University of Technology Sydney
FACULTY OF ENGINEERING

DEVELOPMENT OF A NOVEL FERTILIZER-DRAWN FORWARD OSMOSIS AND ANAEROBIC MEMBRANE BIOREACTOR HYBRID SYSTEM FOR HYDROPONICS

by

YOUNGJIN KIM

A Thesis submitted in fulfilment for the degree of

Doctor of Philosophy

School of Civil and Environmental Engineering
Faculty of Engineering and Information Technology
University of Technology Sydney (UTS)
New South Wales, Australia

February 2017

ACKNOWLEDGEMENTS

First of all, I would like to express my profound gratitude to A/Prof. Hokyong Shon for his guidance and insight. He helped me become a better researcher and a better person. I would also like to thank my external principal supervisor, Prof. Seungkwan Hong from Korea University for giving me the opportunity for the dual degree program. Many thanks as well to my co-supervisors, Dr. Sherub Phuntsho, Dr. Laura Chekli and Dr. Leonard Tijing for their support. Their help and support during my course works helped me and my research a great deal.

I would like to acknowledge MD Johir and Rami Hadad for their help in the laboratory. And the administrative support from Phyllis, Van and Viona as well. A special thanks to my dear friends Yunchul Woo, Sungil Lim, Myongjun Park, Jungeun Kim, Mingwei Yao, Fezeh Lotfi, Nirenkumar Pathak, and Jin Wang.

I also want to express my sincere thanks to Prof. TorOve Leiknes and R/Prof. Noreddine Ghaffour for giving me an opportunity to research at KAUST. And I am grateful for the help of Dr. Sheng Li and Dr. Chunhai Wei. Furthermore, I thank Dr. Sanghyun Jeong for all the great times we had together.

Finally, I would like to express my deepest gratitude to my beloved wife, Ester Yang and my son, Gyuhyeon Kim. Without them, I could not have had the courage and enthusiasm to go day by day in my life and have not gone through all the tough times in life. I would also like to thank my brother-in-law, Hyuntaek Yang for his kind support when I was away and busy with my research.

Last but not least, I would like to acknowledge the University of Technology Sydney for providing me full financial support throughout my time there.

CERTIFICATE OF ORIGINAL AUTHORSHIP

I certify that the work in this thesis has not previously been submitted for a degree nor has it been submitted as part of requirements for a degree except as part of the collaborative doctoral degree and/or fully acknowledged within the text.

I also certify that the thesis has been written by me. Any help that I have received in my research work and the preparation of the thesis itself has been acknowledged. In addition, I certify that all information sources and literature used are indicated in the thesis.

This thesis is the result of a research candidature conducted jointly with another University as part of a collaborative Doctoral degree.

Signature of Student:

Date: 23/02/2017

Journal Articles Published or Submitted**

1. S. Lee, ***Y. Kim***, A. S. Kim, S. Hong, Evaluation of membrane-based desalting processes for RO brine treatment, Desalination and water treatment (2015) 1-8.
2. ***Y. Kim***, S. Lee, H. K. Shon, S. Hong, Organic fouling mechanisms in forward osmosis membrane process under elevated feed and draw solution temperatures, Desalination 355 (2015) 169-177.
3. ***Y. Kim***, S. Lee, J. Kuk, S. Hong, Surface chemical heterogeneity of polyamide RO membranes: Measurements and implications, Desalination 367 (2015) 154-160.
4. ****Y. Kim***, L. Chekli, W. -G. Shim, S. Phuntsho, S. Li, N. Ghaffour, T. Leiknes, H. K. Shon, Selection of suitable fertilizer draw solute for a novel fertilizer-drawn forward osmosis–anaerobic membrane bioreactor hybrid system, Bioresource Technology 210 (2016) 26-34.
5. Y. C. Woo, ***Y. Kim***, W. -G. Shim, L. D. Tijing, M. Yao, L. D. Nghiem, J. -S. Choi, S. -H. Kim, H. K. Shon, Graphene/PVDF flat-sheet membrane for the treatment of RO brine from coal seam gas produced water by air gap membrane distillation, Journal of Membrane Science, 513 (2016) 74-84.
6. *L. Chekli[#], ***Y. Kim***[#], S. Phuntsho, S. Li, N. Ghaffour, T. Leiknes, H. K. Shon*, "Evaluation of Fertilizer-drawn Forward Osmosis for sustainable agriculture and water reuse in arid regions", Journal of Environmental Management 187 (2017) 137-145.
7. J. Wang, N. Pathak, L. Chekli, S. Phuntsho, ***Y. Kim***, D. Li, H. K. Shon*, Performance of a novel fertilizer-drawn forward osmosis aerobic membrane

bioreactor (FDFO-MBR): Mitigating salinity build-up by integrating microfiltration, Water (2017) 9(1), 21.

8. ***Y. Kim***, S. Li, L. Chekli, Y. C. Woo, C. -H. Wei, S. Phuntsho, N. Ghaffour, T. Leiknes, H. K. Shon*, "Assessing the removal of organic micro-pollutants from anaerobic membrane bioreactor effluent by fertilizer-drawn forward osmosis", Journal of Membrane Science, (2017) 533, 84-95.
9. S. Li, ***Y. Kim***, L. Chekli, S. Phuntsho, H. K. Shon, T. Leiknes, N. Ghaffour*, "Impact of reverse nutrient diffusion on membrane biofouling in fertilizer-drawn forward osmosis", Journal of Membrane Science, accepted.
10. ***Y. Kim***, S. Li, L. Chekli, S. Phuntsho, N. Ghaffour, T. Leiknes, H. K. Shon*, "Influence of fertilizer draw solution properties on the performance and microbial community structure in a side-stream anaerobic fertilizer-drawn forward osmosis – ultrafiltration bioreactor", Bioresource Technology, accepted.
11. ***Y. Kim***, Y. C. Woo, S. Phuntsho, L. D. Nghiem, H. K. Shon*, S. Hong*, "Evaluation of fertilizer-drawn forward osmosis for coal seam gas (CSG) reverse osmosis (RO) brine treatment and sustainable agricultural reuse", Journal of Membrane Science, (2017) 237, 22-31.
12. *L. Chekli, J. E. Kim, I. E. Saliby, ***Y. Kim***, S. Phuntsho, S. Li, N. Ghaffour, T. Leiknes, H. K. Shon*, "Fertilizer drawn forward osmosis process for sustainable water reuse to grow hydroponic lettuce using commercial nutrient solution", Separation and Purification Technology, (2017) 181, 18-28.
13. N. Pathak, L. Chekli, J. Wang, ***Y. Kim***, S. Phuntsho, S. Li, N. Ghaffour, T. Leiknes, H. K. Shon*, Performance of a novel baffled OMBR-MF hybrid

system under continuous operation for simultaneous nutrient removal and mitigation of brine discharge, Bioresource Technology, accepted.

14. S. Li, ***Y. Kim***, S. Phuntsho, L. Checkli, H. K. Shon, T. Leiknes, N. Ghaffour*, Methane production in an anaerobic osmotic membrane bioreactor using forward osmosis: Effect of reverse salt flux, Bioresource Technology, accepted.

** Publications made during the PhD candidature including articles not entirely related to the Thesis. * Articles related to the Thesis.

Conference papers and presentation

1. ***Y. Kim***, Y. Woo, J. Wang, H. K. Shon, S. Hong, "Chemical cleaning study in coal seam gas (CSG) RO brine treatment by fertilizer-drawn forward osmosis", 9th International Membrane Science and Technology Conference", Adelaide, Australia, December, 2016.
2. ***Y. Kim***, Y. Woo, S. Phuntsho, L. D. Nghiem, H. K. Shon, and S. Hong, "Accessing fertilizer-drawn forward osmosis for coal seam gas (CSG) reverse osmosis (RO) brine treatment", 2nd International Forward Osmosis Summit, Sydney, Australia, December, 2016.
3. ***Y. Kim***, S. Li, L. Chekli, S. Phuntsho, N. Ghaffour, T. Leiknes and H. K. Shon, "Influence of fertilizer draw solution properties on the performance of a side-stream anaerobic fertilizer-drawn forward osmosis – ultrafiltration bioreactor", 2016 International Conference in Challenges in Environmental Science & Engineering, Kaohsiung, Taiwan, November, 2016.

4. ***Y. Kim***, L. Chekli, S. Phuntsho, S. Li, N. Ghaffour, T. Leiknes and H. K. Shon, "Evaluation of Fertilizer-Drawn Forward Osmosis-Anaerobic Membrane Bioreactor System: Draw Solution Selection and Organic Micro-Pollutants Removal in FDFO", 10th Conference of Aseanian Membrane Society, Nara, Japan, July, 2016.
5. ***Y. Kim***, L. Chekli, W. -G. Shim, S. Phuntsho, S. Li, N. Ghaffour, T. Leiknes and H. K. Shon, "Selection of fertilizers as a draw solute for fertilizer-drawn forward osmosis – anaerobic membrane bioreactor hybrid system", 2nd International Conference on Desalination and Environment, Doha, Qatar, January, 2016.
6. ***Y. Kim***, L. Chekli, S. Phuntsho and H. K. Shon, "Fertilizer-drawn Forward Osmosis-Anaerobic Membrane Bioreactor Hybrid System for Sustainable Agricultural Application", 2015 International Environmental Engineering Conference & Annual meeting of the Korean Society of Environmental Engineers, Busan, Korea, October, 2015.
7. ***Y. Kim***, L. Chekli, S. Phuntsho and H. K. Shon, "Performance of a submerged anaerobic membrane bioreactor with fertilizer-drawn forward osmosis for hydroponics", 2015 International Conference in Challenges in Environmental Science & Engineering, Sydney, Australia, September, 2015.
8. Y. Woo, ***Y. Kim***, W. -G. Shim, L. D. Tijing, M. Yao, J. -S. Choi, L. D. Nghiem, S. -H. Kim and H. K. Shon, "Preparation and fabrication of graphene-enabled cast membrane for the treatment of RO brine from CSG produced water by AGMD", 2015 International Conference in Challenges in Environmental Science & Engineering, Sydney, Australia, September, 2015.

9. S. Lee, ***Y. Kim*** and S. Hong, “Integrated Forward Osmosis (FO) with Membrane Distillation (MD) for RO Brine Treatment”, IWA Regional Conference on Membrane Technology 2014, Ho Chi Minh City, Vietnam, December, 2014.
10. ***Y. Kim***, S. Lee and S. Hong, “Influence of membrane distillation on the performance and fouling behavior of forward osmosis in FO-MD hybrid system for treating primary RO concentrate”, The 7th IWA specialized membrane Technology Conference and Exhibition for water and wastewater treatment and reuse”, Toronto, Canada, August, 2013.

Presentation made during the PhD candidature including proceedings, oral and poster presentations.

LIST OF ABBREVIATIONS

AL-DS	Active layer facing draw solution
AL-FS	Active layer facing feed solution
AnFDFOMBR	Anaerobic fertilizer-drawn forward osmosis membrane bioreactor
AnMBR	Anaerobic membrane bioreactor
BMP	Bio-methane potential
CDI	Capacitive deionization
CEOP	Cake-enhanced osmotic pressure
CMC	Critical micellar concentration
COD	Chemical oxygen demand
CRCP	Cake-reduced concentration polarization
CP	Concentration polarization
CTA	Cellulose triacetate
DI	Deionised
DS	Draw solution
ECP	External concentration polarization
ED	Electrodialysis
EDGs	Electron donating groups
EDX	Energy dispersive X-ray spectroscopy
EPS	Extracellular polymeric substances
EWGs	Electron withdrawing groups
FDFO	Fertilizer drawn forward osmosis
FS	Feed solution
HA	Humic acid

HRT	Hydraulic retention time
ICP	Internal concentration polarization
MAP	Mono-ammonium phosphate
MBR	Membrane bioreactor
MD	Membrane distillation
MF	Microfiltration
MKP	Mono-potassium phosphate
MLSS	Mixed liquor suspended solids
NF	Nanofiltration
NFT	Nutrient film technique
OLR	Organic loading rate
OMBR	Osmotic membrane bioreactor
OMPs	Organic micro-pollutants
PA	Polyamide
PAFDFO	Pressure-assisted fertilizer-drawn forward osmosis
PAO	Pressure-assisted osmosis
PPCPs	Pharmaceutical and personal care products
PRO	Pressure retarded osmosis
RO	Reverse osmosis
RSF	Reverse salt flux
RSFS	Reverse salt flux selectivity
SEM	Scanning electron microscopy
SOA	Ammonium sulphate
SRB	Sulphate reducing bacteria
SRSF	Specific reverse salt flux

SRT	Solid retention time
TAN	Total ammonia nitrogen
TDS	Total dissolved solids
TFC	Thin-film composite
TN	Total nitrogen
TOC	Total organic carbon
TP	Total phosphorous
TS	Total solids
TrOCs	Trace organic contaminants
UF	Ultrafiltration
VFAs	Volatile fatty acids
XRD	X-ray diffraction
ZLD	Zero liquid discharge

Abstract

A novel fertilizer-drawn forward osmosis (FDFO) – anaerobic membrane bioreactor (AnMBR) hybrid system was proposed for the sustainable hydroponic application as well as wastewater reuse. This system consisted of three parts: (i) FDFO for concentrating municipal wastewater and producing diluted fertilizer solution, (ii) AnMBR-FDFO hybrid system for treating concentrated municipal wastewater and producing biogas as well as diluted fertilizer solution, and (iii) supplying produced fertilizer solution to hydroponics.

The FDFO performance was initially investigated to achieve simultaneous water reuse from wastewater and production of nutrient solution for hydroponic application. Bio-methane potential (BMP) measurements, which can be utilized to simulate the anaerobic process in batch mode to assess the bio-methane production potential from different substrates, were carried out to determine the effect of osmotic concentration of wastewater achieved in FDFO on the anaerobic activity. Results showed that 95% water recovery from FDFO was the optimum value for further AnMBR treatment. Nine different fertilizers were then tested based on their forward osmosis (FO) performances (i.e. water flux, water recovery and reverse salt flux (RSF)) and final nutrient concentration. From this initial screening, ammonium phosphate monobasic (MAP), ammonium sulphate (SOA) and mono-potassium phosphate (MKP) were selected for long term experiments to investigate the maximum water recovery achievable. After the experiments, hydraulic membrane cleaning was performed to assess the water flux recovery. SOA showed the highest water recovery rate, up to 76% while MKP showed the highest water flux recovery, up to 75% and finally MAP showed the lowest final nutrient concentration. However, substantial dilution was still necessary to comply with the standards for fertigation even if the recovery rate was increased.

In order to understand and predict the performance behaviour of anaerobic fertilizer-drawn forward osmosis membrane bioreactor (AnFDFOMBR), a protocol for selecting suitable fertilizer draw solute was proposed and evaluated. Among eleven commercial fertilizer candidates, six fertilizers were screened further for their FO performance tests and evaluated in terms of water flux and RSF. Using selected fertilizers, BMP experiments were conducted to examine the effect of fertilizers on anaerobic activity due to reverse diffusion. MAP showed the highest biogas production while other fertilizers exhibited an inhibition effect on anaerobic activity with solute accumulation. Salt accumulation in the bioreactor was also simulated using mass balance simulation models. Results indicated that SOA and MAP were the most appropriate for AnFDFOMBR since they demonstrated less salt accumulation, relatively higher water flux, and higher dilution capacity of draw solution (DS). Given toxicity of sulphate to anaerobic microorganisms, MAP appears to be the most suitable DS for AnFDFOMBR.

Two types of the AnMBR-FDFO hybrid systems were considered for further studies, which are (i) FDFO post-treatment of AnMBR effluent and (ii) AnFDFOMBR. The first was designed to reduce not only the effect of fertilizer DS on the bioreactor but also membrane fouling via microfiltration (MF)/ultrafiltration (UF) as pre-treatment. Besides, contaminants should be treated by three steps: (i) biological treatment, (ii) MF/UF filtration and (iii) FDFO treatment, which can enhance total rejection rate. Therefore, the behaviour of organic micro-pollutants (OMPs) transport including membrane fouling was assessed in FDFO during treatment of AnMBR effluent. The flux decline was negligible when the FO membrane was oriented with active layer facing feed solution (AL-FS) while severe flux decline was observed with active layer facing DS (AL-DS) with di-ammonium phosphate (DAP) fertilizer as DS due to struvite scaling inside the membrane support layer. DAP DS however exhibited the lowest OMPs forward flux or higher OMPs

rejection rate compared to other two fertilizers (i.e., MAP and KCl). MAP and KCl fertilizer DS had higher water fluxes that induced higher external concentration polarization (ECP) and enhanced OMPs flux through the FO membrane. Under the AL-DS mode of membrane orientation, OMPs transport was further increased with MAP and KCl as DS due to enhanced concentrative internal concentration polarization while with DAP the internal scaling enhanced mass transfer resistance thereby lowering OMPs flux. Physical or hydraulic cleaning could successfully recover water flux for FO membranes operated under the AL-FS mode but only partial flux recovery was observed for membranes operated under AL-DS mode because of internal scaling and fouling in the support layer. Osmotic backwashing could however significantly improve the cleaning efficiency.

A side-stream anaerobic FDFO and UF membrane bioreactor hybrid system was proposed and operated for 55 days. The FDFO performance was first investigated in terms of flux decline with various fertilizers DS. Flux decline was very severe with all fertilizers due to the absence of aeration and the sticky property of sludge. Flux recovery by physical cleaning varied significantly amongst tested fertilizers which seriously affected biofouling in FDFO via RSF. Besides, RSF had a significant impact on nutrient accumulation in the bioreactor. These results indicated that nutrient accumulation negatively influenced anaerobic activity. To elucidate these phenomena, bacterial and archaeal community structures were analysed by pyrosequencing. Results showed that bacterial community structure was affected by fertilizer properties with less impact on archaeal community structure, which resulted in a reduction in biogas production and an increase in nitrogen content.

The sustainable reuse of wastewater using FDFO was investigated through osmotic dilution of commercial nutrient solution for hydroponic application. Results from the

bench-scale experiments showed that the commercial hydroponic nutrient solution exhibited similar performance (i.e. water flux and RSF) with other inorganic DS. The use of hydroponic solution provides all the required or balanced macro- and micronutrients in a single solution. Hydraulic cleaning effectively restored water flux up to 75% while osmotic backwashing restored by more than 95% illustrating the low-fouling potential of FDFO. Pilot-scale studies demonstrated that FDFO can produce the required nutrient concentration and final water quality (i.e. pH and conductivity) suitable for hydroponic applications. Coupling FDFO with pressure assisted osmosis (PAO) in the later stages could help in saving operational costs (i.e. energy and membrane replacement costs). However, a trade-off between the process footprint and energy costs associated with the additional pressure needs to be further investigated. Finally, the test application of nutrient solution produced by the pilot FDFO process to hydroponic lettuce showed similar growth pattern as the control without any signs of toxicity or any mortality.

CONTENTS

List of Figures

List of Tables

1. Introduction

1.1 Research background

Recently, freshwater resources are getting scarcer due to the impacts of global warming, and rapid and extensive industrialization and urbanization (Rijsberman, 2006). Furthermore, the agricultural sector still consumes about 70% of the accessible freshwater with about 15-35% of water being used unsustainably (Clay, 2004). Therefore, wastewater reuse as well as seawater desalination has been considered as an alternative water resource in the countries such as Mediterranean countries which are stressed by water shortage for the agricultural purpose (Angelakis et al., 1999b).

Reverse osmosis (RO) membranes have been employed in a wide range of applications including seawater desalination (Almulla et al., 2003), and drinking and industrial water treatment (Al-Agha and Mortaja, 2005) as well as wastewater treatment (Lee et al., 2006, Ang et al., 2006, Vourch et al., 2008). However, its efficient operation is often hampered by high energy consumption and high fouling potential (Semiat, 2008, Herzberg et al., 2009). Recently, forward osmosis (FO) is considered as an alternative process to a conventional RO process due to its low energy consumption, low fouling potential and high recovery rate (McGinnis and Elimelech, 2007, Lee et al., 2010, Mi and Elimelech, 2010).

FO utilizes a highly-concentrated draw solution (DS) as a driving force to induce a net flow of water through the membrane from the feed solution (FS) to DS (Cath et al., 2006, Chekli et al., 2012, Chekli et al., 2016). For that reason, FO can be a lower energy and lower fouling process than other pressurized membrane processes. However, FO requires additional process to produce pure water for the drinking or industrial purposes since it uses very high concentration of DS. For the effective reconstruction of DS and the

effective production of pure water, a variety of post-treatment processes such as distillation, membrane distillation (MD) and nanofiltration (NF) are adopted as shown in **Fig.1** (McCutcheon and Elimelech, 2006, Achilli et al., 2010, Tan and Ng, 2010, Xie et al., 2013a, Kim et al., 2015c, Lee et al., 2015). However, since these recovery processes employ hydraulic pressure or thermal energy to extract water or draw solute from DS, high energy consumption is required. Therefore, it is required to develop a specific FO process without additional DS recovery process.

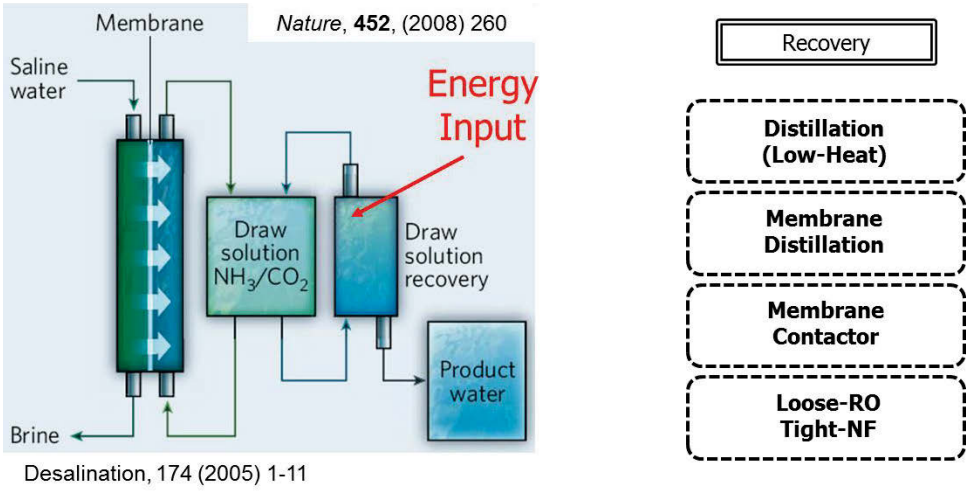

Figure 1. Draw solution recovery in FO (McCutcheon et al., 2005, Shannon et al., 2008).

1.2 A fertilizer-drawn forward osmosis hybrid system for sustainable agriculture and wastewater reuse

Recently, fertilizer-drawn forward osmosis (FDFO) has received increased interest since the diluted DS can be used directly for irrigation purposes and therefore no recovery process is required (Phuntsho et al., 2011, Phuntsho et al., 2012a, Phuntsho et al., 2012b, Phuntsho et al., 2013a, Phuntsho et al., 2014, Phuntsho et al., 2016). In FDFO, fertilizers are used as DS and the fertilizer solution is continuously diluted during operation

(Phuntsho et al., 2011). In the early studies, only single fertilizers, which did not provide sufficient nutrient composition for direct application, were examined. Thus, blended fertilizers were investigated for targeted crops (Phuntsho et al., 2012b). However, the final nutrient concentration was still high and the final fertilizer solution required substantial dilution for direct fertigation. To solve this problem, NF was adopted as post-treatment and the produced fertilizer solution by NF could meet the water quality requirements for fertigation since it has lower rejection rates (i.e., 80-90%) than RO (Phuntsho et al., 2013a). Nevertheless, high energy consumption is still an issue since NF is a pressurized desalting process and should overcome osmotic pressure of diluted fertilizer solution. Finally, pressure-assisted fertilizer-drawn forward osmosis (PAFDFO) was recently developed for enhancing final dilution of fertilizer DS without beyond the point of osmotic equilibrium between FS and DS (Sahebi et al., 2015).

In these days, many researchers have studied anaerobic membrane bioreactor (AnMBR) to treat wastewater since AnMBR has several advantages including low sludge production, high organic rejection and biogas production (Liao et al., 2006). However, AnMBR has low rejection properties on ammonia and phosphorous (Jain et al., 2015). In addition, the conventional AnMBR process exhibits high fouling tendencies which ultimately increases energy requirement (Xu et al., 2010a). To overcome these issues, FO can be utilized instead of traditional pressurized membrane processes of its lower energy consumption and higher fouling reversibility. In addition, by using fertilizer solutions as DS, the diluted fertilizer DS after the osmotic dilution can be directly provided for irrigation purpose without the need of additional recovery process of DS.

For sustainable operation, the FDFO - AnMBR hybrid system is proposed for greenhouse hydroponics as depicted in **Fig. 2**. This system comprises 1st staged FDFO and 2nd staged anaerobic fertilizer-drawn forward osmosis membrane bioreactor (AnFDFOMBR). 1st

staged FDFO plays a role to concentrate municipal wastewater for enhancing biogas production and then 2nd staged AnFDFOMBR is utilized to treat concentrated municipal wastewater. The merits of employing 1st staged FDFO rather than using only AnFDFOMBR are (1) to enhance the anaerobic activity in terms of biogas production and (2) to reduce the footprint of 2nd staged AnFDFOMBR. 2nd staged AnFDFOMBR consists of two parts (i.e., AnMBR and FDFO). In conventional AnMBR, microfiltration (MF) or ultrafiltration (UF) are employed to separate the treated wastewater from the anaerobic sludge. In this study, a FO membrane is used instead and submerged into the bioreactor. In addition, the FO process is here driven by fertilizers and thus the treated water drawn from the wastewater is used to dilute the fertilizer solution which can then be directly used for fertigation. In this system, raw municipal wastewater will be utilized as influent and a highly-concentrated fertilizer solution is used as DS for the AnFDFOMBR process. The diluted fertilizer solution can then be obtained and supplied to greenhouse hydroponics irrigation.

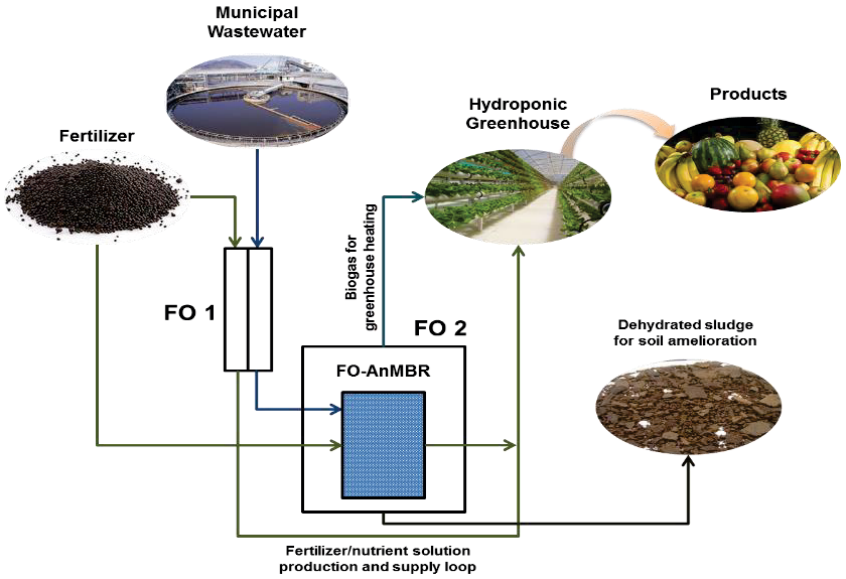

Figure 2. Conceptual diagram of the fertilizer-drawn forward osmosis (FDFO) – anaerobic membrane bioreactor (AnMBR) hybrid process for greenhouse hydroponics.

1.3 Objectives and scope of the research

As mentioned in the last section, the AnMBR-FDFO hybrid process is proposed in this study. And thus it is required to demonstrate the concept of the proposed hybrid process in terms of 1st staged FDFO and 2nd staged AnFDFOMBR separately. Therefore, the proposed scope of the project can be summarised into different segments:

- Demonstrate the concept of hybrid AnMBR-FDFO process (**Fig. 2**) for sustainable hydroponics with an energy neutral balance.
- Evaluate FDFO with fertilizers as DS to produce nutrients solutions for hydroponics.
- Evaluate AnMBR for municipal wastewater treatment and biogas production as the supply of water and energy for operating the hybrid system
- Evaluate the performance of FDFO process as a pre-treatment and post-treatment for AnMBR influent and effluent, respectively.

1.4 Structure of the study

The thesis consists of eight chapters with research background, objectives and scope of the research included in Chapter 1. Introduction.

Chapter 2 covers a literature review on both AnMBR and FDFO including a general introduction of the AnMBR and dominant factors affecting its performance followed by the recent development on FDFO for sustainable irrigation and brackish water treatment.

Chapter 3 focuses on the performance of FDFO to achieve simultaneous water reuse from wastewater and production of nutrient solution for hydroponic application. From this study, the optimum recovery rate of 1st staged FDFO is obtained for optimizing FDFO as

pre-treatment by evaluating bio-methane potential (BMP) experiments with varying recovery rate and testing various single and blended fertilizer combinations.

A systematic protocol for selecting suitable fertilizer draw solute for AnFDFOMBR is developed in Chapter 4. The screening protocol includes evaluations of FO performance, BMP and osmotic membrane bioreactor (OMBR) simulation.

Chapter 5 suggests FDFO as post-treatment of AnMBR for treating municipal wastewater containing organic micro-pollutants (OMPs) and investigates the behaviour of OMPs transport including membrane fouling in FDFO during treatment of AnMBR effluent. The AnMBR-FDFO hybrid process can be optimized from this study.

The performance evaluation of a side-stream anaerobic fertilizer-drawn forward osmosis (FDFO) and ultrafiltration (UF) membrane bioreactor (MBR) hybrid system is described in Chapter 6. Results include FO flux decline, the anaerobic performance and the pyrosequencing analysis.

Chapter 7 targets on the sustainable reuse of wastewater using FDFO through osmotic dilution of commercial nutrient solution for hydroponic application.

Chapter 8 summarises the outcomes, concluding remarks, and recommendations.

2. Literature review

2.1 Introduction: Water scarcity problem

Water scarcity, which is defined as the lack of available water resources to people within a region, has been getting more severe in the world (Jiménez Cisneros and Asano, 2008). Today, around 700 million people in 43 countries suffer from water scarcity. Furthermore, by 2025, 1.8 billion people will be living in regions with absolute water scarcity, and two-thirds of the world's population will be living under water stressed conditions. With the existing climate change scenario, almost half the world's population will be living in areas of high water stress by 2030, including between 75 million and 250 million people in Africa. In addition, water scarcity in some arid and semi-arid places will displace between 24 million and 700 million people. Sub-Saharan Africa has the largest number of water-stressed countries of any region (2014).

Water scarcity can be divided into two mechanisms: (i) physical (absolute) water scarcity and (ii) economic water scarcity (Molden, 2007). The former is the situation caused by a lack of enough water to meet all demands to make ecosystems function effectively. And the latter is originated from a lack of the investment in water infrastructure to meet the water demand for human activity. Therefore, freshwater resources are getting scarcer due to the impacts of global warming, and rapid and extensive industrialization and urbanization (Rijsberman, 2006).

To mitigate the water scarcity problem, particularly in water scarce regions, wastewater reuse in the agricultural sector can be very helpful in sustaining freshwater resources since around 70% (global average) of the accessible freshwater is still consumed by the agricultural sector. Besides, treated wastewater can contribute to an appreciable amount of necessary nutrients for plants (Jeong et al., 2016). Therefore, the use of reclaimed water

for agricultural irrigation has been reported in at least 44 countries (Jiménez Cisneros and Asano, 2008). For example, 30-43% of treated wastewater is used for agricultural and landscape irrigation in Tunisia (Bahri, 2009). In Australia, treated municipal wastewater of about 0.28×10^9 m^3/year is directly reused for irrigation (Nations, 2016).

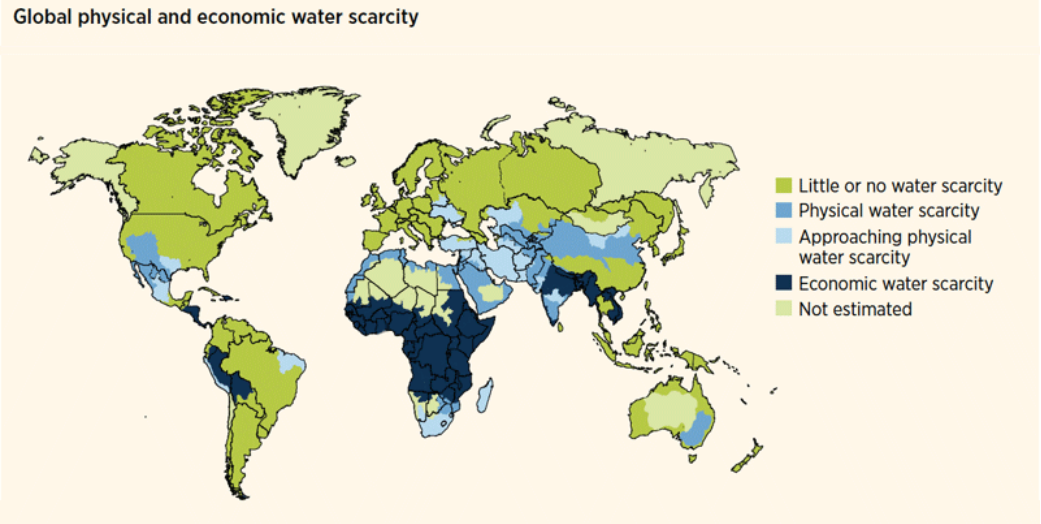

Figure 3. Global physical and economic water scarcity (2012) (WWAP, 2012).

2.2 Anaerobic membrane bioreactor

2.2.1 Basic concept of anaerobic membrane bioreactor

Recently, anaerobic MBR (AnMBR) has been spotlighted for the treatment of a variety of wastewater resources including industrial wastewater, municipal wastewater, and landfill leachate (Lin et al., 2013). AnMBR has many advantages including a complete retention of all microorganisms in the bioreactor by using MF or UF, a small footprint, improved effluent quality, and energy (biogas) production. Due to these merits, the number of studies on AnMBR has been increasing over the past 30 years (**Fig. 4)**. On the other hand, it has also significant problems that are severe membrane fouling compared to aerobic MBR by no aeration (Kim et al., 2014b). Moreover, for wastewater reuse, it is

required to further treat AnMBR effluent due to a low ionic compound rejection property of MF or UF (Hosseinzadeh et al., 2015).

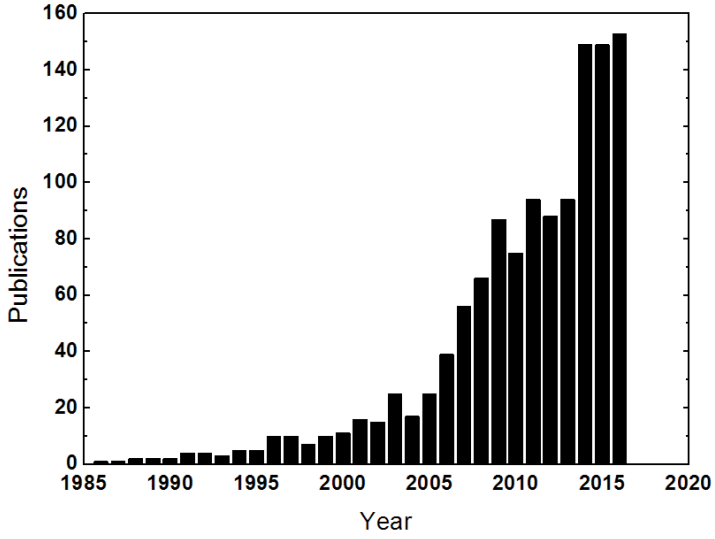

Figure 4. Annual publications of anaerobic membrane bioreactor (AnMBR) for the past 30 years as searched through Scopus (**http://www.scopus.com/**). The investigation was carried out with the range from 1986 to 2016 by using the keyword "anaerobic membrane bioreactor".

AnMBR is the combination of a membrane process (e.g., MF or UF) with an anaerobic bioreactor for municipal and industrial wastewater treatment. According to the way to install membrane modules, it is divided into a submerged AnMBR (i.e., membrane modules are submerged in the bioreactor) and a side-stream AnMBR (i.e., membrane modules are installed externally to the bioreactor) as shown in **Fig. 5**. In the submerged configuration as illustrated in **Fig. 5a**, there is no circulation pump, which makes more energy efficient process compared to the external configuration. The absence of the cross flow (i.e., shear force) leads to low physical stress to microorganisms (Andrade et al., 2014), which can enhance the microbial activity. On the other hand, it has also

disadvantages in terms of membrane fouling. No shear force on the membrane surface may result in more severe membrane fouling. Thus, mixing with biogas or a mechanical stirrer is often utilized in the submerged configuration but their efficiency is limited (Aslan et al., 2014, Zhang et al., 2015). In the side-stream configuration as depicted in **Fig. 5b**, anaerobic sludge is recirculated into the membrane module which is installed outside of the bioreactor. This side-stream can induce the shear force on the membrane surface, which may be utilized to controlling membrane fouling. However, due to the existence of the recirculation pump, the external configuration of AnMBR requires additional energy consumption. Besides, when applying too high cross-flow rate (i.e., more than 2-4 m/s), it can make biomass particle size reduced as well as soluble microbial products (SMP) released (Bornare et al., 2014), which accelerate membrane fouling by pore clogging (Dvořák et al., 2011). For the biogas (bio-methane) production, the efficient operation of the anaerobic bioreactor is most important. Therefore, it needs to understand which factors are dominantly affecting anaerobic processes and it will be discussed in **Section 2.2.2.2 and 2.2.2.3**.

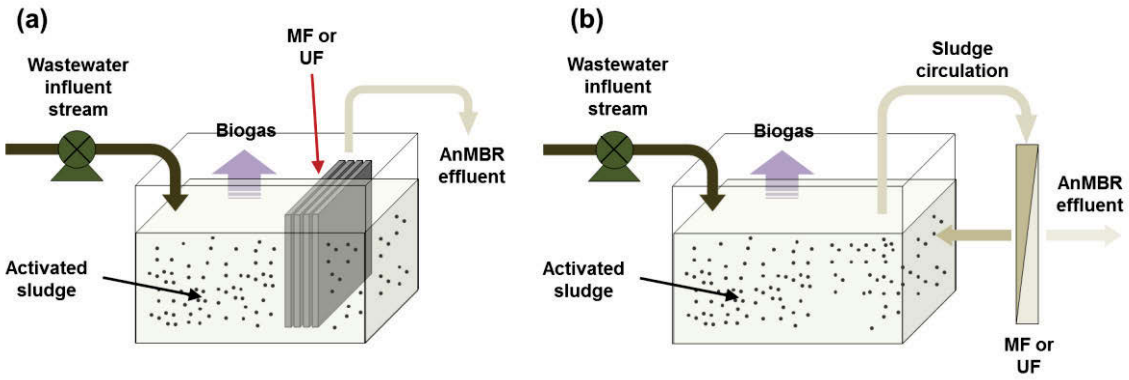

Figure 5. Conceptual illustrations of (a) a submerged AnMBR and (b) a side-stream AnMBR.

AnMBR has been intensively studied for treatment of a variety of wastewater including municipal and industrial wastewaters. Different types of wastewater have different characteristics (i.e., organic composition, salinity, temperature and pH), which can affect the anaerobic biological performance of the bioreactor as well as the membrane performance. Therefore, AnMBR applications is briefly reviewed in terms of wastewater type. The produced amount of industrial wastewater has been significantly increased due to the rapid industrialization. Wastewater generated from food processing, pulp, textile, chemical, pharmaceutical, petroleum, tannery and manufacturing industries may have an extreme physicochemical property (e.g., pH, temperature and salinity) as well as high organic content (Ng et al., 2015, Yurtsever et al., 2016). Therefore, it may be toxic and also have a negative impact on the biological process (Dvořák et al., 2016). **Table 1** presents some recent studies regarding the treatment of the industrial wastewater. Wastewater produced from food industry is readily biodegradable (i.e., higher than 90%) with high concentration of chemical oxygen demand (COD), implying that AnMBR is one of the suitable processes for food industrial wastewater treatment. Wastewater from pulp and paper industry has generally high temperature and thus AnMBR is often operated at thermophilic condition. However, thermophilic operation can induce severe membrane fouling since high temperature causes more release of soluble microbial products and disruption of sludge flocs (Lin et al., 2009).

Compared to industrial wastewater, municipal wastewater has been rarely treated by anaerobic processes due to the difficulty to retain slow-growth anaerobic microorganisms with low hydraulic retention time (HRT) and meet discharge standards for wastewater reuse (Herrera-Robledo et al., 2010). However, by combining anaerobic processes with membrane technology such as MF and UF, municipal wastewater can be treated with some benefits (i.e., low sludge production and biogas production) from the anaerobic

bioreactor. Several studies in municipal wastewater treatment by AnMBR are introduced in **Table 1**.

AnMBR generally achieves higher COD removal rate than other conventional anaerobic processes regardless of the operation type since AnMBR can be operated very long SRT due to the complete sludge retention (Baek et al., 2010). However, total nitrogen (TN) and total phosphorous (TP) are hardly removed in AnMBR. Thus, further treatment for TN and TP is required by combining aerobic and anoxic processes to reclaim the AnMBR effluent. Recently, the treatment of trace organic contaminants (TrOCs) has been getting an increasing attention due to their rapid increasing occurrence in municipal wastewater. Hydrophobicity and specific molecular features such as electron withdrawing groups (EWGs) and electron donating groups (EDGs) have a significant impact on TrOCs removal by AnMBR (Wijekoon et al., 2015). TrOCs containing strong EDGs are easily biodegraded, while TrOCs containing strong EWGs or halogen are not removed by AnMBR (Wei et al., 2015). Moreover, TrOCs with nitrogen and sulphur are readily biodegraded by denitrifying and sulphur-reducing bacteria under the anaerobic condition (Wijekoon et al., 2015).

Synthetic wastewater is often utilized as influent to examine a new design of AnMBR (Qiu et al., 2015, Gu et al., 2015) or study membrane fouling mechanisms due to its significant impact on the efficient operation of AnMBR (Yan et al., 2012). Synthetic wastewater is generally composed of organics (e.g., glucose, starch, yeast and milk power), inorganics (e.g., nitrogen, phosphorous, magnesium, calcium and potassium) and trace metals (e.g., copper, manganese, nickel, zinc and plumbum) (Wei et al., 2015, Gu et al., 2015). **Table 1** shows recent studies regarding the treatment of synthetic wastewater. Since synthetic wastewater has no refractory organic compounds, AnMBR generally exhibited higher that 95% COD removal. In addition, AnMBR can be operated under

lower biomass concentration than other anaerobic processes (e.g., upflow anaerobic sludge blanket (UASB) reactors and expanded granular sludge bed (EGSB) reactors) with high organic loading rate, OLR (i.e., 10 kg COD/m^3/d).

Table 1. Summary of AnMBR performance for the treatment of various wastewater.

Wastewater type		Configuration	Operation condition	COD removal efficiency	Reference
Industrial	Diluted tofu processing wastewater	External	HRT: 4 h pH 5.5 Thermophilic (60 ºC)	Feed: 26,500 mg/L	(Kim et al., 2011)
	Brewery wastewater	External	MLVSS: 12 g/L OLR: 12 kg COD/m^3/d Mesophilic (30 ºC)	Feed: 21,000 mg/L Removal efficiency: 99 %	(Torres et al., 2011)
	Themomechanical pulp	Submerged	MLSS: 5.7 g/L OLR: 2.4 kg COD/m^3/d Mesophilic (35 ºC)	Feed: 2,780-3,350 mg/L Removal efficiency: 90 %	(Gao et al., 2010)
	Brewery wastewater	Submerged	HRT: 44 h, SRT: 30 d MLVSS: 1.8 g/L OLR: 2/5/7.5/10 kg COD/m^3/d Mesophilic (35 ºC)	Feed: 17,000 mg/L Removal efficiency: 98 %	(Chen et al., 2016)
Municipal	Municipal	Submerged	HRT: 10 h MLSS: 6.4-9.3 g/L OLR: 1 kg COD/m^3/d Mesophilic (30 ºC)	Feed: 425 mg/L Removal efficiency: 88%	(Lin et al., 2011)
	Municipal	External	HRT: 3 h, SRT: 100 d Atmospheric (25 ºC)	Feed: 646 mg/L Removal efficiency: 87%	(Herrera-Robledo et al., 2010)
	Domestic	Submerged	HRT: 22 h OLR: 0.8–2.5 COD kg/m3/d Atmospheric (20 ºC)	Feed: 430/460 mg/L Removal efficiency: 95-98%	(Hülsen et al., 2016)
Synthetic	Maltose, glucose, VFA	Submerged	HRT: 14, 16, 20 d MLVSS: 19.5 g/L OLR: 2.5 kg COD/m^3/d Mesophilic (35 ºC)	Feed: 25,000 mg/L Removal efficiency: 99.4 ~ 99.6 %	(Jeong et al., 2010)
	Dairy	External	HRT: 54 h, SRT: 500 d MLVSS: 9.3 g/L OLR: 0.6–1.8 kg COD/m^3/d Atmospheric (24 ºC)	-	(Kjerstadius et al., 2016)
	Whey, sucrose	Submerged	SRT: 30 – 40 d MLVSS: 5.5 - 20.4 g/L OLR: 1.5–13 kg COD/m^3/d Mesophilic (35 ºC)	-	(Spagni et al., 2010)
	Molasses	External	HRT: 16/32 h MLVSS: 1.8/10 g/L OLR:14.9/5.6 kg COD/m^3/d Thermophilic (55 ºC)	Feed: 12,000 mg/L Removal efficiency: 60 – 80 %	(Wijekoon et al., 2011)

2.2.2 Anaerobic processes

2.2.2.1 Fundamentals of anaerobic processes

Anaerobic process is to biodegrade organic matters in absence of oxygen by microorganisms. Biodegradation mechanisms in the anaerobic condition are divided into four steps as shown in **Fig. 6** (Lin et al., 2013, Jain et al., 2015). The first step is enzymatic hydrolysis, which reduces the complex organic matters (i.e., carbohydrate, proteins, and fats) to the soluble organic molecules (i.e., sugars, amino acids, and fatty acids). The second step is fermentation, which converts reduced organics into volatile fatty acids (VFAs), acetic acid, hydrogen, and carbon dioxide. The third step is acetogenesis, which converts VFAs to acetic acid, hydrogen, and carbon dioxide. The final step is methanogenesis, which produces methane from acetate, carbon dioxide, and hydrogen by various methanogenic bacteria. Anaerobic process has many benefits including bio-methane production, fertilizer production, pathogen removal, and pollution control. On the other hand, it has also significant problems in terms of biomass retention by relatively poor settling properties of the biomass (Jain et al., 2015).

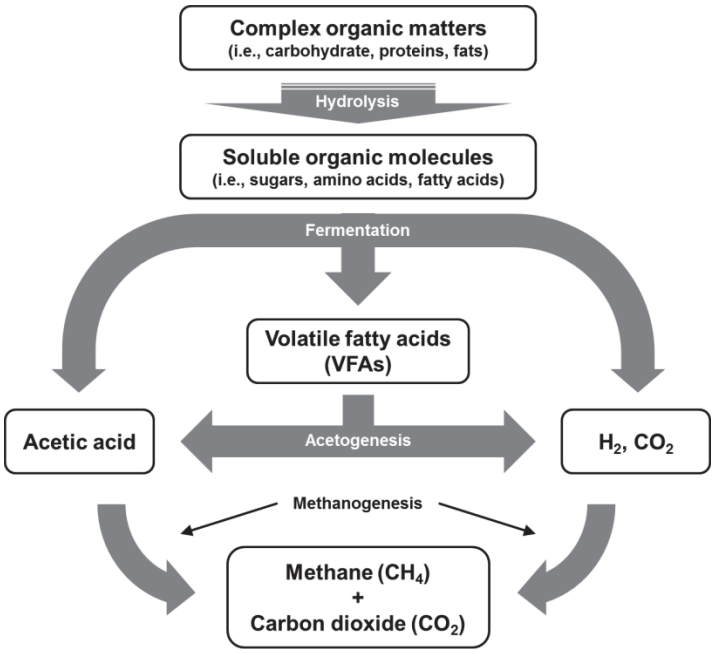

Figure 6. Four-step mechanisms for anaerobic process.

2.2.2.2 Dominant factors affecting anaerobic processes

Many operation factors significantly influence four-step mechanisms (mentioned in **Section 2.2.2.1**) of anaerobic process, which results in deterioration on the effective operation of anaerobic process (Jain et al., 2015). These factors include pH, temperature, total solids (TS) in feed, OLR, seeding, diameter to depth ratio, carbon to nitrogen (C/N) ratio, nutrients, HRT, feed stocks, end products and pressure. Their impacts on anaerobic process are briefly presented in **Table 2**.

In AnMBR, pH is the most important factor dominantly affecting anaerobic process. Between pH 6.5 and 7.5, methanogenic microorganisms are very active, resulting in the efficient bio-digestion in AnMBR (Sutaryo et al., 2012, Zonta et al., 2013). Thus, pH should be maintained in this range to avoid the detriment of the bacterial population. AnMBR can be operated under two different temperature condition (i.e., mesophilic and thermophilic). The optimum temperature for the mesophilic condition is 35 ºC, while that

for the thermophilic condition is 55 ºC (Kim et al., 2002, Hartmann and Ahring, 2006). Higher working temperature can lead to higher biogas production as well as pathogen reduction (El-Mashad et al., 2004). However, due to heating the bioreactor tank, more energy input is required.

Diameter to depth ratio of the reactor tank and stirring is the important designing factors affecting anaerobic processes. When diameter to depth ratio is out of the range of 0.66 - 1.00, temperature can vary with different depths and then non-uniform temperature distribution may negatively influence the anaerobic performance (Kwietniewska and Tys, 2014). Similarly, complete stirring can enhance the anaerobic processes by making low temperature variation and providing food to microorganisms efficiently. However, severe mixing can destroy the cell structure and reduce the anaerobic activity.

In addition to operation conditions, feed quality such as carbon to nitrogen (C/N) ratio critically influences the anaerobic process, especially in terms of the growth of anaerobic microorganisms since microorganisms utilize carbon for energy production and nitrogen for the cell structure. For the anaerobic bacteria growth, a C/N ratio range of 20/1 – 30/1 was recommended (Wang et al., 2012) but an optimal value varies depending on the type of feed stock (Yen and Brune, 2007, Romano and Zhang, 2008). If a C/N ratio is inappropriate, total ammonia nitrogen (TAN) release and VFA accumulation can occur in the bioreactor, which results in the failure of the anaerobic process (Pereira et al., 2003).

Table 2. Operation factors dominantly affecting the anaerobic process.

Factors	Description	Optimum range	Reference
pH	Lower pH than 6.5 or higher pH than 7.5 is detrimental to methanogenic microorganisms.	6.5 – 7.5	(Sutaryo et al., 2012, Zonta et al., 2013)
Temperature	Higher temperature leads higher biogas production.	Mesophilic 35 ºC Thermophilic 55 ºC	(Kim et al., 2002)
Total solids	Increase of TS in feed can make the COD removal and the methane yield reduced.		(Fernández et al., 2008)
Organic loading rate	Too high loading rate can accumulate acid and stop fermentation.	0.5 – 1.6 kg of VS/m3/day	(Luste and Luostarinen, 2010)
Seeding	Methane formers grow more slowly than acid formers.		(Wang et al., 2012)
Diameter to depth ratio	Temperature can vary at different depths.	0.66 – 1.00	(Jain et al., 2015)
Carbon to nitrogen (C/N) ratio	Improper C/N ration can result in releasing high TAN and/or high VFAs which are potential inhibitors.	25/1 (20/1 – 30/1)	(Wang et al., 2012)
Nutrients	Proper amount of P and N_2 should be added since both nutrients may be ignored them in spite of that C, H_2, O_2, N_2, and P are the essential nutrients.		(Alburquerque et al., 2012)
Retention time	Retention time should be over 2 – 4 days since methanogenic microorganisms become double in 2- 4 days.	Over 2 – 4 days	(Kwietniewska and Tys, 2014)
Type of feed stocks	Unwanted materials such as straw, wood shavings, inorganic matters, or polymeric components can cause failures of anaerobic processes.		(van der Wielen et al., 2002, Lu et al., 2007)
End product toxicity	The digested slurry after a certain time can be toxic to the microorganisms due to high concentration of trace elements such as Ca, Mg, and P.		(Chiu et al., 2013)
Pressure	Low pressure is better for the fermentation.		(Cuetos et al., 2010)
Acid accumulation	Intermediate acid products can inhibit anaerobic processes by reducing pH.		(Pereira et al., 2003)

2.2.2.3 Inhibition factors affecting anaerobic processes

There are a lot of inhibition factors affecting anaerobic processes as briefly presented in **Table 3**. Ammonia is generated from the biological degradation of organics containing nitrogen and exists as two forms (i.e., free ammonia (NH_3) and ammonium ion (NH_4^+)) in water (Tchobanoglous et al., 1993). Among both forms, free ammonia can freely diffuse into the cell, which induces proton imbalance and/or potassium deficiency (Gallert et al., 1998). Even though nitrogen is essential nutrient for anaerobic microorganisms, high concentration of ammonia (more than 200 mg/L) inhibits anaerobic processes, resulting in reduced bio-methane production (Liu and Sung, 2002). Furthermore, an increase in pH can affect anaerobic processes by converting ammonium ions to free ammonia (Borja et al., 1996b), which inhibits anaerobic processes as mentioned above. Besides, high concentration of free ammonia can cause a reduction of pH via VFA accumulation (Angelidaki et al., 1993). However, once microorganisms get acclimated to high concentration of free ammonia, anaerobic processes start to function again (Koster and Lettinga, 1988). In addition to pH, working temperature can also influence the anaerobic performance by accelerating the production of free ammonia since the metabolic rate of microorganisms is enhanced under high temperature (Borja et al., 1996a). Interestingly, the presence of other ions including sodium, calcium and magnesium has an antagonistic effect on ammonia inhibition via reducing ammonia toxicity to anaerobic microorganisms (Hendriksen and Ahring, 1991).

The existence of sulphate has also an inhibition effect on anaerobic processes. Sulphate is one of common components of industrial wastewater, and then sulphate is readily reduced to sulphide by sulphate reducing bacteria (SRB) under anaerobic condition (Jan and Barry, 1988). There are two mechanisms to inhibit anaerobic processes: (i) competition of SRB and other anaerobes for common organic and inorganic substrates

(Harada et al., 1994) and (ii) toxicity of sulphide to various bacteria groups (Colleran et al., 1998). During sulphate reduction, SRB reduces lactate to acetate and CO_2, and then reduces acetate to CO_2 and HCO_3^-. Therefore, SRB do not compete with hydrolytic and acidogenic bacteria in the hydrolysis stage since they do not biodegrade natural biopolymers (e.g., glucose, protein and starch). On the other hand, SRB competes with acetogens. Besides, SRB can outcompete hydrogenotrophic methanogens. This is because methanogens cannot compete with SRB for H_2 oxidation, while methanogenesis and sulphate-reduction occur at the same time (Oremland and Taylor, 1978, O'Flaherty and Colleran, 1999). Reduced sulphide may have toxicity to other anaerobes. It is well-known that H_2S is the most toxic form of sulphide. This is because H_2S readily diffuses through the cell membrane and may denature native protein by making the formation of cross-links between sulphide and polypeptide chains (Wood, 1977). To mitigate the effect of sulphate and sulphide on anaerobic processes, two methods are often utilized. The first is to prevent sulphide toxicity by diluting the wastewater stream (Chen et al., 2008) and the second is to reduce sulphate/sulphide concentration by incorporating with sulphate/sulphide removal processes including physicochemical processes (e.g., stripping) and chemical reaction processes (e.g., coagulation and precipitation) (J.W.H et al., 1994, Song et al., 2001).

Light metal ions (i.e., sodium, potassium, calcium and magnesium) with high salt concentration also possibly inhibit anaerobic processes since bacterial cells can be hydrated due to the osmotic pressure difference (Yerkes et al., 1997). At low/moderate concentrations, these ions are beneficial for microbial growth, while excess amounts of ions can slow down the growth rate or cause severe damage to anaerobic bacteria (Soto et al., 1993a). Aluminium can inhibit the anaerobic process by competing iron and manganese which are essential for the bacteria growth or it can adhere on the cell

membrane which results in a reduction of the bacteria growth (Cabirol et al., 2003). Calcium is also an inhibitor even though it is essential for the growth as well as the formation of microbial aggregates (Huang and Pinder, 1995). However, high calcium concentration may lead to scaling formation in the reactor and thus loss of buffer capacity (van Langerak et al., 1998). Potassium at high concentration can lead to a passive influx into cells and neutralize the membrane potential (Jarrell et al., 1984). Moreover, potassium can also extract essential micronutrients such as copper, zinc and nickel and reduce the activity of anaerobic microbes (Ilangovan and Noyola, 1993). Similar to other light metal ions, sodium is one of essential cations at low concentration. However, at high concentration, sodium can influence the activity of microorganisms by interfering with their metabolism (Mendez et al., 1995). Especially, sodium is more toxic to propionic acid-utilizing bacteria rather than acetic acid-utilizing bacteria (Soto et al., 1993b).

Since heavy metals possibly exist in municipal or industrial wastewater, they can be a serious problem in anaerobic processes. They are not biodegradable and thus can be accumulated in microorganisms, which results in disruption of bacterial function and cell structure by binding heavy metals with protein molecules or replacing with other metals (Vallee and Ulmer, 1972, Sterritt and Lester, 1980). Because heavy metals are essential components of the cell, total metal concentration is very important when determining whether heavy metals are inhibitory to anaerobic microorganisms (Zayed and Winter, 2000). Besides, according to chemical forms of heavy metals, their inhibition effects may be varied. Various types of heavy metals exist in wastewater, but only soluble and free form of heavy metals is toxic to microorganisms (Oleszkiewicz and Sharma, 1990). Toxicity-mitigating methods of heavy metals include precipitation, sorption and chelation (Oleszkiewicz and Sharma, 1990). For precipitation, sulphide is well utilized but should be careful due to its inhibitory impact on anaerobic processes (Zayed and Winter, 2000).

Activated carbon and kaolin are used for sorption of heavy metals (Jarrell et al., 1987) and EDTA and PDA are used for chelation by organic ligands (Babich and Stotzky, 1983). In addition to heavy metals, organic compounds in municipal wastewater can be also toxic to microorganisms and inhibit anaerobic processes. The adsorption and accumulation of organics in bacterial membranes may induce the membrane to swell and leak, resulting in the disruption of ion gradients and causing cell lysis eventually (Heipieper et al., 1994). Organic compounds, which are toxic to anaerobic microorganisms, include chlorophenols (Sikkema et al., 1995), halogenated aliphatics (Belay and Daniels, 1987), N-substituted aromatics (Blum and Speece, 1991), LCFAs (Kabara and Vrable, 1977), and lignins and lignin related compounds (Benjamin et al., 1984).

Table 3. Inhibition factors affecting the anaerobic digestion.

Factors		Description	Optimum range	Reference
Ammonia		Free ammonia can freely diffuse into the cell, causing proton imbalance and or potassium deficiency.	Below 200 mg/L	(de Baere et al., 1984, Liu and Sung, 2002)
Sulphide		Competition for common organic and inorganic substrates from SRB. Toxicity of sulphide to various bacteria groups.		(Harada et al., 1994, Jan and Barry, 1988, Colleran et al., 1998)
Heavy metals		Heavy metals can disrupt enzyme function and structure by binding metals with thiol and other groups on protein molecules.		(Vallee and Ulmer, 1972, Jin et al., 1998)
Organics		Organic chemicals can make the membrane swell and leak. - Chlorophenols, Halogenated aliphatics, N-substituted aromatics, LCFAs, Lignins and lignin related compounds		(Renard et al., 1993, van Beelen and van Vlaardingen, 1994, Fang et al., 1995, McCue et al., 2003)
Light metal ions	Aluminium	Aluminium can compete with iron and manganese, or be adhesive to the microbial cell membrane of wall.		(Cabirol et al., 2003)
	Calcium	Calcium is essential for the growth of methanogens, but excessive amounts can lead to precipitation of carbonate and phosphate.	100 ~ 200 mg/L	(van Langerak et al., 1998, Yu et al., 2001)
	Magnesium	High concentration of Mg ions can stimulate the production of single cells.	300 mg/L (Up to 720 mg/L)	(Schmidt and Ahring, 1993)
	Potassium	High potassium concentration can lead to a passive influx of potassium ions that neutralize the membrane potential.	Below 400 mg/L	(Jarrell et al., 1984)
	Sodium	Low concentration of sodium is essential for methanogens.	100 ~ 200 mg/L	(Liu and Boone, 1991)

2.3 Fertilizer-drawn forward osmosis

2.3.1 Forward osmosis

2.3.1.1 Basic concept of forward osmosis

Osmosis is the natural phenomenon that water molecules are transported from FS of higher water chemical potential (i.e., lower solute concentration) to DS of lower water chemical potential (i.e., higher solute concentration) through the semi-permeable membrane (**Fig. 7**). The membrane allows water transport but rejects most of solute molecules or ions. FO utilizes this osmotic pressure differential as the driving force to extract water molecules across the membrane rather than hydraulic pressure differential as used in RO. Therefore, in FO, FS and DS become continuously concentrated and diluted, respectively. On the other hand, solutes are transported from DS to FS across the membrane since solute chemical potential in DS is higher than that in FS. Pressure retarded osmosis (PRO) seems like RO since it applies pressure, but the net water flux is still in the same direction to FO since the driving force in PRO is osmotic pressure gradient through the membrane. Applied pressure just plays a role to retard the water flow across the membrane to make more hydraulic energy for converting chemical energy into electric energy. Compared to RO, FO can be a low energy desalting process with low fouling tendency and high fouling reversibility due to no/low applied hydraulic pressure. Therefore, as shown in **Fig. 8**, the number of studies regarding FO has been rapidly increasing over the past 10 years.

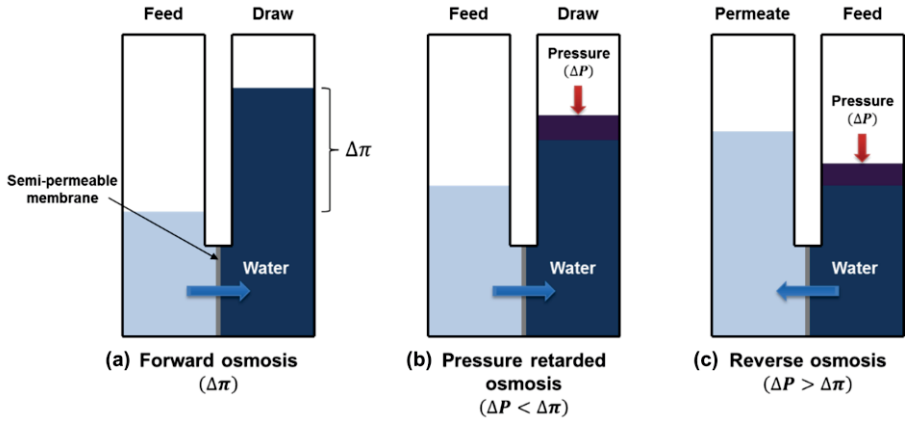

Figure 7. Conceptual description of (a) FO, (b) PRO, and (c) RO. In FO, ΔP is approximately zero and water diffuses to the draw side (i.e., high salinity) of the membrane with the opposite flow direction of draw salts. In PRO, water diffuses to the draw solution under positive pressure (Δπ >ΔP) with the opposite flow direction of draw salts. In RO, water diffuses to the permeate side with the same direction of salt flows due to hydraulic pressure (ΔP >Δπ).

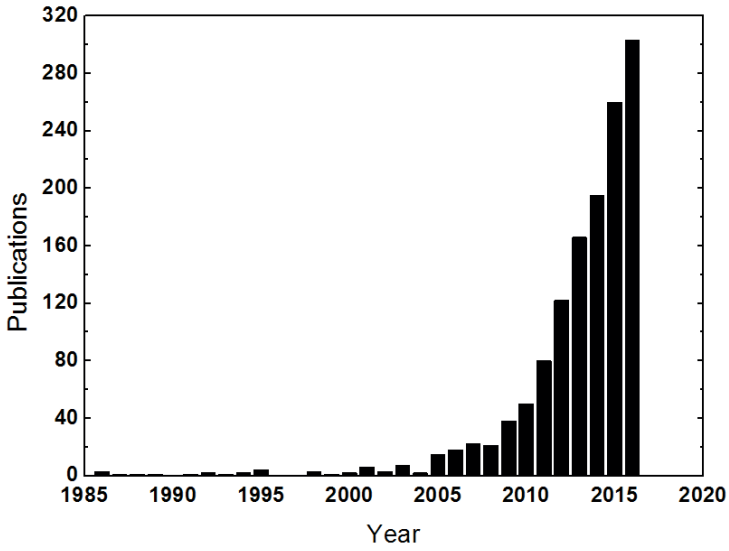

Figure 8. Annual publications of forward osmosis for the past 30 years as searched through Scopus (**http://www.scopus.com/**). The investigation was carried out with the range from 1986 to 2016 by using the keyword "forward osmosis".

2.3.1.2 Concentration polarization in forward osmosis

2.3.1.2.1 External concentration polarization (ECP)

As similar to the pressurized membrane process, concentration polarization (CP) phenomenon occurs in FO since only water molecules pass through the membrane and thus salts are accumulated on the membrane surface (Cath et al., 2006). This is called as external concentration polarization (ECP). In case of a symmetric membrane (**Fig. 9a**), salt concentration increases in the feed side and decreases in the draw side, respectively, since water permeate flows from FS to DS. However, in case of an asymmetric membrane with the active layer facing FS (i.e., FO mode), only concentrative ECP occurs as shown in **Fig. 9b**. On the other hand, in case of an asymmetric membrane with the active layer facing DS (i.e., PRO mode), dilutive ECP happens as shown in **Fig. 9c** since the water flow direction is opposite to that in **Fig. 9b**. This ECP can reduce the driving force by decreasing effective concentration gradient across the active layer of the FO membrane. By improving hydrodynamic properties such as cross-flow velocity, effective concentration gradient can increase and thus water flux can be enhanced. However, in the asymmetric membrane, ECP is not a major factor for the lower-than-expected water flux in FO (McCutcheon and Elimelech, 2006).

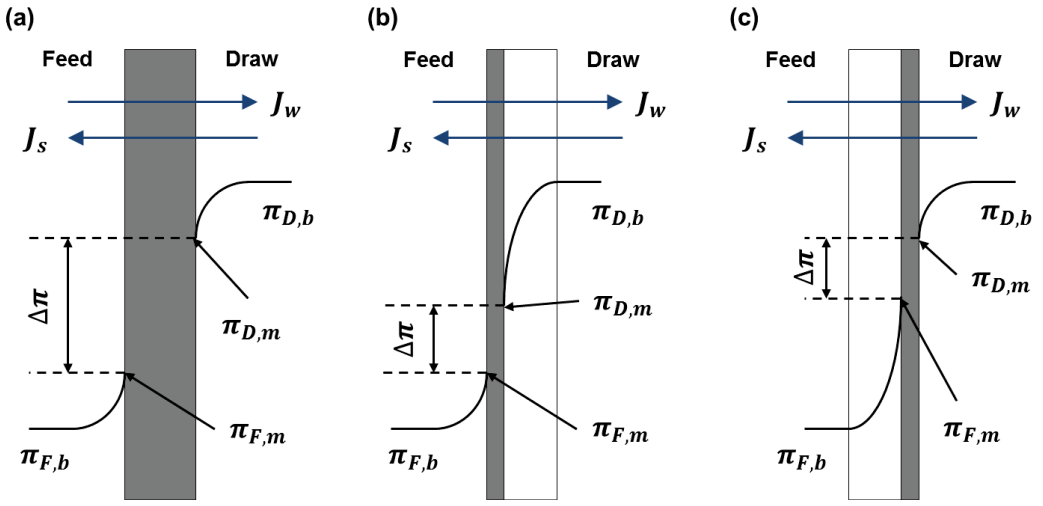

Figure 9. Schematic illustration of concentration profiles: (a) a symmetric dense membrane, (b) an asymmetric membrane with the dense active layer facing feed solution (i.e., FO mode), and (c) an asymmetric membrane with the dense active layer facing draw solution (i.e., PRO mode).

2.3.1.2.2 Internal concentration polarization (ICP)

Since the asymmetric membrane consists of the active layer and the support layer, it exhibits different phenomena compared to the symmetric membrane (McCutcheon and Elimelech, 2006) . The symmetric membrane has both concentrative and dilutive ECPs as shown in **Fig. 9a**, but the asymmetric membrane shows severe CP phenomenon inside the support layer as shown in **Fig. 9b & 9c**. This is called as internal concentration polarization (ICP). In case of **Fig. 9b**, concentration of DS is significantly reduced, so it is referred as diluted ICP. In case of **Fig. 9c**, since concentration becomes concentrated due to the water flux direction, it is referred as concentrative ICP. In the asymmetric membrane, ICP plays more significant role to reduce effective concentration gradient than ECP. Therefore, it should be controlled for enhancing FO performance. Since ICP occurs in the support layer, its structure (i.e., porosity, tortuosity, and thickness) should be

optimized. Many researches have been carried out to optimize the structure of the support layer (Park et al., 2015, Xiao et al., 2015, Yasukawa et al., 2015).

2.3.2 Reverse permeation of draw solute in forward osmosis

FO utilizes highly concentrated DS to induce the osmotic pressure gradient across the active layer as presented in **Fig. 9a**. Thus, draw solutes are readily diffused to FS due to the high concentration gradient between FS and DS in FO (Phillip et al., 2010) unlike RO. Since this reverse diffusion of draw solutes, called as reverse salt flux (RSF), is inevitable in FO, it can seriously affect FO performance. It is well known that RSF contributes to flux decline through accelerated CEOP (cake enhanced osmotic pressure) as shown in **Fig. 10** (Lee et al., 2010). In FO, DS is highly concentrated and thus salt moves from the draw to the feed. The salt is captured by the fouling layer which accelerates CEOP. Thus, the surface concentration of the feed side significantly increases and the permeate flux decreases.

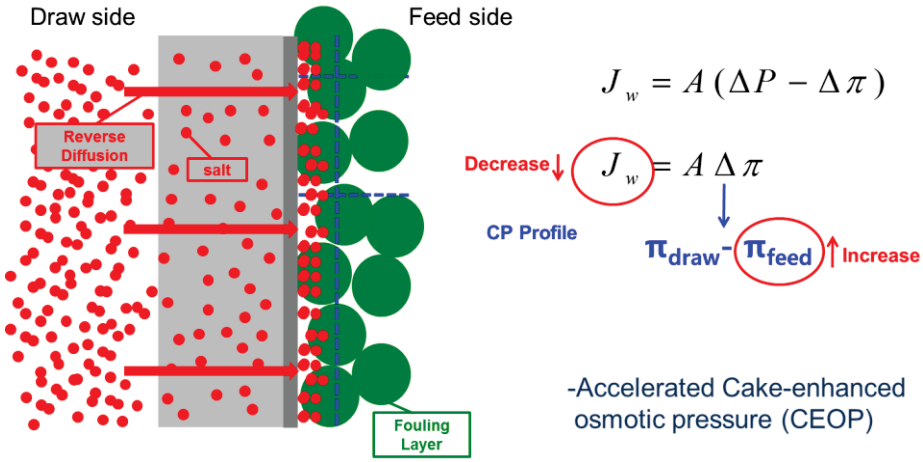

Figure 10. Schematic diagram of accelerated cake-enhanced osmotic pressure (A-CEOP).

In RO, the presence of multivalent cations such as Ca^{2+} or Mg^{2+} in FS can induce severe membrane fouling by making organic-divalent complexes (Hong and Elimelech, 1997). Similarly, in FO, the reverse diffusion of draw solute cations can also promote foulant-membrane and foulant-foulant interactions thereby enhancing membrane fouling (She et al., 2012, Xie et al., 2015a). When examining a variety of inorganic DS (i.e., NaCl, $MgCl_2$, $CaCl_2$ and $Ca(NO_3)_2$), the reverse solute diffusion of draw solute (especially divalent cation) changed the FS chemistry and thus enhanced membrane fouling by alginate, the extent of which is related to the rate of the reverse draw solute diffusion and its ability to interact with the foulant (She et al., 2012). Reverse divalent cation diffusion also severely affected FO biofouling. Reverse Ca^{2+} diffusion led to significantly more serious water flux decline in comparison with reverse Mg^{2+} permeation (Xie et al., 2015a). Unlike magnesium, reverse Ca^{2+} permeation dramatically altered the biofilm architecture and composition, where extracellular polymeric substances (EPS) formed a thicker, denser, and more stable biofilm. This may be because FO biofouling was enhanced by complexation of calcium ions to bacterial EPS.

Similar with RO, in FO, the presence of scaling precursor ions such as Ca^{2+} and PO_4^{3-} on the membrane surface may exceed its solubility limits of inorganic minerals such as $CaCO_3$ (calcite) and $Ca_3(PO_4)_2$ (tricalcium phosphate) (Greenberg et al., 2005), resulting in the formation of scales on the membrane surface thereby reducing the water flux. For efficient recovery of DS in FO, ammonia-carbon dioxide (NH_3-CO_2) was suggested as the novel DS (McCutcheon et al., 2006). HCO^{3-} in the NH_3-CO_2 DS was reversely transported to FS and chemically reacted with Ca^{2+} when NH_3-CO_2 was used as DS to treat the Ca^{2+}-containing FS (Lee and Kim, 2017). Thus, $CaCO_3$ scales were formed on the active layer (**Fig. 11**). In addition to ammonia-carbon dioxide DS, fertilizers were utilized as DS for a fertigation process (Phuntsho et al., 2012a, Phuntsho et al., 2012b).

During treating brackish water by FO with fertilizer DS, severe membrane scaling was observed with di-ammonium phosphate DS (Phuntsho et al., 2014). The concentration of PO_4^{3-} ions and pH of FS were significantly influenced by RSF, and thus struvite scaling occurred on the membrane surface.

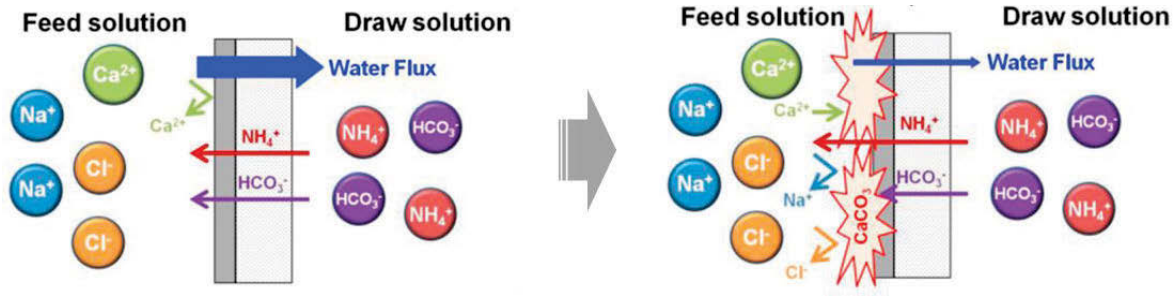

Figure 11. Schematic illustration of the mechanism for $CaCO_3$ scaling formation on the active layer and bidirectional solute transport during the FO experiment using NH_3-CO_2 to treat a Ca^{2+}-containing feed solution (Lee and Kim, 2017).

Recently, OMBR has been spotlighted due to its several advantages including complete rejection of suspended solids, low sludge production, and high organic rejection (Nawaz et al., 2013, Gu et al., 2015, Kim et al., 2016). However, since most of draw solutes consist of inorganics, their reverse transport may be toxic to microbial bacteria in the bioreactor. Nawaz et al. showed that chlorides of calcium and magnesium depicted more support to growth as compared to sodium and potassium. Ammonium bicarbonate solution could only be used with a high aeration intensity in the aerobic OMBR since bicarbonate ions are toxic to microorganisms. Sulphate salts of ammonium, sodium and potassium can potentially be used in the FO-MBR. Nawaz suggested that surfactants are suitable alternatives due to the high molecular weight of micellar aggregates, they exhibit a value for J_s/J_w which is 100–150 times lower than that for inorganic salts, but they should be

used at concentrations above their critical micellar concentration (CMC) (Nawaz et al., 2013). The compatibility of each draw solute with subsequent anaerobic treatment was assessed by BMP analysis to simulate anaerobic FO-MBR. The effect of each draw solute (at concentrations corresponding to RSF at ten-fold pre-concentration of wastewater) on methane production was also evaluated. The results show that ionic organic draw solutes (e.g., sodium acetate) were most suitable for FO application and subsequent anaerobic treatment (Ansari et al., 2015). Mono-ammonium phosphate (MAP) showed the highest biogas production while other fertilizers exhibited an inhibition effect on anaerobic activity with solute accumulation (Kim et al., 2016).

Even though RSF has a negative impact on FO performance, many researchers have tried to utilize FO for the beneficial purpose, for example, the food industry. Petrotos et al. tried to concentrate tomato juice by examining six DS (Petrotos et al., 1998). Sodium chloride brine was found to be the best osmotic medium due to its very low viscosity. The operation parameters also appeared to be of paramount importance regarding the effectiveness of an osmotic medium. Higher osmotic medium concentrations yielded to higher osmotic permeation rates. Increasing the juice temperature was found to markedly increase the permeation flux. However, only a slight enhancement of flux was observed by increasing the juice flow rate. Moreover, higher juice concentrations up to approximately 128 Brix led to a lowering of the osmotic flux. Garcia-Castello investigated FO for concentrating sugar solutions (Garcia-Castello et al., 2009). Using NaCl as a surrogate DS, FO could lead to sucrose concentration factors that far exceed current pressure-driven membrane technologies, such as RO. Water fluxes were found to be lower than those commonly obtained in RO, which is a consequence of the significantly higher concentration factors in conjunction with ICP.

In addition, there is a few studies to apply RSF to treat solution having high scaling potential by using an antiscalant as DS. Gwak et al. proposed Poly (aspartic acid sodium salt) (PAspNa) as a novel DS (Gwak et al., 2015). PAspNa exhibited superiority in high water flux and low RSF in FO. Besides, PAspNa could be readily recovered by both NF and MD. They suggested that the reversely flowed PAspNa in FO could act as an antiscalant. Zhang et al. investigated the effect of RSF on FO scaling as presented in **Fig. 12** (Zhang et al., 2017) . They found out that RSF of scaling precursors (Ca^{2+}, PO_4^{3-}, etc.) can promote severe $Ca_3(PO_4)_2$ scaling, while RSF of anti-scaling agents (i.e., H+, EDTA, etc.) can suppress $Ca_3(PO_4)_2$ scaling.

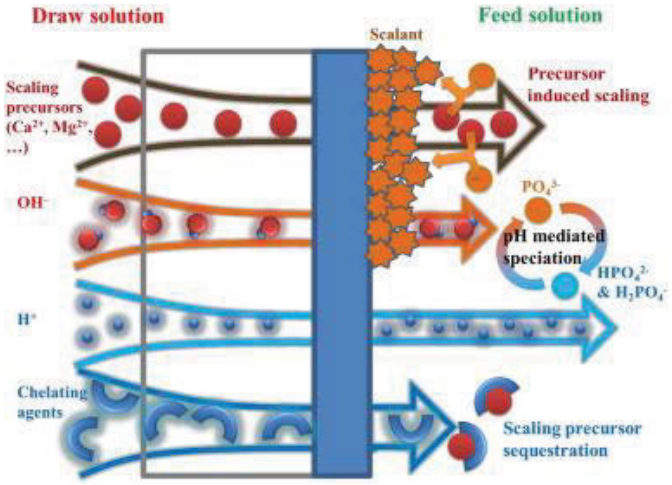

Figure 12. Conceptual diagram illustrating the role of RSF in promoting or reducing scaling in ODMPs (Zhang et al., 2017).

2.3.3 Potential applications of forward osmosis

FO is possibly utilized for several applications such as seawater/brackish water desalination, wastewater treatment, fertigation, and others. For the seawater or brackish water desalination, FO has been investigated as a direct desalination process combined with the DS recovery process or an advanced desalination pre-treatment process. Since

the driving force in FO is osmotic pressure gradient, there is no/low hydraulic pressure unlike NF or RO. As a result, the fouling layer formed on the membrane surface can be readily removed by physical cleaning (Mi and Elimelech, 2010, Lee et al., 2010, Kim et al., 2014c). Thus, many studies have focused on the recovery of DS with high or stable FO performance. NH_4HCO_3 DS was proposed for FO desalination by McCutcheon et al. since it can be efficiently recovered by simple heating with quite low temperature and easily re-generated as DS as shown in **Fig. 13a** (McCutcheon et al., 2005, McCutcheon et al., 2006, McGinnis and Elimelech, 2007). Specific energy consumption of this hybrid system was significantly lower than other thermal distillation methods with high water recovery rate but water quality does not meet the WHO standard for ammonia. In addition, the FO-MSF or MED hybrid process (**Fig. 13b**) was also evaluated with concentrated brine as DS. Simulation results demonstrated that FO could completely remove divalent ions from FS which mitigates the scaling on the surface of heat exchangers. FO-MED system was less energy intensive and had greater recovery rate compared to FO-MSF. As presented in **Fig. 13c**, MD could be also combined with FO to effectively recover diluted DS (Yen et al., 2010, Guo et al., 2014, Lee et al., 2015, Gwak et al., 2015). FO successfully achieved not only recovery rate of more than 90% but also high quality product water (Li et al., 2014). However, TrOCs could migrate across FO membrane and accumulate in DS but when system was coupled with GAC and UV, it could remove more than 99.5% of TrOCs (Xie et al., 2013a). Besides, when treating oily wastewater, acetic acid concentration increased in DS which decreased its osmotic pressure (Zhang et al., 2014).

FO desalination was investigated with recovering DS by NF or RO as presented in **Fig. 13d**. With glucose DS, water recovery was limited due to the low osmotic efficiency of glucose which also created high ICP effect due to its large molecular weight. When

recovering various organic and inorganic DS by NF, high salt rejection (i.e. up to 97.9% for NF process) and good quality product water (i.e. meeting the drinking water total dissolved solids (TDS) standard) could be achieved due to a multiple barrier (Tan and Ng, 2010). Compared to standalone RO process, the FO-NF hybrid process exhibited lower operating pressure, less flux decline due to membrane fouling, higher flux recovery after cleaning, higher quality of product water (Zhao et al., 2012).

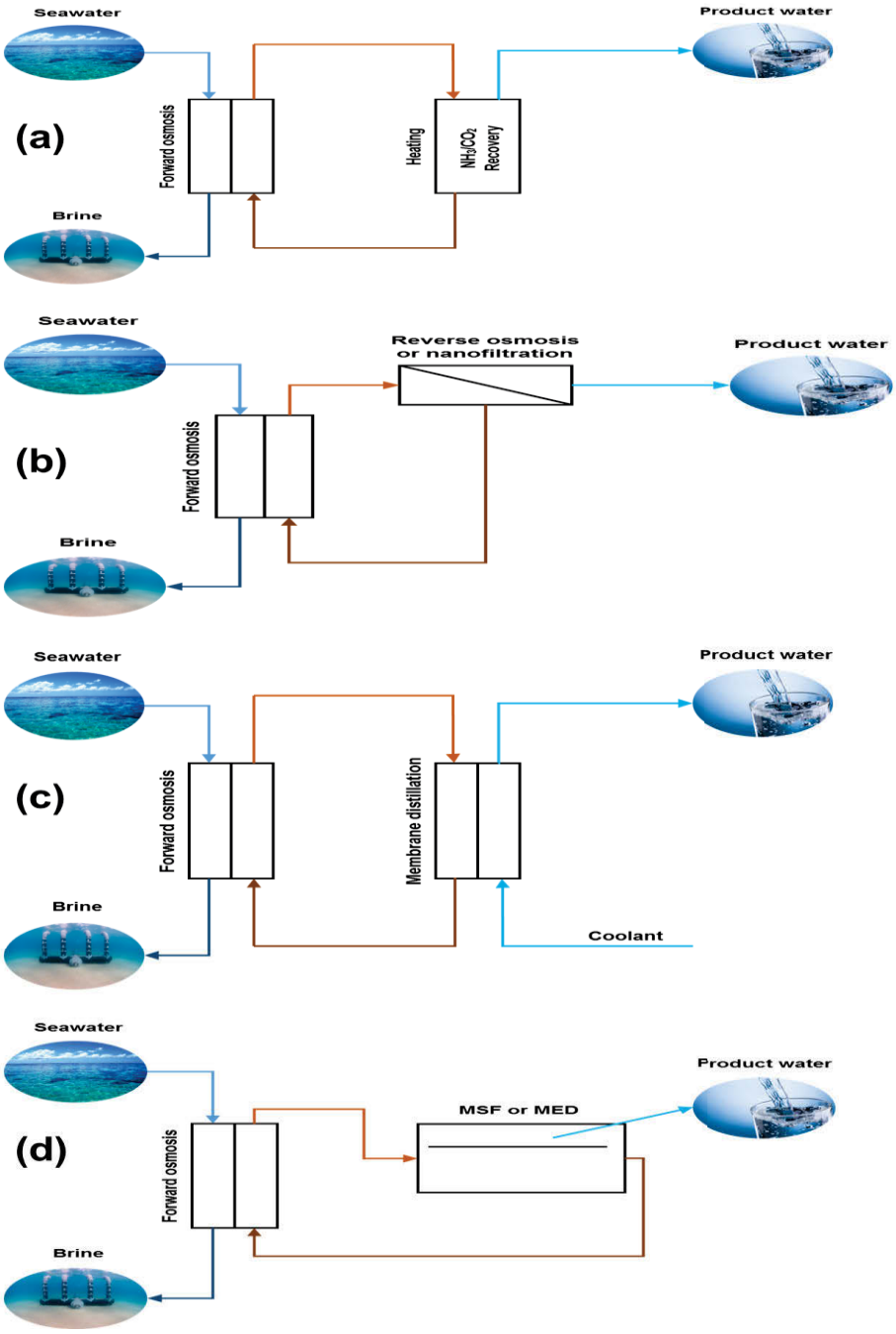

Figure 13. Schematic diagram of the FO hybrid process combined with (a) heating for NH3/CO2 draw solution recovery, (b) MSF or MED, (c) membrane distillation, and (d) reverse osmosis or nanofiltration.

As described above, many researchers tried to use FO as an advanced pre-treatment process instead of direct treatment of seawater or brackish water (Chekli et al., 2012,

Chekli et al., 2016). Yaeli firstly suggested the FO hybrid system as an alternative to standalone RO which suffered from high fouling tendency (Yaeli, 1992). Here, FO was used as a pre-treatment to reduce the fouling propensity of feedwater in the subsequent RO process. In the hybrid FO–RO system, FO effectively operates as a pre-treatment for RO by rejecting a wide range of contaminants helping to mitigate membrane fouling and scaling in the RO process (Hancock et al., 2011). In fact, FO used as a pre-treatment was found to enhance the performance of conventional desalination technologies (e.g. RO) and can surpass the current pre-treatment technologies that are currently not designed to remove dissolved solids (Greenlee et al., 2009). The benefit of FO pre-treatment to remove dissolved solids can also assist RO in meeting the demanding drinking water quality standards. In fact, there are two types of dissolved contaminants for which RO process does not demonstrate total rejection and which present a health risk even at trace levels: TrOCs and boron. In a recent review article on the performance of FO membranes in rejecting TrOCs (Coday et al., 2014), it was explained that the hybrid FO–RO system demonstrates significantly high TrOCs rejection (i.e. more than 99%) due to the dual barrier provided by both membrane processes. Besides, it was also demonstrated that FO alone can achieve higher rejection of TrOCs than RO process (Xie et al., 2012a). Similarly, in a recent bench-scale study (Kim et al., 2012), FO showed higher boron rejection than RO mainly due to RSF in FO that likely reduced boron flux. In fact, the diffusion of boron through the FO membrane was found to be inversely related to the extent of reverse draw salt diffusion. In another study (Shaffer et al., 2012), simulation results showed that boron removal through the hybrid FO–RO desalination system can be more energy efficient than the conventional two-pass RO process. However, it was also emphasised that the rejection of these contaminants may ultimately result in their accumulation in the DS when a closed-loop system is used (i.e. when RO is simultaneously used to produce high

quality water and recover the DS) (D'Haese et al., 2013, Xie et al., 2013a). This will likely lead to the contamination of the product water and therefore additional methods need to be developed to reduce cumulative contaminant accumulation.

For wastewater treatment, MBR, which is composed of low-pressure membrane processes such as MF or UF, has been recently getting an increased attention. This is mainly due to its higher and consistent effluent quality compared with conventional treatment processes (Arévalo et al., 2009). However, one of the main limitation of MF and UF membranes is the poor rejection rate of low molecular weight constituents such as TrOCs, ions and viruses (Ottoson et al., 2006). Besides, the energy demand of MBR is higher than conventional wastewater treatment, especially due to the need to apply pressure as well as due to membrane fouling with both MF/UF membranes and RO membranes caused by the presence of natural organic matter and biofouling (Cornelissen et al., 2008).

To circumvent these limitations, many recent studies investigated the potential of FO membranes as an alternative to MF and UF in MBR. This osmotic MBR (OMBR) depicted in **Fig. 14** provides an ideal multi-barrier protection which can be used for indirect or direct potable reuse applications (Cornelissen et al., 2008, Alturki et al., 2012). In fact, the main advantages of integrating FO membranes into bioreactors instead of conventional low-pressure membrane processes are their lower energy consumption (driving force is generated by the osmotic pressure of the DS), their lower membrane fouling propensity and higher rejection of macromolecules, ions and TrOCs from the wastewater (Hancock et al., 2011, Valladares Linares et al., 2011, Hancock et al., 2013). Usually, a high salinity DS such a concentrated NaCl or pre-treated seawater is used and in some studies, RO has been integrated into the hybrid OMBR system to re-concentrate the diluted DS and produce ultrapure water (Achilli et al., 2009, Bowden et al., 2012).

Despite the several advantages and applications of OMBRs, several studies have identified that one of the major limitations of this hybrid system is the cumulative accumulation of dissolved solutes in the feed stream and other dissolved constituents inside the reactor as they are highly rejected by the FO membrane (Achilli et al., 2009, Lay et al., 2011, Zhang et al., 2012). Accumulation of draw solutes in the bioreactor also occurs due to the reverse diffusion of draw solutes to the bioreactor through the FO membrane. These generally result in lowering the osmotic pressure difference (or driving force) across the FO membrane and thus lowering the water flux as well as affecting the microbial activity inside the bioreactor at elevated solute dissolved concentration (Ye et al., 2009). Some recent studies (Xiao et al., 2011, Bowden et al., 2012, Kim et al., 2016) have proposed salt accumulation models and their results showed that the solids retention time (SRT) is the main factor responsible for the steady state salt concentration in the reactor. A short SRT may therefore contribute to a reduction in the salts concentration in the bioreactor. However, this will also limit the biological nitrogen removal and reduce the water recovery (Ersu et al., 2010).

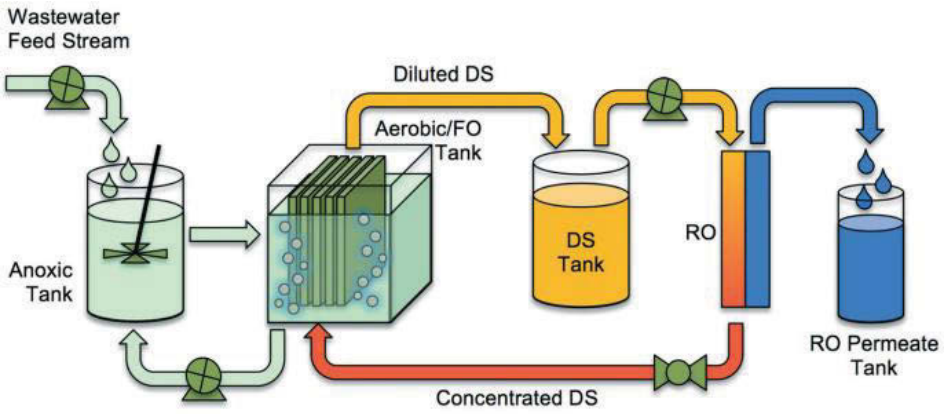

Figure 14. A schematic of an integrated OMBR system containing an FO MBR and RO system for reconcentration of draw solution (Holloway et al., 2015).

2.3.4 Fertilizer-drawn forward osmosis

For the agricultural application, the concept of FDFO was initially proposed by Moody (Moody, 1977). Recently, Phuntsho et al. designed the detail concept of FDFO (**Fig. 15a**) for direct fertigation and systematically investigated the possibility of FDFO in terms of FO performance (i.e., water flux, RSF, and reverse salt flux selectivity (RSFS)) for brackish groundwater and seawater as target feedwater (Phuntsho et al., 2011). They found out that potassium chloride is the best draw solute among screened fertilizer chemicals in terms of the performance ratio as well as water flux. However, in terms of RSF, the ammonium compounds of sulphate and phosphate, and $Ca(NO_3)_2$ containing divalent anions were most suitable for FO due to low RSF. This study has a limitation that only single fertilizers were evaluated since mixture of nutrients is utilized for fertigation in reality. In addition, during brackish water treatment by FDFO, Phuntsho et al. also found that some fertilizers could cause severe membrane scaling due to the existence of scaling precursors such as PO_4^{3-}, Ca^{2+} and Mg^{2+} (Phuntsho et al., 2014).

To meet the water quality requirements for direct fertigation, blended fertilizers were investigated and compared with single fertilizers (Phuntsho et al., 2012b). In this study, loss of nutrients by RSF and final nutrient concentration in FO when using single fertilizers and blended fertilizers were investigated. Based on these experiments, final nutrient concentrations using the blended fertilizer (i.e., $NaNO_3$, $(NH_4)_2SO_4$, KCl, and MKP) as DS were calculated and compared with recommended concentrations for target plants. This study demonstrated that the final nutrient concentration in FDFO could be significantly decreased by using the blended fertilizers. However, reducing the final nutrient concentration for direct fertigation still remains a challenge because of the limitations offered by the osmotic equilibrium, especially when using high salinity feedwater.

Phuntsho et al. has suggested NF as either pre-treatment to reduce TDS or post-treatment for partial recovery of draw solutes for further recycling and reuse in the processes reducing the nutrient concentration and making diluted acceptable for direct fertigation (Phuntsho et al., 2013a). NF as pre-treatment (**Fig. 15b**) could significantly reduce the feed concentration and achieve target nutrient concentrations by enhancing the water extraction capacity of fertilizers. NF as post-treatment (**Fig. 15c**) could reduce the final nutrient concentrations in the final produced water due to high rejection of multivalent ions by NF. Both hybrid processes are acceptable for direct fertigation, but NF post-treatment could be more useful in terms of process efficiency and energy consumption (i.e., low fouling potential). Altaee et al. suggested that a dual-staged low-pressure RO is effective for regenerating diluted DS as well as producing suitable fertilizer solution (Altaee et al., 2016).

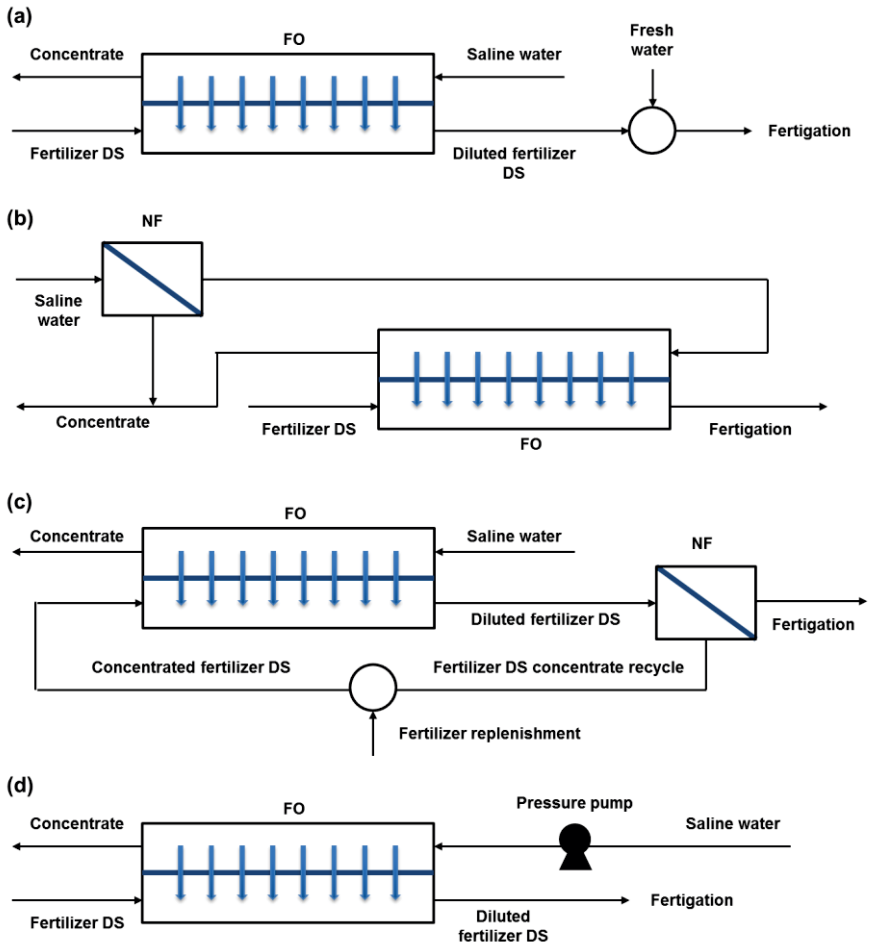

Figure 15. The conceptual illustration of (a) fertilizer-drawn forward osmosis (Phuntsho et al., 2011), (b) fertilizer-drawn forward osmosis combined with nanofiltration as pre-treatment (Phuntsho et al., 2013a) (c) fertilizer-drawn forward osmosis combined with nanofiltration as post-treatment, and (d) pressure-assisted fertilizer-drawn forward osmosis (Sahebi et al., 2015).

A concept of the FDFO and NF hybrid process has been evaluated and demonstrated in a pilot-scale system for direct fertigation (Kim et al., 2013, Phuntsho et al., 2016). Kim et al. firstly studied a NF system as post-treatment of diluted fertilizer DS from FDFO by using ammonium sulphate (SOA) DS. In this study, feed concentration exhibited more significant impact on the specific water flux and N rejection even though operation factors

(i.e., applied pressure and cross-flow rates) played a certain role in the performance of the pilot-scale NF process (Kim et al., 2013). Furthermore, a pilot-scale 8040 FO membrane module was investigated for brackish groundwater desalination by FDFO with SOA DS under different operation conditions (i.e., feed flow rates, feed salinity, DS concentrations) (Kim et al., 2015b). Phuntsho et al. operated a pilot-scale FDFO and NF hybrid system for 6 months by using saline coalmine water as FS in the field. Results showed that FDFO could be stably operated for treating saline coalmine water and diluting SOA DS with efficient water flux recovery by physical cleaning (Phuntsho et al., 2016). Besides, water quality from the FDFO-NF system meets standard for fertigation. Results imply that high selectivity FO membrane is essential for reducing salt diffusion on both feed and draw sides.

To enhance water flux and recovery rate in FDFO, hydraulic pressure (Sahebi et al., 2015) as well as osmotic pressure was applied as the driving force (**Fig. 15d**). The effect of applied pressure on the water flux and RSF was significantly investigated. Results showed that the additional water flux by the applied pressure could dilute DS beyond the point of osmotic equilibrium making the PAFDFO process potential for application as a standalone process without the need of additional post-treatment process such as NF to reduce the final fertilizer concentration to acceptable level for direct fertigation. Besides, Altaee et al. suggested that PAFDFO is more energy efficient process than simple FDFO (Altaee et al., 2016).

Since single or blended reagent grade fertilizer chemicals were examined for FDFO studies, the performance of FDFO desalination might be different when using commercial liquid/solid fertilizers. Xie et al. investigated the commercial liquid fertilizers as DS in FDFO for the osmotic dilution of wastewater for fertigation of green walls and suggested that FDFO with commercial liquid fertilizers could meet greenwall nutrient requirement,

thereby sustaining the greenwall irrigation process. (Xie et al., 2015b). Moreover, when treating wastewater by FDFO, energy consumption was evaluated with commercial liquid fertilizer DS. Results showed that a higher initial DS caused lower energy consumption while the primary effluent induced higher energy demand due to a significant reduction in water flux (Xiang et al., 2017). In addition, there was a try to develop a new fertilizer DS suitable for FDFO. Duan et al. proposed sodium lignin sulfonate (NaLS) as DS since NaLS could generate high osmotic pressure as well as reasonable performance in FDFO (Duan et al., 2014).

2.4 Conclusions

In this chapter, the recent development of AnMBR and FO (especially, FDFO) was comprehensively reviewed. Previous studies demonstrated that AnMBR is a very promising technology in terms of wastewater treatment and bio-energy production. However, they also indicated that AnMBR is very sensitive to operating factors (e.g., pH, temperature, OLR, and pressure) and feed composition (e.g., ammonia, heavy metals, organics and sulphide). Thus, it is concluded that AnMBR should be very carefully operated to avoid its failure. Many researches on FO have been carried out due to its low energy requirement and high fouling reversibility. They found out that FO can successfully treat various water resources including seawater, brackish water, municipal and industrial wastewaters, and shale gas produced water even though they have high fouling potential. However, the FO operation is limited due to the requirement of DS recovery. Besides, the existence of reverse diffusion of draw solute often has a negative effect on membrane fouling. FDFO has been spotlighted since it does not require the DS recovery. However, FDFO also has similar problems such as RSF. Consequently, the

combination of AnMBR and FDFO may have many obstacles to overcome and should be investigated with a focus on the impact of FDFO on AnMBR.

3. Evaluation of fertilizer-drawn forward osmosis for sustainable agriculture and water reuse in arid regions

3.1 Introduction

Freshwater resources are getting scarcer, particularly in arid, semi-arid and coastal areas, while agricultural sector consumes about 70% of the accessible freshwater with about 15-35% of water being used unsustainably (Assessment, 2005, Clay, 2013). In arid regions, the development of agriculture is not only hindered by the limited freshwater resources but also by the scarcity of fertile lands. Hydroponics is a subset of hydroculture with several advantages over conventional soil culture. In fact, it is a soilless process using synthetic mineral solution to grow crops (Jensen, 1997). As such, it eliminates the problems associated with soil culture; i.e. poor soil culture, poor drainage, soil pollution and soil-borne pathogens. Therefore, hydroponics has been widely used in commercial greenhouse vegetable production around the world. However, hydroponics requires a nutrient solution to fertilize the plants under a controlled environment (e.g., concentration, flow rate, temperature). As a result, this process also consumes a large amount of fresh water to prepare the fertilizer solution. This water-food nexus is becoming a critical issue in most arid regions and therefore, sustainable solutions to assure water and food security must be explored.

Recently, increased consideration has been given to the concept of FDFO. In fact, the novelty of the concept relies on the low-energy osmotic dilution of the fertilizer DS which can then be applied directly for irrigation since it contains the essential nutrients required for plant growth. Although early studies on FDFO (Phuntsho et al., 2011, Phuntsho et al., 2012a) demonstrated that most fertilizers can be suitable DS, the limit posed by the osmotic equilibrium between FS and DS will dictate the final nutrient concentration,

which, in most cases, was found to exceed the standards for irrigation. This means that the final DS still requires additional dilution which is not acceptable, especially in the context of freshwater scarcity. To circumvent this issue, NF was proposed as pre or post-treatment for FDFO with the aim of reducing the nutrient concentration in the final product water (Phuntsho et al., 2013a). Results from this study showed that the product water was suitable for direct application when NF was used as post-treatment and when brackish water with low TDS (i.e. < 4000 mg/L) was employed as FS. However, the use of an additional process will increase the energy consumption of the system and thus the final cost of produced water especially because NF is a pressure-driven membrane process. Recently, PAFDFO was tested as an alternative solution to eliminate the need for NF post-treatment (Sahebi et al., 2015). Pressure-assisted osmosis (PAO) used an additional hydraulic driving force to simultaneously enhance the water flux and dilute the DS beyond the point of osmotic equilibrium. In this study, it was concluded that the use of PAO instead of NF can further dilute the fertilizer DS, thereby producing permeate water that meets the acceptable nutrient concentrations for direct fertigation.

To date, all FDFO studies have either used brackish water (Phuntsho et al., 2013a, Phuntsho et al., 2014, Raval and Koradiya, 2016), treated coalmine water with a TDS of about 2.5 g/L (Phuntsho et al., 2016) or seawater (Phuntsho et al., 2011, Phuntsho et al., 2012b, Phuntsho et al., 2012a, Phuntsho et al., 2013b) as the FS. However, the relatively low salinity of most impaired waters makes them potentially suitable candidate for such dilution (Lew et al., 2005). Besides, drawing the water from impaired sources to produce nutrient solution for hydroponic culture seems a very promising and sustainable approach to solve the freshwater scarcity issue in most arid regions. This concept can be further extended if the concentrated impaired water from FDFO is sent to AnMBR for additional treatment and biogas production to supply energy to the hybrid process.

The main objective of this study is therefore to evaluate the potential of FDFO process for simultaneous water reuse and sustainable agriculture. The optimum recovery rate for feeding the AnMBR process will be first determined through BMP measurements. Then, bench-scale FO experiments will be carried out to optimize the fertilizer formula and process configuration in order to simultaneously achieve the optimum recovery rate and favourable nutrient supply for hydroponics.

This chapter is an extension of the research article published by the author in Journal of Environmental Management.

3.2 Experiments

3.2.1 FO membrane and draw solutions

The FO membrane used in this study was a commercial TFC PA FO membrane (Toray Industry Inc.). The properties (i.e., water & salt permeability coefficients and structural parameter) of the FO membrane are 2.07 L/m2/h/bar, 0.49 kg/m2/h and 204 μm, respectively. This membrane has All chemical fertilizers used in this study were reagent grade (Sigma Aldrich, Australia). DS were prepared by dissolving fertilizer chemicals in DI water. Detail information of fertilizer chemicals are provided in **Table 4**. Osmotic pressure and diffusivity were obtained by OLI Stream Analyzer 3.1 (OLI System Inc., Morris Plains, NJ, USA).

Table 4. Properties of the fertilizer solutions used in this study. Thermodynamic properties were determined at 1 M concentration and 25 ºC by using OLI Stream Analyzer 3.2.

Chemicals	Formula	Molecular weight (g/mole)	Osmotic pressure (atm)	Diffusivity (10^{-9} m^2/s)
Ammonium nitrate	NH_4NO_3	80.04	33.7	1.65
Ammonium sulphate (SOA)	$(NH_4)_2SO_4$	132.1	46.1	1.14
Ammonium chloride	NH_4Cl	53.5	43.5	1.85
Calcium nitrate (CAN)	$Ca(NO_3)_2$	164.1	48.8	1.01
Potassium chloride	KCl	74.6	44	1.79
Ammonium phosphate monobasic (MAP)	$NH_4H_2PO_4$	115.0	43.8	1.06
Ammonium phosphate dibasic (DAP)	$(NH_4)_2HPO_4$	132.1	50.6	0.912
Potassium nitrate	KNO_3	101.1	37.2	1.78
Potassium phosphate monobasic (MKP)	KH_2PO_4	136.09	36.5	1.02

3.2.2 Bio-methane potential experiments

The BMP experiment was carried out using the BMP apparatus described in our previous study (Kim et al., 2016) to investigate the effect of water recovery in the FO process on the performance of the post-AnMBR process. The BMP apparatus consisted of 6 fermentation bottles submerged in a water bath connected to a temperature control device to maintain a temperature of 35±1 ºC. These bottles were connected to an array of inverted 1,000 mL plastic mass cylinders submerged in the water bath filled with 1 M NaOH solution to collect and measure the biogas (**Fig. 16**). The NaOH solution plays an important role to sequester both CO_2 and H_2S to evaluate only CH_4 production potential.

Air volume in each mass cylinder was recorded twice a day. Detailed description of BMP apparatus used in this study is given elsewhere (Nghiem et al., 2014, Ansari et al., 2015).

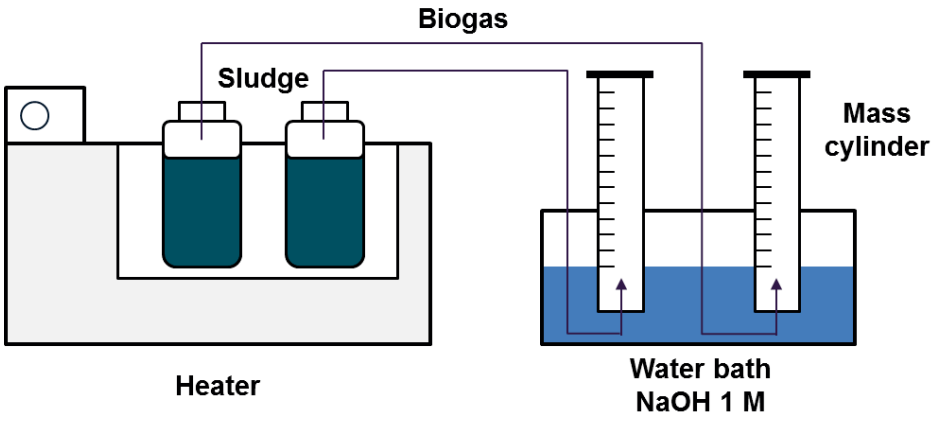

Figure 16. Schematic diagram of bio-methane potential apparatus.

Six different recovery rates were tested in this study (i.e. 0%, 20%, 40%, 60%, 80% and 95%) and the concentrated synthetic wastewater was prepared accordingly. 50 mL of each solution was then mixed with 700 mL of digested sludge. All bottles were purged with nitrogen gas, and connected to the biogas collecting equipment. The BMP experiment was carried out until the methane production stopped.

3.2.3 Bench-scale FO system

The performance of the FO process was conducted in a closed-loop bench-scale FO system (**Fig. 17**) in which detailed characteristics can be found elsewhere (Lee et al., 2010, Kim et al., 2015c). This lab-scale FO unit has an effective membrane area of 20.02 cm^2 with a channel dimension of 77 mm long, 26 mm wide, and 3 mm deep. The FO cell had two symmetric channels on both sides of the membrane for co-current flows of FS and DS. Variable speed gear pumps (Cole-Parmer, USA) were used to pump the liquid in a

closed loop. The DS tank was placed on a digital scale and the weight changes were measured by a computer in real time to determine water flux. Conductivity and pH meters (HaCH, Germany) were connected to a computer to monitor RSF of draw solutes in the FS tank.

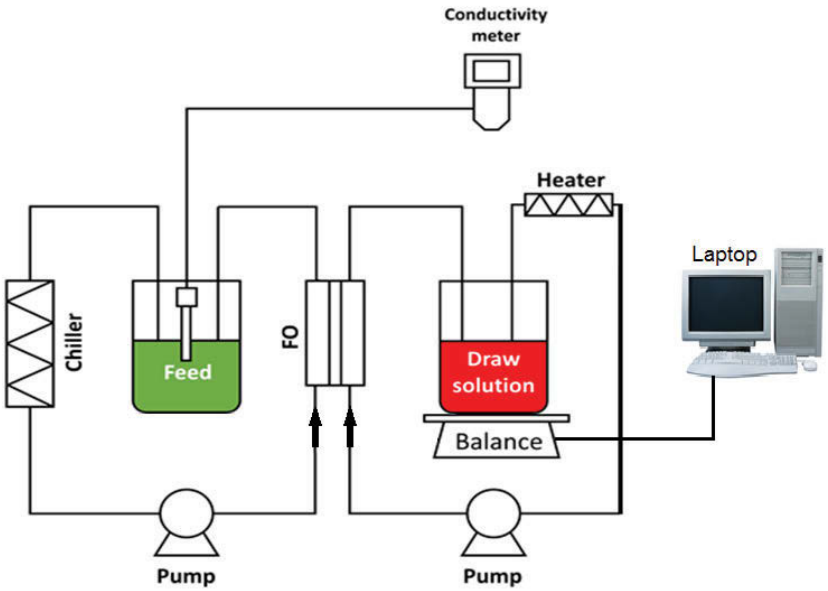

Figure 17. Schematic of the bench scale FO setup used in this study. The FO cell has two symmetric channels on both sides of the membrane for co-current flows of feed and draw solutions.

FO experiments were conducted in the FO mode where the active layer is facing the FS. Before each performance experiment, the FO membrane was stabilized for 30 mins with DI water as FS and fertilizer solution as DS. Once stabilized, the water flux was measured continuously throughout the experiment with a 3 mins time interval. All experiments were conducted at a cross-flow velocity of 8.5 cm/s, and a constant temperature of 25 ºC.

3.2.3.1 Short-term FO performance experiments – Initial Screening

The performance of each fertilizer (**Table 4**) as DS was assessed with either DI water (for RSF experiments) or with synthetic wastewater simulating municipal wastewater (**Table 5**) as FS. In all experiments, a concentration of 1M was used for each fertilizer DS, unless otherwise stated. For the RSF experiment, the FS was collected after 2 h operation and RSF was determined by analysing the components of each tested DS. The experiments, using synthetic wastewater as FS, were carried out for one day (i.e. 24 h) during which the water flux was measured continuously (i.e. one measurement every three mins). At the end of the experiments, the final recovery rate and nutrient(s) concentration were calculated. The water flux, RSF, recovery rate and final nutrient composition were used to determine the optimum fertilizers to carry out long-term experiments (i.e. four days). The effect of DS concentration was also investigated by running experiments at 2M fertilizer DS concentration. Finally, this study also evaluate the performance of selected blended fertilizers (based on (Phuntsho et al., 2012b)) at 1M:1M ratio.

Table 5. Composition and characteristics of the synthetic wastewater used in this study (Chen et al., 2014b).

Parameters	Value
Glucose (mg/L)	275
Peptone (mg/L)	100
Beef extract (mg/L)	100
Urea (mg/L)	10
$NaHCO_3$ (mg/L)	100
KH_2PO_4 (mg/L)	20
NH_4Cl (mg/L)	25
$MgCl_2 \cdot 6H_20$ (mg/L)	10
$CaCl_2 \cdot 2H_20$ (mg/L)	5
pH	6.58
EC (mS/cm)	0.226
TOC (mg/L)	175.6
Osmotic Pressure (bar)*	0.14

*The osmotic pressure was calculated using ROSA software (Version 9.1, Filmtech Dow Chemicals, USA).

3.2.3.2 Long term FO performance experiments

Long-term experiments were carried out with the optimum DS selected during the first stage screening and synthetic wastewater as FS. These experiments were run for four days

during which the water flux was monitored continuously. At the end of the experiment, the final recovery rate and nutrients concentration were calculated.

A new FO membrane was used for each experiment, and the initial baseline flux of the virgin membrane was obtained using 1M NaCl as DS and DI water as FS under the operating conditions described earlier (i.e. cross-flow velocity of 8.5 cm/s, and a constant temperature of 25 ºC). At the end of the long-term experiments, physical membrane cleaning was performed to evaluate the water flux recovery. The DS and FS were replaced with DI water, and the FO process was operated at triple cross-flow rate (i.e. 1,200 mL/min) for 15 mins. Following this physical cleaning, the flux recovery was assessed by measuring the flux under the same conditions as the baseline experiment (i.e. 1M NaCl as DS and DI water as FS). The percentage ratio of the recovered flux after cleaning to initial virgin baseline flux (normalised) was assessed as the water flux recovery.

3.3 Results and discussion

3.3.1 Bio-methane potential measurements

BMP measurements were carried out for 11 days to determine the effect of water recovery/osmotic concentration of wastewater in FDFO on the anaerobic biological process. **Fig. 18a** shows the influence of water recovery achieved in FDFO on biogas production by activated sludge. It is clear from these results that biogas production increased with increasing recovery rate. In fact, 95% water recovery showed the highest cumulative biogas production, almost three times higher than the results obtained with 80% water recovery. It has been demonstrated previously that municipal wastewater usually needs to be concentrated five to ten times before reaching an acceptable level, in terms of COD, for subsequent anaerobic treatment and energy recovery via biogas

production (Verstraete and Vlaeminck, 2011, Burn et al., 2014). Results in **Fig. 18b** confirmed that there is a strong (i.e. $R^2 = 0.9953$) linear correlation between the final volume of biogas produced and the COD in wastewater. For example, from 0% water recovery to 20% recovery, the increase in COD value is not very significant (i.e. from 390 mg/L to 487.5 mg/L) which explains the very low biogas production for these two samples. However, from 0% water recovery to 40% water recovery, the COD in the concentrated wastewater increases by 1.7 times and similarly the final volume of biogas produced increases by 1.8 times. Therefore the COD contribution is crucial to promote a fast and adequate rate of methane production as it was already demonstrated in previous research (Grobicki and Stuckey, 1989, Ansari et al., 2015). For these reasons, 95% was chosen as the optimum recovery rate to achieve for the wastewater via osmotic concentration in FDFO. It is interesting to note that the biogas production per COD removal (i.e., 0.92 L/g COD for 0% to 0.7 L/g COD for 95%) was very similar regardless of recovery rate. However, the biogas production per COD removal was lowest at 95% since too high organic loading can accumulate acid and influence fermentation.

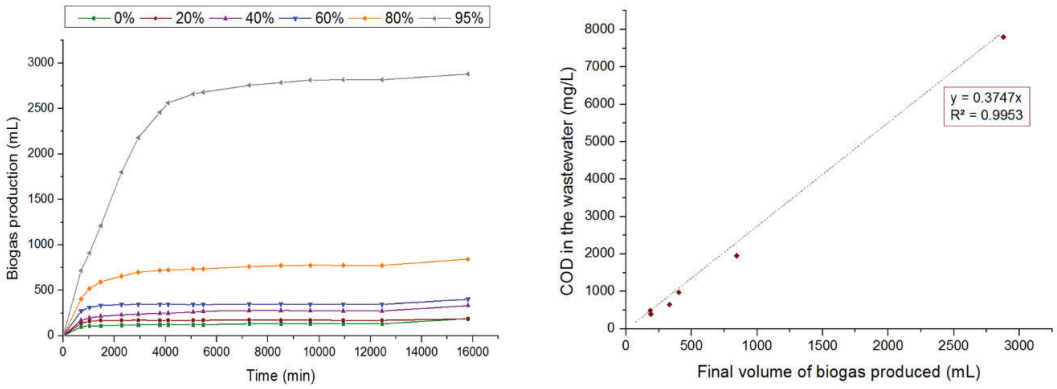

Figure 18. (a) Influence of water recovery in FDFO on biogas (i.e. methane) production by activated sludge and (b) relationship between the COD in wastewater and the final volume of biogas produced.

3.3.2 Performance of single fertilizers as draw solution

3.3.2.1 Water flux, water recovery and reverse salt flux

The performance of single fertilizers was initially evaluated in terms of water flux, water recovery and RSF; three essential criteria for agriculture and water reuse applications. In fact, a high water flux is desirable for the economic viability of the process since it will affect the total membrane area and thus the capital cost. Then, a high water recovery/wastewater concentration (i.e. target of 95% as discussed in the previous section) will ensure optimum biogas production in the subsequent AnMBR process and also help in achieving the required final nutrient concentration in the diluted DS. Finally, low RSF is preferable since the accumulation of DS in the feed water due to its reverse movement can have detrimental effect on the anaerobic microbial activity in the post-AnMBR process (Ansari et al., 2015). Based on those criteria and previous studies on FDFO (Phuntsho et al., 2011, Phuntsho et al., 2012b), nine different fertilizers were selected for this study. The thermodynamic properties of the selected DS are gathered in **Table 4** and

were determined using OLI Stream Analyzer 3.2 (OLI System Inc., Morris Plains, NJ, USA). Diammonium phosphate (DAP) showed the highest osmotic pressure (i.e. 50.6 atm) followed by $Ca(NO_3)_2$ and ammonium sulphate (SOA) while NH_4Cl has the highest diffusivity ($1.85\times10^{-9}\ m^2/s$) followed by KCl and KNO_3. The performance tests were carried out for one day (i.e. 24 h) using synthetic wastewater (cf. **Table 5**) or DI water as FS under similar operating conditions at 1M DS concentration and the results are gathered in **Table 6**.

Table 6. Performance of single fertilizers as draw solution in FDFO using synthetic wastewater and DI water as feed.

		Synthetic wastewater as feed solution				DI water as feed solution				
Fertilizers	**Osmotic pressure at 1M (bar)**	**Initial flux (LMH)**	**Final flux (LMH)**	**Flux decline (%)**	**Recovery rate (%)**	**RSF (gMH)**	**RSFS (L/g)**	**Nutrient loss by RSF (mg/L)**		
								N	**P**	**K**
NH_4NO_3	33.7	17.1	9.7	43.2	32.9	14.6	1.169	714.5	-	-
KNO_3	37.7	18.6	8.3	55.4	33.7	24.5	0.760	255.8	-	837.5
NH_4Cl	43.5	21.1	11.2	46.8	42.2	7.5	2.817	109.1	-	-
KCl	44.6	21.1	10.7	49.2	38.6	11.2	1.891	-	-	345.8
KH_2PO_4	36.5	13.2	10.6	19.4	28.5	2.3	5.819	-	17.9	133.7
$Ca(NO_3)_2$	49.4	16.7	9.2	44.8	33.2	4.0	4.220	52.5	-	-
SOA	46.7	15.5	7.9	49.1	28.4	1.7	9.343	30.8	-	-
MAP	44.4	13.8	11.5	16.7	29.9	1.0	14.092	54.1	10.8	-
DAP	51.3	13.3	11.8	11.3	30.3	3.4	3.878	202.1	17.5	-

RSF: Reverse Salt Flux; **RFS**: Reverse Flux Selectivity. **Recovery rate** is the ratio between the accumulated volume of water transferred from the feed solution to the draw solution and the initial feed solution volume. Results obtained after 1-day operation.

Similarly to earlier studies on FDFO (Phuntsho et al., 2011, Phuntsho et al., 2012b), KCl showed the highest initial water flux (i.e. 21.1 LMH) together with NH_4Cl and followed by KNO_3 while MKP and DAP had the lowest among the different tested fertilizers (i.e. 13.2 LMH and 13.3 LMH respectively). Theoretically, since the osmotic pressure difference across the membrane is the main driving force in the FO process, the water flux trend among the fertilizers should follow the same trend as the osmotic pressure. However, results in both **Table 4** and **Table 6** show that there is no direct correlation between the osmotic pressure of the DS and the water flux. For instance, while DAP

generated the highest osmotic pressure, this fertilizer showed one of the lowest water flux. This is due to the concentration polarization (CP) effects and more importantly to the extent of internal CP (ICP) effects induced by the solute resistance (K) inside the membrane support layer facing the DS (McCutcheon et al., 2006, McCutcheon and Elimelech, 2007). The solute resistance is, in fact, a function of the diffusivity of the solute and thus, a DS having a high diffusivity will have a low K value and therefore generate a high water flux. This is confirmed by the results obtained in this study as data showed a fairly good correlation (i.e. $R^2 = 0.8077$) between the water flux generated by a DS and its diffusivity (**Fig. 19**).

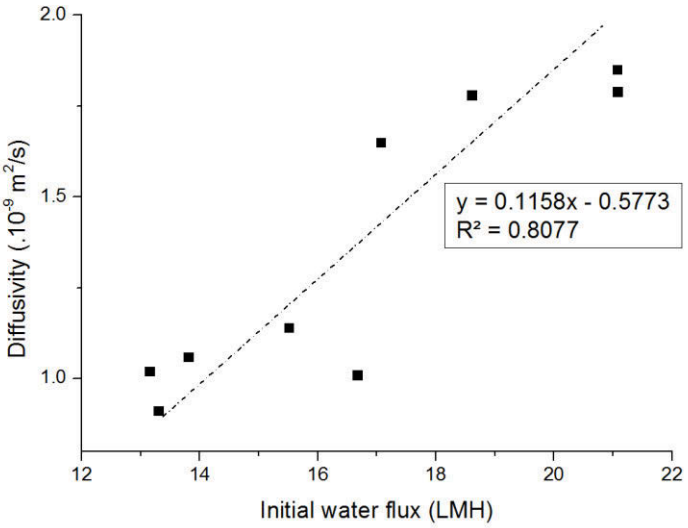

Figure 19. Diffusivity of fertilizer draw solutions as a function of initial water flux in FDFO using synthetic wastewater effluent as feed solution.

The recovery rate after 1-day operation shows similar trend to the initial water flux (i.e. linear correlation, $R^2 = 0.8397$, **Fig. 20**) with NH_4Cl and KCl having the highest water recovery (i.e. 42.2% and 38.6% respectively). Comparing the results with the FDFO desalination studies using either seawater or brackish water as FS, the water flux obtained

in this study (i.e. using synthetic wastewater as FS) is much higher, up to 80% (**Table 7**). In fact, the osmotic pressure of the synthetic wastewater used in this study (i.e. 0.149 atm) is considerably lower than, for instance, the brackish water used in Phuntsho, Shon et al., (2012b) (i.e. 3.9 atm) and therefore the initial difference in osmotic pressure across the membrane (i.e. which is the driving force of the FO process) is significantly higher, resulting in a higher initial water flux. This suggests that, if available, low-strength wastewater might be a more suitable FS for FDFO when targeting high water flux and water recovery. However, it should be noted that a different membrane has been employed in this study (i.e. Toray TFC PA membrane instead of HTI CTA membrane) so the increase in water flux might also be partially related to the better performance of this novel membrane.

Table 7. Comparison between the initial water fluxes obtained in FDFO operating with either brackish water or wastewater as feed solution.

	Initial water flux (μm/s)	
	Brackish water as feed (Phuntsho et al., 2012b)	**Wastewater as feed (improvement %)**
NH_4NO_3	1.92	4.74 (+59)
SOA	1.71	4.31 (+60)
MAP	1.32	3.84 (+65)
KCl	2.31	5.86 (+60)
KNO_3	1.17	5.17 (+77)
MKP	1.61	3.65 (+56)
$Ca(NO_3)_2$	2.04	4.63 (+56)
DAP	1.48	3.69 (+60)
NH_4Cl	2.27	5.85 (+61)

SOA: Ammonium sulphate, MAP: ammonium phosphate monobasic, DAP: ammonium phosphate dibasic.

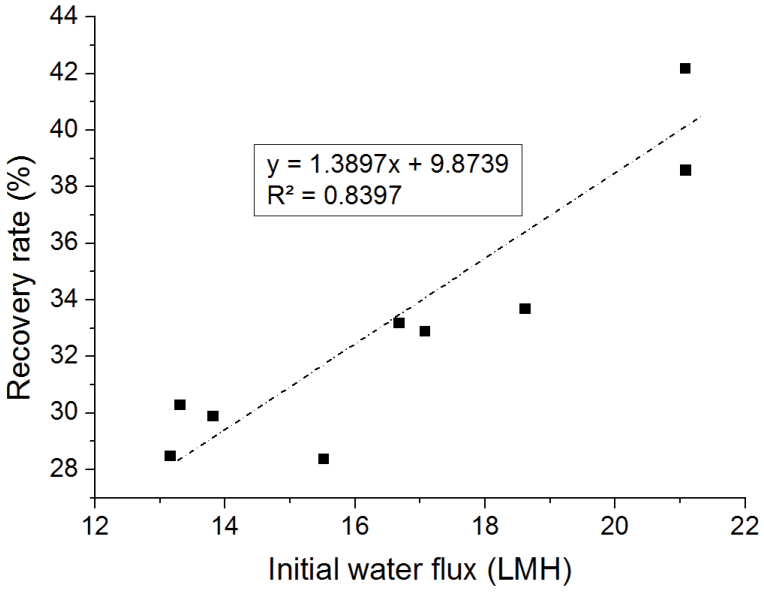

Figure 20. Final recovery rate as a function of initial water flux in FDFO using different fertilizers as draw solution and synthetic wastewater effluent as feed solution.

After one day of operation, both KNO_3 and KCl showed the highest flux decline (i.e. 55.4% and 49.2%, respectively) while the water flux generated by DAP, mono-ammonium phosphate (MAP) and MKP only decreased by less than 20%. This trend can be explained by the fact that an initial higher water flux level can generally be coupled with elevated rate of RSF resulting in more severe fouling (Hancock and Cath, 2009, Tang et al., 2010, Phillip et al., 2010). Besides, both KCl and KNO_3 have ionic species with small hydrated diameter (i.e. K^+, Cl^- and NO_3^-) which will therefore readily diffuse through the membrane compared to fertilizers having larger-sized hydrated anions (i.e. SO_4^{2-} and PO_4^{2-}) regardless of the paired cations (Achilli et al., 2010). It is well established that a greater rate of RSF will significantly affect the feed water chemistry which may cause more severe fouling (She et al., 2016).

Reverse salt flux selectivity (RSFS = J_w/J_s), which represents the ratio of the forward water *flux* (J_w) to the *RSF* (J_s), was also calculated and results are displayed in **Table 6**.

This ratio is very useful to estimate how much salts from the DS are lost through RSF during the FO process operation. It is usually preferable to have a DS with a high RSFS in terms of replenishment cost but also for sustainable FO operation (Achilli et al., 2010). **Table 6** shows that MAP, SOA and MKP exhibited the highest RSFS suggesting that all three DS can produce the highest volume of permeate per gram of lost draw salts. This is very crucial in our study since the target is to produce a highly-diluted DS for possible direct hydroponic application while concentrating the wastewater with minimum reverse diffusion from the DS to minimize the impact on the microbial activity in the subsequent AnMBR process. Because for hydroponics, one of the most important parameters to evaluate is the final nutrient concentration, the RSF in FDFO has also been evaluated in terms of loss of essential nutrients (i.e. N, P and K) per unit volume of water extracted from the FS as described in Phuntsho, Shon et al., (2012b). Results in **Table 6** showed that KNO_3, KCl and NH_4NO_3 had the highest loss of nutrient which correlates with the RSF data for these three fertilizers. SOA, MAP and MKP exhibited the lowest loss of nutrient by reverse diffusion for N, P and K, respectively. In fact, these fertilizers have divalent ions (i.e. SO_4^{2-}, PO_4^{2-}) which display significantly lower loss through RSF due to their larger hydrated ions.

3.3.2.2 Final nutrient concentration after 1 day operation

Fig. 21 presents the final nutrient (i.e. N, P and K) concentrations in the final diluted DS after 1-day operation for all nine tested fertilizers. Based on earlier FDFO studies (Phuntsho et al., 2012b), the final NPK concentration is highly dependent on the feed water (i.e. seawater, brackish water, wastewater) as well as the percentage of a particular nutrient in the DS and the final recovery rate. In fact, by comparing MAP and DAP fertilizers, which have the same counter ion (i.e. PO_4^{2-}) but a different percentage of N

(i.e. 12.2% and 21.2 %, respectively), the final diluted DS contained 10.8 and 21.5 g/L of N, respectively. The lowest nutrient concentration for N was observed for NH_4Cl (i.e. 9.8 g/L) which generated one of the highest water flux and recovery rate (**Table 6**). All DS containing either P or K resulted in similar final concentration in the diluted DS after 1-day and this concentration remained fairly high (i.e. about 24 g/L for P and 30 g/L for K).

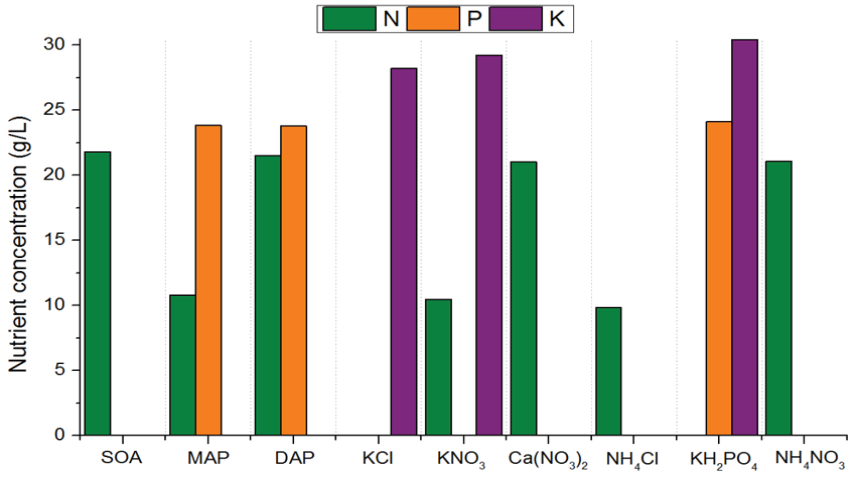

Figure 21. Final NPK nutrient concentration of fertilizer solution (Initial concentration: 1M) after one day operation of FDFO using synthetic wastewater as feed solution.

However, the results presented in **Fig. 20** indicate that the final nutrient concentration after 1-day operation remains significantly higher than the standards for hydroponics. In fact, depending on the crop types and growth stages, the required nutrient concentration varies significantly with a maximum recommended concentration of 200 mg/L for N, 50 mg/L for P and 300 mg/L for K (Resh, 2012). Taking tomatoes as an example, the nutritional requirement for hydroponics varies from 70-150 mg/L for N, 50 mg/L for P (i.e. no variation during the different growth periods) and 120-200 mg/L for K (Hochmuth and Hochmuth, 2001). It is clear from these data that the results obtained in **Fig. 20** after 1-day operation are significantly higher than the standards for hydroponics suggesting

that the final DS still requires a substantial dilution before being applied to hydroponic crops. Additional post-treatment (e.g. NF) or alternative process configuration (e.g. use of blended fertilizers or PAO) might help in obtaining the desired nutrient concentration as demonstrated in previous FO studies (Tan and Ng, 2010, Phuntsho et al., 2012b, Zhao et al., 2012, Phuntsho et al., 2013a, Sahebi et al., 2015).

3.3.2.3 Effect of fertilizer draw solution concentration

Short-term experiments were also carried out at 2.0 M DS concentration since higher water flux has been generally observed at higher fertiliser concentrations. Results for this study are presented in **Table 8** (i.e. water flux and recovery rate) and **Fig. 22** (i.e. final NPK concentrations). With the exception of MKP which has a maximum solubility of 1.8 M, all fertilizer DS generated a higher water flux at 2.0 M concentration (**Table 8**). However, the improvement ratio (i.e. percentage increase in water flux from 1.0 M to 2.0 M concentration) is different among the tested fertilizers. In fact, previous studies have already shown that DS concentration influences the FO process performance (Seppälä and Lampinen, 2004, McCutcheon et al., 2006, Achilli et al., 2009, Choi et al., 2009, Hancock and Cath, 2009, Xu et al., 2010b). It was demonstrated that the relationship between DS concentration and water flux is not linear and different among the DS types, especially at high DS concentration where the relation has been found logarithmic. This has been attributed to ICP effects in the membrane support layer which become more important at higher permeate flux resulting in less effective water flux improvement (Tan and Ng, 2010). The lower improvement ratio for MAP and DAP (i.e. less than 5%) suggests that the percentage of the bulk osmotic pressure effectively available did not improve significantly when increasing the solute concentration (Phuntsho et al., 2013a).

Table 8. Effect of fertilizer draw solution concentration on water flux and recovery rate in FDFO using synthetic wastewater as feed solution.

	Initial Water Flux (LMH)			Recovery Rate (%)		
Fertilizer	1M	2M	Improvement ratio (%)	1M	2M	Improvement ratio (%)
NH_4NO_3	17.1	22.2	23.0	32.9	46.2	28.8
KNO_3	18.6	21.2	12.3	33.7	34.4	2.0
NH_4Cl	21.1	26.6	20.7	42.2	40	-5.5
KCl	21.1	26.4	20.1	38.6	39.5	2.3
MKP	13.1	Not measured – above max. solubility		28.5	Not measured – above max. solubility	
$Ca(NO_3)_2$	16.7	21.1	20.9	33.2	42	21.0
SOA	15.5	19.5	20.5	28.4	34.8	18.4
MAP	13.8	14.1	2.1	29.9	29.7	-0.7
DAP	13.3	13.8	3.6	30.3	31.8	4.7

The recovery rate after 1-day operation also increased with the increase in DS concentration, with the exception of NH_4Cl and MAP. However, the improvement ratio (i.e. percentage increase) in comparison with the results obtained with 1.0 M DS concentration is quite heterogeneous among the tested fertilizers. In fact, it has been previously demonstrated that, although the increase in DS concentration can increase the initial water flux, it can also exacerbate membrane fouling due to the greater hydraulic drag force promoting more foulant deposition on the membrane (Mi and Elimelech, 2008, Zou et al., 2011, She et al., 2012) as well as an increase in the solute reverse diffusion from the DS (Hancock and Cath, 2009, Phillip et al., 2010). Besides, it is evident that the membrane fouling behaviour and especially the foulant-membrane interactions, are closely dependent on the type of DS (i.e. diffusivity, solubility, molecular weight, soluble

species, etc.) and therefore, different fertilizer DS will have different impacts on membrane fouling resulting in different water flux trends (i.e. and thus final recovery rate) which explains the results obtained in **Table 8**.

The final nutrient (i.e. NPK) concentrations for all DS (i.e. except MKP) are shown in **Fig. 21**. Considering the negligible improvement in terms of water flux and more importantly in terms of recovery rate, it is not surprising that the final NPK concentrations, using 2.0 M initial DS concentration, are almost twice for the values obtained with 1.0 M DS concentration. This result suggests that increasing the initial DS concentration might not be the best approach to achieve lower nutrient concentration in the final diluted DS.

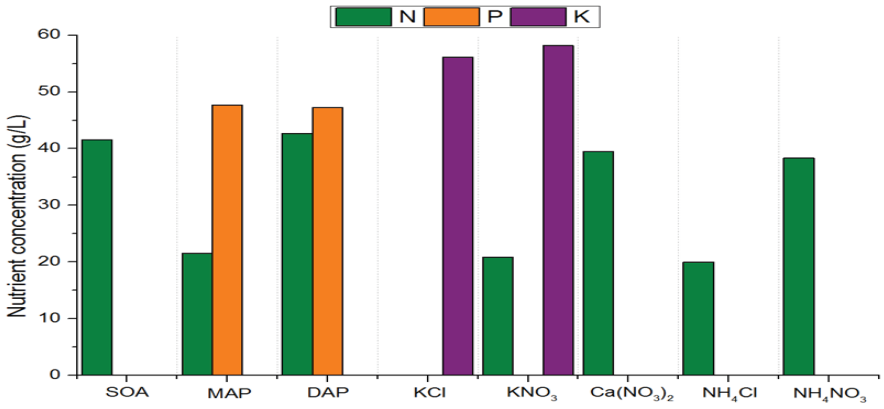

Figure 22. Final NPK nutrient concentration of fertilizer solution (Initial concentration: 2M) after one day operation of FDFO using synthetic wastewater as feed solution.

3.3.3 Performance of blended fertilizers as draw solution

A previous FDFO study (Phuntsho et al., 2012b) demonstrated that blending two or more fertilizers as DS can help in reducing the final nutrient (i.e. NPK) concentration compared to the use of single fertilizer. Based on this finding, four different combinations of two fertilizers (i.e. at 1 M: 1 M ratio) were selected since they already exhibited good

performance among all the blended solutions tested. Results, in terms of water flux, recovery rate and final NPK concentration are gathered in **Table 9**.

Similarly to the previous FDFO study on blended fertilizers, all four blended solutions generated a higher water flux than the individual fertilizers but it was still lower than the sum of the water fluxes obtained with the two single fertilizers. This was previously explained as a result of complex interactions occurring between the ions and counterions of the two fertilizers leading to a decreased number of formed species in the final solution (Phuntsho et al., 2012b). The coexistence of two different species in the same solution was also found to affect the diffusivity of a specific compound which will indirectly affect the internal CP (ICP) effects and thus the water flux in the FO process (Gray et al., 2006, McCutcheon and Elimelech, 2006, Tan and Ng, 2008, Tang et al., 2010).

Table 9. Performance of selected blended fertilizers (1 M: 1 M ratio) as draw solution in FDFO using synthetic wastewater as feed solution.

Fertilizer combinations (1M:1M)	Osmotic Pressure (bar)	Initial flux (LMH)	Recovery rate (%)	Final nutrient concentration (g/L)		
				N	P	K
NH_4Cl : MKP	80.0	21.5	38.2	10.1	22.4	28.3
MAP : KCl	89.0	22.6	38.0	10.1	22.4	28.3
NH_4NO_3 : MKP	70.2	19.2	33.0	21.1	23.3	29.4
NH_4NO_3 : NH_4Cl	77.2	26.1	38.2	30.4	0.0	0.0

The highest water flux and recovery rate were generated by the NH_4NO_3 + NH_4Cl blend while NH_4NO_3 combined with MKP produced the lowest water flux and recovery rate. In most cases, the final NPK concentration was slightly lower than with single fertilizers but the difference was not significant, especially when considering the increase in cost when

using an additional fertilizer. For instance, when NH_4NO_3 and MKP were used individually, the final NPK concentration in the final diluted DS was 21.1/0/0 mg/L and 0/24.1/30.4 mg/L, respectively but when mixed together, the final NPK concentration only reduced to 21.1/23.3/29.4 mg/L. This suggests that blended fertilizers at 1 M: 1 M ratio might not be the best strategy to reduce the final NPK concentration. In fact, a better approach would be to prepare blended fertilizers (i.e. two or more) with different NPK grade (i.e. percentage of each nutrient in the blended solution) to target specific crop requirement. For instance, if the targeted crop is tomato which has a maximum NPK requirement of 150/50/200 mg/L then the initial NPK grade for the blended fertilizers could be 15/5/20. This approach has already shown the promising results for the FDFO desalination process when the DS was prepared by mixing four different fertilizers (i.e. $NaNO_3$, SOA, KCl and MKP) at targeted NPK grade (Phuntsho et al., 2012b). Further studies are needed in this area and should focus on finding the optimum blended fertilizers solution according to the type of crops and feed waters. This will significantly help in achieving the required final NPK concentration for direct agriculture application and thus potentially eliminate the need for further post-treatment or additional dilution.

3.3.4 Long-term experiments – Maximum water recovery, fouling behaviour and final NPK concentration

Based on the results obtained in section 3.3.2, SOA, MAP and MKP were selected for longer-term operation (i.e. 4 days) due to their high RSFS combined with low nutrient loss by reverse diffusion. Besides, because of their low RSF, these three fertilizers present a relatively low inhibition impact on anaerobic activity (i.e. biogas production) due to lower salt accumulation inside the bioreactor (Chen et al., 2008, Chen et al., 2014a).

The performance of the selected fertilizers, in terms of water flux, water recovery rate and water flux recovery after hydraulic cleaning is presented in **Table 10**. Among the three selected fertilizers, SOA showed the best performance in terms of initial water flux (i.e. 17.2 LMH) and final recovery rate (i.e. 76.2%). In fact, it was already demonstrated in the previous FDFO studies (Phuntsho et al., 2011, Phuntsho et al., 2013a) that SOA generates one of the highest water flux combined with a relatively low RSF and was therefore employed in pilot-scale investigations of FDFO (Kim et al., 2013, Kim et al., 2015b). In terms of fouling behaviour, all three fertilizers showed severe flux decline (i.e. about 70%) along the 4-day operation. However, since flux decline was fairly similar among all three tested fertilizers, this suggests that it might most likely be related to the continuous osmotic dilution of the DS resulting in the reduction of the osmotic pressure difference across the membrane (i.e. the driving force of the FO process) rather than the intrinsic properties of the DS. Nevertheless, since membrane fouling is a rather complex phenomenon, it is very likely that flux decline was also associated with foulant-membrane interactions, CP effects and reverse diffusion of the draw solutes (She et al., 2016). For instance, both MAP and MKP exhibited low flux decline (i.e. less than 20%) during short-term experiments (**Table 6**). However, after 4-day operation, results in **Table 10** showed severe flux decline for both fertilizers. This is most likely related to the osmotic concentration of the feed water combined with the back-diffusion of PO_4 which can cause membrane scaling on the feed side (i.e. formation of calcium phosphate) resulting in much severe flux decline (Greenberg et al., 2005, Phuntsho et al., 2014). In fact, **Fig. 23** (i.e. SEM images of membrane surface) and **Table 11** (i.e. EDX results) showed higher scaling for both MAP and MKP after long-term operation and EDX results revealed a higher concentration of phosphate on the active layer of the membrane during long-term operation.

Table 10. Performance of selected single draw solution in FDFO during long-term (i.e. 4 days) operations.

Fertilizers	Initial flux (LMH)	Flux decline (%) after 4 days	Recovery rate (%) after 4 days	Water flux recovery after hydraulic cleaning (%)
SOA	17.2	68	76.2	60.5
MAP	13.3	70.7	66.1	47.0
MKP	12.6	71.4	66.8	75.1

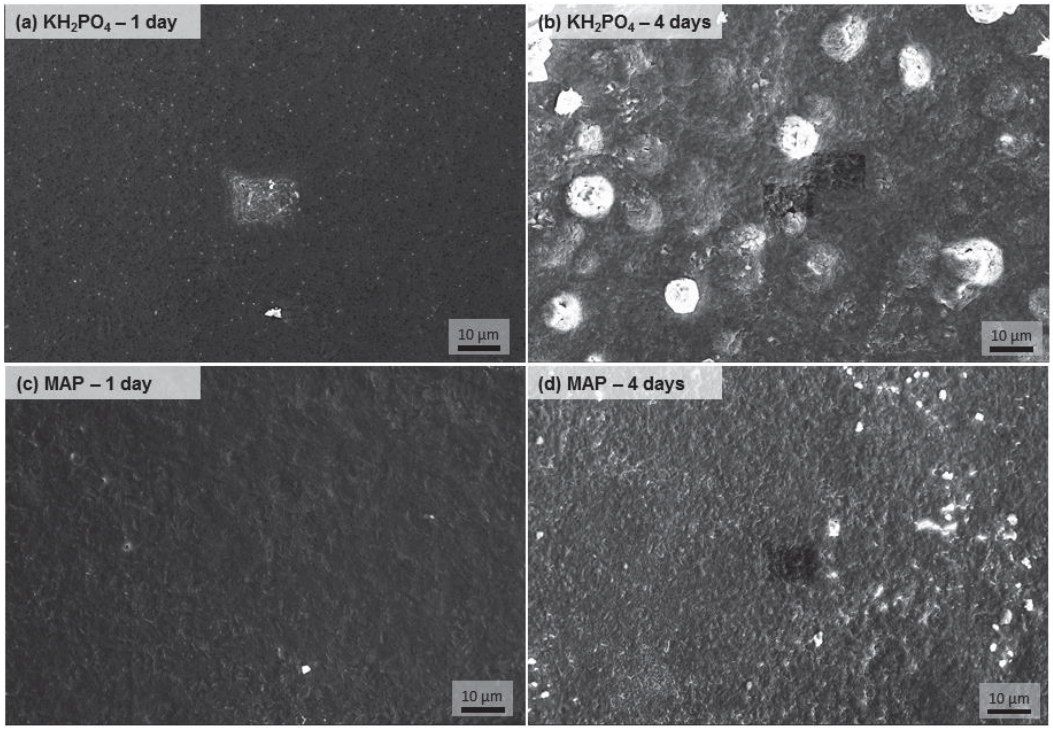

Figure 23. SEM images of membrane surface (active layer) after short-term (i.e. 1 day) and long-term (i.e. 4 days) FDFO operations using MKP and MAP as fertilizer DS and synthetic wastewater as feed.

Table 11. EDX results of membrane surface (active layer) after short-term (i.e. 1 day) and long-term (i.e. 4 days) FDFO operations using MKP and MAP as fertilizer DS and synthetic wastewater as feed.

	Atomic %				
	C	O	P	K	N
MKP – 1 day	57.55	38.7	2.61	1.14	N/D
MKP – 4 days	51.17	42.25	**3.27**	0.31	N/D
MAP – 1 day	44.56	34.97	2.37	1.14	16.95
MAP – 4 days	36.95	35.55	**7.12**	5.69	14.68

After the 4-day experiments, physical cleaning (i.e. membrane surface flushing by enhancing the shear force – triple cross flow – along the membrane surface) was performed to remove the deposited foulants. In fact, this method has already been proved to be very effective against membrane fouling in the FO process (Mi and Elimelech, 2010, Arkhangelsky et al., 2012). However, results in **Table 10** and **Fig. 24** (i.e. pictures of membrane surface after physical cleaning) show a partial membrane cleaning and water flux recovery varying from 47.0% for MAP to 75.1% for MKP. This result clearly indicates that internal fouling within the support layer (i.e. due to ICP effects) occurred during the operation since the membrane surface flushing was not effective in restoring the original water flux (Arkhangelsky et al., 2012). Besides, the extent of internal fouling varied among the fertilizers with MAP having the lowest water flux recovery (i.e. 47.0%) and thus had potentially the highest internal fouling which can be likely related to its molecular weight, being the lowest among the three tested fertilizers. In order to mitigate internal fouling, many researchers have suggested the use of osmotic backwashing to remove the foulants blocked within the support layer (Yip and Elimelech, 2013, Boo et al., 2013, Valladares Linares et al., 2013). This membrane cleaning technique can thus be

adopted in the present FDFO process as a more efficient way to reduce fouling during continuous operation.

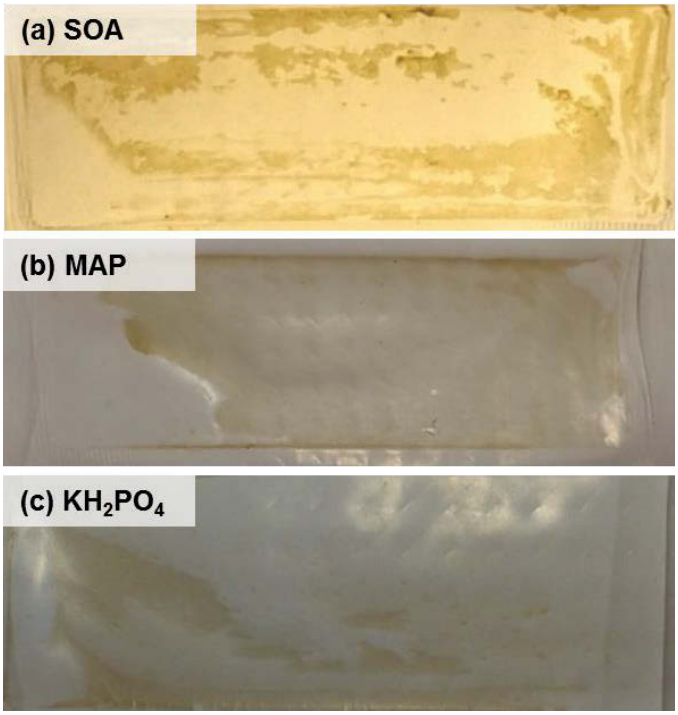

Figure 24. Pictures of membrane surface after physical cleaning (i.e. DI water on both sides, cross-flow rate: 1,200 mL/min, 15-min operation) following long-term FDFO operations using SOA, MAP and MKP as fertilizer DS and synthetic wastewater as feed.

The final NPK concentration after four days operation is shown in **Fig. 25a**. Compared to the results obtained in section 3.3.2.2. (i.e. short-term operation), there is a slight reduction in the final nutrient concentrations of about 20-25% depending on the nutrient and the fertilizer DS. This reduction was found higher with SOA (i.e. 27% reduction for N compared to 22% for MAP) since it achieved the highest initial water flux and final water recovery. However, for all three fertilizers, the final nutrient concentrations were still not suitable for hydroponics and yet required substantial dilution (i.e. about 100 times if targeting tomato crops) before application.

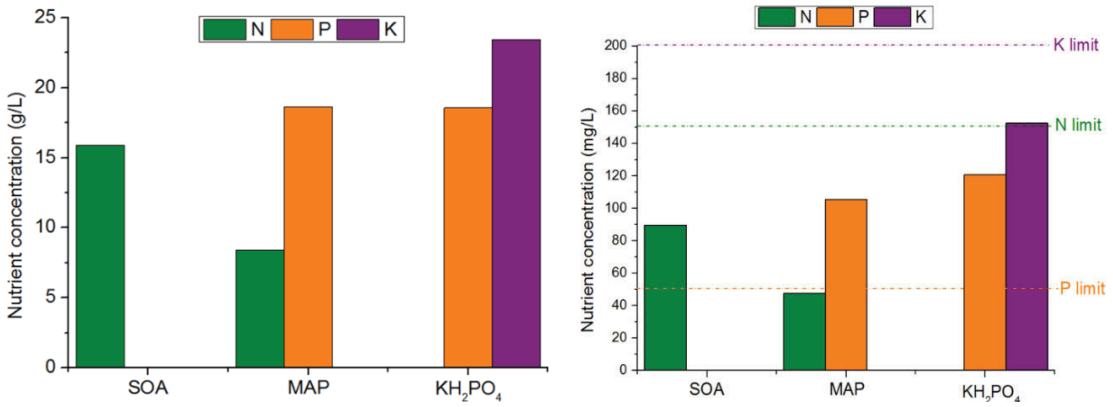

Figure 25. Final NPK nutrient concentration of fertilizer solution (Initial concentration: 1M) (a) after four days operation and (b) at the point of osmotic equilibrium of FDFO using synthetic wastewater as feed solution. The NPK limits were derived from (Hochmuth and Hochmuth, 2001).

Fig. 25b shows the estimated final NPK concentrations if the process is operated until the bulk osmotic equilibrium between the fertilizer DS and wastewater FS is reached (i.e. when the osmotic pressure of the fertilizer DS equals that of the wastewater FS (0.149 atm) as described in Phuntsho et al. (2012b). Osmotic pressure of the different fertilizer DS as a function of molar concentrations was predicted using OLI Stream Analyser 3.1 (OLI Inc, USA) at 25°C (**Fig. 26**). Results indicate that, at the point of osmotic equilibrium, the final nutrient concentrations are considerably reduced, even below the standard requirements for both N and K nutrients (i.e. if considering tomato as the targeted crop). This clearly emphasizes the benefit of using a low-salinity feed water such as municipal wastewater in FDFO to meet the nutrient standard requirements for hydroponics. However, for both MAP and MKP, the final P nutrient concentration still exceeded the acceptable threshold (i.e. 50 mg/L), suggesting that further dilution or post-treatment may be required. Besides, as discussed previously by Phuntsho et al. (2012b),

operating FDFO until the osmotic equilibrium might not be an economically viable solution considering the significant reduction in water flux due to the continuous osmotic dilution of the fertilizer DS.

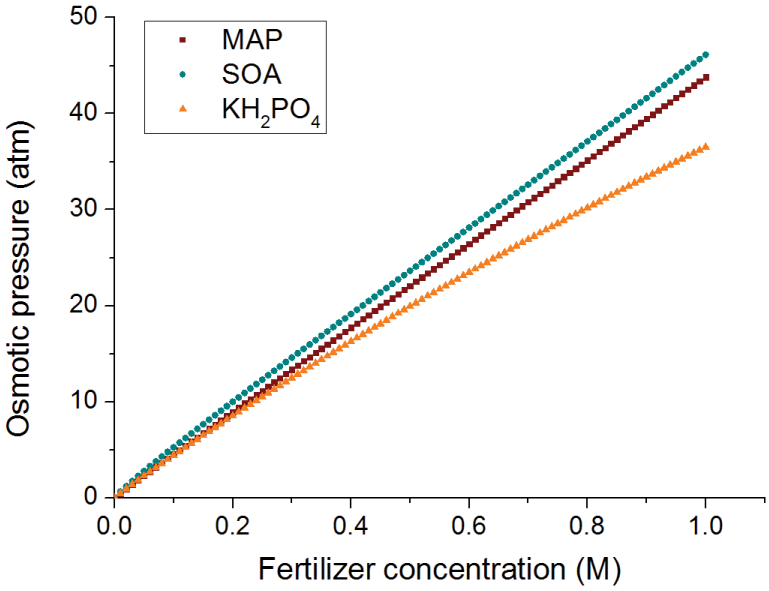

Figure 26. Osmotic pressure of fertilizer draw solutions as a function of molar concentrations. Osmotic pressure was predicted using OLI Stream Analyser 3.1 (OLI Inc, USA) at 25°C. N.B. Ammonium sulphate: SOA and ammonium phosphate monobasic: MAP.

3.4 Conclusions

This study investigated the potential of FDFO to achieve simultaneous water reuse from wastewater and sustainable agriculture application. Results showed that 95% was the optimum water recovery to achieve in FDFO for further AnMBR treatment. The performance of different fertilizers (i.e. single and blended) as DS was assessed in terms of water flux, RSF, water recovery and final nutrient concentration. While KCl and NH_4Cl showed the highest water flux and water recovery, MAP, MKP and SOA

demonstrated the lowest RSF and thus loss of nutrient through back diffusion. The use of wastewater effluent instead of brackish or seawater as FS in FDFO proved to be beneficial in terms of reducing the final nutrient concentration. In fact, the water fluxes obtained with wastewater as FS was substantially higher than those obtained with high salinity FS (i.e. up to 80% higher). Increasing the DS concentration or blending fertilizers at equal ratio (i.e. 1 M: 1 M) did not provide significant improvement in terms of water flux and final NPK concentration. Finally, although high recovery rate can be achieved during long-term operations (i.e. up to 76.2% for SOA after 4-day operation), the final diluted DS still required substantial dilution (i.e. up to 100 times depending on the targeted crop) before meeting the nutrient standard requirements for hydroponics.

4. Selection of suitable fertilizer draw solute for a novel fertilizer-drawn forward osmosis – anaerobic membrane bioreactor hybrid system

4.1 Introduction

Freshwater resources are getting scarcer due to the impacts of global warming, and rapid and extensive industrialization and urbanization (Rijsberman, 2006). Moreover, agricultural sector still consumes about 70% of the accessible freshwater with about 15-35% of water being used unsustainably (Clay, 2004). Therefore, countries such as in the Mediterranean region, which are stressed by water shortage, have considered wastewater reuse as a viable alternative water resource for agricultural purposes (Angelakis et al., 1999b). Adequate treatment of wastewater before reuse as irrigation is essential not only to protect the human health from consumption and plant health but also enhance the value of the crops grown through wastewater reuse. Many researchers have studied the feasibility of wastewater reuse for irrigation by using a variety of treatment methods (Ferro et al., 2015, Alderson et al., 2015).

For wastewater reuse, however, advanced treatment processes (e.g., RO, NF or advanced oxidation) are generally required as a post-treatment process since wastewater could contain pollutants which are not removed by conventional treatment processes such as heavy metals, pharmaceutics and trace organic contaminants (Ahluwalia and Goyal, 2007). AnMBR has been studied to treat wastewater and has several advantages including complete rejection of suspended solids, low sludge production, high organic rejection and biogas production (Stuckey, 2012). Moreover, both AnMBR and post-treatment (e.g., RO and NF) exhibit high fouling issues which ultimately increase energy requirements since these processes are driven by the hydraulic pressure as a driving force (Kim et al., 2014b). To overcome these issues, OMBR has been proposed by integrating AnMBR with FO

instead of conventional pressurized membrane processes (Achilli et al., 2009, Wang et al., 2016, Chekli et al., 2016). OMBR can provide high rejection of contaminants, low fouling propensity and high fouling reversibility but also has limitations that pure water should be extracted from DS and reversely transported draw solute can be toxic or inhibit the biological processes (Achilli et al., 2009).

Lately, FDFO has received increased interest since the diluted DS can be used directly for irrigation purposes and therefore no recovery process is required (Phuntsho et al., 2011, Phuntsho et al., 2012b). In FDFO, fertilizers are used as DS and the fertilizer solution is continuously diluted during operation (Phuntsho et al., 2011). In the early studies, only single fertilizers, which did not provide sufficient nutrient composition for direct application, were examined. Thus, blended fertilizers were investigated for targeted crops (Phuntsho et al., 2012b). However, the final nutrient concentration was still high and the final fertilizer solution required substantial dilution for direct fertigation. To solve this problem, NF was adopted as post-treatment and the produced fertilizer solution by NF could meet the water quality requirements for fertigation since it has lower rejection rates (i.e., 80-90%) than RO (Phuntsho et al., 2013a). Nevertheless, high energy consumption is still an issue since NF is a pressurized desalting process and should overcome osmotic pressure of diluted fertilizer solution. Finally, PAFDFO was recently developed for enhancing final dilution of fertilizer DS without beyond the point of osmotic equilibrium between FS and DS (Sahebi et al., 2015).

In this study, we propose for the first time a FDFO-AnMBR hybrid system (AnFDFOMBR) for simultaneous wastewater treatment for greenhouse hydroponic application based on the concept described in **Fig. 27**. This hybrid system consists of two parts (i.e., AnMBR and FDFO). In conventional AnMBR, MF or UF are employed to separate the treated wastewater from the anaerobic sludge. In this study, a FO membrane

is used instead and submerged into the bioreactor. In addition, the FO process is here driven by fertilizers (FDFO process) and thus the treated water drawn from the wastewater is used to dilute the fertilizer solution which can then be directly used for fertigation. In this system, raw municipal wastewater will be utilized as influent and a highly concentrated fertilizer solution will be used as DS for the AnFDFOMBR process. The diluted fertilizer solution can then be obtained and supplied to greenhouse hydroponics irrigation.

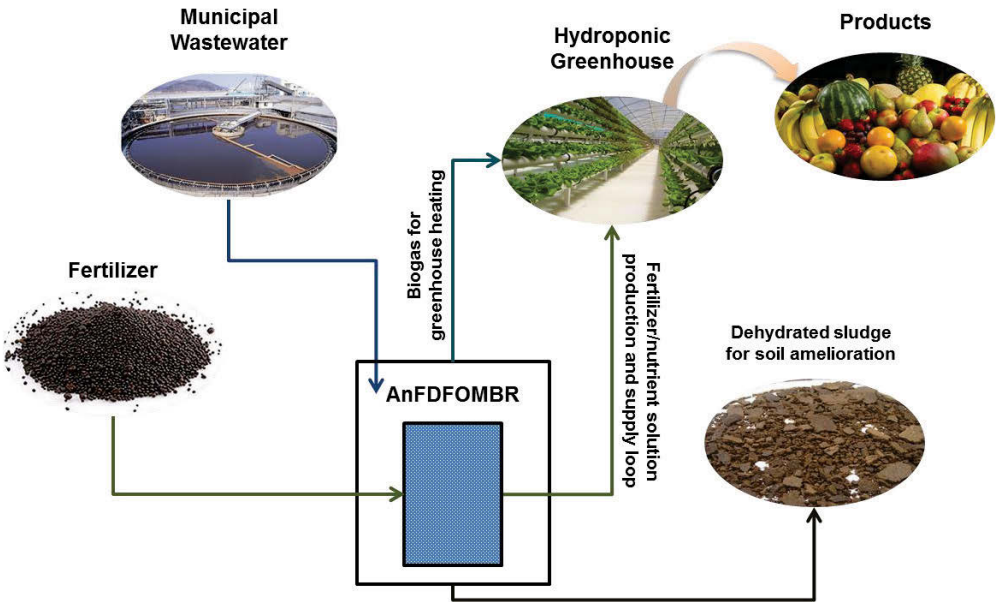

Figure 27. The conceptual diagram of the fertilizer-drawn forward osmosis – anaerobic membrane bioreactor hybrid process for greenhouse hydroponics

The main objective of this study is to investigate a protocol for selecting the optimum DS for the novel AnFDFOMBR process. For selecting a suitable fertilizer as draw solute, FO performance was first investigated in terms of water flux and RSF. BMP was then measured to evaluate the potential effect of the fertilizer due to reverse diffusion on inhibiting the microbial activity in the bioreactor for methane production. Finally, salt

accumulation in the AnFDFOMBR was simulated based on theoretical models derived from mass balance.

This chapter is an extension of the research article published by the author in Bioresource Technology.

4.2 Experiments

4.2.1 FO membrane

The FO membrane used in this study was provided by Hydration Technology Innovations (Albany, OR, USA). This membrane is made of cellulose-based polymers with an embedded polyester mesh for mechanical strength. Detailed characteristics of this commercial membrane can be found elsewhere (Tiraferri et al., 2013).

Properties of FO membrane are commonly classified into the water permeability coefficient (*A*) and the salt permeability coefficient (*B*) of the active layer, and the structure parameter (S) of the support layer. The mathematical method (Tiraferri et al., 2013) which can simultaneously measure three parameters under the non-pressurized condition was used in this study. Experimental measurements were conducted in a lab-scale FO unit with an effective membrane area of 20.02 cm^2. Operating temperature was 25 ºC and the cross-flow velocities of both the solutions were maintained at 25 cm/s. The methods to determine the *A*, *B* and *S* parameters **(**see **Table 12)** are described elsewhere in detail (Tiraferri et al., 2013, Yip and Elimelech, 2013).

Table 12. Experimental data for HTI CTA FO membrane properties (i.e., water and salt (NaCl) permeability coefficients of the active layer and the structural parameter of the support layer).

	Water permeability coefficient, A ($L/m^2/h/bar$)	**Salt permeability coefficient, B ($kg/m^2/h$)**	**Structural parameter, S (10^{-6} m)**
HTI CTA FO membrane	0.368	0.191	289

4.2.2 Draw solutions

All chemical fertilizers used in this study were reagent grade (Sigma Aldrich, Australia). DS were prepared by dissolving fertilizer chemicals in DI water. Detail information of fertilizer chemicals are provided in **Table 13**. Osmotic pressure and diffusivity were obtained by OLI Stream Analyzer 3.2 (OLI System Inc., Morris Plains, NJ, USA).

Table 13. Details of the fertilizer chemicals used in this study. Thermodynamic properties were determined at 1 M concentration and 25 ºC by using OLI Stream Analyzer 3.2.

Chemicals	Formula	Molecular weight (g/mol)	Osmotic pressure (atm)	Diffusivity ($\times 10^{-9}$ m^2/s)
Ammonium nitrate	NH_4NO_3	80.04	33.7	1.65
Ammonium sulphate	$(NH_4)_2SO_4$	132.1	46.1	1.14
Ammonium chloride	NH_4Cl	53.5	43.5	1.85
Calcium nitrate	$Ca(NO_3)_2$	164.1	48.8	1.01
Sodium nitrate	$NaNO_3$	85.0	41.5	1.42
Potassium chloride	KCl	74.6	44	1.79
Mono-ammonium phosphate	$NH_4H_2PO_4$	115.0	43.8	1.06
Di-ammonium phosphate	$(NH_4)_2HPO_4$	132.1	50.6	0.91
Potassium nitrate	KNO_3	101.1	37.2	1.78
Urea	CH_4N_2O	60.06	23.7	0.13
Potassium phosphate monobasic	KH_2PO_4	136.09	36.5	1.02

4.2.3 FO performance experiments

FO performance experiments were carried out using a lab-scale FO system similar to the one described elsewhere (Lee et al., 2015, Kim et al., 2015c). The FO cell had two symmetric channels on both sides of the membrane each for FS and DS. Variable speed gear pumps (Cole-Parmer, USA) were used to provide crossflows under co-current directions at a crossflow rate of 8.5 cm/s and solution temperature of 25°C and the solutions were recirculated in a loop resulting in a batch mode of process operation. The DS tank was placed on a digital scale and the weight changes were recorded by a computer in real time to determine the water flux. Conductivity and pH meters (HACH, Germany) were connected to a computer to monitor RSF of draw solutes in the feed tank.

FO experiments were conducted in the AL-FS mode. The fertilizer DS concentrations were fixed at 1 M for all the experiments. Before each performance experiment, the FO membrane was stabilized for 30 mins with DI water as FS and 1 M fertilizer solution as DS. Once stabilized, the water flux was measured continuously throughout the experiment every 3 mins time interval. After 1 h of operation, FS was collected and then RSF was measured by analysing its composition.

4.2.4 Selection of suitable fertilizer draw solution for anaerobic fertilizer-drawn forward osmosis membrane bioreactor process

4.2.4.1 Determination of reverse salt concentration in a bioreactor based on a dilution factor

When considering a typical submerged AnFDFOMBR as depicted in **Fig. 28**, salt accumulation will take place in the bioreactor from both the influent and DS. This is due to wastewater continuously being fed into the bioreactor and the FO membrane rejecting

almost 100% of ionic compounds and the back diffusion of DS. Salt concentration will continuously increase and therefore may affect the microbial activity of the anaerobic bacteria as well as FO performances. This salt concentration in the bioreactor can be calculated through the solute mass balance with the assumption of no change of water flux and RSF during operation (**Eq. (1)**). In this study, no sludge discharge is also assumed since AnFDFOMBR is usually operated under high solids retention time (SRT) (Qiu and Ting, 2014), and the concept of dilution factor (DF), which is defined as a ratio of final volume to initial volume (**Eq. (2)**), was adopted since total permeate volume will be different for each fertilizer at a similar operation time. Thus, an equation for salt concentration induced by RSF in the bioreactor can be obtained as **Eq. (3)**.

$$\left(\frac{dC_{R,RSF}}{dt}\right)V_R = Q_{in}C_{in,feed} + J_{s,RSF}A_m - Q_sC_{R,RSF} = J_{s,RSF}A_m \qquad \textbf{Equation 1}$$

$$\mathrm{DF} = \frac{V_{D,f}}{V_{D,i}} = \frac{V_{D,i}+J_wA_mt}{V_{D,i}} = 1 + \frac{J_wA_mt}{V_{D,i}} \qquad \textbf{Equation 2}$$

$$\boldsymbol{C_{R,RSF} = \frac{1}{(J_w/J_{s,RSF})}\frac{V_{D,i}}{V_R}(DF - 1)} \qquad \textbf{Equation 3}$$

where, $C_{R,RSF}$ is the bioreactor concentration caused by RSF, J_w and $J_{s,RSF}$ is the water flux and RSF in FO, respectively, $V_{D,i}$ is the initial volume of DS, V_R is the bioreactor volume, and DF is the dilution factor.

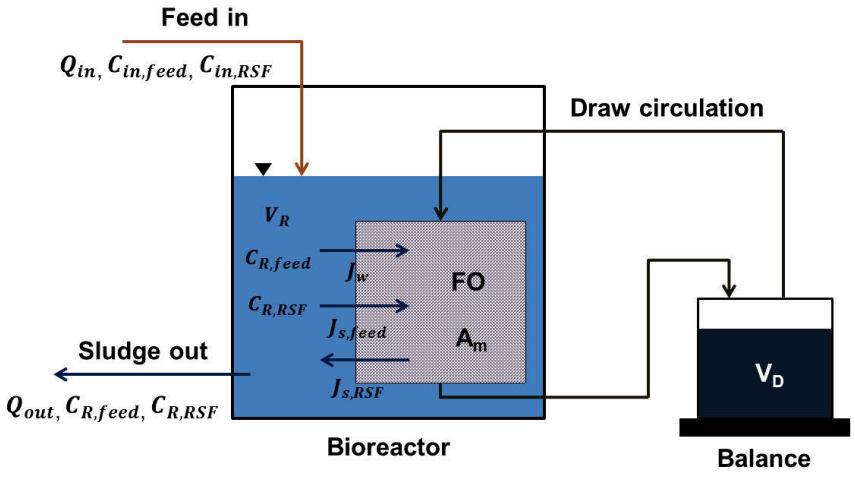

Figure 28. Schematic diagram of the AnFDFOMBR system. $\boldsymbol{A_m}$ is the membrane area, $\boldsymbol{C_{in,feed}}$ and $\boldsymbol{C_{in,RSF}}$ are the influent concentrations containing the respective influent and draw solutes, $\boldsymbol{C_{R,feed}}$ and $\boldsymbol{C_{R,RSF}}$ are the bioreactor concentrations caused by the respective influent and RSF, $\boldsymbol{J_w}$, $\boldsymbol{J_{s,feed}}$ and $\boldsymbol{J_{s,RSF}}$ is the respective water flux, FSF and RSF in FO, $\boldsymbol{Q_{in}}$ and $\boldsymbol{Q_{out}}$ are flow rates of the respective influent and sludge waste, and $\boldsymbol{V_D}$ and $\boldsymbol{V_R}$ are volumes of the respective draw tank and bioreactor.

4.2.4.2 Bio-methane potential experiments

BMP experiments, which can be utilized to simulate the anaerobic process in batch mode to assess the bio-methane production potential from different substrates (Ansari et al., 2015), were carried out using the BMP apparatus depicted in **Fig. 16** to investigate the effect of RSF on the performance of the AnFDFOMBR. The BMP apparatus consisted of 7 fermentation bottles submerged in a water bath connected to a temperature control device to maintain a temperature of 35±1 ºC. These bottles were connected to an array of inverted 1000 mL plastic mass cylinders submerged in the water bath filled with 1 M NaOH solution to collect and measure the biogas. 1 M NaOH solution plays an important role to remove CO_2 and H_2S from biogas to evaluate only CH_4 production potential. Air

volume in each mass cylinder was recorded 2 times per a day. Detailed description of BMP apparatus used in this study is given elsewhere (Ansari et al., 2015).

To determine the amount of fertilizer chemicals to be added to the digested sludge, **Eq. (6)** was used on the assumption that the bioreactor volume is 6 L, the initial volume of DS is 2 L, and DS is diluted 9 times (i.e., DF is 9 by the end of the experiment). The determined amount of each fertilizer salt was dissolved in 50 mL of DI water and then mixed with 700 mL of digested sludge. For the control, 700 mL of digested sludge mixed with 50 mL of DI water was prepared. All bottles were purged with nitrogen gas, and connected to the biogas collecting equipment. The substrate in each bottle was characterized in terms of TS, MLSS, pH, and COD. pH was measured using pH meter (Hach, Germany), and COD was determined using a COD cell test kit (Merck Millipore, Germany) following the standard method (DIN ISO 15705). TS and MLSS were measured using standard methods (Federation and Association, 2005).

4.2.5 Models for salt accumulation in anaerobic fertilizer-drawn forward osmosis membrane bioreactor

4.2.5.1 Water flux

Many studies have reported that experimental water flux is significantly lower than the ideal water flux obtained by using bulk osmotic pressure difference (McCutcheon and Elimelech, 2006, Chekli et al., 2012). This significant difference is caused by CP when feed salt is accumulated near the active layer in the salt rejecting membrane process, which is referred to as concentrative ECP, and draw salt is diluted across the support layer, which is referred to as dilutive ICP. McCutcheon and Elimelech (McCutcheon and Elimelech, 2006) derived the simplified equation for water flux in FO as follows, taking

into account both the dilutive ICP and concentrative ECP under the FO mode of membrane orientation:

$$\boldsymbol{J_w = A\left[\pi_{D,b} exp(-J_w K) - \pi_{F,b} exp(J_w/k)\right]} \quad \textbf{Equation 4}$$

where, *A* is the water permeability coefficient, *K* is the mass transfer resistance in the support layer, *k* is the mass transfer coefficient in FS, and $\pi_{F,b}$ and $\pi_{D,b}$ are bulk osmotic pressures of FS and DS, respectively.

In this study, we assumed the bioreactor as a completely stirred reactor tank where the mass transfer coefficient is infinite ($k \rightarrow \infty$,), and thus ECP can be ignored ($\exp(J_w/k) \rightarrow 1$). Therefore, **Eqn. (5)** can be modified as:

$$\boldsymbol{J_w = A\left[\pi_{D,b} \exp(-J_w K) - \pi_{F,b}\right]} \quad \textbf{Equation 5}$$

The mass transfer resistance, K, is obtained by dividing the membrane structure parameter by the solute diffusion coefficient.

$$\boldsymbol{K = \frac{S}{D}} \quad \textbf{Equation 6}$$

RSFS is defined as the ratio of water flux to RSF in FO as presented in **Eqn. (7)**. The RSFS is independent of membrane support layer properties and can quantitatively describe FO membrane performance.

$$\frac{J_w}{J_s} = \frac{A}{B} n R_g T$$ **Equation 7**

where, n is the number of species that draw solute dissociates into $n = 2$ for NaCl, and R_g is the gas constant, and T is the absolute temperature.

4.2.5.2 Salt accumulation

In AnMBR, MF or UF is utilized for separating water from FS, but both processes have low rejection rates for ionic solutes. To enhance the produced water quality, FO can be integrated with AnMBR since it has high rejection rate of all compounds including ions. At the same time, however, the rejected salts can accumulate in the bioreactor. In addition, RSF from DS can also cause an increase of salt concentration in the bioreactor. In order to understand AnFDFOMBR, it is important to determine salt accumulation in the bioreactor as a function of time based on solute mass balance in terms of both feed and draw solutes since draw solutes may be different from feed solutes in real applications. Mass balance for water can be written as **Eqn. (8)** since the reactor volume is constant.

$$\mathbf{Q_{in} = Q_{out} + J_w A_m}$$ **Equation 8**

The mixed liquor salt concentration can be separated into two solute components: salt concentrations induced by FS ($C_{R,feed}$) and DS ($C_{R,RSF}$). Mass balance for feed solutes in AnFDFOMBR can be written in the form of **Eqn. (9)**. As shown in **Fig. 28**, $J_{s,feed}$ indicates the forward solute flux (FSF) through FO membrane, and this term can be neglected assuming perfect salt rejection of the FO membrane due to the hindrance effect

of RSF on FSF (Xie et al., 2012a, Kim et al., 2012). Thus, **Eqn. (9)** can be modified as **Eqn. (10)**.

$$\left(\frac{\partial C_{R,feed}}{\partial t}\right) V_R = Q_{in} C_{in,feed} - J_{s,feed} A_m - Q_{out} C_{R,feed} \quad \textbf{Equation 9}$$

$$\frac{\partial C_{R,feed}}{\partial t} = \frac{(Q_{out} + J_w A_m)}{V_R} C_{in,feed} - \frac{Q_{out}}{V_R} C_{R,feed} \quad \textbf{Equation 10}$$

where, $C_{R,feed}$ is the accumulated solute concentration in the bioreactor rejected from the influent flow or FS by the FO membrane, $C_{in,feed}$ is the influent or FS solute concentration, and $J_{s,feed}$ is the FSF to DS.

Mass balance for draw solutes in the AnFDFOMBR can be represented using **Eqn. (11)**. In this equation, the term ($C_{in,RSF}$) can be neglected since influent does not contain any draw solute. Thus, **Eqn. (11)** can be modified as **Eqn. (12)** by substituting **Eqn. (7)** into **Eqn. (11)**.

$$\left(\frac{\partial C_{R,RSF}}{\partial t}\right) V_R = Q_{in} C_{in,RSF} + J_{s,RSF} A_m - Q_{out} C_{R,RSF} \quad \textbf{Equation 11}$$

$$\frac{\partial C_{R,RSF}}{\partial t} = \frac{1}{V_R}\left(\frac{B_{RSF}}{A n R_g T}\right) J_w A_m - \frac{Q_{out}}{V_R} C_{R,RSF} \quad \textbf{Equation 12}$$

where, B_{RSF} is the salt permeability coefficient of draw solutes.

4.2.5.3 Draw solution dilution

To obtain the variations of water flux over time, the change in the volume and concentration of DS in the DS tank should be determined via mass balance equations as follows.

$$\frac{\partial V_D}{\partial t} = J_w A_m \qquad \textbf{Equation 13}$$

$$\frac{\partial C_D}{\partial t} = -\frac{1}{V_D}\left(\frac{B}{AnR_gT}\right)J_w A_m - \frac{C_D}{V_D}\frac{dV_D}{dt} \qquad \textbf{Equation 14}$$

where, V_{D} is the DS volume and C_D is the concentrations of DS.

4.3 Results and discussion

4.3.1 Draw solution selection protocol for anaerobic fertilizer-drawn forward osmosis membrane bioreactor and initial screening

A flow diagram for selecting the best fertilizer as draw solute for AnFDFOMBR is illustrated in **Fig. 29**. A comprehensive list of fertilizer chemicals was initially screened based on solubility in water, osmotic pressure, their popularity as fertilizers, and their potential toxicity to the microorganisms in the bioreactor. For the application of DS, fertilizer chemicals should be highly soluble in water and also should generate higher osmotic pressure than target FS. In addition, DS should not react with the feed solutes to form precipitates and membrane scaling during the reverse diffusion of draw solutes (Chekli et al., 2012). Based on this preliminary screening, a total of eleven different fertilizers were finally selected for further study. Their thermodynamic properties listed in **Table 12** were obtained by using OLI Stream Analyzer 3.2 (OLI System Inc., Morris

Plains, NJ, USA). In terms of osmotic pressure, di-ammonium phosphate (DAP) has the highest value (132.1 atm) followed by $Ca(NO_3)_2$, ammonium sulphate (SOA), mono-ammonium phosphate (MAP), and NH_4Cl. In terms of diffusivity, NH_4Cl has the highest value ($1.85\times10^{-9}\ m^2/s$) followed by KCl, KNO_3, NH_4NO_3, and $NaNO_3$. These fertilizers are commonly used for fertigation (Phuntsho et al., 2011, Phuntsho et al., 2012b). We excluded volatile fertilizers such as ammonium carbonate and ammonia carbonate due to the handling problem although they have sufficient water solubility and osmotic pressure. The eleven selected fertilizers candidates were further screened by conducting FO performance experiments measured in terms of water flux and RSF, and then finally six fertilizers were chosen and further evaluated for bio-methane production experiments and AnFDFOMBR simulation. Based on these approaches of evaluation, the most suitable fertilizers as draw solute was finally determined.

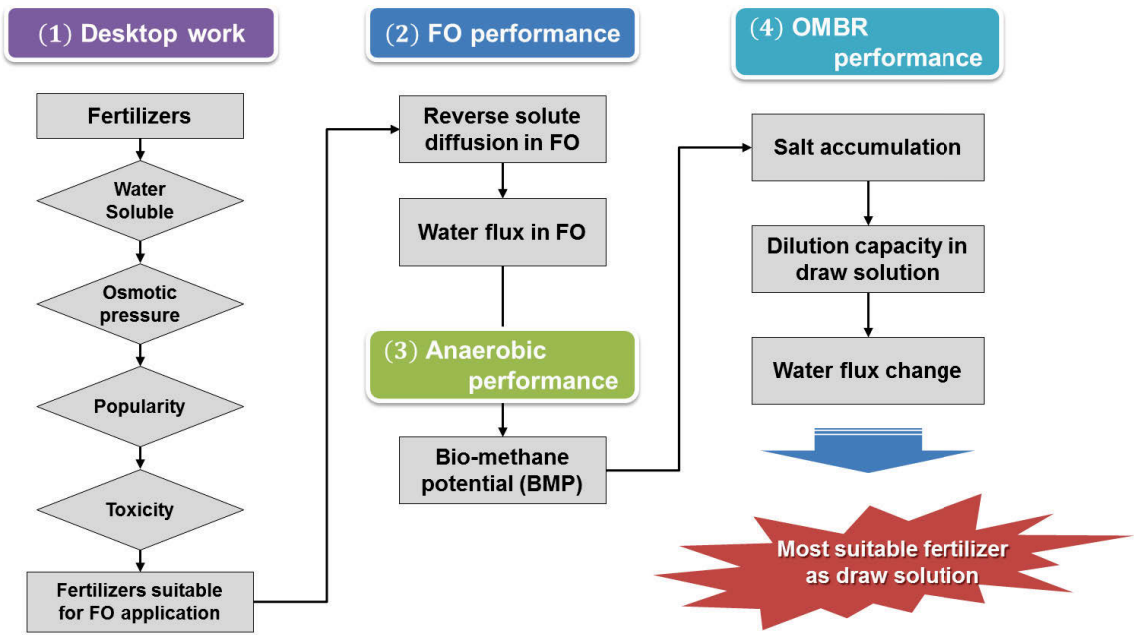

Figure 29. Illustration of flow diagram for draw solution selection in AnFDFOMBR.

4.3.2 FO performance

In order to evaluate the performance of each fertilizer DS, FO process performance experiments were carried out using 1 M concentration DS and DI water as FS, and their water flux measured (see **Fig. 30a**). Results showed that KCl has the highest water flux (11.13 L/m^2/h) followed by NH_4Cl, NH_4NO_3, and KNO_3, while urea has the lowest water flux (2.12 L/m^2/h). However, the osmotic pressure of fertilizers shows a different trend compared to water flux. In fact, DAP shows the highest osmotic pressure (50.6 atm) followed by $Ca(NO_3)_2$, SOA, and MAP. This difference in water flux between fertilizers is explained from the variations of the extent of ICP effects induced by the mass transfer resistance (K) within the membrane support layer (McCutcheon and Elimelech, 2006, Phuntsho et al., 2011). As shown by **Eqn. (6)**, mass transfer resistance refers to the ratio between the S parameter and diffusivity of DS, and thus a draw solute with higher diffusion coefficient has low mass transfer resistance and should have high water flux. Even though DS has low mass transfer resistance, however, it is possible to have low water flux if it has low osmotic pressure.

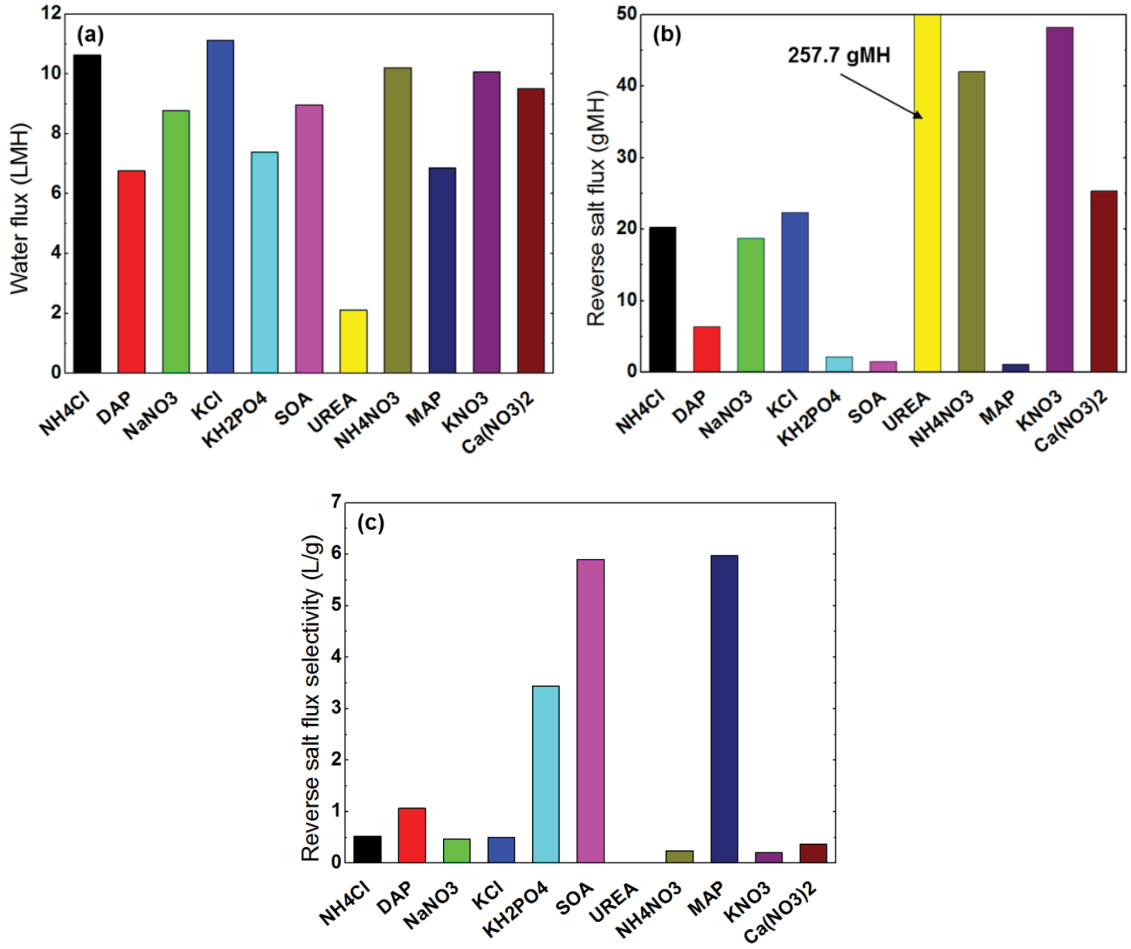

Figure 30. FO performance for different fertilizer draw solutions: (a) water fluxes, (b) reverse salt fluxes, and (c) reverse salt flux selectivity (RSFS). Performance ratio was determined by divided the experimental water flux with the theoretical water flux which was calculated by **Eqn. (6)**, and RSFS was obtained by using **Eqn. (7)**. Experimental conditions of performance experiments: 1 M fertilizer draw solution; cross-flow velocity of 25 cm/s; and temperature of 25 ºC.

RSF of the fertilizer was also measured at 1 M DS concentration to evaluate the suitability of the fertilizer candidates (see **Fig. 30b**) since RSF can be a useful indicator of the extent of draw solute that can be lost during the FO process. Results showed that urea has the highest RSF (257.68 $g/m^2/h$) followed by KNO_3, NH_4NO_3, and $Ca(NO_3)_2$. On the other

hand, MAP has the lowest RSF (1.15 g/m^2/h) followed by SOA, MKP, and DAP. Unlike water flux which increased at higher diffusivity however, the trend for RSF with diffusivity was quite different. This is because RSF is theoretically a function of not only the effective concentration gradient between DS and FS at the active layer surface of the FO membrane but also the salt rejecting properties of the membrane characterised by the salt permeability coefficient (*B* value) which varies with each fertilizer (Kim et al., 2015c) as shown in **Table 14**. The high RSF of urea could be explained because of the high *B* parameter which is likely due to very low diffusivity (in fact lowest amongst all the fertilizer solutes) which could induce high ICP effects. Besides, urea has low molecular size and low hydrated diameter and also forms a neutral solution in water which accelerated its permeation through the FO membrane resulting in significantly higher RSF compared to other fertilizer solutes (Phuntsho et al., 2011). On the other hand, SOA showed low ICP and low RSF which could be due to its low *B* parameter value. A lower RSF could be preferable for AnFDFOMBR since the accumulation of inorganic salt ions in the active bioreactor could potentially inhibit the anaerobic microbial activity (Ansari et al., 2015).

Table 14. Experimental salt permeability coefficients (B) in the active layer and solute resistance in the support layer (K) with respect to fertilizer chemicals. The B parameter was obtained by using $\mathbf{B} = \boldsymbol{J_s}/\Delta \boldsymbol{C_m}$, and the K parameter was obtained based on **Eqn. (6)** by using the diffusion coefficient shown in **Table 15**.

Fertilizers	**Solute resistance in the support layer, K (m^2h/kg)**	**Salt permeability coefficient, B ($kg/m^2/h$)**
Mono-ammonium phosphate	0.076	0.024
Ammonium sulphate	0.0706	0.022
Potassium phosphate monobasic	0.0789	0.029
Di-ammonium phosphate	0.0883	0.134
Sodium nitrate	0.0567	0.39
Ammonium chloride	0.0435	0.577
Potassium chloride	0.0450	0.441
Calcium nitrate	0.0797	0.296
Ammonium nitrate	0.0488	0.646
Urea	0.6099	17.885
Potassium nitrate	0.0452	0.657

For efficient and sustainable operation of the FO process, high RSFS is therefore desirable (Achilli et al., 2010). For example, RSFS of 6 L/g indicates that 6 L of permeate can be produced per gram of a draw solute lost by RSF. Results showed that MAP has the highest RSFS (5.98 L/g) followed by SOA, MKP, and DAP (see **Fig. 30c**), which means that MAP can produce the highest permeate per gram of lost draw solute. As mentioned previously, low RSF can be beneficial for the anaerobic process. However, since RSFS is the ratio of water flux and RSF, high RSFS means high water flux or low RSF. Therefore, when evaluating DS, both water flux and RSF should be considered.

Two parameters (i.e., water flux and RSF) were used to evaluate the performance of fertilizer as DS. These parameters were normalized to find out the optimum fertilizer as shown in **Table 15**. In case of water flux, each value of fertilizers was divided by the highest value and the ratios ($J_w/J_{w,Highest}$) were obtained for each fertilizer chemical. Similarly, the ratio ($J_{s,Lowest}/J_s$) for RSF was also determined by dividing RSF by the lowest RSF. In terms of water flux, KCl, NH_4Cl, and NH_4NO_3 ranked high, while in terms of RSF, MAP, SOA, and MKP ranked high.

From these results, it is evident that MAP, SOA, MKP, KCl, NH_4NO_3 and NH_4Cl could be ranked high and thus could be considered as the most suitable fertilizers in terms of FO performance. These selected fertilizers can be divided into two groups. The first group (i.e., MAP, SOA, and MKP) is a group with low RSF with moderate water flux, and the second group (i.e., KCl, NH_4NO_3, and NH_4Cl) with higher water flux with relatively high RSF. Therefore, the comparison of two different groups is expected to provide useful information. Consequently, these six selected fertilizers will be examined for their influence on the performance of AnFDFOMBR measured in terms of anaerobic activity on BMP due to salt accumulation.

Table 15. Ratios between the best draw solution and the draw solution itself for water flux, performance ratio, and reverse salt flux. Each draw solution was evaluated at concentration of 1 M.

Fertilizers	Relative water flux $(J_w/(J_w)_{KCl})$	Relative reverse salt flux $((J_s)_{MAP}/J_s)$
NH_4NO_3	0.917	0.027
SOA	0.806	0.755
NH_4Cl	0.956	0.057
$Ca(NO_3)_2$	0.854	0.045
$NaNO_3$	0.788	0.061
KCl	1	0.051
MAP	0.616	1
DAP	0.607	0.181
KNO_3	0.906	0.024
Urea	0.19	0.004
MKP	0.664	0.534

4.3.3 Bio-methane potential measurements

For BMP experiments, concentrations of fertilizer in the AnFDFOMBR were estimated using **Eqn. (3)** with the assumption of 9 dilution factor and the draw and reactor volumes of 2 L and 6 L, respectively. As shown in **Table 16**, high RSFS resulted in low concentration of fertilizer in the reactor since the equation derived in this study was reversely related to RSFS.

Table 16. Concentrations of selected fertilizers in the bioreactor. These values were determined based on **Eq. (8)** with assumption of 9 dilution factor, and respective draw and reactor volumes of 2 L and 6 L.

	MAP	SOA	MKP	KCl	NH_4NO_3	NH_4Cl
Concentration (g/L)	0.44	0.45	0.78	5.35	10.98	5.08

To investigate the effect of selected fertilizers on the anaerobic biological process, BMP experiments were carried out at determined fertilizer concentrations (see **Table 16**) during 4 days of operation. The substrate characteristics after BMP experiments were analysed and shown in **Table 17**. Results showed that MAP has the highest bio-methane production among six fertilizers as shown in **Fig. 31a** but all fertilizers had lower bio-methane production compared to the control (DI water addition) thereby indicating that these inorganic chemical fertilizers could inhibit anaerobic microbial activity even at their low concentrations (Chen et al., 2008, Ansari et al., 2015). The results in **Fig. 31b** further confirm that the biogas production linearly decreases as the fertilizer concentration due to RSF increases in the bioreactor except for MAP which did not fit it within the regression line. This likely shows that the presence of MAP in the bioreactor is likely to have a significantly different influence on the AnMBR compared to the other fertilizers. For the fertilizer group with high concentration (i.e., KCl, NH_4NO_3, and NH_4Cl), they exhibited lower biogas production (i.e., 122 mL, 66 mL, and 84 mL, respectively) than the fertilizer group with low concentrations.

Table 17. Substrate characteristics before and after BMP experiments.

	Sludge	KCl	SOA	NH_4Cl	NH_4NO_3	MAP	KH_2PO_4	DI water
TS (%)	3.03	2.18	1.7	2.17	2.67	2.64	2.56	2.86
MLSS (g/L)	27.9	18.0	15.7	17.4	18.8	25.5	26.0	27.2
COD (mg/L)	1,860	1,230	1,580	1,540	1,960	1,610	1,360	1,460
pH	7.19	7.23	7.2	7.31	7.66	7.01	7.02	7.03

The lower concentration group (i.e., MAP, SOA, and MKP) showed significantly different behaviours in the biogas production. The difference in the biogas production between MKP and MAP was 313 mL after 4 days, while their difference in molar concentration was only 5.7 mM. This result indicates that MKP and SOA have higher inhibition impact on anaerobic activity than MAP. In the case of SOA, SRB can reduce sulphate to sulphide in the presence of sulphate ions. Thus, in the presence of sulphate ions, the SRB have to compete with methanogen bacteria for common organic and inorganic resources. In addition, reduced sulphide ion is toxic to other bacteria groups thereby likely inhibiting or killing certain bacterial species useful for the BMP (Chen et al., 2008, Chen et al., 2014a). In the case of MKP, the presence of potassium ions could also inhibit the anaerobic process since high potassium concentration can lead to a passive influx of potassium ions which neutralize the membrane potential (Chen et al., 2008). However, in this study, potassium concentration was under 250 mg/L and thus MKP is expected to have less inhibition effect based on the previous study (Chen et al., 2008).

Therefore, in order to understand more about the influence of the potassium ions using MKP, further study would be required.

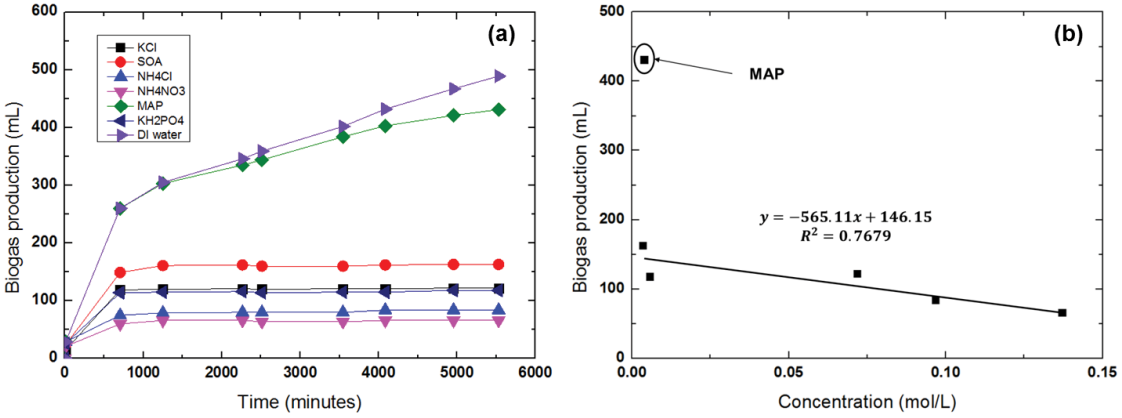

Figure 31. Bio-methane potential results: (a) influence of fertilizers on the biogas production for 4 days of operation, and (b) comparison of biogas production with fertilizer concentration. Biogas production volumes with respect to fertilizers were determined after 4 days of operation. Experimental conditions: 700 mL of digested sludge with addition of 50 mL of each fertilizer solution; and temperature of 35 ºC.

4.3.4 Salt accumulation in anaerobic fertilizer-drawn forward osmosis membrane bioreactor

Fig. 32 shows the modelled water flux versus the experimental water flux for all the eleven fertilizer initially selected for this study. The theoretical model used in this study was derived by accounting ECP effect on the feed side of the active layer and ICP effect in the support layer (McCutcheon and Elimelech, 2006). Results showed that the modelled water flux reasonably agreed with the experimental data. Therefore, the models for salt accumulation by feed and draw solutes in the bioreactor were derived based on this basic water flux model as presented in **Section 4.2.5**.

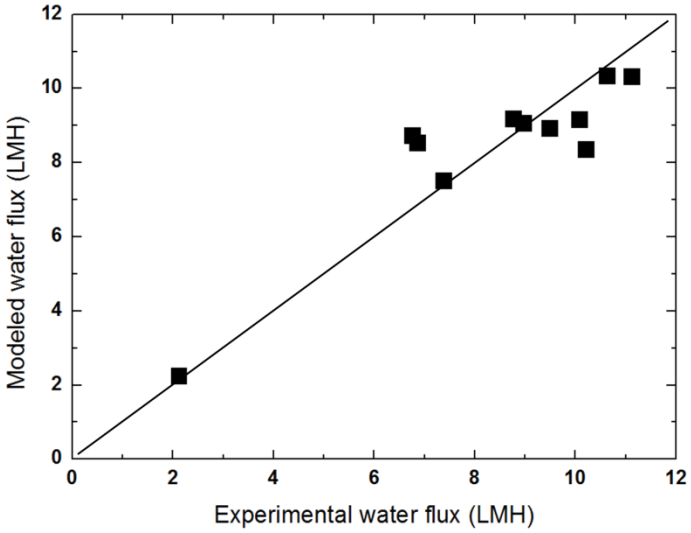

Figure 32. Comparison of experimental water fluxes with modelled water fluxes. Modelled water fluxes were calculated based on **Eqn. (4)** by using A and S parameters shown in **Table 12** and diffusivity of fertilizers shown in **Table 14**.

Based on the salt accumulation models, time-dependent water flux and reactor concentration were determined under the simulation conditions shown in **Table 18**, and the effect of fertilizer chemicals on salt accumulation was investigated. FO mode of membrane orientation was adopted since PRO mode previously showed severe fouling potential in the support layer (Kim et al., 2015a). Influent solute concentration was determined as 10 mM NaCl. SRT was determined for 10 days to see how much sludge waste can affect salt accumulation. Initial HRT used in this study was determined based on the initial water fluxes of fertilizer draws solutions. To simulate the OMBR integrated with FDFO, we assumed that DS is diluted unlike usual OMBR that constant draw concentration is applied since diluted DS is recovered by post-treatment (e.g., RO, NF, MD, etc.). A set of ordinary differential equations (ODEs) described in **Section 5.2.5** were numerically solved to simulate AnFDFOMBR.

Table 18. Simulation conditions for predicting salt accumulation in the bioreactor.

Items	Values
Reference membrane	HTI CTA FO membrane (see **Table 12**)
Membrane area	0.05 m^2
Membrane orientation	FO mode (AL-FS)
Reactor and draw tank volumes	6 L
Influent salt concentration	10 mM NaCl
Draw solution concentration	1 M fertilizer chemicals
Solid retention time (θ_{SRT})	10 days

To investigate the effect of the presence of fertilizer salts on the performance of OMBR, water flux, HRT and salt concentrations in the bioreactor and the draw tank solution was simulated over time. Results showed that water flux for all the fertilizers severely declined with time as shown in **Fig. 33a** since FS and DS in FO were continuously diluted and concentrated with time. After 240 h of operation, SOA exhibited the highest water flux (1.58 L/m^2/h) followed by MAP and MKP despite the fact that NH_4Cl had the highest initial water flux (10.33 L/m^2/h) followed by KCl and SOA. This different flux decline behaviour of each fertilizer was likely due to the differences in the salt accumulation rate by RSF as shown in **Fig. 33b**. In the case of NH_4NO_3, it had not only high water flux (10.21 L/m^2/h) but also high RSF (42.01 g/m^2/h). Therefore, a significant amount of draw solutes moved from DS to the bioreactor and thus the concentration gradient was significantly reduced. On the contrary for MAP, it had low water flux (6.86 L/m^2/h) but also low RSF (1.15 g/m^2/h) and thus only small amount of draw solutes were expected to move to the bioreactor. Although it has the lowest final salt concentration (42.37 mM) in the bioreactor, MAP exhibited the second highest final water flux (1.55 L/m^2/h) following

by SOA which had lower *K* parameter (0.071 m^2h/kg) and higher osmotic pressure (46.1 atm) than MAP. Besides bioreactor concentration, change in the draw concentration also affects the change in the water flux based on **Eqn. (6)**

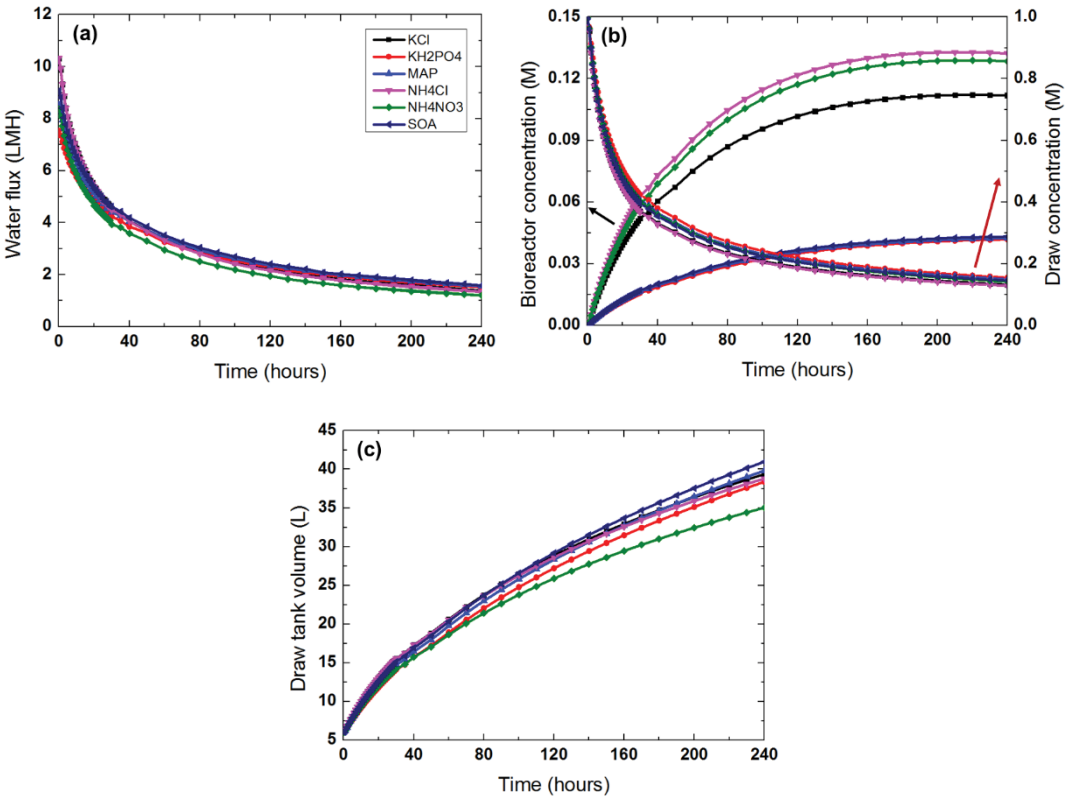

Figure 33. Simulated (a) water fluxes, (b) salt concentration in a bioreactor (left axis) and fertilizer concentration in draw tank (right axis), and (c) draw tank volume as a function of operation time.

Results (see **Figs. 31b & 31c**) show that NH_4Cl had the lowest final draw concentration (0.13 M) followed by KCl and NH_4NO_3 by the end of the experimental duration of 240 h despite the fact that SOA had the highest dilution capacity (i.e., DF 6.83) which is an important factor in FDFO to supply diluted fertilizer solution for the agricultural purpose (Phuntsho et al., 2013a). This variation in the dilution trend between draw concentration

and draw volume is due to the differences in their salt accumulation rates of each fertilizer DS. Since fertilizers with high initial water flux showed more severe flux decline and also high RSF, their average water flux became lower than fertilizers having lower initial water flux and RSF and thus dilution capacity also became lower. However, the loss of draw solutes due to RSF also played an important role in reducing the draw concentration with time. In the case of NH_4Cl, it had the fourth highest average water flux but also resulted in the highest solute concentration in the bioreactor. Therefore, NH_4Cl could achieve the lowest final draw concentration at the end of the operation but, as shown in **Fig. 31**, it is possible for higher inhibition potential on the anaerobic microbial activity due to high RSF and hence high solute accumulation rate. From these results, it can be concluded that DS should have low RSF for the stable long-term operation of the AnFDFOMBR.

The rate of solute accumulation in the bioreactor by feed and draw solutes is separately simulated and presented in **Fig. 34**. As shown in **Fig. 34a**, the solute concentration in the bioreactor caused due to rejection of influent feed solutes continuously increased over time although the rate of accumulation decreased at the later stages of the operation time. This slight decrease in the rate of feed solute accumulation in the bioreactor was due to decrease in the water flux with time as a result of the cumulative dilution of DS with time when operated in a batch process. Similarly, the accumulation of draw solutes in the bioreactor increased continuously with time but the rate of accumulation gradually decreased over time beyond certain operation time which is also due to reduction in the DS concentration with the cumulative dilution of DS in the tank. As evident in **Fig. 34b**, the first group of fertilizer (KCl, NH_4NO_3 and NH_4Cl) with high RSF exhibited significantly higher concentration of accumulated draw solute while the second group (SOA, MAP, MKP) showed significantly lower concentration of accumulated draw solute.

Interestingly, fertilizers with high RSF (first group) exhibited slower rate of salt accumulation in the bioreactor after 180 h of operation compared to the second group which showed a continuous and rather linear rate of accumulation. This decrease in the rate of draw solute accumulation in the bioreactor for the first group is attributed to the reduction in the RSF due to cumulative decrease in the DS concentration with time. From these results, it can be concluded that DS for the AnFDFOMBR should have desirably low RSF for stable operation.

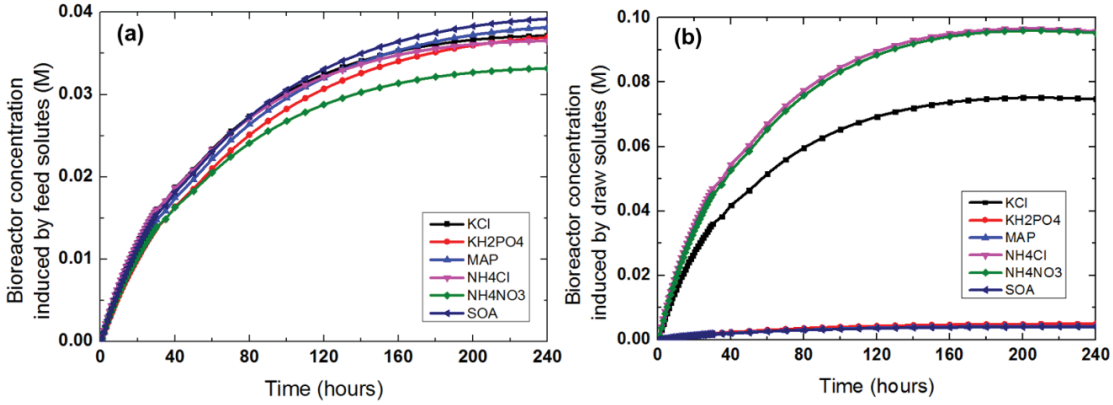

Figure 34. Influence of fertilizers on salt accumulation in the bioreactor: (a) induced by feed solutes rejected by the FO membrane and (b) induced by the back diffusion of draw solutes.

Comparing **Fig. 34a and 34b** shows that the rate of feed solute accumulation is not significantly affected by the types of fertilizer DS while the rate of draw solute accumulation is highly influenced by the types of DS used. This is because the rate of feed solute accumulation mostly depends on the feed solute rejection rate of the FO membrane. The differences in the water flux generated by each fertilizer also slightly influences the accumulation rates in the batch process as it affects the influent flow rate and hence the mass of the feed solutes that reaches the bioreactor.

4.3.5 Most suitable fertilizer draw solution for anaerobic fertilizer-drawn forward osmosis membrane bioreactor

Among eleven pre-screened fertilizer candidates, the fertilizer chemicals which ranked particularly high in terms of the water flux are NH_4NO_3, KCl, and NH_4Cl, while the fertilizer chemicals which ranked best in terms of RSF are MAP, SOA, and MKP. Considering both the criteria, six fertilizers (i.e., MAP, SOA, MKP, KCl, NH_4Cl, and NH_4NO_3) are ranked high for further investigation. Since all fertilizer chemicals are inorganic salts which can inhibit the biological activities of the anaerobic microorganisms, low RSF is therefore desirable for the biological application as well as for maintaining stable operation and reducing salinity build-up in the bioreactor. In terms of BMP, MAP exhibited better potential as DS for AnFDFOMBR than other fertilizers. In addition, in terms of salt accumulation, MAP and SOA ranked best considering the water flux sustainability and salinity build-up by DS. Thus, MAP is projected as likely the best DS for the AnFDFOMBR process.

The other criterion which must be considered while selecting a suitable fertilizer draws solution candidate is the influence of the draw solute on the fouling and scaling potential during the AnFDFOMBR process. Based on the earlier studies (Phuntsho et al., 2014), MAP has been observed to have low scaling or fouling potential compared to other fertilizers. DAP has been reported to have very high scaling potential especially when feed water contains calcium and magnesium ions (Phuntsho et al., 2014). The presence of scaling precursor ions such as Ca^{2+} and PO_4^{3-} on the membrane surface may exceed its solubility limits of inorganic minerals such as $CaCO_3$ (calcite) and $Ca_3(PO_4)_2$ (tricalcium phosphate) (Greenberg et al., 2005) resulting in the formation of scales on the membrane surface thereby reducing the water flux. In addition to scaling, fertilizers containing

multivalent cations such as Ca^{2+} or Mg^{2+} can induce severe membrane fouling. The reverse diffusion of draw solute cations could promote foulant-membrane and foulant-foulant interactions thereby enhancing membrane fouling (She et al., 2012, Xie et al., 2015a).

4.4 Conclusions

Primary findings drawn from this study are summarized as follows:

- A selection procedure of fertilizers as DS for novel AnFDFOMBR was investigated.
- From preliminary screening and FO experiments, six fertilizers (i.e., MAP, SOA, MKP, KCl, NH_4NO_3, and NH_4Cl) were selected.
- MAP exhibited the highest biogas production since other fertilizers exhibited the inhibition effect on the anaerobic activity under determined concentrations.
- Simulation results showed that SOA and MAP were appropriate to OMBR integrated with FDFO since they had less salt accumulation and relatively higher water flux.
- For these reasons, MAP can be the most suitable DS for AnFDFOMBR.

5. Assessing the removal of organic micro-pollutants from anaerobic membrane bioreactor effluent by fertilizer-drawn forward osmosis

5.1 Introduction

Freshwater scarcity is getting more severe due to the impacts of climate change, rapid population growth and extensive industrialization (Rijsberman, 2006). Furthermore, about 70% (global average) of the accessible freshwater is still consumed by the agricultural sector (Clay, 2004). Particularly in water scarce regions, wastewater reuse in the agricultural sector can be very helpful in sustaining freshwater resources. Besides, treated wastewater can contribute an appreciable amount of necessary nutrients for plants (Jeong et al., 2016). Therefore, the use of reclaimed water for agricultural irrigation has been reported in at least 44 countries (Jiménez Cisneros and Asano, 2008). For example, 30-43% of treated wastewater is used for agricultural and landscape irrigation in Tunisia (Bahri, 2009). However, wastewater reuse is often limited due to the presence of harmful heavy metals, industrial waste, pharmaceutical and personal care products (PPCPs), and excess salts. Organic micro-pollutants (OMPs), originating from PPCPs, herbicides and pesticides, and industry, could have potential harmful impacts on public health and the environment because of their bioaccumulation (Snyder et al., 2003). Therefore, OMPs should be effectively removed to enable reuse of wastewater for irrigation (2004).

AnMBR has been studied for wastewater treatment as the treatment scheme has several advantages, including complete rejection of suspended solids, low sludge production, high organic rejection and biogas production (Stuckey, 2012). Recent studies on the efficiency of OMPs removal in the AnMBR process indicated that bio-transformation is the dominant OMPs removal mechanism (Wang et al., 2014a) and there is a correlation between hydrophobicity, specific molecular features (i.e., EWGs and EDGs) and OMPs

removal efficiency (Wijekoon et al., 2015). Especially, most readily biodegradable OMPs contain strong EDGs while most refractory OMPs contain strong EWGs or halogen substitute (Wei et al., 2015). Besides, some OMPs can be captured by the fouling layer on the membrane surface thereby enhancing their removal efficiencies (Monsalvo et al., 2014). Even though OMPs can be biodegraded and removed by AnMBR, their removal rate is not sufficient for the wastewater reuse since some OMPs are rarely treated by AnMBR (Wei et al., 2015, Wijekoon et al., 2015).

For wastewater reuse advanced post-treatment processes (e.g., NF, RO, FO or advanced oxidation) are often required to enhance the removal efficiency since most OMPs, even at very low concentration levels, may have a negative effect on the environment. Stand-alone NF can remove OMPs with their rejection rates from about 20% to almost 100% depending on their different characteristics (i.e., hydrophobicity and molecular shape) (Kiso et al., 2001). By combining AnMBR with NF, the OMPs removal efficiency can be improved up to 80 – 92% (Wei et al., 2015). Furthermore, TFC PA RO membranes have a 57 – 91% rejection range for OMPs, which is lower than the salt rejection rate since OMPs are generally of low molecular size and are neutral compounds (Kimura et al., 2004). On the other hand, FO has a higher OMPs removal efficiency than RO since OMPs forward flux is likely hindered by RSF of the draw solute (Xie et al., 2012a). However, since FO utilizes highly concentrated DS as a driving force, additional desalting processes (e.g., NF, RO or MD) are required to extract pure water from DS (Cath et al., 2006).

Recently, FDFO has received increased attention since the diluted fertilizer solution can be utilized directly for irrigation purpose and thus a separation and recovery process for the diluted DS is not required (Phuntsho et al., 2011, Phuntsho et al., 2012b, Xie et al., 2015b). In the early studies, both single and blended fertilizers were investigated for direct application, however the diluted fertilizer solution still required substantial dilution as the

final nutrient concentration exceed the standard nutrient requirements for irrigation, especially using feed water sources with high salinity (Phuntsho et al., 2011, Phuntsho et al., 2012b). For high salinity feed water, a NF process can be employed as a post-treatment for further dilution thereby meeting the water quality requirements for fertigation (Phuntsho et al., 2013a). A pilot-scale FDFO and NF hybrid system was recently evaluated for 6 months in the field (Phuntsho et al., 2016). However, the energy consumption of the NF process is still a challenge for such a FDFO-NF hybrid system. PAFDFO is another suitable option for further enhancing final dilution of fertilizer DS beyond the point of osmotic equilibrium between DS and FS (Sahebi et al., 2015).

FDFO is viewed to be more suitable for the treatment of low salinity impaired water sources so that a desired fertilizer dilution can be achieved without the need of a NF post-treatment process. Recent reports have shown FDFO has been applied using commercial liquid fertilizers for the osmotic dilution of wastewater for fertigation of green walls (Xie et al., 2015b, Zou and He, 2016). For both wastewater reuse and irrigation purposes, a novel FDFO-AnMBR hybrid system for a greenhouse hydroponic application was proposed and reported in our earlier study (Kim et al., 2016). Despite the recent efforts to develop and understand FDFO for wastewater treatment (Chekli et al., 2017), OMPs removal in FDFO has not yet been investigated, in particular the impact of fertilizer properties, fertilizer concentration and FO membrane orientation. Moreover, by combining FDFO with AnMBR, total OMPs removal rates can be significantly enhanced since FDFO can treat non-biodegradable OMPs from AnMBR.

The main objective of this study is therefore to investigate the feasibility of FDFO for treatment of AnMBR effluents with a particular emphasis on OMPs removal and membrane fouling. Atenolol, atrazine, and caffeine were utilized as representatives of OMPs due to their low removal propensity in AnMBR. The study also looked at how

membrane fouling may be affected during the treatment of AnMBR effluents by FDFO as a function of types of fertilizer DS used in relation to their concentrations and thermodynamic properties and membrane orientation. Finally, the effect of membrane fouling on OMPs transport was also investigated.

This chapter is an extension of a research article published by the author in Journal of Membrane Science.

5.2 Experiments

5.2.1 FO membrane

Cellulose triacetate (CTA) FO membranes embedded in a woven polyester mesh, provided by Hydration Technology Innovations, HTI (Albany, OR, USA), was used in this study. The detail characteristics of this commercial membrane can be found elsewhere (McCutcheon and Elimelech, 2008, Kim et al., 2015c).

5.2.2 Feed solution

AnMBR effluent used for FDFO treatment was collected from a lab-scale AnMBR system. The lab-scale AnMBR system consisted of a commercial anaerobic stirred tank reactor (CSTR, Applikon Biotechnology, Netherland) with an effective volume of 2 L and a side-stream hollow-fiber polyvinylidene fluoride (PVDF) UF membrane with a nominal pore size of 30 nm (Wei et al., 2014, Wei et al., 2015). The recipe of synthetic wastewater with COD of 800 mg/L used in this system can be found elsewhere (Wei et al., 2014). The operational conditions of this system were as follows: temperature 35 ± 1 °C, pH 7 ± 0.1, stirring speed 200 ± 2 rpm, MBR water flux of 3 L/m^2/h and HRT of 24 h. For all the FDFO experiments in this study, AnMBR effluent was collected every day for 2 weeks, mixed together and stored in a refrigerator at 4 °C to obtain a homogeneous

feed water composition throughout the study. Detail information of AnMBR effluent used as feed in this study is provided in **Table 19**.

Table 19. Water quality of anaerobic membrane bioreactor effluent used in this study. The analysis was conducted repeatedly.

Components	Values	Components	Values
COD (ppm)	57.2 (±9.12)	K^+ (ppm)	11.8 (±2.69)
Conductivity (mS/cm)	1.68 (±0.28)	Na^+ (ppm)	23.5 (±3.27)
TP (ppm PO_4-P)	32.2 (±2.97)	Mg^{2+} (ppm)	3.95 (±0.57)
TN (ppm N)	84.8 (±13.79)	Cl^- (ppm)	9.21 (±1.42)
Turbidity	0.77 (±0.02)	SO_4^{2-} (ppm)	1.04 (±0.14)
pH	8 (±0.13)		

Three different OMPs (Atenolol, Atrazine and Caffeine), received in powder form from Sigma Aldrich (Saudi Arabia), were used as representative OMPs since they are generally found in wastewater but not readily removed in AnMBR (Wei et al., 2015). Atenolol and atrazine contain both EDGs and EWGs and are therefore possible refractory compounds, and also caffeine has a low removal rate at the initial stage due to its prolonged adaption time even though caffeine has a strong EDG, which is supported by experimental results (Wei et al., 2015). Their key properties are provided in **Table 20**. Stock solution of 3 g/L (i.e., 1 g/L for each OMP) was prepared by dissolving total 3 mg of OMP compounds (i.e., 1 mg for each OMP) in 1 mL of pure methanol and the stock solution was then stored in a refrigerator at 4 °C prior to the experiments.

Table 20. Physicochemical properties of OMPs used in this study.

	Atenolol	Atrazine	Caffeine
Structure *	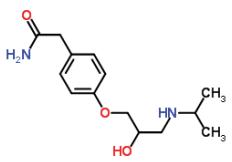	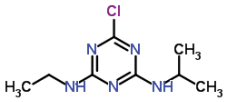	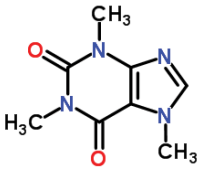
Application	Beta-blocker	Herbicide	Stimulant
Formula	$C_{14}H_{22}N_2O_3$	$C_8H_{14}ClN_5$	$C_8H_{10}N_4O_2$
Molecular weight	266.3 Da	215.7 Da	194.2 Da
Charge [9]	Positive	Neutral	Neutral
pK_a*	9.6	1.7	10.4
Log K_{ow}*	0.16	2.61	-0.07

* Data from ChemSpider website (http://www.chemspider.com).

5.2.3 Draw solutions

Three different chemical fertilizers of reagent grade were used in this study (Sigma Aldrich, Saudi Arabia) and they consisted of mono-ammonium phosphate (MAP), di-ammonium phosphate (DAP) and potassium chloride (KCl). MAP and DAP are composed of the same components (N and P) but have different thermodynamic properties such as osmotic pressure and diffusivity while KCl has a different composition but has a similar osmotic pressure with MAP (Kim et al., 2016). DS was prepared by dissolving fertilizers in DI water. Detailed information of fertilizer chemicals is provided

in **Table 21**. Osmotic pressure, diffusivity and viscosity of three fertilizers were obtained by OLI Stream Analyzer 3.2 (OLI System Inc., Morris Plains, NJ, USA).

Table 21. Details of the fertilizer chemicals used in this study. Thermodynamic properties were determined at temperature of 20 ºC by using OLI Stream Analyzer 3.2. Mass transfer coefficients in the flow channel were calculated based on **Eqns. (17) ~ (22)**.

Chemicals	MAP		DAP		Potassium chloride	
Formula	$NH_4H_2PO_4$		$(NH_4)_2HPO_4$		KCl	
Molecular weight (g/mol)	115.0		132.1		74.6	
Concentration	1 M	2 M	1 M	2 M	1 M	2 M
Osmotic pressure (atm)	43.4	86.14	49.85	93.57	43.3	87.95
Diffusivity ($\times \mathbf{10^{-9}}$ m^2/s)	1.05	1.08	0.87	0.87	1.59	1.55
Viscosity (mPa • s)	1.33	1.73	1.11	1.20	0.99	0.99
Mass transfer coefficients ($\times \mathbf{10^{-5}}$ m/s)	1.01	1.03	0.89	0.89	1.33	1.31

5.2.4 FDFO experiments

5.2.4.1 Lab-scale FO system

All FDFO experiments were carried out using a lab-scale FO system similar to the one described in our previous studies (Lee et al., 2015, Kim et al., 2015c). The FO cell had two symmetric channels (i.e., 100 mm long, 20 mm wide and 3 mm deep) on both sides of the membrane each fed with FS and DS respectively. Variable speed gear pumps (Cole-Parmer, USA) were used to provide crossflows under co-current directions at a crossflow rate of 8.5 cm/s. Solution temperature was 20°C. Both solutions were recirculated in a closed-loop system resulting in a batch mode process operation. The DS tank was placed on a digital scale and the weight changes were recorded by a computer in real time every 3 mins interval to determine the water flux.

5.2.4.2 AnMBR effluent treatment by FDFO

FDFO experiments were carried out under either AL-FS or AL-DS modes at 1 M or 2 M fertilizer DS concentrations. Detailed descriptions of FO experiments are available elsewhere (Phuntsho et al., 2014, Lee et al., 2015, Kim et al., 2015c). Crossflow velocities of DS and FS were set at 8.5 cm/s and temperature at 20°C. For FDFO performance experiments, DI water was utilized as FS with fertilizer DS. In order to investigate the OMPs transport behaviours in FDFO during AnMBR effluent treatment, prior to all experiments, 10 μL of OMPs stock solution was spiked into 1 L FS (i.e., AnMBR effluent) to obtain a final concentration of 10 μg/L each of the three OMPs, giving a total of 30 μg/L (Wei et al., 2015). For understanding OMPs transport behavior, average water flux during FDFO experiments was obtained and compared with OMPs forward flux.

$$J_{w,a} = \frac{V_p}{A_m t} = \frac{V_{Df} - V_{Di}}{A_m t}$$ **Equation 15**

where, $J_{w,a}$ is the average flux during AnMBR effluent treatment (L/m^2/h), V_p is the permeate volume (L), V_{Di} is the initial volume of DS (L), V_{Df} is the final volume of DS (L), A_m is the membrane area (m^2), and t is time (h). Mass transfer coefficients were further obtained to elucidate the FO performance in terms of water flux and physical cleaning efficiency. Firstly, Reynolds number was determined by **Eqn. (16)** to see whether the type of flow in the channel is laminar or turbulent. Then, Schmidt number and hydraulic diameter (for fully filled rectangular duct) were obtained based on **Eqns. (17) and (18)**, respectively. By using Reynolds number, Schmidt number and hydraulic diameter, Sherwood number was calculated as **Eqns. (19) or (20)** for laminar or turbulent flows in fully filled rectangular duct, and thus a mass transfer coefficient could be lastly obtained as **Eqn. (21)**.

$$\boldsymbol{Re} = \frac{\boldsymbol{v d_h}}{\boldsymbol{\nu}}$$ **Equation 16**

$$\boldsymbol{Sc} = \frac{\boldsymbol{\nu}}{\boldsymbol{D}}$$ **Equation 17**

$$\boldsymbol{d_h} = \frac{\boldsymbol{2ab}}{\boldsymbol{a+b}}$$ **Equation 18**

$$\boldsymbol{Sh} = \boldsymbol{1.85(Re \cdot Sc \cdot d_h/L)^{0.33}}$$ **Equation 19**

$$\boldsymbol{Sh} = \boldsymbol{0.04 Re^{0.75} \cdot Sc^{0.33}}$$ **Equation 20**

$$\boldsymbol{k} = \frac{\boldsymbol{Sh \cdot D}}{\boldsymbol{d_h}}$$ **Equation 21**

where, *Re* is Reynolds number, *Sc* is Schmidt number, d_h is the hydraulic diameter of the flow channel (m), *Sh* is Sherwood number, *k* is mass transfer coefficient (m/s), ν is the average crossflow rate (m/s), *a* is the width of the flow channel (m), *b* is the height of the

flow channel (m), D is diffusivity of DS (m^2/s), υ is kinematic viscosity (m^2/s), and L is the length of the flow channel (m). Since DS is gradually diluted during FDFO operation, osmotic pressure difference was reduced during FDFO experiments. To evaluate the effect of membrane fouling only on flux decline, a baseline test was carried out for 10 h with DI water as FS prior to each experiment and the resulting flux curves were utilized as a baseline to correct the flux curves obtained (Kim et al., 2015c).

5.2.4.3 Physical cleaning

In order to investigate the effect of physical (or hydraulic) cleaning on flux recovery, two different physical cleaning methods were adopted for all FDFO experiments. Osmotic backwashing was however investigated only for those experiments conducted under the AL-DS mode. Physical cleaning consisted of flushing DI water inside the DS and FS channels at 3 times higher crossflow velocity (25.5 cm/s) for 30 mins. Osmotic backwashing was conducted for 30 mins by flushing 1M NaCl solution on the support layer side of the membrane and DI water on the active layer side (both at 8.5 cm/s crossflow velocity) in order to provide water flux in reverse direction to the experiment conducted under AL-DS mode of membrane orientation. After each physical cleaning, baseline FDFO experiments were conducted using fertilizers DS and DI FS to evaluate the water flux recovery rate.

5.2.5 Analytical methods for organic micro-pollutants

OMPs in samples were analyzed following the procedures described in previous studies (Alidina et al., 2014, Wei et al., 2015). 100 mL samples were prepared and spiked with the corresponding isotopes (Cambridge Isotope Laboratories, Inc., USA). OMPs samples

were first extracted via solid phase extraction (Dione Autotrace 280 solid-phase extraction instrument and Oasis cartridges) and then concentrated via evaporation. OMPs concentration was then measured by liquid chromatography (Agilent Technology 1260 Infinity Liquid Chromatography unit, USA) connected to mass spectrometry (AB SCIEX QTRAP 5500 mass spectrometer, Applied Biosystems, USA). OMPs forward flux to DS can be obtained based on mass balance for OMPs species (Kim et al., 2012, Kim et al., 2014a).

As the initial OMPs concentration in DS is zero, OMPs mass balance yields:

$$\boldsymbol{C_{OMPs}(V_{Di} + J_w A_m t) = J_{OMPs} A_m t} \qquad \textbf{Equation 22}$$

where, C_{OMPs} is the OMPs concentration in DS (mM/L), J_w is the measured water flux (L/m^2/h), and J_{OMPs} is the OMPs forward flux to DS (mM/m^2/h). For OMPs forward flux, **Eqn. (22)** can be modified as:

$$\boldsymbol{J_{OMPs} = \frac{C_{OMPs}(V_{Di}+J_w A_m t)}{A_m t} = \frac{C_{OMPs} V_{Df}}{A_m t}} \qquad \textbf{Equation 23}$$

OMPs rejection in FDFO can be calculated by using the permeate concentration, yielding (Xie et al., 2012b):

$$\boldsymbol{R_{OMPs} = \left(1 - \frac{C_{OMPs}}{C_{OMPs,f}}\right) \times 100\%} \qquad \textbf{Equation 24}$$

where, $C_{OMPs,f}$ is the OMPs concentration in the FS (mM/L).

5.2.6 Characterization of the membrane surface

Membrane surface characterization was conducted by collecting membrane coupons after experiments, soaking them in DI water for a few seconds to remove FS and DS, and then dried in a desiccator for 1 day. The surface and cross-sectional morphologies of the FO membrane were observed and analyzed by scanning electron microscopy (SEM, Zeiss Supra 55VP, Carl Zeiss AG, Germany) and energy dispersive X-ray spectroscopy (EDX) following the procedures described in a previous study (Woo et al., 2016). Samples taken from each membrane were first lightly coated with Au/Pd and then the SEM imaging was carried out at an accelerating voltage of 10 kV.

X-Ray diffraction (XRD) (Siemens D5000, USA) analysis was also performed over Bragg angles ranging from 10° to 60° (Cu Kα, λ=1.54059 Å) to investigate the dominant species responsible for scaling on the membrane surface.

Contact angles of fouled FO membranes were measured by the sessile drop method using an optical subsystem (Theta Lite 100) integrated with an image-processing software following the procedures described in a previous study (Woo et al.). Membrane samples were placed on a platform, and DI water droplets of 10 μL were dropped automatically on the membrane surface. A real-time camera captured the image of the droplet, and the contact angle was estimated by a computer. At least 3 measurements were taken for each membrane sample and the average value was used.

5.3 Results and discussion

5.3.1 AnMBR effluent treatment by FDFO

5.3.1.1 Basic FDFO performance: Water flux and reverse salt flux

Three different fertilizers (MAP, DAP and KCl) were selected as DS for this study. MAP and DAP are composed of the same components (N and P) but have different thermodynamic properties such as osmotic pressure and diffusivity while KCl has a different composition but has a similar osmotic pressure with MAP (Kim et al., 2016). As shown in **Table 23**, MAP exhibited similar water flux with DAP under the AL-FS mode, even though DAP has higher osmotic pressure. This is due to lower diffusivity of DAP species which enhances the ICP effects that lowers the water flux (Kim et al., 2015c). However, under the AL-DS mode, DAP exhibited higher water flux than MAP due to less pronounced effects on ICP (Cath et al., 2006).

KCl showed a much higher water flux than MAP under all experiments despite having similar osmotic pressures, which is attributed to the higher diffusivity of KCl that lowers ICP effects under the AL-FS mode of operation. KCl also shows higher water flux compared to MAP under the AL-DS mode even though ICP effect should have been eliminated for both DS since DI water was used as FS in the support layer side of the membrane. This higher water flux of KCl is related to the higher mass transfer coefficient (i.e., $1.33 \times 10^{-5}\ m/s$ and $1.01 \times 10^{-5}\ m/s$ for KCl and MAP, relatively) compared to MAP that results in lower dilutive ECP effects. The KCl has higher diffusivity and lower viscosity compared to the MAP that significantly enhances its mass transfer coefficient (refer **Table 21**). The mass transfer coefficient of the draw solute depends on the average solute diffusivity and solution viscosity, assuming that the other operating conditions were similar for both KCl and MAP.

The performance of the three fertilizer DS was also investigated in terms of RSF. KCl showed the highest RSF in all cases probably due to its highest solute diffusivity and also lower hydrated diameters of both K^+ and Cl^- species (Achilli et al., 2010). Interestingly, DAP showed much higher RSF than MAP even though they have similar components and DAP has much lower diffusivity as shown in **Table 23**. This can probably be explained due to the differences in their species formed in the water with DAP and MAP. Speciation analysis was carried out for 1 M DAP and 1 M MAP using OLI Stream Analyzer and their data is presented in **Table 22,** where the three major species (NH_4^+, $H_2PO_4^-$ and NH_3) are considered to be of particular interest for comparison. It can be seen that 1 M DAP DS contains about 1.974 M NH_4^+ compared to 1.0 M NH_4^+ for MAP DS. This is one potential reason why the RSF of NH_4^+ for DAP was observed to be higher than MAP in **Table 24**. Besides, 1 M DAP DS also contains 0.026 M NH_3 (in aqueous form) as one of the species and this uncharged aqueous NH_3 being small in molecular size is highly likely to reverse diffuse through the FO membrane towards the feed further contributing to the RSF value. This is also probably the main reason why the pH of the FS was observed to increase above pH 9 when the FO was operated with DAP as DS. Once in the FS, NH_3 is expected to slightly dissociate further to produce NH_4^+ increasing OH^- ions that give the pH rise.

Table 22. Speciation analysis results of 1 M MAP and DAP by using OLI Stream Analyzer.

Species	MAP (mole/L)	DAP (mole/L)
H_2O	55.526	55.524
H^+	1.032×10^{-4}	3.393×10^{-8}
OH^-	2.225×10^{-10}	9.519×10^{-7}
$H_2P_2O_7^{2-}$	1.735×10^{-2}	1.558×10^{-5}
$H_2PO_4^-$	0.953	2.066×10^{-2}
$H_3P_2O_7^-$	4.22×10^{-5}	4.699×10^{-12}
H_3PO_4	5.932×10^{-3}	2.55×10^{-8}
$H_4P_2O_7$	6.167×10^{-8}	1.352×10^{-18}
$HP_2O_7^{3-}$	6.612×10^{-4}	5.5×10^{-3}
HPO_4^{2-}	5.411×10^{-3}	0.947
NH_3	5.212×10^{-6}	2.593×10^{-2}
NH_4^+	1.00	1.974
$P_2O_7^{4-}$	1.03×10^{-7}	1.06×10^{-2}
PO_4^{3-}	2.098×10^{-10}	2.664×10^{-4}
Total	57.508	58.508

The RSF of total PO_4 ions, however, was observed to be higher for MAP compared to DAP, which is probably due to the differences in concentrations of $H_2PO_4^-$ species in their solutions. $H_2PO_4^-$ is one of the major species common to both MAP and DAP and is a monovalent species. Thus, it is likely to reversely diffuse more compared to other species which are mostly multivalent. **Table 22** shows that 1 M MAP (0.953 M of $H_2PO_4^-$) has much higher concentration of $H_2PO_4^-$ than 1 M DAP DS (0.021 M of $H_2PO_4^-$). This likely explains why MAP has higher RSF for total PO_4 ions compared to DAP as presented in **Table 24**.

Table 23. Water flux and reverse salt flux with different membrane orientation and draw solution concentration. Experiment conditions of FO experiments: DI water as feed solution; crossflow rate of 8.5 cm/s; temperature of 20 ± 1°C.

	AL-FS mode (1 M DS)			AL-FS mode (2 M DS)			AL-DS mode (1 M DS)		
	MAP	DAP	KCl	MAP	DAP	KCl	MAP	DAP	KCl
Water flux ($L/m^2/h$)	7.71	7.64	11.64	9.46	9.19	17.12	14.28	16.18	18.08
Reverse salt flux ($mmol/m^2/h$)	0.68	2.46	6.42	0.64	3.78	12.30	1.03	2.00	11.33

Table 24. Reverse salt flux of ionic species with different membrane orientation and draw solution concentration. Experiment conditions of FO experiments: feed solution of DI water; cross-flow rate of 8.5 cm/s; temperature of 20 ± 1 °C.

	AL-FS mode (1 M DS)		AL-FS mode (2 M DS)		AL-DS mode (1 M DS)	
	MAP	DAP	MAP	DAP	MAP	DAP
NH_4^+ (mmol/m^2/h)	0.02	0.12	0.02	0.18	0.02	0.08
HPO_4^{2-} (mmol/m^2/h)	0.02	0.01	0.02	0.01	0.03	0.02

5.3.1.2 Flux decline during AnMBR effluent treatment by FDFO

FDFO experiments were conducted using AnMBR effluent as FS and the three fertilizers as DS. Flux data are presented as normalized flux in **Fig. 35**. When FDFO experiments were first carried out at 1 M DS under the AL-FS mode of membrane orientation, KCl (11.77 L/m^2/h) exhibited the highest initial water flux followed by MAP (7.82 L/m^2/h) and DAP (7.33 L/m^2/h), shown in **Table 25**, which is consistent with our earlier studies (Phuntsho et al., 2014, Kim et al., 2016). As shown in **Fig. 35a**, all fertilizers tested did not show any flux decline during the 10 h of FO operation. Compared to the SEM image of the virgin membrane surface in **Fig. 35a,** the SEM images of the FO membrane surfaces after FO experiments in **Fig. 36b and 36c** with MAP and KCl appear very similar to the virgin membrane surface, suggesting that no significant fouling/scaling layer was formed on the membrane surface. However, results with DAP clearly show the presence

of a partial scaling layer on the membrane surface (**Fig. 36d**), although no flux decline was also observed with this fertilizer (**Fig. 35a**).

Table 25. Initial water flux and average water flux with different membrane orientation and draw solution concentration. Experiment conditions of FO experiments: AnMBR effluent as feed solution; cross-flow rate of 8.5 cm/s; temperature of 20 ± 1°C.

	AL-FS mode (1 M DS)			AL-FS mode (2 M DS)			AL-DS mode (1 M DS)		
	MAP	DAP	KCl	MAP	DAP	KCl	MAP	DAP	KCl
Initial water flux ($L/m^2/h$)	7.82	7.33	11.77	9.4	9.16	17.62	13.25	12.84	15.64
Average water flux ($L/m^2/h$)	7.58	7.35	11.20	9.23	8.72	16.32	10.48	5.10	9.44

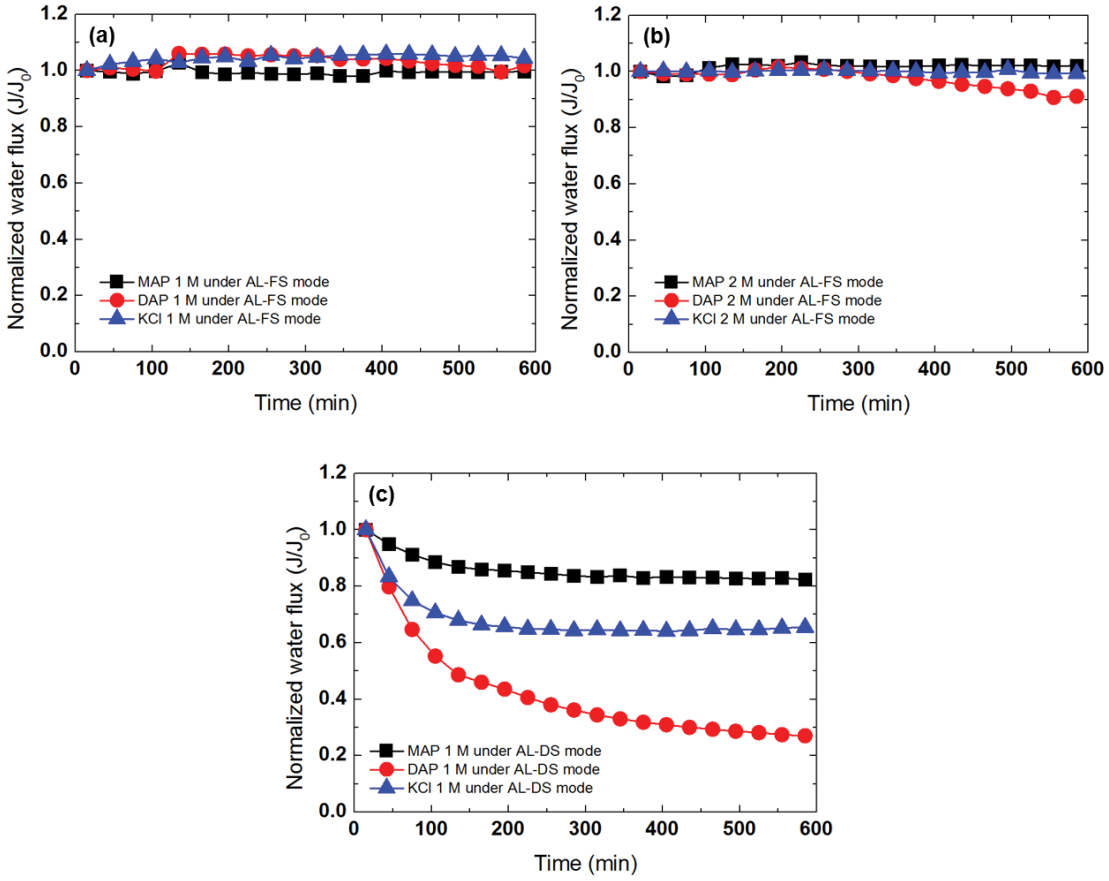

Figure 35. Flux-decline curves obtained during FO experiments (a) under AL-FS mode at 1 M draw solution, (b) under AL-FS mode at 2 M draw solution, and (c) under AL-DS mode at 1 M draw solution. Experimental conditions of all FO experiments: AnMBR effluent as feed solution; crossflow velocity of 8.5 cm/s; and temperature of 20 ± 1 °C.

A closer observation of membrane scales in **Fig. 36d** reveals that columnar jointing shaped crystals are formed on the membrane surface for DAP as DS. The deposition of scaling crystals on the membrane surface is in fact expected to increase the membrane resistance resulting in the water flux decline, however, such flux decline was not observed with DAP as DS. This could probably be explained by the membrane surface becoming more hydrophilic due to the presence of hydrophilic scales on the membrane surface. A slight decrease in the contact angle of the fouled membrane with DAP compared to virgin

membrane was found, shown in **Table 27**. By improving its hydrophilicity, the membranes can exhibit higher water flux due to more favorable transport of water molecules through improved membrane wetting (Kaur et al., 2012, Pendergast et al., 2013). Hydrophilic scaling often occurs in the early stage of the scaling formation (Woo et al., 2015) which can enhance the transport of water molecules. Any slight flux decline from the increased membrane resistance due to partial scale formation on the membrane surface can thus be offset by the enhanced water flux from the improved hydrophilicity of the FO membrane surface.

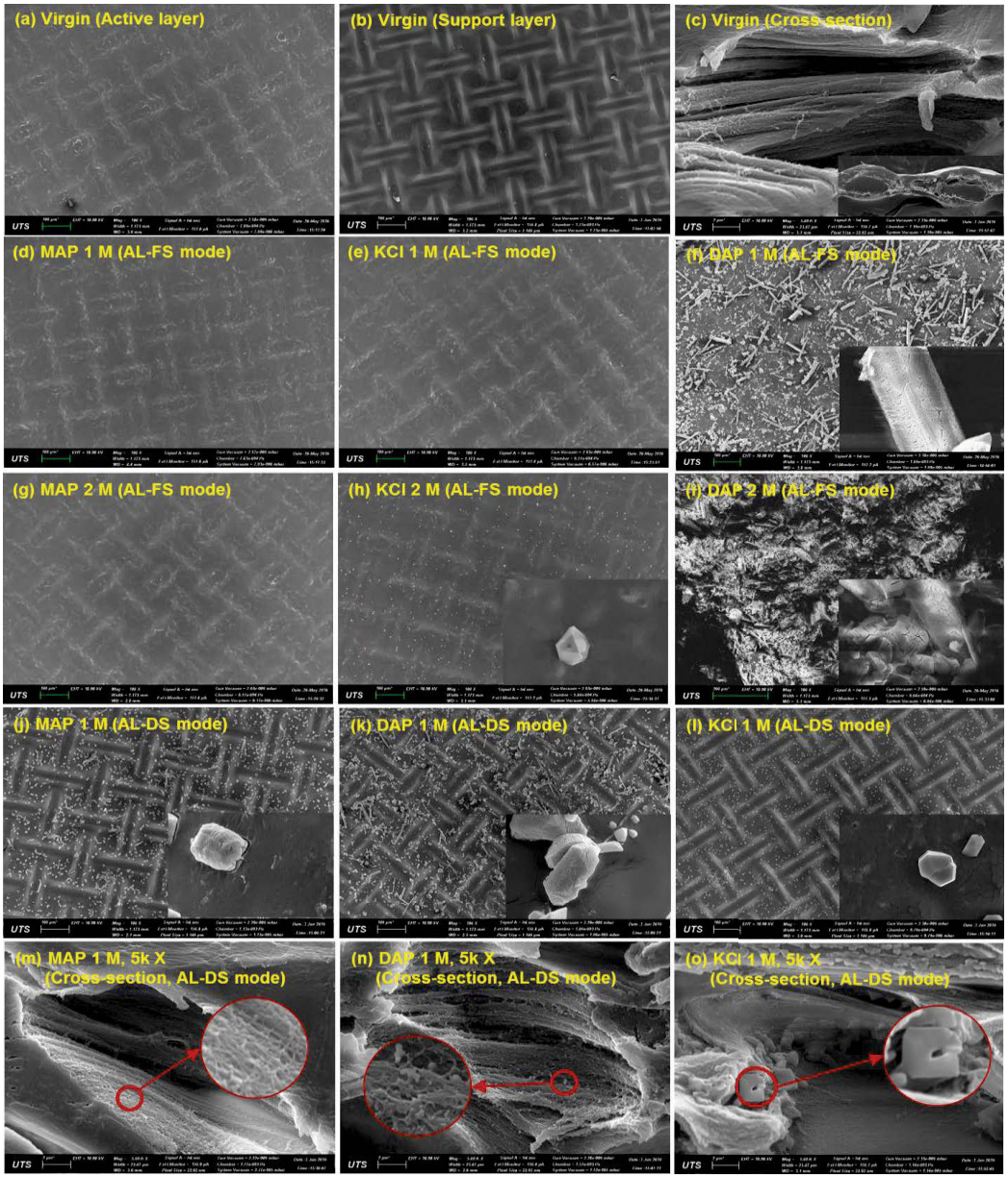

Figure 36. SEM images of the active layer of (a) virgin membrane and fouled membrane under AL-FS mode at (b) MAP 1 M, (c) KCl 1 M, (d) DAP 1 M, (e) MAP 2 M, (f) KCl 2 M and (g) DAP 2 M, the support layer of (h) virgin membrane and fouled membrane under AL-DS mode at (i) MAP 1 M, (j) DAP 1 M and (k) KCl 1 M, and the cross-section under 5k X magnification of (l) virgin membrane and fouled membrane under AL-DS mode at (m) MAP 1 M, (n) DAP 1 M and (o) KCl 1 M.

To investigate the effect of fertilizer concentration, FDFO experiments were conducted at 2 M DS under the AL-FS mode. By doubling the DS concentrations, the initial water fluxes in all fertilizers were enhanced, shown in **Table 25**. Operating the FO process at higher flux is expected to not only to enhance dilutive ICP but also increase the permeation drag that could further result in fouling and more severe flux decline (Kim et al., 2015c). However, as shown in **Fig. 35b**, only DAP exhibited a slight flux decline while MAP and KCl DS did not show any noticeable flux decline. The membrane surface with MAP (**Fig. 36g**) does not appear to show occurrence of fouling, appearing similar to the virgin membrane surface (**Fig. 36a**). On the other hand, the membrane surface with 2 M KCl (**Fig. 36h**) was partially covered by small crystal-shaped scales, which are likely due to the KCl from the RSF that formed scales on the membrane surface as the RSF of KCl was quite significant compared to the other fertilizer DS **(Table 23)**. However, it may be said that the scale formation due to RSF of KCl may be fairly low and not enough to cause significant flux decline during the 10 h of FO operation. In the case of DAP DS, about 10 % decline in water flux was observed, probably because the membrane surface was fully covered by scales as shown in **Fig. 36i**. Interestingly, only scaling was observed on the membrane surface even though AnMBR effluent is a complex mixture including organics, inorganics and contaminants. This may be because AnMBR effluent has quite low COD (**Table 19**) due to high organic removal capability of AnMBR and thus only scaling was formed by the effect of RSF. However, it can be expected that, if FDFO is operated in the long term, biofouling/organic fouling will be a significant problem.

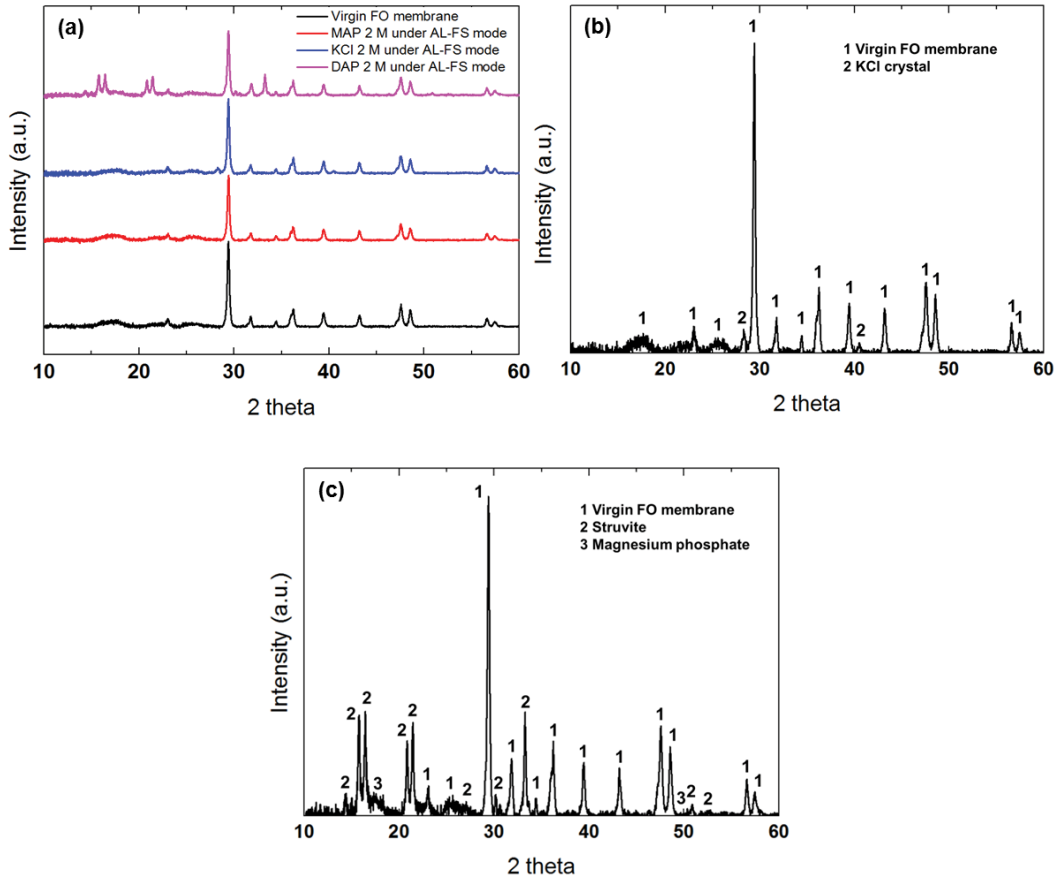

Figure 37. XRD patterns of virgin and fouled membranes: (a) comparison of XRD peaks between virgin membrane and fouled membranes with three fertilizer draw solution, (b) comparison of XRD peaks between fouled membranes with KCl 2 M and KCl crystal, and (c) comparison of XRD peaks between fouled membranes with DAP 2 M, magnesium phosphate, and magnesium ammonium phosphate (struvite). XRD analysis was performed on the active layer of FO membranes.

The scaling layer formed during FDFO experiments with DAP as DS was further studied by EDX analysis, which indicated the presence of magnesium and phosphorus elements (**Fig. 38**). Even though AnMBR effluent contains both Mg^{2+} and PO_4^{3-} as listed in **Table 19**, only DAP caused magnesium and phosphate related scales. During FDFO experiments, pH of FS with DAP as DS slightly increased from 8 to 8.8 (**Table 26**) due

to reverse diffusion of species found in the DAP DS which might have created a more ideal condition for phosphate precipitation with Ca^{2+} or Mg^{2+} cations (Ariyanto et al., 2014) (e.g. magnesium phosphate ($Mg(H_2PO_4)_2$) or magnesium ammonium phosphate ($NH_4MgPO_4 \cdot 6H_2O$) (struvite). Although FS was different, the results from this study are consistent with the results from our earlier study for brackish water desalination in FDFO (Phuntsho et al., 2014).

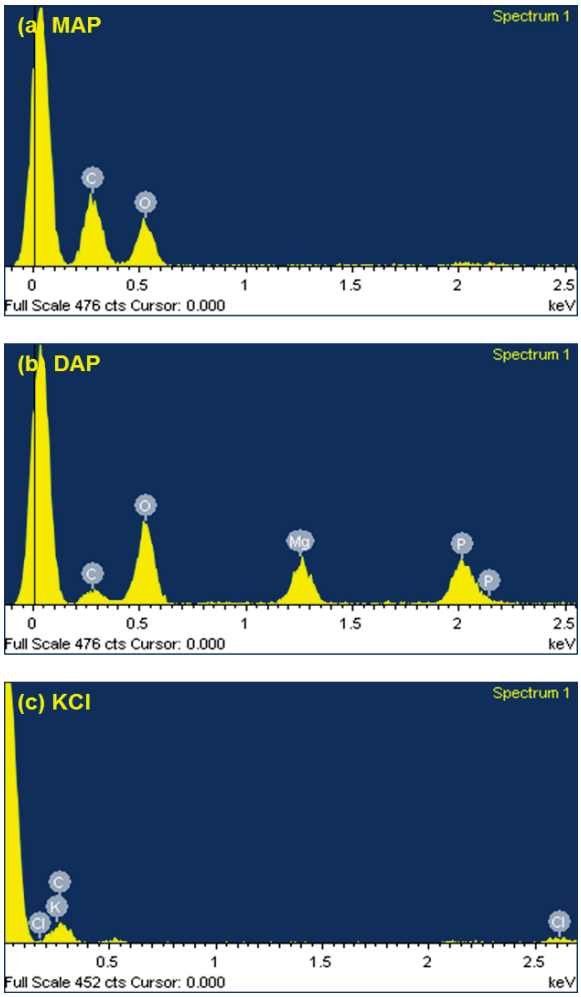

Figure 38. EDX results of fouled membranes with (a) MAP, (b) DAP and (c) KCl.

To further identify the composition of the scaling layer, XRD analysis was carried out on the scaled membrane surface. **Fig. 37a** showed that the membrane with MAP has similar XRD peaks to the virgin membrane, indicating that no scaling layer was formed on the membrane surface. On the other hand, the XRD pattern for the FO membrane surfaces with KCl and DAP as DS exhibited different peaks than the virgin FO membrane peaks. XRD analysis confirmed that KCl crystals formed on the membrane surface in **Fig. 36h** with KCl as DS (**Fig. 37b**), and is likely from the reverse diffusion of KCl. Since magnesium and phosphorous were found from EDX analysis, XRD peaks with DAP were first compared to reference peaks of magnesium phosphate (**Fig. 37c**), but the result was not conclusive. The XRD peaks agreed well when compared to the reference peaks of struvite (**Fig. 37c**), indicating that the scaling layer was primarily composed of struvite. This insoluble scaling formation can be caused by a combination of pH increase, the presence of Mg^{2+} in FS and supply of NH_4^+ and HPO_4^{2-} from DS as **Eqn. (25)** (Ariyanto et al., 2014)**.**

$$\mathbf{HPO_4^{2-} + Mg^{2+} + NH_4^+ + 6H_2O \rightarrow NH_4MgPO_4{\bullet}6H_2O\downarrow + H^+} \qquad \textbf{Equation 25}$$

For struvite formation, HPO_4^{2-} ions should exist in solution, and they can only be formed under high pH (pKa 7.21). Speciation analysis in **Table 22** also shows 0.947 M of HPO_4^{2-} ions formed in 1 M DAP (negligible for MAP) which is also likely to reverse diffuse towards the feed. In addition, a pH increase of FS with DAP as shown in **Table 26** provided a more favorable condition for struvite formation (Ariyanto et al., 2014). Moreover, higher RSF of the NH_4^+ with DAP as DS also created more favorable conditions for struvite scaling.

Table 26. pH of feed solutions after 10 h operation.

Feed solution	AL-FS mode 1 M DS			AL-FS mode 2 M DS			AL-DS mode 1 M DS		
	MAP	DAP	KCl	MAP	DAP	KCl	MAP	DAP	KCl
DI water	6.0	9.2	7.6	6.3	9.7	6.0	6.1	9.3	7.0
AnMBR effluent	7.9	8.8	8.2	7.7	8.9	8.1	7.7	8.8	8.1

To investigate the influence of membrane orientation on flux decline, the FDFO experiments were carried out under AL-DS mode at 1 M DS, with flux results presented in **Fig. 35c**. Unlike the AL-FS mode of membrane orientation, the fouling and scaling are expected to occur inside the membrane support layer as the membrane support layer is in contact with the feed water. As expected, the initial water fluxes under the AL-DS mode were significantly higher (shown in **Table 25)** compared to those in AL-FS mode at the same concentration since ICP phenomenon became negligible under the AL-DS mode of membrane orientation (McCutcheon and Elimelech, 2006). However, the flux decline was observed to become more severe with all the fertilizer DS, with DAP showing the highest flux decline followed by KCl and MAP. Despite DAP and MAP having similar initial water flux, DAP showed much higher flux decline compared to MAP. Comparing SEM images in **Fig. 36c and 36k,** it appears that the membrane surface of the support layer side with DAP was covered by a slightly higher amount of scales compared to MAP. However, the surface scaling results alone do not appear to be sufficient to explain the significant flux decline observed with DAP. Therefore, a cross-section of fouled FO

membranes was also analyzed to have further insight into scaling issues inside the membrane inner structure. **Fig. 36n** shows the presence of a large amount of small scales inside the support layer with DAP, while the support layer with MAP (**Fig. 36m**) was very similar to the virgin membrane (**Fig. 36c**). Based on these results, it can be speculated that phosphate precipitates, such as struvite scales, may also be formed within the pores of the support layer thereby contributing to the severe flux decline.

KCl showed higher flux decline than MAP, which may be explained by its higher initial water flux that results in a higher permeation drag force and higher concentrative CP which enhances the deposition and accumulation of foulants on the membrane support layer. Although KCl (**Fig. 36l**) shows a slightly less scale deposition on the membrane support surface compared to with MAP (**Fig. 36j**), this is also a possible reason why KCl had a higher flux decline compared to MAP. Unlike the AL-FS mode of FO operation, the foulant deposition occurs inside the support layer where the hydrodynamic crossflow shear is not effective in removing the foulant from the membrane resulting in a higher flux decline. In addition, **Fig. 36o** appears to show some form of inorganic scaling crystals present inside the membrane support layer with KCl as DS, however, it is not clear whether these crystals were actually insoluble precipitates that contributed to flux decline or KCl from the DS itself not fully removed before taking the membrane samples for SEM imaging. K_2SO_4 being much lower in solubility, is a potential candidate that can cause scaling with KCl DS when operated at a higher water flux, and further aggravated by higher RSF of the KCl that can slightly enhance concentrative ICP on the support layer side of the FO membrane.

5.3.1.3 Influence of physical cleaning on flux recovery

The effectiveness of physical (hydraulic) cleaning on the FO water flux recovery after AnMBR effluent treatment is presented in **Fig. 40a**. It was observed that under the AL-FS mode, FO membrane water fluxes were fully recovered for all the fertilizer DS tested, irrespective of DS concentrations used since high crossflow could induce high shear force (i.e., Re increased from 491 to 1474 due to turbulent flow). This further supports findings (**Section 5.3.1.2)** that the membrane fouling layer formed on the active layer could be readily removed by physical hydraulic cleaning. It is interesting to note that the water flux was also fully recovered for FO membranes subjected to scaling when operated with 2 M DAP as DS. In order to confirm whether the fouling layer was completely removed, SEM analysis was carried out using the fouled FO membranes with DAP since membrane fouling was the severest with this DS. **Fig. 39a and 39b** show that the scaling layer was almost fully removed by physical washing. Results of contact angle analysis were also consistent with the SEM analysis. After physical cleaning, contact angles of cleaned FO membrane surfaces with all fertilizers under AL-FS mode were almost restored, shown in **Table 27**.

Table 27. Contact angles of fouled FO membranes. When dropping a water droplet on the fouled FO membrane at 2 M DAP DS, the water droplet was immediately absorbed by the surface and thus contact angle couldn't be measured.

Contact angle (°)	AL-FS mode (1 M DS) (Active layer)			AL-FS mode (2 M DS) (Active layer)			AL-DS mode (1 M DS) (Support layer)		
	MAP	DAP	KCl	MAP	DAP	KCl	MAP	DAP	KCl
Fouled membrane	50.7 (±3.4)	26.27 (±4.3)	59.8 (±3.1)	48.2 (±5.6)	N/D*	26.6 (±4.4)	74.6 (±5.4)	74.9 (±3.9)	83.07 (±9.0)
Physical washing	74.29 (±1.9)	78.74 (±3.0)	65.54 (±3.0)	70.50 (±2.5)	81.16 (±3.3)	48.40 (±6.5)	74.96 (±1.9)	85.58 (±5.0)	65.25 (±2.0)
Osmotic backwashing	• Virgin active layer: 64.5 (±2.2) • Virgin support layer: 84.6 (±3.4)						67.37 (±4.1)	87.31 (±4.1)	61.79 (±5.1)

* N/D: Not detectable

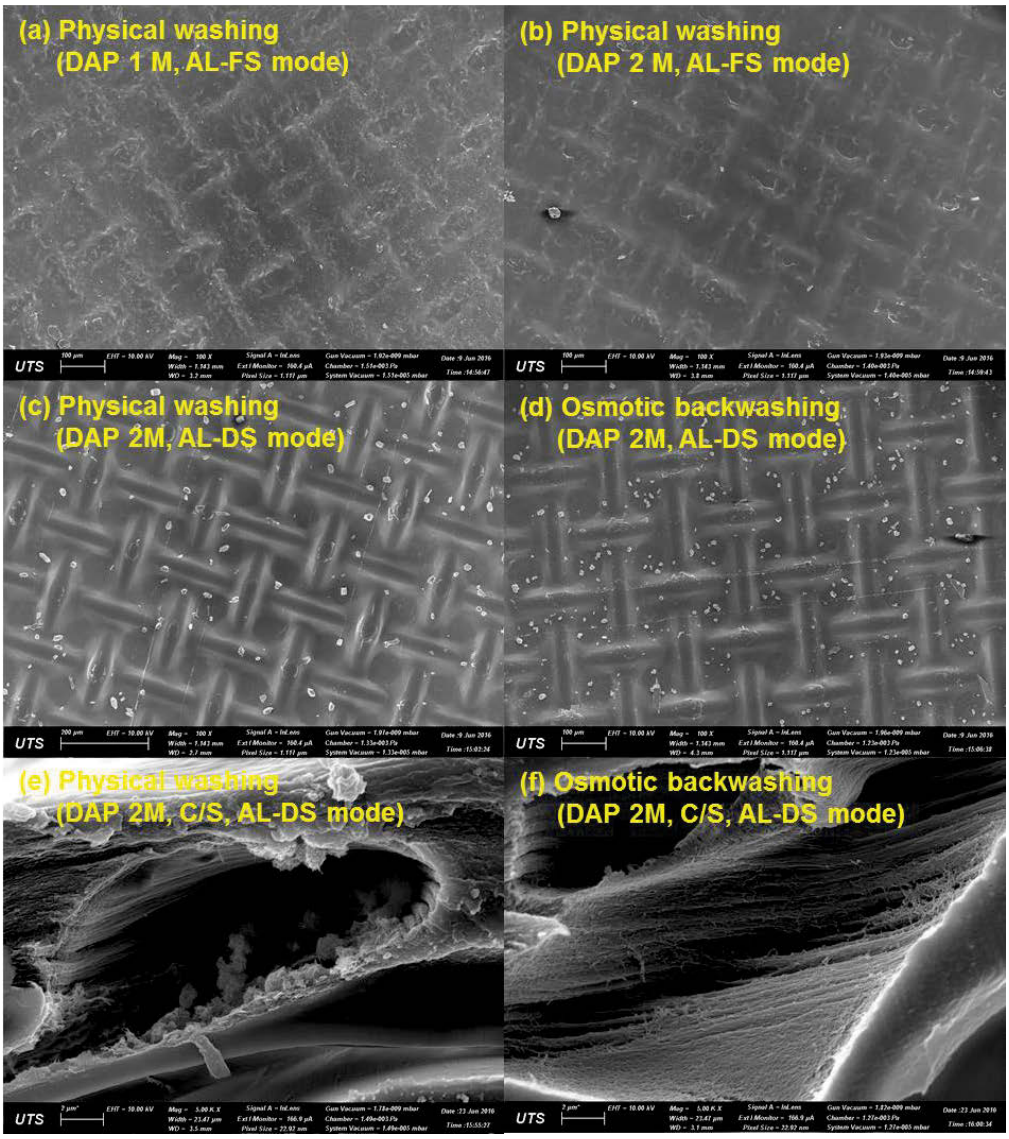

Figure 39. SEM images of (a) the active layer of cleaned FO membrane (AL-FS mode, DAP 1M) by physical washing, (b) the active layer of cleaned FO membrane (AL-FS mode, DAP 2M) by physical washing, (c) the support layer of cleaned FO membrane (AL-DS mode, DAP 1M) by physical washing, (d) the support layer of cleaned FO membrane (AL-DS mode, DAP 1M) by osmotic backwashing, (e) the cross-section of cleaned FO membrane (AL-DS mode, DAP 1M) by physical washing, and (f) the cross-section of cleaned FO membrane (AL-DS mode, DAP 1M) by osmotic backwashing.

The water fluxes could not be fully recovered after physical cleaning for the FO membranes operated under the AL-DS mode, where MAP and KCl showed >90% recovery while DAP was only about 25%. However, it is interesting to note that physical cleaning was effective to restore the water flux by more than 90% for KCl and MAP DS despite the fact that the fouling is expected to occur inside the support layer side of the FO membrane which is unaffected by the crossflow velocity shear. This may be related to the structure of the FO membrane where it is apparent that CTA FO membranes do not have a distinct support layer and active layer unlike the TFC FO membranes (Yip et al., 2010). The woven backing fabric generally considered as a support layer for the CTA FO membrane is in fact embedded within the cellulose triacetate layer which is the active rejection layer, thereby giving a FO membrane without a distinct porous support layer. This is also the main reason why CTA FO membranes do not have a significant FO pure water flux difference when operated under AL-FS or AL-DS modes of membrane orientations, unlike TFC FO membranes where pure water fluxes under the AL-DS mode is significantly higher (Yip et al., 2010, Fam et al., 2013). Therefore, it is apparent that physical cleaning was quite effective in removing the foulant deposited on the support layer side of the CTA FO membrane although it was not as effective in cleaning the active layer side of the FO membrane.

The poor flux recovery rate of FO membranes operated with DAP DS shows that hydraulic cleaning was not effective in removing the membrane foulant and scales formed on the support layer (**Fig. 39c**) as well as on the surface (**Fig. 39e**). While it is expected that some of the foulants and scales deposited on the surface of the support layer are removed by physical cleaning, those formed inside the support layer are not influenced by the crossflow. Besides, struvite is only sparingly soluble in DI water under neutral and

alkaline conditions thereby rendering the physical washing ineffective for FO membrane operated with DAP DS.

In order to enhance the cleaning efficiency for FO membranes operated under the AL-DS mode, osmotic backwashing was investigated for fouled FO membranes using DI water on the active layer and 1 M NaCl on the support layer side at the same crossflow velocity (i.e., 8.5 cm/s for 30 mins). **Fig. 40b** shows that water flux recovery after osmotic backwashing was not significantly better than physical cleaning for MAP and KCl and hence still did not result in 100% flux recovery. Interestingly, the FO water flux with DAP was restored to about 80%, indicating that osmotic backwashing was effective in removing the foulants and scales deposited inside the FO support layer, shown in **Fig. 39f**. During osmotic backwashing, the water flux is reversed and the permeation drag force occurs from the active layer side to the support layer side of the FO membranes. This mode of cleaning is expected to partially remove the foulants and scales present in the pores and remove them out of the membrane support layer. It should be noted that the use of NaCl salt solution as a cleaning agent might induce other phenomena such as changing the structure of the cross-linked gel layer on the membrane surface by an ion exchange reaction which can break up calcium-foulant bonds when the fouling layer is exposed to the salt solution (Lee and Elimelech, 2007, Mi and Elimelech, 2010, Corbatón-Báguena et al., 2014). Similarly, DS with 1 M NaCl might affect struvite dissolution through an ion exchange reaction. As a result, osmotic backwashing was a more effective cleaning method than physical washing to remove the scales present within the support layer.

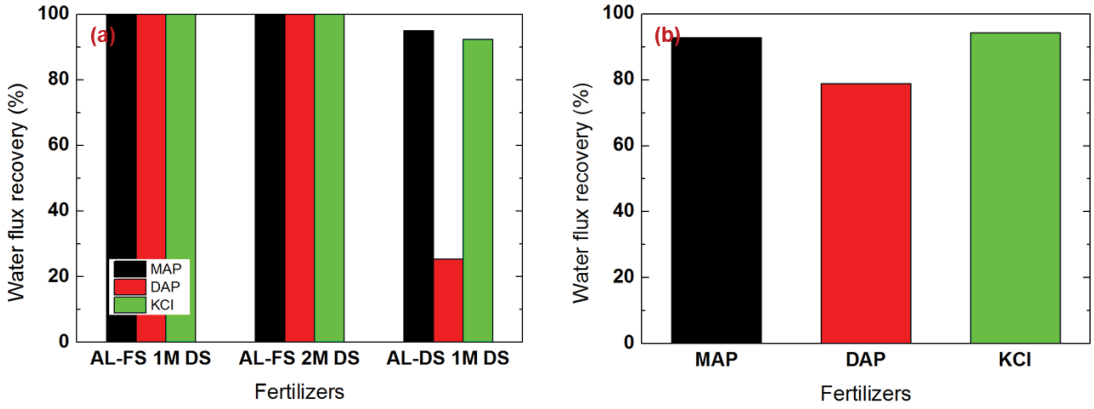

Figure 40. Water flux recovery after (a) physical washing and (b) osmotic backwashing. Experimental conditions for physical washing: DI water as feed and draw solutions; crossflow velocity of 25.5 cm/s; cleaning duration of 30 min; and temperature of 20 ± 1 °C. Experimental conditions for osmotic backwashing: 1M NaCl as feed solution; DI water as draw solution; crossflow velocity of 8.5 cm/s; cleaning duration of 30 min; and temperature of 20 ± 1 °C.

5.3.2 Influence of fertilizer DS properties on OMPs transport

During FDFO operations using AnMBR effluent treatment, OMPs transport behavior was also studied by measuring the OMPs forward flux, presented in **Fig. 41**. It is clear from **Fig. 41a** that the highest OMPs flux was observed with KCl as DS, except for Atenolol where the OMPs fluxes were fairly similar with all the three fertilizer DS, while the OMPs fluxes for MAP and DAP were comparable. For the three OMPs tested, the highest flux was observed for Caffeine, closely followed by Atrazine, and Atenolol showing the lowest flux with all the fertilizer DS. Since a higher flux relates to a lower OMPs rejection rate by the FO membrane, a lower OMPs flux is desirable for FDFO. The specific OMPs permeate concentrations and their rejection rates by the FO membrane are presented in **Table 28**.

The higher OMPs flux for KCl compared to MAP and DAP may be explained by the higher average FO water flux of KCl (11.2 L/m^2/h in **Table 25**) compared to MAP (7.58 L/m^2/h) and DAP (7.35 L/m^2/h) DS. The average water flux in this particular case was calculated by dividing the total volume of FO permeate that crossed the FO membrane from the feed to the DS tank, divided by the effective membrane area and the duration of the FO operation in the batch process. In any salt-rejecting membrane processes, ECP plays an important role in determining the forward salt flux and rejection rates (Srinivasan and Chi, 1973). At higher water fluxes, salt concentration at the membrane surface increases due to enhanced concentrative ECP (under the AL-FS mode) and thus increases the forward salt flux through the membrane. MAP and DAP have comparable average water fluxes under the AL-FS mode at 1 M concentration (**Table 25**) which contributes to almost similar concentrative ECP and hence resulting in comparable OMPs fluxes. Generally, the rejection rate in FO is higher than that in the RO process, where previous studies have linked this to a probable hindrance effect of RSF on the forward transport (Xie et al., 2012a). Based on this assumption, KCl with the highest RSF is expected to have lower OMPs forward flux compared to MAP and DAP that have significantly lower RSF. Although the water fluxes of the MAP and DAP fertilizer DS are similar (**Table 25**), the RSF of DAP is significantly higher than MAP while their OMPs forward fluxes are observed to be similar. These results suggest that the effect of ECP by permeation drag force is more significant than the hindrance effect by RSF, which is consistent with a previous study (Kim et al., 2012). For instance, if certain DS has higher water flux as well as higher RSF than others, rejection rates can be seriously reduced even though high RSF has a potential impact on enhancing a rejection propensity.

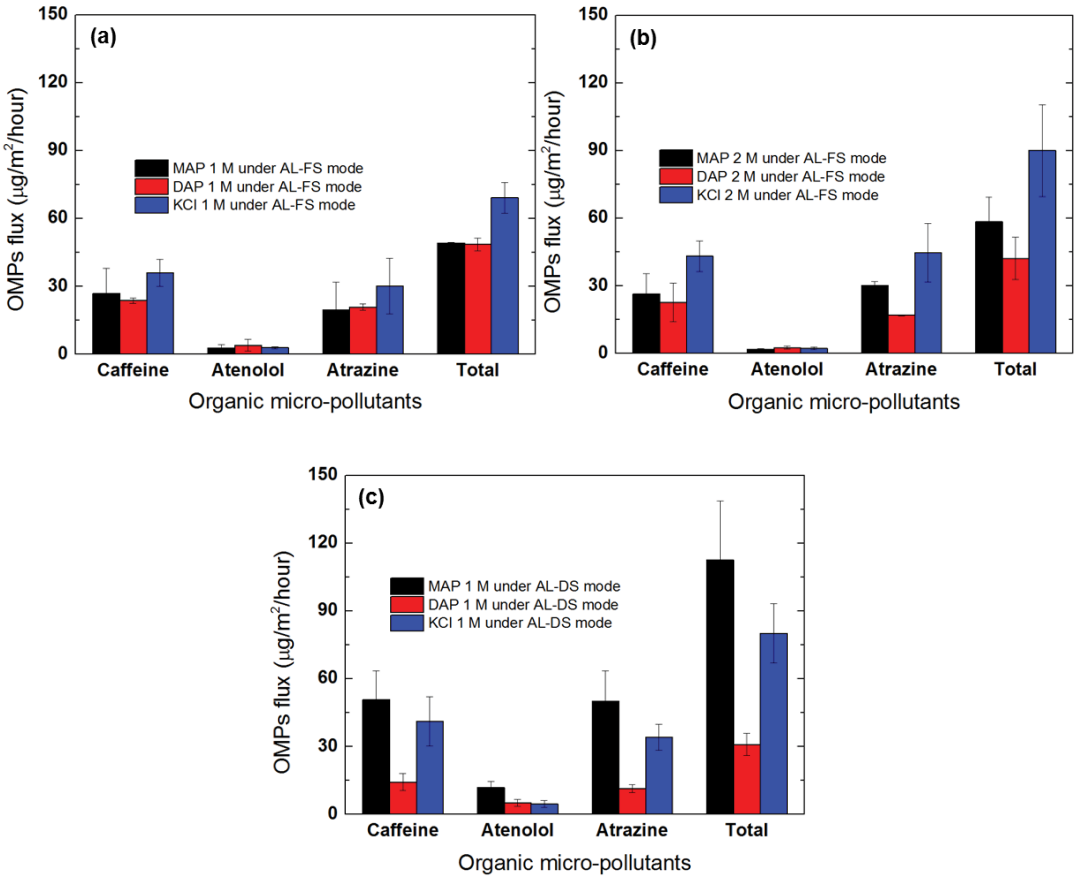

Figure 41. Comparison of OMPs forward flux in FDFO between MAP, DAP and KCl: (a) under AL-FS mode at 1 M draw solution, (b) under AL-FS mode at 2 M draw solution, and (c) under AL-DS mode at 1 M draw solution. The error bars represent the standard deviation from duplicate measurements. Experimental conditions for OMPs transport behaviors: AnMBR effluent with 10 μg/L OMPs as feed solution; crossflow velocity of 8.5 cm/s; 10 h operation; and temperature of 20 ± 1 °C.

Table 28. Permeate OMPs concentration and OMPs rejection with different membrane orientation and draw solution concentration. Experimental conditions for OMPs transport behaviors: AnMBR effluent with 10 μg/L OMPs as feed solution; crossflow velocity of 8.5 cm/s; 10 h operation; and temperature of 20 ± 1 °C.

		AL-FS mode (1 M DS)			AL-FS mode (2 M DS)			AL-DS mode (1 M DS)		
		MAP	DAP	KCl	MAP	DAP	KCl	MAP	DAP	KCl
Permeate concentration (μg/L)	Caffeine	0.47	0.41	0.59	0.45	0.39	0.65	0.94	0.25	0.82
	Atenolol	0.05	0.07	0.05	0.03	0.04	0.03	0.23	0.08	0.09
	Atrazine	0.34	0.36	0.49	0.51	0.29	0.67	0.78	0.20	0.59
	Total	0.85	0.85	1.13	0.99	0.72	1.36	1.94	0.53	1.50
Rejection (%)	Caffeine	95.3	95.9	94.1	95.5	96.1	93.5	90.6	97.5	91.8
	Atenolol	99.5	99.3	99.5	99.7	99.6	99.7	97.7	99.2	99.1
	Atrazine	96.6	96.4	95.1	94.9	97.1	93.3	92.2	98.0	94.1
	Total	97.2	97.2	96.2	96.7	97.6	95.5	93.5	98.2	95.0

The OMPs transport behavior is also significantly affected by OMPs properties (i.e., molecular weight, surface charge, and surface hydrophobicity). In both RO and FO, OMPs molecular weights have a significant impact on OMPs transport behavior by the steric hindrance that depends on the mean effective pore size of the membrane used (Xie et al., 2012a, Xie et al., 2014). In addition, the surface charges of the OMPs also significantly affect the OMPs transport behavior by electric repulsion with membranes that contain surface charges (Xie et al., 2012b). Furthermore, rejection of OMPs with

hydrophobic properties can be enhanced by hydrophobic-hydrophilic repulsion when using hydrophilic membranes (Valladares Linares et al., 2011).

In this study, atenolol showed the lowest OMPs flux and therefore the highest rejection rates (> 99%) followed by atrazine (95-96.5%) and caffeine (94-96%), giving a total OMPs rejection rate between 96-97% for the three fertilizer DS. The highest rejection rate for Atenolol is likely because it has the largest molecular weight compared to the other two OMPs. The forward OMPs flux is a function of the molecular weight (shown in **Fig. 42**) where the linear decrease in the rejection rate observed with the increase in the molecular weight is consistent with other studies (Kiso et al., 2001, Kimura et al., 2004, Xie et al., 2014). High molecular weight OMPs can be more easily rejected by FO membranes through steric hindrance (Xie et al., 2014). In addition to molecular weight, the surface charge of OMPs may also have an influence on OMPs transport behavior. Table 2 presents that atenolol is positively charged while atrazine and caffeine are neutral. Thus, atenolol has much higher hydrated molecular dimension as well as higher molecular weight itself compared to uncharged OMPs (i.e., atrazine and caffeine). Since CTA membrane is relatively uncharged under the conditions tested in this study, these results indicate that the steric hindrance by the FO membrane is likely the dominant rejection mechanisms affecting OMPs transport behavior.

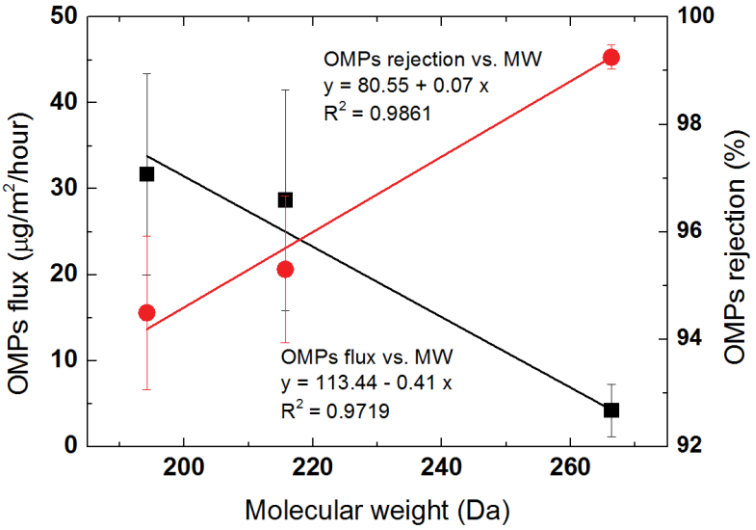

Figure 42. Relationship of molecular weights of OMPs with OMPs flux and rejection, respectively.

Table 28 shows the OMPs concentrations measured in the FO permeate. These results indicate that the individual OMP concentrations in the permeate was consistently lower than 1 μg/L for all three fertilizers as DS, under conditions applied in this study. This concentration is well within the permissible limit for irrigation where the maximum allowable concentration is 1 μg/L (2004). However, since we considered only three OMPs despite many types of OMPs, more investigation is required by operating the AnMBR-FDFO hybrid system continuously.

5.3.3 Influence of DS concentration on OMPs transport

In order to investigate the influence of fertilizer DS concentration on OMPs transport, FDFO OMPs flux data for 1 M (**Fig. 41a**) DS concentration is compared with the 2 M (**Fig. 41b**) DS concentrations under the AL-FS mode. The total OMPs forward flux for MAP and KCl increased slightly at higher DS concentration (2 M), which is likely due to the enhanced concentrative ECP as their average water fluxes at 2 M is higher than 1 M

DS concentrations. However, the same trend did not apply to DAP as its total OMPs forward flux rather decreased at 2 M compared to 1 M although the average water flux increased from 7.35 L/m^2/h to 8.72 L/m^2/h (**Table 25**). This unexpected behavior is likely due to membrane fouling, where about 10% flux decline was observed with 2 M DAP as DS and not observed with 1 M DAP as DS. When the fouling layer is formed on the membrane surface, it alters the surface properties and hence the solute rejection properties depending on the severity and type of fouling layer formed (Hoek and Elimelech, 2003, Kim et al., 2009). In a colloidal fouling, for example, a porous fouling layer induces cake-enhanced concentration polarization (CECP) and accelerates feed salt permeability (Hoek and Elimelech, 2003). In organic fouling, however, a non-porous and dense fouling layer leads to cake-reduced concentration polarization (CRCP) which reduces salt permeability and hence improves salt rejection (Kim et al., 2009). With 2 M DAP as DS, the non-porous, thick and dense fouling layer was formed (shown in **Fig. 36g)** where both scaling and organic fouling could have likely caused a CRCP effect resulting in lower OMPs forward flux. In terms of OMPs rejection rates in **Table 28**, increasing DS concentration under AL-FS mode lowers the OMPs rejection rates for all the fertilizer DS due to enhanced water flux that enhances concentrative ECP.

5.3.4 Influence of FO membrane orientation on OMPs transport

OMPs forward flux with MAP as DS was significantly enhanced when operated under the AL-DS mode of membrane orientation (**Fig. 41c**), compared to the AL-FS mode (**Fig. 41a**). Similarly, OMPs forward flux increased with KCl as DS although the increase was not as high as with MAP. Interestingly, the OMP flux significantly decreased with DAP

as DS. These phenomena may be likely due to the concentrative ICP effect and fouling occurring inside the membrane support layer.

The water flux for 1 M MAP under the AL-DS mode was 10.5 L/m^2/h, higher than under the AL-FS mode (7.6 L/m^2/h). This higher water flux enhances the concentrative ICP thereby likely increasing the OMPs concentration at the membrane and hence its flux through the FO membrane (Xie et al., 2012b). Under the AL-DS mode, the water fluxes are generally higher due to higher effective concentration difference across the membrane active layer (McCutcheon and Elimelech, 2006). As per earlier observations (**Fig. 40a**), a slight membrane fouling had occurred with 1 M MAP under the AL-DS mode of membrane orientation, where the water flux was not fully recovered by physical cleaning. As this fouling likely occurred inside the support layer side of the FO membrane, the deposited foulant or cake layer could reduce back-diffusion of the OMPs thereby likely contributing to enhanced OMPs flux.

The average water flux for KCl under the AL-DS mode (9.44 L/m^2/h) was lower compared to the AL-FS mode (11.2 L/m^2/h), however, the OMPs forward flux increased under the AL-DS mode. This phenomenon can be elucidated due to the combined effects of enhanced concentrative ICP and fouling inside the FO membrane support layer. Under the AL-DS mode of membrane orientation, foulants can be easily deposited inside the membrane support layer due to high initial permeation drag force since KCl had a much higher initial water flux (15.6 L/m^2/h in **Table 25**) although the average water flux decreased to around 9.4 L/m^2/h during the period of operation. This increased fouling inside FO membrane support layer not only lowers water flux but also can potentially prevent back-diffusion of OMPs to the feed side, similar to the observation with MAP, thereby increasing its flux through the FO membrane. This phenomenon as outlined is schematically presented in **Fig. 43a**.

The decrease in the OMPs flux with DAP under the AL-DS mode of membrane orientation is likely due to the combination of a much reduced average water flux compared to under the AL-FS mode. This reduction in average water flux might induce the decrease in OMPs flux by mitigating concentrative ICP. Moreover, the severe flux decline observed with DAP under the AL-DS mode is probably due to both struvite scaling and organic fouling, which may reduce the membrane porosity and pore size thus likely reducing the mass transfer of the OMPs and increasing the OMPs solute rejection by size exclusion (Polyakov and Zydney, 2013) and hence decreasing the OMPs flux as explained in **Fig. 43b**.

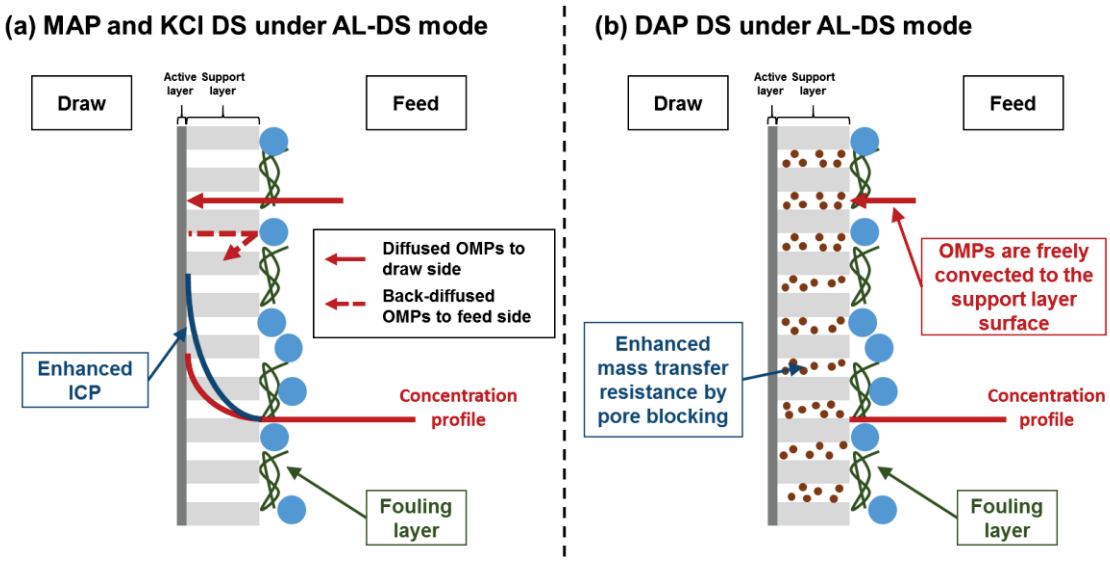

Figure 43. Schematic description of OMPs transport mechanisms under AL-DS mode: (a) MAP and KCl, and (b) DAP.

5.4 Conclusions

In this study, fouling behavior in FDFO was systematically investigated using three different fertilizer DS and included OMPs transport behavior during AnMBR effluent treatment. The primary findings from this study are summarized as follows:

- Under the AL-FS mode of membrane orientation, water flux with FDFO did not decline significantly due to the hydrophilicity of the scaling layer, even though severe scaling occurred when DAP fertilizer was used as DS.
- Under the AL-DS mode, DAP fertilizer DS showed the highest flux decline followed by KCl and MAP, where scaling was observed within the support layer pores when DAP fertilizer was used as DS.
- Physical/hydraulic cleaning successfully recovered water flux for the FO membranes operated under the AL-FS mode of membrane orientation. However, for the membranes operated under AL-DS mode, the flux was not fully recovered as the fouling and scaling occurred inside the support layer. Osmotic backwashing significantly enhanced the cleaning efficiency and flux recovery for FO membranes operated under the AL-DS mode.
- During the AnMBR effluent treatment by FDFO, DAP fertilizer DS exhibited the lowest OMPs forward flux (or the highest OMPs removal of up to 99%) compared to MAP and KCl fertilizers as DS. The higher OMPs flux resulted in higher water flux that enhanced concentrative ECP on the membrane active surface and no significant influence of RSF was observed on the OMPs flux.

Findings from this study have significant implications for optimizing FDFO in terms of AnMBR effluent treatment and OMPs rejection. The trade-off between getting high

dilution of DS (i.e., high water flux and low flux decline) and enhancing OMPs rejection (i.e., low OMPs forward flux) should be considered in FDFO design and optimization.

6. Influence of fertilizer draw solution properties on the process performance and microbial community structure in a side-stream anaerobic fertilizer-drawn forward osmosis - ultrafiltration bioreactor

6.1 Introduction

Freshwater resources are getting scarcer due to the impacts of global warming, and rapid and extensive industrialization and urbanization (Rijsberman, 2006). Agricultural sectors consume about 70% of the accessible freshwater with about 15 -35% of water being used unsustainably (Clay, 2004). Therefore, Mediterranean countries, which are stressed by water shortage, have considered wastewater reuse as a viable alternative water resource for agricultural purposes (Angelakis et al., 1999b). However, since wastewater reuse is often limited due to the presence of harmful heavy metals, industrial waste, PPCPs, and excess salts (Snyder et al., 2003), adequate treatment of wastewater before reuse as irrigation is essential not only to protect the human and plant health but also to enhance the value of the crops grown through wastewater reuse (Ferro et al., 2015). Therefore, advanced treatment processes (e.g., RO, NF or advanced oxidation) are generally required as a post-treatment process since wastewater could contain pollutants which are not removed by conventional treatment processes (Ahluwalia and Goyal, 2007).

AnMBR has been studied to treat wastewater and has several advantages including complete rejection of suspended solids, low sludge production, high organic rejection and biogas production (Stuckey, 2012). However, post-treatment processes such as RO and NF exhibit high fouling issues which ultimately increase energy requirements since these processes are driven by the hydraulic pressure as a driving force (Kim et al., 2014b). To overcome these issues, OMBR has been proposed by integrating AnMBR with FO instead of conventional pressurized membrane processes (Achilli et al., 2009). OMBR can

provide high rejection of contaminants, low fouling propensity and high fouling reversibility but has limitations that pure water should be extracted from DS and reversely transported draw solute can be toxic or inhibit the biological processes (Achilli et al., 2009, Kim et al., 2016).

FDFO has received increased attention since the diluted fertilizer solution can be utilized directly for irrigation purpose and thus the diluted DS separation and recovery process is not required (Phuntsho et al., 2011, Phuntsho et al., 2012b, Phuntsho et al., 2013a). However the diluted fertilizer solution still requires substantial dilution since the final nutrient concentration can exceed the standard nutrient requirements for irrigation especially using feed water sources with high salinity (Phuntsho et al., 2011, Phuntsho et al., 2012b). Thus, NF can be employed as a post-treatment process for further dilution and in meeting the water quality requirements for fertigation (Phuntsho et al., 2013a). However, FDFO is seen to be more suitable for the treatment of low salinity impaired water sources such as municipal wastewater so that desired fertilizer dilution can be achieved without the need of a NF post-treatment process. Thus, AnFDFOMBR was proposed by combining FDFO and AnMBR for simultaneous wastewater treatment for greenhouse hydroponic application in the previous study (Kim et al., 2016).

Despite many advantages (i.e., complete rejection of pollutants, low energy requirement and high fouling reversibility) of the AnFDFOMBR hybrid system, it also has critical issues including salt accumulation in the bioreactor. When considering the typical submerged AnFDFOMBR hybrid system, salt accumulation takes place in the bioreactor from both the influent and DS. This is due to wastewater continuously being fed into the bioreactor and the FO membrane rejecting almost 100% of ionic compounds and the back diffusion of the DS. Salt concentration will continuously increase and therefore may affect the microbial activity of the anaerobic bacteria as well as FO performances.

Therefore, many researchers have tried to mitigate the salt accumulation by combining OMBR with porous membrane technologies (e.g., MF and UF) (Wang et al., 2014b) and desalting technologies (e.g., capacitive deionization (CDI) and electrodialysis (ED)) (Lu and He, 2015).

In this study, a side-stream anaerobic FDFO-UF-MBR hybrid system (An-FDFO-UF-MBR) is proposed for simultaneous wastewater treatment for greenhouse hydroponic application based on the concept described in **Fig. 44**. Side-stream FO and UF membrane modules are used since membrane fouling in the side-stream system is readily controlled by simple physical cleaning compared to the submerged system. UF plays an important role to reduce and mitigate salt accumulation in the bioreactor. In this system, raw municipal wastewater is utilized as the influent and a highly-concentrated fertilizer solution is used as DS. Thus, the diluted fertilizer solution can then be obtained and supplied to greenhouse hydroponic irrigation. The UF permeate can be also utilized to recover fertilizers due to its high nutrient content (Luo et al., 2016).

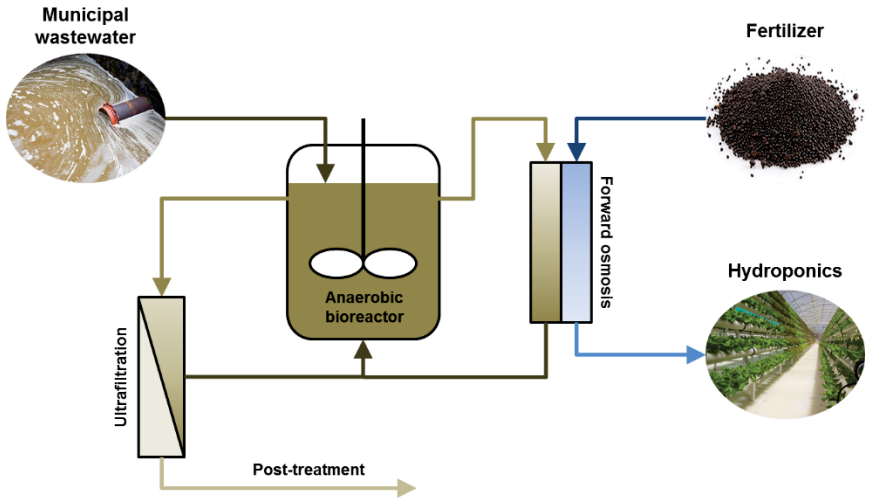

Figure 44. Conceptual diagram of a side-stream anaerobic fertilizer-drawn forward osmosis – ultrafiltration bioreactor.

Therefore, this study aims to investigate the feasibility of the anaerobic FDFO-UF-MBR hybrid process for treating municipal wastewater. FO performance in terms of flux decline was firstly evaluated with various fertilizer DS. During the operation, salt accumulation and biogas production were monitored. Besides, bacterial and archaeal community structures of the sludge were characterized through pyrosequencing analysis to investigate the effect of fertilizer DS on variations of bacterial and archaeal structures and their relationship to biogas production and composition.

This chapter is an extension of a research article published by the author in Bioresource Technology.

6.2 Experiments

6.2.1 Feed and draw solutions

Synthetic municipal wastewater with COD of 400 ± 10 mg/L consisting of food ingredients, chemical compounds and trace metals was used as FS in this study (**Table 29**). Three different chemical fertilizers (i.e., mono-ammonium phosphate (MAP), mono-potassium phosphate (MKP) and potassium chloride (KCl)) as DS were prepared by dissolving fertilizers in the DI water. Detailed information of fertilizer chemicals is provided in **Table 30**. Osmotic pressure, diffusivity and viscosity of three fertilizers were obtained by OLI Stream Analyzer 3.2 (OLI System Inc., Morris Plains, NJ, USA). All chemicals of reagent grade were received in powder form from Sigma Aldrich (Saudi Arabia).

Table 29. Detailed composition of the synthetic municipal wastewater used in this study (Wei et al., 2014).

Chemical compounds	Conc. (mg/L)	Food ingredients	Conc. (mg/L)	Trace metals	Conc. (mg/L)
Urea	91.7	Starch	122	$Cr(NO_3)_3 \cdot 9H_2O$	0.770
NH_4Cl	12.8	Milk power	116	$CuCl_2 \cdot 2H_2O$	0.536
Na-acetate	79.4	Yeast	52.2	$MnSO_4 \cdot H_2O$	0.108
Peptone	17.4			$NiSO_4 \cdot 6H_2O$	0.336
$MgHPO_4 \cdot 3\ H_20$	29.0			$PbCl_2$	0.100
KH_2PO_4	23.4			$ZnCl_2$	0.208
$FeSO_4 \cdot 7H_2O$	5.8				

Table 30. Details of the fertilizer chemicals used in this study. Thermodynamic properties were determined at 1 M concentration and 25 ºC by using OLI Stream Analyzer 3.2.

Chemicals	**Potassium chloride**	**Ammonium phosphate monobasic (MAP)**	**Potassium phosphate monobasic (MKP)**
Formula	KCl	$NH_4H_2PO_4$	KH_2PO_4
Molecular weight (g/mol)	74.6	115.0	136.09
Osmotic pressure (atm)	45.27	44.52	37.53
Diffusivity ($\times \mathbf{10^{-9}}$ m^2/s)	2.24	1.50	1.46
Viscosity (cP)	0.7324	0.9352	0.9504

6.2.2 A lab-scale side-stream anaerobic fertilizer-drawn forward osmosis – ultrafiltration membrane bioreactor

A lab-scale side-stream An-FDFO-UF-MBR unit (**Fig. 45**) consisted of a completely mixing bioreactor (Applikon Biotechnology, the Netherlands) with effective volume of 2 L controlled by a level sensor (temperature 35 ± 1 ºC, pH 7 ± 0.1 and stirring speed 200 ± 2 rpm), a side-stream crossflow hollow fibre UF membrane module and a side-stream crossflow flat-sheet FO membrane module. The FO membrane was provided by Hydration Technology Innovations (Albany, OR, USA) and made of cellulose-based polymers with an embedded polyester mesh for mechanical strength. The UF membrane

is composed of polyvinylidene fluoride with nominal pore size of 30 nm. The effective membrane surfaces of FO and UF modules were 100 cm^2 (i.e., 10 cm × 10 cm) and 310 cm^2, respectively. Operation temperature was 35 ± 1 ºC and crossflow velocity of FO and UF modules were 2.3 cm/s and 20 cm/s, respectively. Reynolds number in the FO module was 273. The hybrid system was operated for 55 days with HRT 20 - 24 h. Initially, AnMBR was operated without FO operation for 6 days to stabilize the system. FO was then operated with KCl DS for 6 days and stopped for 9 days to stabilize anaerobic microorganisms. Then, FO was run again with MAP DS for 15 days. After that, FO operation was stopped and the bioreactor was operated for 7 days to restabilise the system. FO was also operated with MKP DS for 12 days. In this study, the operational period of FDFO was determined according to the anaerobic performance (represented as biogas production). In order to recover water flux, physical cleaning was applied every day since water flux severely declined within 1 day of continuous operation. Physical cleaning consisted of flushing DI water inside the DS and the sludge solution FS channels at 3 times higher crossflow velocity (6.9 cm/s) for 30 min.

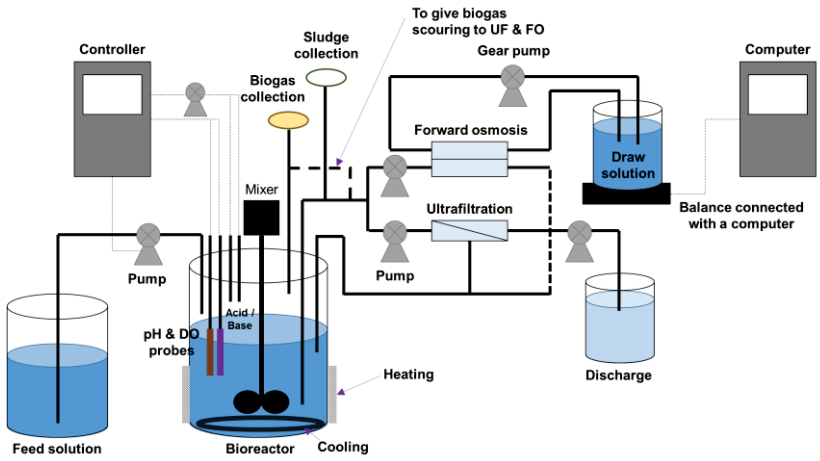

Figure 45. Schematic diagram of the lab-scale side-stream anaerobic FDFO-UF hybrid system.

6.2.3 Analytical methods

COD was determined using a COD cell test kit (Hach, Germany) following the standard method (DIN ISO 15705). Total nitrogen (TN) was determined using a TN test kit according to the persulfate digestion method. Total phosphorous (TP) was analysed by ion chromatography (Dionex ICS-5000). MLSS was measured using standard methods (American Public Health et al., 2005). Biogas composition and volume (reported under a temperature of 25 ºC and pressure of 1 atm) were measured according to the gas bag method (Ambler and Logan, 2011) based on gas chromatography.

6.2.4 Pyrosequencing analysis

6.2.4.1 DNA extraction

DNA was extracted through the FastDNA Spin kit for soil (MP Biomedicals, USA), using 4x the normal bead beating to enable recovery of bacteria that are difficult to lyse (Albertsen et al., 2015).

6.2.4.2 16S rRNA amplicon library preparation

The procedure for bacterial 16S rRNA amplicon sequencing targeting the V1-3 variable regions is based on Caporaso et al. (2012), using primers adapted from the Human Gut Consortium (Jumpstart Consortium Human Microbiome Project Data Generation Working, 2012). Archaeal V3-5 16S sequencing libraries were prepared by a custom protocol based on the 16S metagenomic sequencing library preparation protocol (Part # 15044223 Rev. B). 10 ng of extracted DNA was used as template and the PCR reaction (25 μL) contained dNTPs (400nM of each), $MgSO_4$ (1.5 mM), Platinum® Taq DNA

polymerase HF (2mU), 1X Platinum® High Fidelity buffer (Thermo Fisher Scientific, USA), and barcoded library adaptors (400 nM) containing Bacteria V1-3 specific primers: 27F AGAGTTTGATCCTGGCTCAG and 534R ATTACCGCGGCTGCTGG and Archaea V3-5 (Pinto and Raskin, 2012): 5'-CCCTAHGGGGYGCASCA (Arch-340F) and 5'-GWGCYCCCCCGYCAATTC (Arch-915R). PCR was set as below: Initial denaturation at 95°C for 2 min, 30 cycles of 95°C for 20 s, 56°C for 30 s, 72°C for 60 s and final elongation at 72°C for 5 min. All PCR reactions were run in duplicate and pooled afterwards. The amplicon libraries were purified using the Agencourt® AMpure XP bead protocol (Beckmann Coulter, USA) with the following exceptions: the sample/bead solution ratio was 5/4, and the purified DNA was eluted in 33 µL nuclease-free water. Library concentration was measured with Quant-iT™ HS DNA Assay (Thermo Fisher Scientific, USA) and quality validated with a Tapestation 2200, using D1K ScreenTapes (Agilent, USA). Based on library concentrations and calculated amplicon sizes, the samples were pooled in equimolar concentrations and diluted to 4 nM.

6.2.4.3 DNA sequencing

The purified sequencing libraries were pooled in equimolar concentrations and diluted to 4 nM. The samples were paired end sequenced (2x301bp) on a MiSeq (Illumina) using a MiSeq Reagent kit v3, 600 cycles (Illumina) following the standard guidelines for preparing and loading samples on the MiSeq. 10% and 20% Phix control library for respective bacterial and archaeal analyses were spiked in to overcome low complexity issue often observed with amplicon samples.

6.2.4.4 16S rRNA amplicon bioinformatic processing

Forward and reverse reads were trimmed for quality using Trimmomatic v. 0.32 with the settings SLIDINGWINDOW:5:3 and MINLEN:275. The trimmed forward and reverse reads were merged using FLASH v. 1.2.7 with the settings -m 25 -M 200. The merged reads were dereplicated and formatted for use in the UPARSE workflow. The dereplicated reads were clustered, using the usearch v. 7.0.1090 -cluster_otus command with default settings. OTU abundances were estimated using the usearch v. 7.0.1090 -usearch_global command with -id 0.97. Taxonomy was assigned using the RDP classifier (Wang et al., 2007) as implemented in the parallel_assign_taxonomy_rdp.py script in QIIME (Caporaso et al., 2010), using the MiDAS database v.1.20 (McIlroy et al., 2015). The results were analysed in R (Team, 2015) through the Rstudio IDE using the ampvis package v.1.24.0 (Albertsen et al., 2015).

6.3 Results and discussion

6.3.1 Influence of fertilizer properties on FO performance

The lab-scale side-stream An-FDFO-UF-MBR hybrid system was operated with three different fertilizers (i.e., KCl, MAP and MKP) as DS for a period of 55 days. The water flux data are presented as normalized flux as shown in **Fig. 46**. The effect of each fertilizer DS on the performance of An-FDFO-UF-MBR was first investigated since these three fertilizers have different nutrient (i.e., NPK) combinations. All fertilizers showed severe flux decline (i.e., up to almost 80%) even within 1 day operation with fairly similar initial fluxes (i.e., 9.06 L/m^2/h – 9.82 L/m^2/h). This is because the sludge with high MLSS (i.e., 3.06 ± 0.06 g/L at the initial stage) was treated by the FO membrane under quite low cross-flow velocity (i.e., 2.3 cm/s) with no aeration (Nguyen et al., 2013). In addition,

anaerobic sludge is more sticky than aerobic sludge, and thus it can accelerate membrane fouling.

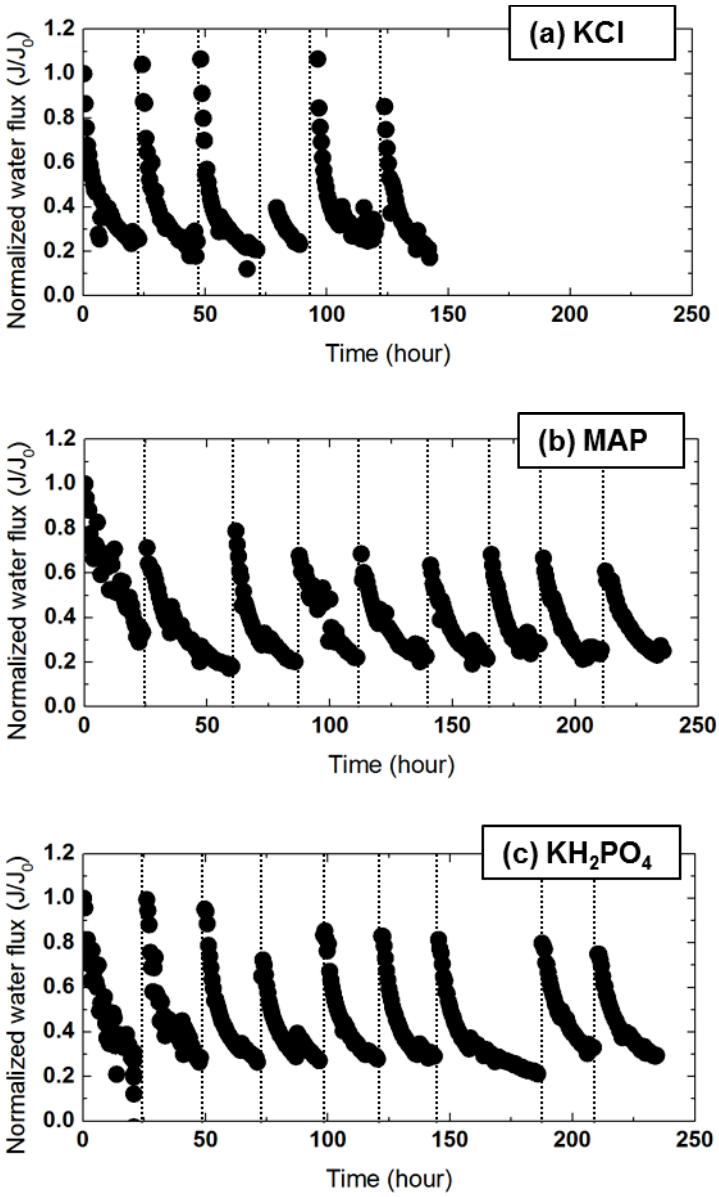

Figure 46. Flux-decline curves obtained during the anaerobic FDFO-UF-MBR hybrid system under AL-FS mode with (a) 1 M KCl DS, (b) 1 M MAP DS and (c) 1 M MKP DS. Experimental conditions of all experiments: synthetic municipal wastewater as FS, crossflow velocity of 2.3 cm/s and 20 cm/s for FO and UF, respectively, pH 7 ± 0.2, temperature of 35 ± 1 ºC, and HRT of 24 hrs. Membrane cleaning was conducted every 24 ~ 30 h by applying crossflow velocity of 6.9 cm/s with DI water as DS.

To remove membrane fouling and recover water flux, physical cleaning was applied by flushing it for 30 mins as well as replacing DS with DI water to provide the osmotic backwashing effect. Compared to similar flux decline in FDFO regardless of fertilizer types, water flux recovery by physical cleaning was significantly affected by fertilizer DS properties. When considering KCl DS as shown in **Fig. 46a**, water flux was fully recovered after physical cleaning until the 5^{th} cycle. Besides, the cleaned surface was also clearly visible during the operation, indicating that the membrane surface could be perfectly cleaned by physical cleaning when using KCl DS. With MAP DS, water flux was recovered by about 70% as presented in **Fig. 46b**. It was observed that FO membrane was partially cleaned by physical cleaning. With MKP DS, water flux was fully recovered until the 3rd cycle. However, after 3rd cycle, water flux started to be only recovered by about 80% (**Fig. 46c**).

MLSS of the sludge was measured to elucidate the different behaviour of water flux recovery and evaluate the effect of different fertilizer DS on microorganisms. When FO was operated with KCl, MLSS was 1.64 – 1.71 g/L. With MAP DS, MLSS was initially 1.42 ± 0.03 g/L and slightly reduced to 1.25 ± 0.13 g/L. Moreover, MLSS with MKP DS was lower (i.e., from 1.01 ± 0.01 g/L to 0.92 ± 0.23 g/L) compared to other fertilizers. These results indicate that microorganisms in the bioreactor were damaged by FO operation, consistent with our previous study (Kim et al., 2016).

It is very interesting to compare water flux recovery with MLSS of the sludge. KCl DS exhibited 100% recovery rate even though MLSS was very high. On the other hand, MAP DS exhibited lower recovery rate despite of lower MLSS than KCl DS. To identify the reason behind this different trend, the DNA concentration of the fouling layer was measured and presented in **Table 31**. MAP DS exhibited much higher DNA concentration than KCl DS, indicating that severe biofouling was formed on the FO membrane surface

with MAP DS. This is because KCl DS has higher RSF than MAP DS as presented in our previous studies (Phuntsho et al., 2011, Kim et al., 2016). Therefore, microorganisms attached on the surface of FO membrane could be inactivated due to high salt concentration (Johir et al., 2013). In case of MKP, water flux recovery was fully recovered at the initial stage, but afterward, it was continuously reduced. This could be explained by the fact that the sludge with MKP DS had a low fouling potential (i.e., low MLSS). Thus, the membrane surface was readily cleaned by physical cleaning. Besides, MKP DS has low RSF due to its low diffusivity as shown in **Table 30** (Phuntsho et al., 2011, Phuntsho et al., 2012b). Therefore, biofouling occurred severely similar to the results obtained with MAP and consistent with the DNA results presented in **Table 31**.

Table 31. DNA concentration of the fouling layer collected from the fouled membrane surface with three different fertilizer DS.

	KCl	MAP	MKP
DNA concentration (ng/nL)	160.2 (± 1.5)	467.8 (± 28.1)	504.6 (± 72.2)

6.3.2 Influence of fertilizer properties on salt/nutrient accumulation in the bioreactor

Salt/nutrient accumulation in the bioreactor is presented in **Fig. 47a**. When the hybrid system was operated without FO operation, TN, TP and conductivity were initially stable: 63.06 ± 4.91 mg/L, 12.11 ± 0.71 mg/L and 0.81 ± 0.07 mS/cm, respectively. However, when operating FO with KCl DS, conductivity started to significantly increase up to 5.39

mS/cm. This is because KCl shows high RSF probably due to its highest solute diffusivity as shown in **Table 30** and also lower hydrated diameters of both K^+ and Cl^- species (Phuntsho et al., 2011, Kim et al., 2016). To stabilize the anaerobic bioreactor and reduce the conductivity caused by RSF from DS, FO operation was stopped for a few days while UF was continuously operated to extract the salts from the bioreactor. As a result, salt/nutrient concentrations were recovered to the original values (after approx. 6 days). Then, FO operation restarted with MAP DS. Results showed that conductivity gradually increased to 2.44 mS/cm with a significant increase in concentrations of both TP and TN from 69.81 mg/L and 83.5 mg/L to 712.87 mg/L and 246.8 mg/L, respectively. When stopping FO operation, it was observed that TN, TP and conductivity were rapidly reduced. FO was operated again with MKP DS. **Fig. 47a** shows that both conductivity and TP in the bioreactor increased with no change in TN since MKP DS consists of potassium and phosphate. However, the increasing rate with MKP DS was lower than that with MAP DS, implying that MKP has lower RSF than MAP. From these results, it can be concluded that UF is not sufficient to mitigate salt accumulation in the bioreactor when operated simultaneously with FO.

6.3.3 Influence of fertilizer properties on biogas production

Biogas production from the anaerobic bioreactor was monitored and the results are presented in **Fig. 47b**. When operating AnMBR without FO operation, methane content was continuously increased with decreasing nitrogen and carbon dioxide contents. This indicates that the anaerobic activity was gradually taking place in the bioreactor. When FO was operated with KCl DS, the biogas production rate was slightly increased from 0.178 L/g COD to 0.301 L/g COD in 2 days while methane content slightly decreased,

which is consistent with another study (Song et al., 2016) where it was shown that the bulk organic removal and biogas/methane production decreased as the bioreactor salinity increased. Interestingly, after only 2 days of FO operation, biogas production completely stopped, which indicates that the increased salt concentration in the bioreactor (**Fig. 47a)** had a negative impact on anaerobic microorganisms (Kim et al., 2016). To recover anaerobic activity, FO operation was stopped while UF operation was continued. Afterward, salt concentration in the bioreactor was reduced to its original value and biogas started to be produced again with an increase in methane content. Thus, FO was operated again with MAP DS and biogas production rate was slightly reduced to 0.084 L/g COD with a small decrease in methane content (from 36.81% to 30.03%). For the sludge stabilization, FO operation was stopped for 7 days. However, methane content continuously decreased while nitrogen content increased, which implies that anaerobic microorganisms were critically damaged. Lastly, when starting again FO operation with MKP DS, biogas production rate was still low at 0.04 L/day and methane concentration kept decreasing to 18.25% which was accompanied by a continuous increase in nitrogen concentration. Lastly, when starting again FO operation with MKP DS, biogas production rate was still low at 0.05 L/g COD and methane concentration kept decreasing to 18.25% which was accompanied by a continuous increase in nitrogen concentration. As a consequence, it was implied that FO operation with inorganic fertilizer DS affects negatively anaerobic activity.

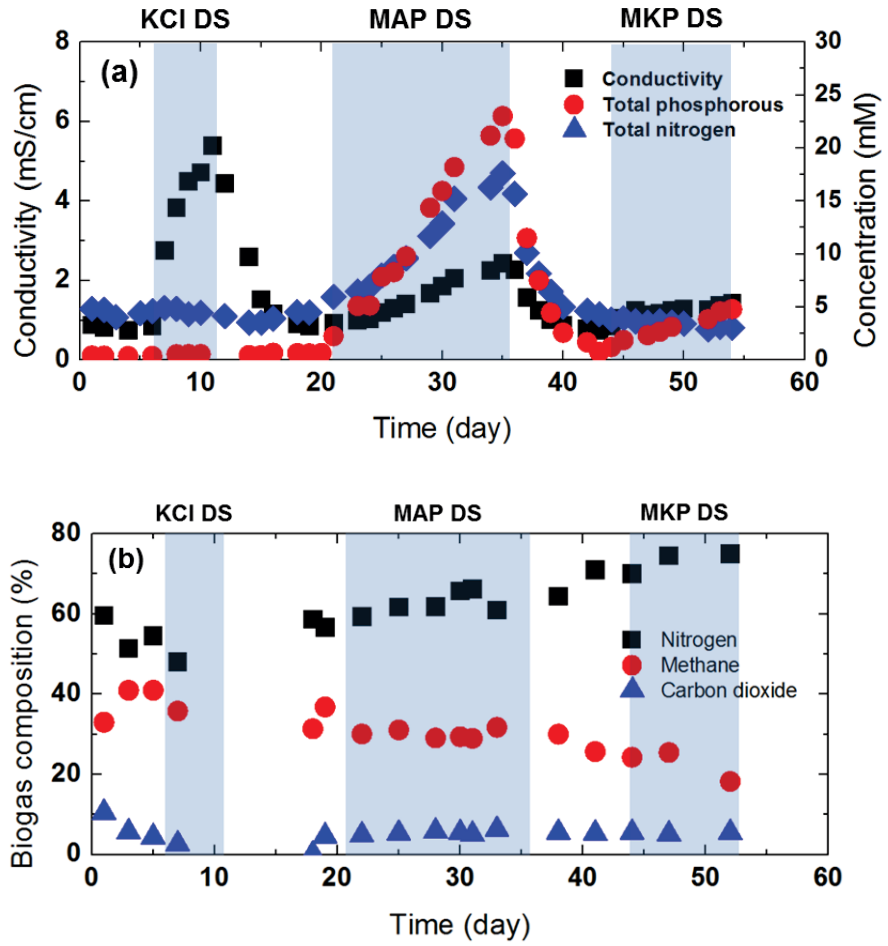

Figure 47. Influence of fertilizer DS on (a) salt/nutrient accumulation caused by RSF and (b) biogas composition. Salt and nutrient accumulations were monitored by measuring conductivity (representing potassium ions with KCl DS), total nitrogen and total phosphorous. Biogas composition was monitored by GC-FID.

6.3.4 Influence of fertilizer properties on bacterial community structure from pyrosequencing analysis

To elucidate the variations in the performance of the bioreactor, the bacterial community structure was analysed by pyrosequencing and presented in **Fig. 48**. Before operating FO, *Gelria* (18.8%) was the most dominant species followed by *Longilinea*, *VadinBC27*, *Pertimonas*, *Brooklawnia*, and *Comamonas* (i.e., 12.5%, 9.0%, 8.6%, 8.4% and 5.9%,

respectively). Based on the literature, *Gelria* is an anaerobic thermophilic glutamate-degrading bacterium which oxidizes glutamate to propionate, H_2, NH_4^+ and CO_2 (Plugge et al., 2002). *Longilinea* is associated with efficiency in hydrolytic and acidogenetic fermentation (Ambuchi et al., 2016). *VadinBC27* degrades recalcitrant organic contaminants (Riviere et al., 2009) and *Pertimonas* ferments glucose to produce acetate, H_2 and CO_2 as well as reduces elemental sulphur to sulphide and reduces nitrate to ammonium (Grabowski et al., 2005). *Brooklawnia* plays a significant role for hydrolysis and acidogenesis (Bae et al., 2006). *Comamonas* is a denitrifying bacterium which reduces nitrate to nitrogen gas (Gumaelius et al., 2001). Results from previous studies focusing on bacteria species indicated that all the aformentioned bacteria are essential to ensure the procedures from hydrolysis to acetogenesis and thus to successfully achieve methane production in the bioreactor as shown in **Fig. 47b**.

When FO operation started with KCl DS, the bacterial community structure was significantly changed (**Fig. 48**) and the biogas production stopped (**Fig. 47b)**. Results describe that *Comamonas* (54.3%) became the most dominant species followed by *Longilinea*, *VadinBC27*, *Curvibacter*, and *Clostridium sensu stricto 1* (i.e., 7.4%, 4.9%, 4.2% and 3.6%, respectively), which indicates that beneficial bacteria for bio-methane production were no longer present or deactivated in the bioreactor. This is because TDS in the bioreactor was significantly increased since KCl has very high RSF (Phuntsho et al., 2011, Kim et al., 2016). Besides, the presence of potassium ions could inhibit the anaerobic process since high potassium concentration can lead to a passive influx of potassium ions which neutralize the membrane cell potential (Kim et al., 2016).

To recover the anaerobic activity, the An-FDFO-UF-MBR hybrid system was operated without FO operation. Results in **Fig. 48** show that beneficial bacteria (i.e., *Longilinea*, *VadinBC27*, *Brooklawnia*, *Gelria* and *Comamonas*) for methane production became

dominant, and biogas production was re-started together with an increase in methane content. When operating FO with MAP DS, *Comamonas* (35.5%) was dominant followed by *VadinBC27*, *Gelria* and *Longilinea* (i.e., 5.1%, 4.8% and 4.1%, respectively), which is consistent with the results of biogas composition. With MAP DS, biogas was continuously produced as shown in **Fig. 47b** but nitrogen content was increased with a decrease in methane content. This is because the population of anaerobic bacteria (i.e., *VadinBC27*, *Gelria* and *Longilinea*) which are beneficial for hydrolysis, fermentation and acetogenesis (Plugge et al., 2002, Riviere et al., 2009, Ambuchi et al., 2016), was reduced while the population of anoxic bacterium (*Comamonas*) which is a denitrifying bacterium (Gumaelius et al., 2001), was increased.

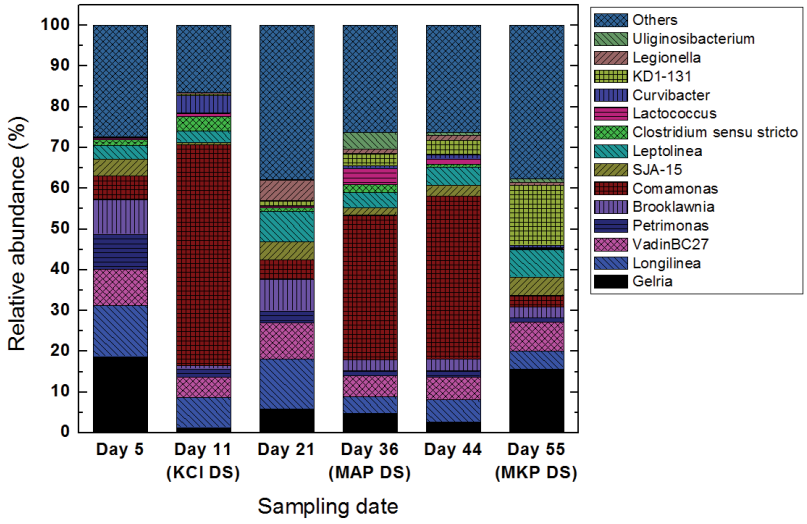

Figure 48. Variations of bacterial community structures of the sludge collected from the anaerobic bioreactor.

Therefore, FO operation was stopped again to re-stabilize anaerobic bacteria in the bioreactor. Results show that *Comamonas* (40.0%) was the most dominant species followed by *Longilinea*, *VadinBC27*, *f_KD1-131_OTU_3* and *Brooklawnia* (i.e., 5.6%,

5.5% 3.7% and 3.0%, respectively). It is interesting to note that the bacterial community structure was slightly different than the original one, which is different from the results obtained after FO operation with KCl. This implies that the anaerobic bacteria population was seriously damaged and thus nitrogen content was increased with a decrease in methane content. This is because inorganic chemical fertilizers could inhibit anaerobic microbial activity even at low concentration (Kim et al., 2016).

The An-FDFO-UF-MBR hybrid system was operated with MKP DS even though the anaerobic activity in the bioreactor was not restored to its original value. Interestingly, *Gelria* (15.6%) became the most dominant species followed by *f_KD1-131_OTU_3*, *VadinBC27*, *c_SJA-15_OTU_10* and *Longilinea* (i.e., 14.7%, 7.2%, 4.6% and 4.5%, respectively), while *Comamonas* was significantly reduced from 40.0% to 2.8%. This implies that biogas production and methane content should be enhanced. However, biogas production was still low with a continuous reduction in methane content. Therefore, it can be hypothesized that if methanogens were activated with MKP DS, biogas production and methane content would have increased with a longer operation.

To further investigate the effect of fertilizer properties on biogas production, the archaeal community structure was analysed by pyrosequencing and presented in **Fig. 49**. Initially, Methanosaeta (45.7%) was dominant followed by Methanomethylovorans and Methanobacterium (i.e., 28.6% and 14.4%, respectively) with a total of 97.92% of methanogens. With KCl DS, the archaeal community structure was not significantly changed but its relative abundance was slightly affected. During operation, Methanosaeta was getting more abundant in the sludge while the population of Methanomethylovorans was reduced. This indicates that the archaeal community structure is affected by inorganic fertilizers in the bioreactor. However, from these results, it was observed that methanogens were still the dominant species (i.e., 95% ~ 98%) regardless of the types of

fertilizer DS. Nevertheless, methane content was continuously decreased with low biogas production. This is because the anaerobic bacterial community was seriously influenced by fertilizer DS and thus biodegradation and biogas production mechanisms did not work effectively.

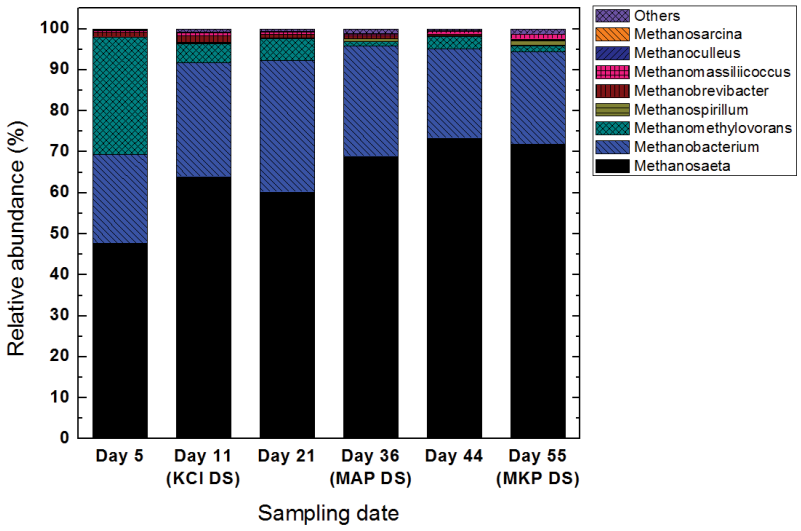

Figure 49. Variations of archaeal community structures of the sludge collected from the anaerobic bioreactor.

Findings from this study have significant implications for optimizing the proposed An-FDFO-UF-MBR hybrid system. The present hybrid system has two major problems: the first is the severe membrane fouling in FDFO resulting in flux decline. The second issue is the negative impact on anaerobic activity caused by reversely diffused fertilizer draw solutes in the bioreactor. The RSF issue is more problematic since membrane fouling in a side-stream FO membrane module could be easily controlled by optimizing the system design (e.g., module design and system configuration) and the operation conditions (e.g., critical water flux, cross-flow rate and cleaning methods). Thus, three solutions can be implemented to overcome the RSF issue. The first would reduce RSF by optimizing the

DS composition. For example, inorganic DS can be mixed with surfactant such as Triton X-114 (Nguyen et al., 2015) and thus RSF can be significantly reduced . The second would be to enhance the anaerobic activity by taking advantage of the RSF. For instance, inorganic fertilizer DS can be mixed with organics which can enhance anaerobic activity or organic fertilizer with low RSF can be developed. The last solution would be to reduce salt accumulation in the bioreactor. In this study, UF was applied for removing salts in the bioreactor, but this was not effective. Thus, alternative macro porous membrane technology (e.g., MF or membrane cartridge filtration) which can retain sludge or electric desalination technology (e.g., CDI, ED (Lu and He, 2015) or ion exchange) can be employed.

6.4 Conclusions

Primary findings drawn from this study are summarized as follows:

- Flux decline was very severe regardless of fertilizer DS due to the absence of aeration and the sticky sludge, while flux recoveries were different amongst the tested fertilizer DS since their effect on biofouling was different.
- Nutrient accumulation in the bioreactor was influenced by fertilizer properties and exhibited a significant impact on anaerobic activity as well as the sludge.
- Bacterial community structure was affected by nutrient accumulation while archaeal community structure remained fairly stable, implying that anaerobic activity was mainly depending on variations in bacterial community structure.

7. Fertilizer-drawn forward osmosis process for sustainable water reuse to grow hydroponic lettuce using commercial nutrient solution

7.1 Introduction

With increasing pressure on natural resources due to rapid and extensive urbanization and industrialization, freshwater resources are becoming limited, particularly in arid, semi-arid and coastal areas. On the other hand, the agricultural sector consumes about 70% of the accessible freshwater with about 15-35% of water being used unsustainably (i.e. wasted) (Cai and Rosegrant, 2003, Assessment, 2005, Clay, 2013). Besides, in arid regions, agriculture is not only hindered by the limited freshwater resources but also by the scarcity of fertile lands. Hydroponics, a subset of hydroculture, is being increasingly used in commercial greenhouse vegetable production worldwide. In fact, being a soilless process, it eliminates all the problems associated with soil culture (e.g. poor drainage, soil pollution or soil-borne pathogens) and offers the possibility of using areas typically unsuitable for conventional farming such as arid regions (Jensen, 1997). However, this technique requires nutrient solutions to grow plants and therefore also consumes a large amount of freshwater although the water efficiency is much higher compared to open farming in the soil. This water-food nexus has become a critical issue in most arid regions and therefore, the development of technologies to sustain water and food security must be explored.

Wastewater reuse for irrigation of plants and crops has gradually become a common practice worldwide since it represents a viable alternative water source (Angelakis et al., 1999a). However, wastewater effluent from a typical biologically treated effluent is generally not suitable for direct application due to the presence of pathogens (e.g. E-coli, faecal coliform, Giardia and Cryptosporidium, viruses etc.), organic and inorganic

pollutants (e.g. heavy metals and micro pollutants) which are detrimental to both plants and human health (EPA, 2012, Wang et al., 2016). Therefore, advanced treatment process (e.g. membrane technologies) is essential to eliminate any health risks which are usually done using UF or RO or both.

FDFO has received increased interest since its concept relies on the natural osmotic dilution of fertilizer DS which can then be applied directly for irrigation without the need of a DS recovery process as for the other FO applications (Phuntsho et al., 2011, Phuntsho et al., 2012a, Phuntsho et al., 2012b, Phuntsho et al., 2013a). Although previous FDFO studies focused on the desalination of either brackish or seawater, the relatively low salinity and high organic content of most impaired waters makes them suitable candidate for the wastewater treatment through osmotic dilution (Lew et al., 2005). Besides, due to the limit posed by the osmotic equilibrium between FS and DS, which will ultimately affect the final nutrient concentration, using FS having a lower salinity (i.e. lower osmotic pressure) will help in meeting the standard requirements for irrigation. Finally, it has been demonstrated that FO alone can be effective for the treatment of impaired waters, especially for the removal of persistent trace organic compounds, making it a suitable technology for wastewater reuse (Coday et al., 2014).

To date, several inorganic fertilizer salts have been tested as a potential DS either separately or in blended form (Phuntsho et al., 2011, Phuntsho et al., 2012b). However, by using single or blended salts as fertilizers, the final diluted DS does not have the required balanced nutrients (i.e. macronutrients and micronutrients) for plant growth. Therefore, two recent bench-scale studies (i.e. targeting greenwall and conventional soil irrigation) have suggested the use of commercial fertilizers containing all essential nutrients with the required balanced ratio (Xie et al., 2015b, Zou and He, 2016). Although these preliminary bench-scale studies showed promising results and demonstrated the

potential feasibility of water recovery by the FO process using commercial liquid fertilizers, the response of plants grown in nutrient solution produced by FDFO has not been assessed. Hydroponic nutrient solutions are the most versatile medium where plants can grow with little care. They can be easily prepared, modified, and replaced. The production of lettuce (*Lactuca sativa* L.) in hydroponic systems is well studied under different conditions and scenarios (Domingues et al., 2012, Smoleń et al., 2014, Park et al., 2016).

Therefore, the main objective of the present study is to demonstrate the feasibility of FDFO to produce nutrient solutions suitable for hydroponics via osmotic dilution of secondary wastewater effluent using commercial hydroponic nutrient solution as DS. Bench-scale experiments were firstly conducted to evaluate the performance of the commercial hydroponic nutrient solution in comparison to standard single inorganic fertilizer DS. Pilot-scale operation of FDFO was then carried out to investigate the potential of FDFO to produce a nutrient solution suitable for hydroponic application. Finally, the response (i.e. growth performance) of hydroponic lettuce plants grown in nutrient solutions produced by the pilot FDFO process was tested and compared with standard hydroponic formulation.

This chapter is an extension of a research article published by the author in Separation and Purification Technology.

7.2 Experiments

7.2.1 Bench-scale FO experiments

7.2.1.1 FO membranes and commercial hydroponic nutrient solution

A commercially available TFC PA FO membrane (Toray Industry Inc.) was used for all the bench-scale experiments. In fact, to ensure data consistency, this membrane was obtained from a spiral wound 8040 TFC FO membrane module, similar to the one used for the subsequent pilot-scale experimental studies. The pure water permeability coefficient (A value) and salt rejection rate of the TFC PA FO membrane determined based on the previous experimental protocol (Cath et al., 2013) were found as follow: A = 8.9 ± 0.14 $L.m^{-2}.h^{-1}.bar^{-1}$ and salt rejection of 85% (1.2 g/L Red Sea salt).

The commercial hydroponic nutrient solution (Optimum Grow - twin pack hydroponic nutrient) used in this study as DS was obtained from Fernland Agencies Pty Ltd (Queensland, Australia). This is a standard hydroponic nutrient solution usually employed in plant nurseries and commercial greenhouses. This commercial nutrient solution consists of two concentrated solutions, namely “Part A” and “Part B” which is typical of any hydroponic recipes (Jones Jr, 2016). In fact, as shown in **Table 32**, Part A contains calcium while Part B contains phosphates and sulphates which can both form insoluble precipitates with calcium if mixed in the concentrated form. This also indicates that, Part A and B solutions will have to be processed by FDFO process separately either in a parallel stage or use only one of the solutions as DS while the other can be later mixed in dilute form. **Table 32** also shows that the commercial nutrient solution contains a significant concentration of organics which usually comes from humic-like materials or organic chelating agents such as ethylenediaminetetraacetic acid (EDTA) used to

facilitate nutrient uptake or urea as a source of nitrogen. The impact of the presence of organics in the DS on the FO performance (i.e. water flux and RSF) remains largely unknown and requires further insights.

Bench-scale and pilot-scale FO experiments were conducted with Part B only since it contains all essential macronutrients (i.e. N, P, K) as well as other important micronutrients (i.e. Mg, S, Mn, B, Zn and Mo). For the hydroponic experiments, Part A was simply added, at the required ratio, and mixed to the final nutrient solution produced by the FDFO pilot.

Table 32. Characteristics of the commercial liquid fertilizer used in this study.

Parameters	Part A*	Part B*
EC (mS/cm)	119.6	107.2
pH	2.63	4.26
TDS (mg/L)	95100	67300
TOC (mg/L)	1136	519.5
Osmotic pressure (bar)**	95.2	66.3
TN (mg/L)	41000	12000
$N\text{-}NO_3^-$ (mg/L)	33600	8700
$N\text{-}NH_4^+$ (mg/L)	3800	1400
$N\text{-}NO_2^-$ (mg/L)	N/D	N/D
$P\text{-}PO_4^{2-}$ (mg/L)	0	9000
K^+ (mg/L)	25400	36800
Ca^{2+} (mg/L)	36600	0
Mg^{2+} (mg/L)	0	10340
SO_4^{2-} (mg/L)	0	12900

*Part A also contains Fe and Part B contains essential micronutrients (i.e. Mn, B, Zn and Mo). **The osmotic pressure was calculated using ROSA software (Version 9.1, Filmtech Dow Chemicals, USA).

7.2.1.2 Bench-scale FO setup

The performance of the FO process was firstly evaluated in a batch mode of FO operation similar to the one used in previous studies (Lee et al., 2010, Kim et al., 2015c). The FO cell has two symmetric channels on each side of the membrane and the system was operated under co-current flow mode. The cell has internal dimensions of 7.7 cm length, 2.6 cm width and 0.3 cm depth (i.e. effective membrane area of 0.002 m^2). Variable speed gear pumps (Cole Parmer, USA) were employed to circulate FS and DS. The DS tank

was placed on a digital scale connected to a computer to enable the determination of the water flux by measuring the weight changes over time. A conductivity and pH meter (Hach, Germany) was connected to the feed tank to record the pH and RSF of draw solutes. The experiments were conducted under the AL-FS mode. A new membrane was used for each experiment and the FO membrane was stabilised for 30 mins using DI water on both sides of the membrane prior to the start of the experiment. Once stabilised, FS and DS were replaced and the water flux was measured continuously every 3 mins. All experiments were conducted at a cross-flow velocity of 8.5 cm/s, and a constant temperature of 25 ºC maintained with the help of temperature control bath connected to a heating/chilling unit.

7.2.1.3 Short and long term performance

Preliminary short-term experiments (i.e. up to 25% water recovery) were conducted to evaluate the basic performance (i.e. water flux and RSF) of the commercial hydroponic nutrient solution (Part B only) against NaCl, a widely used standard DS. NaCl solution was prepared at 1.4 M concentration which corresponds to an osmotic pressure of 66 bar, similar to the one of Part B fertilizer (**Table 32**). The osmotic pressure was calculated using ROSA software (Version 9.1, Filmtech Dow Chemicals, USA). Experiments using 1.4 M NaCl with 500 mgC/L (i.e. corresponding to 1.8 g/L humic acid) as DS were also conducted to evaluate the effect of organics in the DS on the FO performance (i.e. water flux, RSF and reverse organic compounds flux). These short-term experiments were conducted with DI water as FS. Water flux was measured continuously and the average water flux obtained after 25% water recovery was reported. Reverse salts and organic compounds fluxes were quantified by analysing their concentration in FS at the beginning

and end of each experiment. Samples from FS were taken at the start and completion of each experiment for inorganic and organic compounds analysis.

Long-term experiments (i.e. up to 75% water recovery) were then conducted using the liquid fertilizer (Part B) as DS and synthetic wastewater simulating municipal wastewater effluent (**Table 33**) as FS. Upon completion of the experiments, different physical cleaning methods were tested to evaluate their effectiveness on water flux recovery. Membrane surface flushing (or hydraulic cleaning) was conducted by replacing both the solutions with DI water and recirculating for 30 mins at triple crossflow (i.e. 25.5 cm/s). Osmotic backwashing was also employed during which FS was replaced with 1M NaCl and DS with DI water to create a negative water flux. Osmotic backwashing was conducted at crossflow rates of 8.5 cm/s for 30 mins. After physical cleaning or osmotic backwashing, initial FS and DS (i.e. synthetic wastewater and commercial liquid fertilizer) were switched back to the system and water flux was monitored for an additional 2 h after which the water flux recovery rates were calculated.

Table 33. Composition and characteristics of the synthetic wastewater used in this study (based on (Chen et al., 2014b)).

Parameters	Value
Glucose (mg/L)	275
Peptone (mg/L)	100
Beef extract (mg/L)	100
Urea (mg/L)	10
$NaHCO_3$ (mg/L)	100
KH_2PO_4 (mg/L)	20
NH_4Cl (mg/L)	25
$MgCl_2 \cdot 6H_20$ (mg/L)	10
$CaCl_2 \cdot 2H_20$ (mg/L)	5
pH	6.58
EC (mS/cm)	0.226
TOC (mg/L)	175.6
Osmotic Pressure (bar)*	0.14

*The osmotic pressure was calculated using ROSA software (Version 9.1, Filmtech Dow Chemicals, USA).

7.2.1.4 Analytical methods

Macro and micronutrients (i.e. $N\text{-}NH_4^+$, $N\text{-}NO_3^-$, $N\text{-}NO_2^-$, TN, $P\text{-}PO_4^{3-}$, K^+, SO_4^{2-}, Mg^{2+} and Ca^{2+}) concentrations were determined using Merck cell tests and spectrophotometer (Spectroquant NOVA 60; Merck, Germany). The total organic content of FS was measured using a TOC analyser (TOC-VCPH, TNM-1, Shimadzu, Japan).

The surface of virgin, fouled and cleaned membranes were analysed by SEM (Zeiss Supra 55VP, Carl Zeiss AG, Germany). Samples were firstly dried under air purging and then lightly coated with Au/Pd. The SEM imaging was performed at an accelerating voltage of 10kV at different magnifications and at various points.

7.2.2 Operation of pilot-scale FDFO unit

Fig. 50 illustrates the layout of the pilot-scale FO unit operated in this study and more detail on its design and control are provided in our previous study (Kim et al., 2015b). Here, an 8" spiral wound TFC PA FO membrane module with a total membrane area of 15.3 m^2 (Toray Industries, Korea) was used. All experimental studies were conducted in FO mode or AL-FS mode. FS and DS flow rates were maintained at 70 and 6 L/min, respectively, throughout the experiments. FS and DS were the same used during the bench-scale tests (i.e. synthetic wastewater and commercial liquid fertilizer Part B). FS was kept constant throughout the experiments (i.e. conductivity was measured at frequent intervals and adjusted when necessary) to maintain the same osmotic pressure on the feed side of the membrane while DS was continuously diluted.

The system was operated under a combination of FO and PAO modes (Sahebi et al., 2015). In FO mode (referred as stage 1), the osmotic driving force of the DS was solely responsible for generating the water flux and FO unit was operated until the DS tank (1,000 L) was full with the diluted fertiliser DS. The diluted DS from stage 1 was then used as DS in PAO operations (referred as stage 2 and stage 3). For PAO operations, hydraulic pressure was applied on the feed side of the membrane module and used as an additional driving force to enhance water flux (Sahebi et al., 2015). In order to achieve the targeted fertilizer dilution for direct hydroponic application (i.e. 250 times dilution as indicated by the manufacturer) two stages of PAO was necessary at an applied pressure of 2 bar (i.e. maximum pressure rating of the feed pump). The first PAO experiment (i.e. stage 2) was continued until the DS tank was full with the diluted fertiliser DS and this solution was in turn used as the DS for the second PAO experiment (stage 3). The pilot operation was stopped when the targeted dilution factor was achieved. At the end of the experiments, the diluted DS (i.e. Part B) was mixed with the required ratio of Part A

solution (**Table 32**) and stored in 200 L tanks for the subsequent hydroponic experiments. About 120 L of nutrient solution was delivered to the Royal Botanic Gardens every week for hydroponic testing. All containers were initially disinfected using 70% ethanol solution and rinsed with MQ water to avoid bacterial growth. Conductivity and pH were measured twice a week to ensure both parameters remain within the acceptable range for hydroponics (i.e. pH 6.0-6.5 and conductivity 1.5-2.0 mS/cm) and hydrogen peroxide (50% v/v) was applied once a week at a rate of 2 mL per 10 L of nutrient solution to prevent microorganism growth in the tanks.

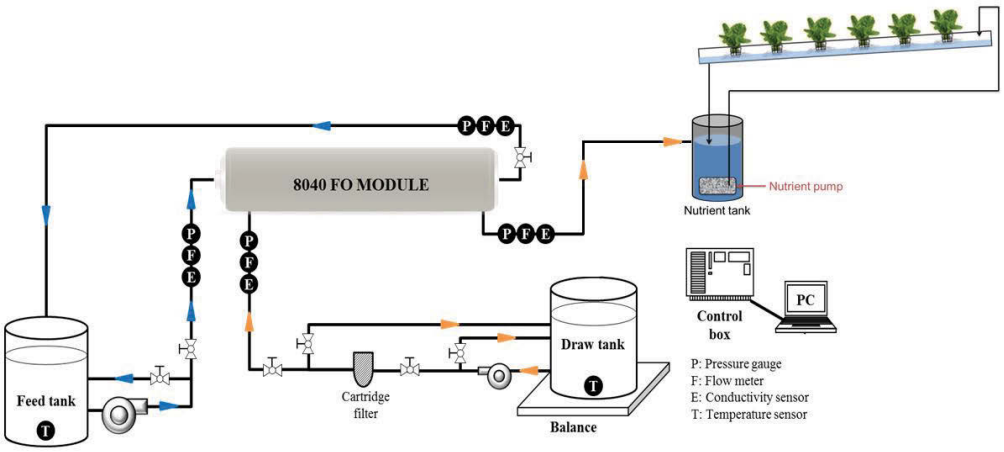

Figure 50. Schematic diagram of the pilot-scale FO experimental set up and illustration of 8040 spiral wound TFC PA FO modules manufactured by Toray Inc.

7.2.3 Hydroponic lettuce plants experiments

7.2.3.1 Nutrient film technique (NFT) and experimental procedures

Different types of hydroponic systems are used for the production of lettuce and include still solution hydroponics, substrate hydroponics with recirculating solution and the nutrient film technique (NFT); the latest being the most popular system has been selected

for this study. In NFT, the plants are supported in a gently sloping (i.e. about 1.5-2.0°) shallow gully in which the roots are suspended in a flowing stream containing the nutrient solution as shown in **Fig. 51**. This marginal slope allows the nutrient solution to flow back into the recirculation tank from which it is pumped back to the top of the gully making it a closed recirculating flow system. The circulation of the nutrient solution down the gullies also helps in making the solution sufficiently aerated. The NFT units typically used in Australia consist of PVC channels having rectangular base and fitted with plastic covers containing plant holes. The NFT units used in this study have been purchased from Sage Horticultural (Hallam, Vic., Australia).

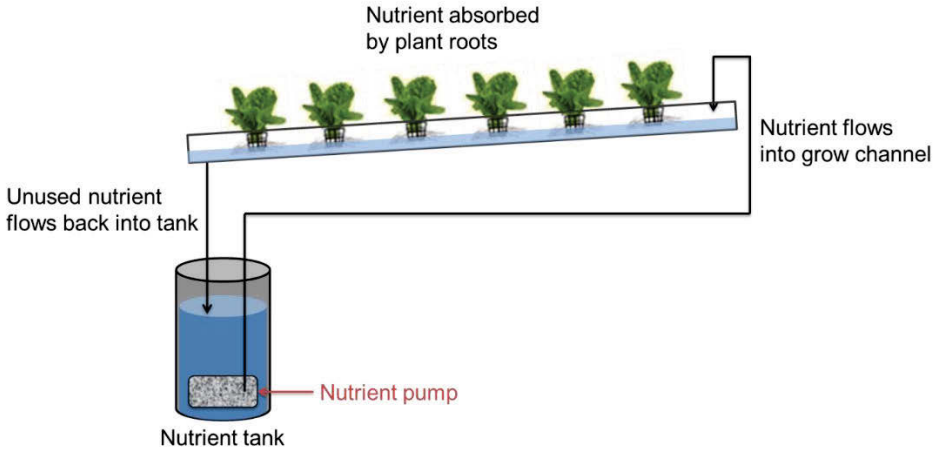

Figure 51. Schematic diagram of the nutrient film technique (NFT) used in this study.

The experiment was conducted in a controlled environment greenhouse at the Royal Botanic Garden nursery in Sydney from April to June 2016. The diluted nutrient solution obtained from the pilot FDFO unit was used to grow lettuce in NFT units. The experiment consisted of three different treatments: i) FDFO nutrient solution as T1; ii) Optimum Grow (i.e. same hydroponic nutrient solution used as DS in FO experiments) diluted with distilled water as T2; and iii) Half-strength Hoagland's solution as T3 (**Table 34 and 35**).

Table 34. Chemicals composition of Half-Strength Hoagland's solution [a].

	Amounts per volume of water	
	Stock concentrate #1	
Compounds	**500 mL**	**1 L**
KNO_3	25.26 g	50.52 g
KH_2PO_4	14.42 g	28.84 g
$MgSO_4.6H_2O$	11.48 g	22.96 g
Micronutrient concentrate	50 mL	100 mL
	Stock concentrate #2	
$Ca(NO_3)_2$ [b]	45.69 g	91.38 g
Fe-EDTA 13%	2.41 g	4.82 g
	Micronutrient concentrate	
	200 mL	**1L**
H_3BO_3 [c]	0.57 g	2.85 g
$MnSO_4.H_2O$	0.30 g	1.5 g
$ZnSO_4.7H_2O$	0.04 g	0.2 g
$CuSO_4.5H_2O$	0.01 g	0.05 g
$MoO_3.2H_2O$	0.004 g	0.02 g

[a] All chemicals were analytical or reagent grade.

[b] The iron chelate was thoroughly mixed before adding the dissolved $Ca(NO_3)_2$

[c] H_3BO_3 was dissolved in boiling water. Other salts were added and mixed in 100 mL of water. The dissolved H_3BO_3 was added to the rest and the final volume adjusted.

Table 35. Nutrient solution preparation using Half-Strength Hoagland's solution.

	To make final nutrient solution*	
	50 L	**100 L**
Stock concentrate #1	250 mL	500 mL
Stock concentrate #2	250 mL	500 mL

*EC and pH would be approximately 1050 µs/cm and 6.24, respectively.

7.2.3.2 Response of hydroponic lettuce plants: Growth performance

Lettuce seeds (*Lactuca sativa* L. 'Green Mignonette', Mr. Fothergill's Seeds Pty Ltd.) were first sown on Rockwool cells in a germination glasshouse under controlled temperature (18-27 °C) and grown for three weeks. A total of 57 seeds (**Fig. 52**) were germinated in individual cells within trays filled with Optimum nutrient solution (EC = 700 µs/cm and pH = 6.0). After three weeks, seedlings were then transferred to the NFT units and grown for eight weeks under the three aforementioned treatments (19 plants per treatment, **Fig. 53**). All nutrient solutions were prepared to an EC of 1100 µs/cm and a pH of 6 adjusted with distilled water, phosphoric acid and potassium hydroxide, respectively. At the end of the experiment (**Fig. 54**), data were collected from 5 randomly selected plants on different growth parameters such as fresh biomass production (aerial parts and roots) and dried biomass (oven dried at 60 °C for 72 h).

Figure 52. Lettuce seedlings germinated in Rockwool.

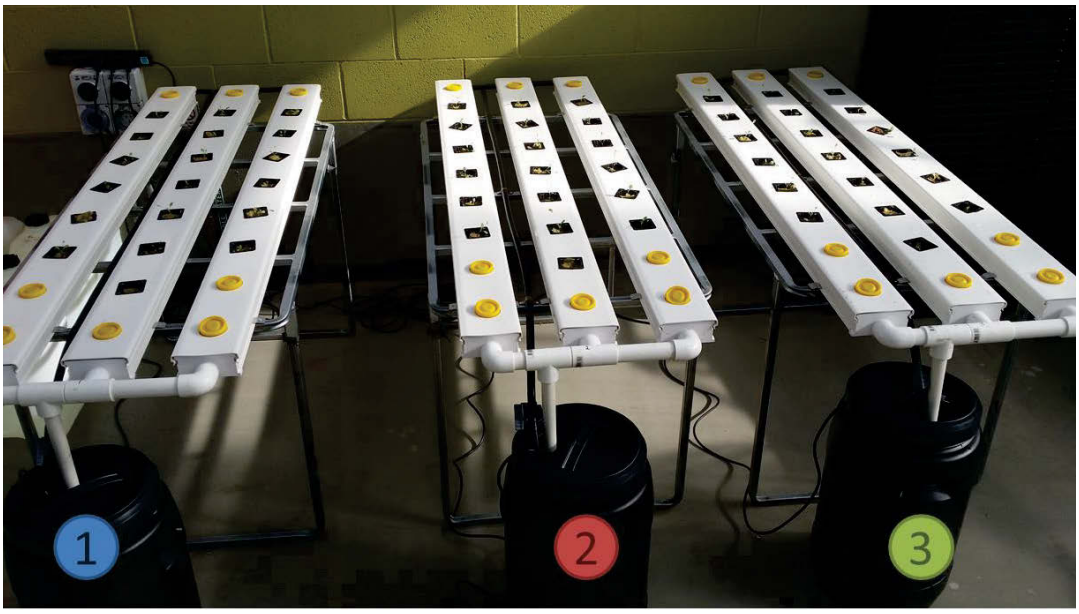

Figure 53. Lettuce seedlings in NFT units with three different treatments: (1) feed with FDFO nutrient solution, (2) feed with commercial fertilizer diluted with distilled water and (3) feed with half-strength Hoagland's solution.

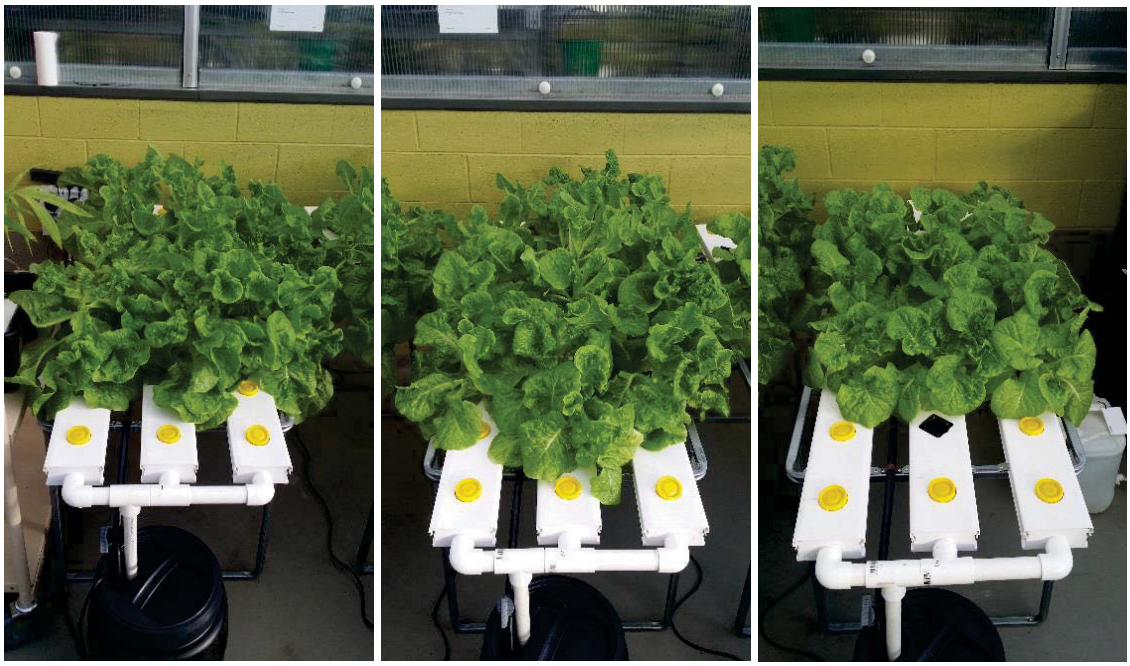

Figure 54. End of experiment with three different treatments: NFT unit feed with FDFO nutrient solution (left), NFT unit feed with commercial fertilizer diluted with distilled water (centre) and NFT unit feed with half-strength Hoagland's solution (right).

7.3 Results and discussion

7.3.1 Bench-scale performance of commercial fertilizer

The performance of the commercial fertilizer in terms of water flux, final TOC concentration in FS and RSF is presented in **Fig. 55**. At similar initial driving force (i.e. initial osmotic pressure of 66.3 bar), the average water flux produced by the commercial fertilizer was slightly lower than the one obtained with NaCl (i.e. 15.9 ± 0.7 LMH against 19.7 ± 0.9 LMH for the commercial fertilizer and 1.4 M NaCl, respectively). Although, theoretically, the osmotic pressure difference across the membrane is the main driving force in the FO process, it has been shown previously that the extent of ICP effects inside the membrane support layer facing the DS will have significant impact on the water flux (McCutcheon et al., 2006, McCutcheon and Elimelech, 2007). Therefore, a DS having a higher diffusivity (e.g. NaCl) will generate a high water flux because of the lower ICP effects inside the membrane support layer. The presence of multiple solutes in the commercial fertilizer including those solutes with lower diffusivities probably lowers the average diffusivity of the DS thereby resulting is slightly lower water flux. **Fig. 55a and 55d** show that the presence of humic acid (HA) (i.e. 500 mg/L of carbon or mgC/L) in the DS did not affect the FO water flux performance. In fact, there was no significant difference in the average water flux (**Fig. 55a**) which indicates that HA did not accumulate on the membrane support layer to induce a potential fouling layer which would have created an additional resistance to the water flux. This is in accordance with previous studies showing that the water permeation drag (i.e. from FS to DS) prevents the accumulation of HA on the support layer (Boo et al., 2013, Xie et al., 2015b).

At similar initial TOC content (i.e. 500 mgC/L), there were more organic compounds diffusing to FS with the commercial fertilizer compared with 1.4 M NaCl with humic acid

(**Fig. 55b**). This clearly demonstrates that the commercial fertilizer contains other organic compounds beside HA, which can diffuse easily through the membrane towards the DS. Other sources of organics in the commercial fertilizer solution include chelating agents such as EDTA or urea, as a source of nitrogen. Chelating agents, such as EDTA, have large molecular weight (e.g. molecular weight of EDTA is 292.24 g/mol) so it is very unlikely that these organic compounds will diffuse to FS. However, the high reverse solute transport of urea has already been demonstrated (Phuntsho et al., 2012b) attributed to its low molecular size (i.e. 60.06 g/mol) combined with the fact that it remains neutral in solution, increasing its reverse diffusion through the FO membrane (Hancock and Cath, 2009). This hypothesis is further confirmed by the high reverse diffusion of N compounds from the commercial fertilizer (**Fig. 55c**).

The loss of nutrients from the commercial fertilizer by reverse diffusion during its osmotic dilution is an important factor that needs to be evaluated since it will affect the final nutrient concentration available to the plants. A well-balanced macro and micronutrients solution is essential to ensure favourable plant growth and health. **Fig. 55c** shows the reverse permeation of the different nutrients present in the commercial fertilizer. First, it can be seen that the solutes having the lower hydrated solute radii (i.e. K^+, NH_4^+ and NO_3^-) had the highest RSF while the solutes having the larger solute radii (i.e. PO_4^{3-}, SO_4^{2-} and Mg^{2+}) showed the lowest reverse permeation; indicating that steric hindrance played a role in the reverse diffusion of nutrients (Linares et al., 2011, Alturki et al., 2013). Phosphate and sulphate ions, besides having a relatively high hydrated radius, possess negatively charged multivalent ions and are thus subjected to electrostatic repulsion resulting in lower RSF. The difference of RSF amongst the solute ions can also be explained based on their initial concentration. In fact, previous studies have shown that RSF increases with the increase in draw solutes concentration (Ge et al., 2012, Phuntsho

et al., 2013b). Potassium had the highest concentration (36.8 g/L) while NH_4^+ ions had the lowest (1.4 g/L) followed by NO_3^- (8.7 g/L) in the commercial liquid fertilizer DS. Based on their hydrated radii and diffusivity, these solutes may appear to have similar reverse diffusion transport behaviour. However, results in **Fig. 55c** show that the reverse diffusion of K^+ was significantly higher than for NH_4^+ and NO_3^- which may be related to their differences in the initial concentration. Another explanation for the difference in RSF between K^+, NH_4^+ and NO_3^- could be ion pairing. For instance, some fraction of KCl and NH_4Cl could be present in the non-dissociated form instead of free ions and such uncharged solutes could more easily diffuse through the FO membrane compared to charged species (Wishaw and Stokes, 1954). On the other hand, $NH_4H_2PO_4$ also contains NH_4^+ ions but their diffusion will be limited in order to maintain electrical neutrality of DS since the corresponding anion (i.e. HPO_4^{2-}) has a much larger hydrated radius; reducing its reverse permeation. Therefore, depending on their associated ions, the reverse transport of different solutes will be different.

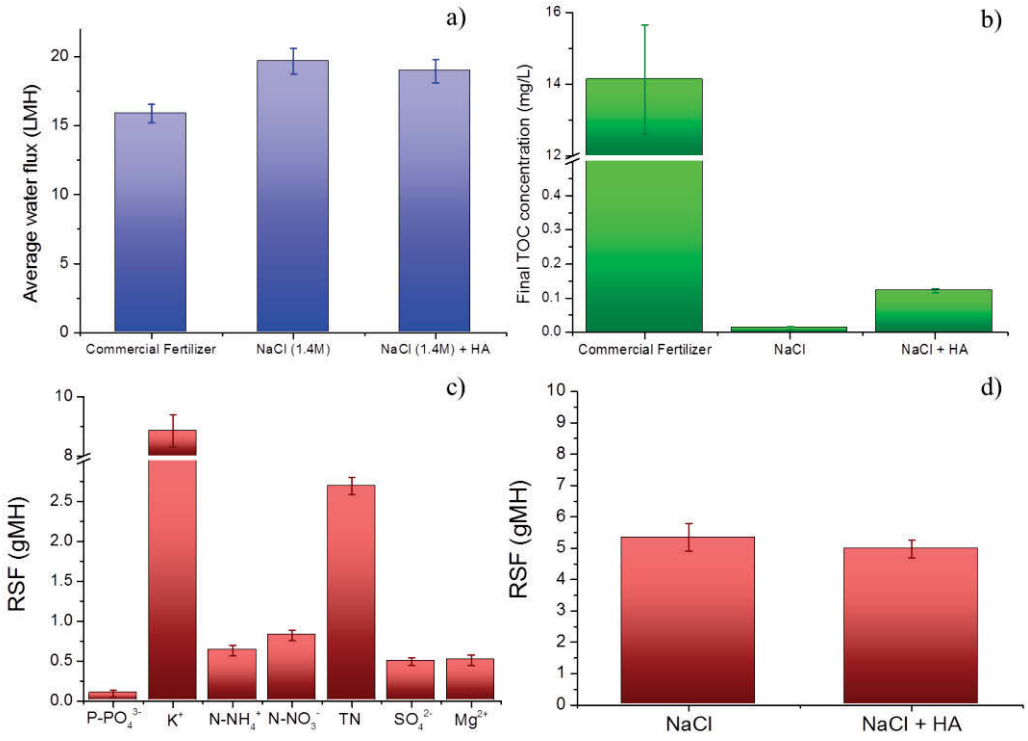

Figure 55. (a) Average water flux, (b) Final TOC concentration in the feed solution, (c) Reverse nutrient fluxes of commercial liquid fertilizer and (d) Reverse salt flux of 1.4M NaCl and 1.4M NaCl with 500 mgC/L humic acid draw solutions. Experimental conditions were: feed solution: DI water; draw solutions: commercial fertilizer Part B, 1.4M NaCl and 1.4 M NaCl with 500 mgC/L humic acid; crossflow velocity: 8.5 cm/s; temperature: 25°C; Operating time: up to 25% water recovery. Error bars are standard deviation of duplicate measurements.

The long-term FDFO operation was carried out to achieve a wastewater feed recovery of up to 75% using commercial hydroponic nutrient solution as DS in a batch process and the performance assessed in terms of water flux, RSF and water flux recovery after hydraulic cleaning and osmotic backwashing (**Fig. 56 and 57**). **Fig. 57a** shows that the water flux was fairly stable initially up to 25% recovery rate and then the flux significantly decreased to about 85% on reaching recovery rate of 75%. The water flux decline is

mostly caused due to continuous decrease of the osmotic pressure driving force (i.e. dilution of the fertilizer DS and concentration of FS in a batch mode of operation) and also likely due to the deposition of foulants on the membrane surface, increasing the resistance to water permeation through the membrane. In fact, visual observation of the membrane surface after the experiment showed a brownish cake layer formed with a loose structure (data not shown).

At the end of each FDFO performance experiments, two physical cleaning methods (i.e. hydraulic cleaning and osmotic backwashing) were adopted to remove the deposited foulants and recover the initial water flux. Results in **Fig. 57a** show a partial water flux recovery of only about 75% after the hydraulic cleaning indicating that internal fouling within the support layer might have also occurred inside the membrane support layer (Arkhangelsky et al., 2012). Osmotic backwashing, however, was able to restore up to 95% of the initial water flux (**Fig. 57a**). In fact, this cleaning method was employed in previous studies and showed better performance for the removal of foulants within the support layer (Yip and Elimelech, 2013, Boo et al., 2013, Valladares Linares et al., 2013). **Fig. 56** shows the SEM images of the virgin membrane, the fouled membrane and the membrane surface after hydraulic cleaning and osmotic backwashing. It can be clearly seen that the surface of the membrane after both cleaning methods is very similar to the virgin membrane; indicating that most of the foulants deposited of the membrane surface were easily removed by physical hydraulic cleaning. However, after the hydraulic cleaning, a partial gel layer can still be observed which was probably attached strongly on the membrane surface and not easily removed by simple hydraulic flushing.

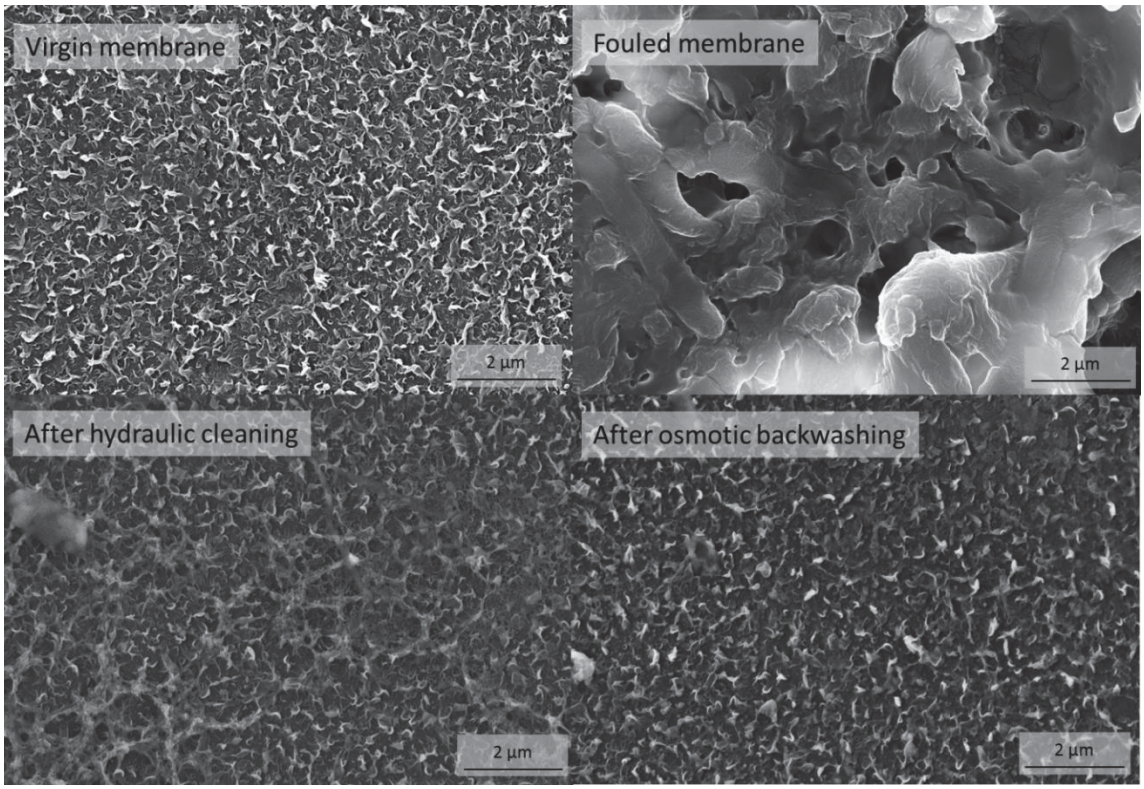

Figure 56. SEM images of the active layer of the virgin membrane, fouled membrane, and cleaned membrane after hydraulic cleaning and osmotic backwashing under 10,000 X magnification.

The reverse nutrient diffusion during long-term operation using synthetic wastewater as feed showed a similar trend but slightly lower values compared to the results obtained during the short-term experiments using DI water as feed. This can be attributed to the lower average water flux as well as to the formation of the organic foulant cake layer that reduced the reverse solute transport through the membrane. In fact, it has been demonstrated previously that the formation of organic fouling layer rendered the membrane surface negatively charged which reduces the reverse transport of negatively charged solutes (e.g. HPO_4^{2-}) by enhanced electrostatic repulsion with the fouling layer. Thus, to maintain the electrical neutrality of DS, the reverse diffusion of the coupled positive ions also improves (Xie et al., 2013b, Xie et al., 2015b).

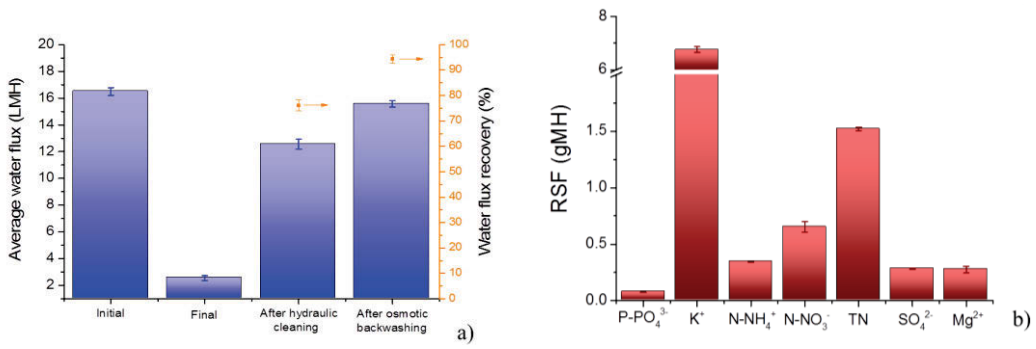

Figure 57. (a) Average water flux at the initial stage (i.e. up to 25% water recovery), final stage (after 75% water recovery), after hydraulic cleaning and after osmotic backwashing and water flux recovery after hydraulic cleaning and osmotic backwashing (b) Reverse nutrient fluxes of commercial liquid fertilizer. Experimental conditions were: feed solution: synthetic wastewater; draw solutions: commercial fertilizer Part B; crossflow velocity: 8.5 cm/s; temperature: 25°C; Operating time: up to 75% water recovery. Error bars are standard deviation of duplicate measurements.

7.3.2 Performances of pilot-scale FDFO operations

According to the manufacturer, the commercial hydroponic solution used in this study must be diluted 250 times while the final pH and conductivity must fall within the range 6.0-6.5 and 1.5-2.0 mS/cm, respectively. The osmotic dilution using synthetic wastewater as feed was carried out for the commercial fertilizer Part B only in three stages as described in section 7.2.2. The first stage has been performed in FO mode (i.e. using osmotic driving force only) while the second and third stages have been carried out under PAO mode (i.e. using osmotic driving force combined with an applied hydraulic pressure of 2 bar). These 3 stages were necessary as the pilot-scale FO process has to be operated in a batch mode and hence the desired dilution could not be achieved in a single stage. In

fact, a recent FDFO study (Sahebi et al., 2015) demonstrated that the additional hydraulic driving force not only enhances the permeate flux when the osmotic driving force is significantly reduced (i.e. the osmotic pressure of the diluted DS approaches that of FS) but also could further dilute the DS beyond the point of osmotic equilibrium which is not possible under the FO mode of operation alone. Therefore, PAO could eliminate the need for an additional post-treatment process such as NF for enhancing the fertiliser dilution (Phuntsho et al., 2013a) and thus reduce the overall process footprint. Besides, this study also demonstrated that the effective gain in water flux was higher when the DS concentration becomes closer to the osmotic equilibrium when the osmotic driving force approaches zero. This is also one of the reasons why, in this study, PAO was applied in the second and third stages and not in the first stage.

The results from the pilot-scale investigations are gathered in **Fig. 58, Tables 36 and 37**. **Fig. 58a and 58b** show the water flux, the osmotic pressure of the commercial fertilizer and the accumulated permeate volume during the three different stages of pilot operation. During stage 1 (i.e. FO mode), the gradual decrease in water flux is related to the continuous dilution of the commercial fertilizer since both are following the same trend (**Fig. 58a and 58b**) and the bench-scale experiments showed a relatively low fouling potential under the FO mode of operation. At the end of stage 1, the osmotic pressure from the commercial hydroponic solution fell down to 5.5 bar (i.e. which corresponds to a conductivity of 8.6 mS/cm) while the water flux decreased to 5.9 LMH. The additional 2 bar pressure applied during stage 2 of the FO operation increased the initial water flux by 57% while the same additional pressure only resulted in a 20% water flux increase at the beginning of stage 3. A recent PAO study (Blandin et al., 2013) showed that the application of hydraulic pressure contributes positively on the water flux but also resulted in more severe CP effects affecting the efficiency of the osmotic pressure, especially

when the hydraulic pressure contribution becomes predominant. **Fig. 58d** shows that, at the beginning of stage 2, the contribution of the osmotic pressure is still predominant over the hydraulic pressure (i.e. 5.5 bar for the diluted DS with a conductivity of 8.6 mS/cm against 2 bar applied pressure); however, at the beginning of stage 3, the osmotic pressure of the diluted DS was only 0.4 bar (i.e. which corresponds to a conductivity of 1.2 mS/cm), which is very close to the osmotic pressure of the synthetic wastewater feed (i.e. 0.14 bar) and much lower than the additional 2 bar pressure. Therefore, CP effects were most likely more prominent towards the end of stage 2, limiting the expected flux enhancement. Another likely explanation for this lower water flux improvement can be the enhanced membrane fouling due to PAO operation during stage 2. In fact, it has been explained in previous studies (Yun et al., 2014, Blandin et al., 2013) that in PAO, both fouling layer compaction (i.e. similar to RO) and CEOP (i.e. similar to FO) are expected to occur resulting in slightly higher fouling propensity compared to FO. It is very likely that, under stage 2, a more compact fouling layer has been formed on the membrane surface resulting in an additional barrier for water permeation.

Finally, **Fig. 58c** shows the RSF results at the end of each pilot stage. During stage 1 (FO mode), the reverse nutrients transport was quite similar to the values obtained during the bench-scale experiments with synthetic wastewater as feed. However, during both stage 2 and 3 under the PAO mode of operations, the RSF is significantly reduced. In fact, unlike in the FO process where an increase in the water flux also leads to more severe RSF due to higher concentration difference. In the PAO process however, the enhanced water permeation increases the dilutive ICP that reduces the draw solute concentration at the membrane interface which results in lower RSF (Blandin et al., 2013). Besides, as discussed previously, more CP effects are observed under the PAO mode of operation

which decreases the net osmotic pressure across the membrane and therefore limits the reverse diffusion of salts.

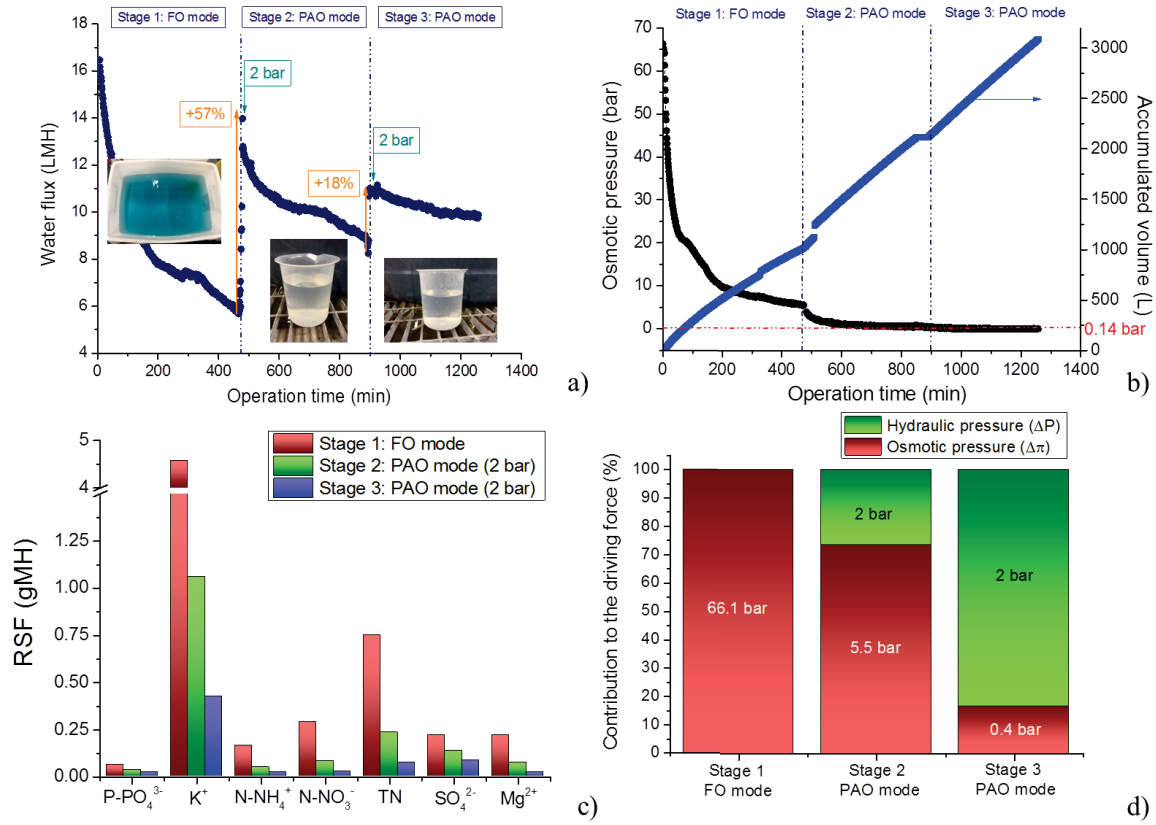

Figure 58. (a) Water flux, (b) Osmotic pressure of commercial fertilizer and accumulated permeate volume, (c) Reverse nutrient fluxes and (d) Relative contribution of osmotic pressure and hydraulic pressure to the driving force during pilot-scale operation. Experimental conditions were: feed solution: synthetic wastewater; draw solutions: commercial fertilizer Part B; Initial DS and FS volumes were 75 L and 1000 L respectively; Operating time: Up to 250 times dilution (based on EC value). The osmotic pressure of diluted draw solution was calculated using the ROSA software (Version 9.1, Filmtec DOW^{TM} Chemicals, USA) based on continuously measured EC values.

Combining FDFO process with PAO, it could help save the overall operating costs (i.e. energy and membrane costs). However, in order for this hybrid FDFO-PAO process to be economically feasible, a trade-off between membrane and energy costs (i.e. from the additional pressure) has to be determined. **Table 36** displays the energy and membrane replacement costs for different process configurations (i.e. FDFO alone, FDFO coupled with PAO at different DS osmotic dilution and PAO alone). It is clear from this table that using osmotic dilution alone will result in higher membrane replacement cost and footprint (i.e. higher total membrane area) while using PAO only will result in higher energy consumption and thus higher energy cost. To optimise this hybrid process, it is necessary to find out at which stage (i.e. DS concentration) PAO should be applied. Although previous studies have found that applying PAO at lower DS concentration is more beneficial in terms of water flux enhancement. This also means that the initial feed concentration will be higher due to increased recovery rates. The draw solute concentration in the feed stream due to RSF will also be much higher. Both these increased solute concentrations increases the need for a higher applied pressure thereby increasing the energy consumption of the PAO feed pump to achieve similar final DS concentration (Phuntsho et al., 2016). Besides, **Table 36** shows that if the FO process is operated at higher recovery rate (i.e. to achieve higher DS dilution), then the contribution of applied pressure (PAO) to the water flux gain will be lower which will in turn increase the total membrane area and thus the membrane replacement cost. Further studies are therefore needed in this area in order to find the optimum process configurations for this hybrid FDFO-PAO system.

Table 36. Operation costs under different process configurations.

Operation	Energy consumption [a] (kWh/m^3)	Energy cost [b] ($/m^3)	Total membrane area (m^2)	Membrane replacement cost [b] ($/m^3)
FDFO	0.072	0.020	377,600	0.13
FDFO-PAO (Dilution factor in FO = 70%)	0.226	0.066	341,700	0.12
FDFO-PAO (Dilution factor in FO = 60%)	0.225	0.065	301,900	0.10
FDFO-PAO (Dilution factor in FO = 50%)	0.225	0.065	279,000	0.09
PAO	0.236	0.069	168,500	0.06

[a] FDFO and PAO energy consumption calculations were based on the specific energy consumption of the feed and draw solutions pumps. PAO water flux were calculated using the equation adapted from (Blandin et al., 2015).

[b] FO module cost was assumed to be $1,250/element and energy cost was assumed to $0.29/kWh.

Finally, **Table 37** presents the water quality of the diluted fertilizer at each stage of the pilot-scale operation as well as the final nutrient solution (i.e. diluted part B mixed with Part A). It is clear from the results that the concentration of nutrients is decreasing at each stage due to the continuous dilution of the fertilizer DS. The pH and conductivity of the final product complied with the hydroponic requirements (i.e. pH 6.0-6.5 and conductivity 1.5-2.0 mS/cm), demonstrating the feasibility of the FDFO-PAO process to produce nutrient solution suitable for hydroponics application. The pH of hydroponic solutions should usually fall between 5.5 and 6.5 since previous studies have shown that

nutrient deficiencies can occur outside this acceptable range because the pH can affect greatly the availability of fertilizer salts (Parks, 2011, Brechner et al.).

A diluted fertilizer solution was also separately prepared with distilled water in order to remove the presence of draw solutes from reverse diffusion and obtain the correct nutrients concentration following the manufacturer's guidelines for hydroponic solution as presented in brackets in **Table 37**. It can be seen that the use of FDFO to prepare the hydroponic solution resulted in the loss of some essential nutrients to variable extent. Nutrient deficiencies can greatly affect the plant health and growth and typical symptoms generally include reduced plant growth, yellowing and/or scorching of leaves and growing tips as depicted in **Table 38**. The type of symptoms and their extent on plant growth and health will depend on the nutrient(s) being deficient (Parks, 2011, Brechner et al.). For instance, nitrogen deficiency will lead to severe stunting while potassium deficiency will lead to yellowing and scorching of old leaves, highlighting the importance of these macronutrients. **Table 39** shows the hydroponic formulation of two standard recipes (i.e. Huett and Hoagland hydroponic formulations (Hoagland and Arnon, 1950, Huett, 1993)) and the nutrients concentration in the final FDFO solution are within the range of these two standard hydroponic solutions suggesting that nutrient deficiencies should not be expected for the hydroponic lettuce.

Table 37. Water quality of diluted draw solution at different stages of pilot-scale operation and final nutrient solution for hydroponic application.

	After FO	After PAO 1	After PAO 2	Final Product (Part A + Part B)
pH	5.91	6.84	7.12	6.15
EC (mS/cm)	8.53	1.22	0.47	1.65
TDS (mg/L)	5500	751	262	696
TOC (mg/L)	21.12	9.74	0.65	5.54
TN (mg/L)	800	100	45	204 (212)*
NO_3^- (mg/L)	610	82	33.5	159 (169)*
NH_4^+ (mg/L)	93	9.5	3.5	17.5 (20.5)*
$P\text{-}PO_4^{3-}$ (mg/L)	660	90	30	29.5 (36)*
K^+ (mg/L)	2180	270	100	201 (249)*
Ca^{2+} (mg/L)	0**	0**	0**	137 (146)*
Mg^{2+} (mg/L)	750	100	38	31.5 (41.5)*
SO_4^{2-} (mg/L)	940	120	45	42 (51.5)*

* Values in brackets are the ones obtained when diluted the fertilizer with distilled water.

** Part B does not contain calcium.

Table 38. Nutrient deficiencies and their symptoms (adapted from (Parks, 2011)).

Nutrient deficiency	Symptoms
Nitrogen	Plants are weak and extremely stunted; older leaves become pale or yellow. Reddening of stems and older leaves can also occur
Phosphorus	Plants are stunted and leaves are small; Grey-green or purple colouring of older leaves can also occur
Potassium	Plants are slightly stunted; Yellowing or scorching of older leaves can also occur
Calcium	Scorching of growing tips and the margins of new leaves. Leaves cup while they grow. Yellowing between the leaf veins can occur and precede scorching and leaf death
Iron	Yellowing of young leaves between leaf veins
Magnesium	Mild growth reduction; Yellowing and scorching of older leaves between veins and progressing inwards from margins
Zinc	Restricted leaf size and stem length; Yellowing can occur between leaf veins and progress into scorching between veins
Boron	Yellowing and scorching can occur between leaf veins at growing points
Copper	Dark blue-green colouring of leaves
Sulphur	Yellowing and purpling of new and old leaves between veins; Older leaves show marginal scorching
Manganese	Yellowing between leaf veins progressing to scorching

Table 39. Standard hydroponic formulations.

Nutrients	Huett hydroponic formulation (Huett, 1993)	Hoagland hydroponic formulation (Hoagland and Arnon, 1950)
N (mg/L)	116	210
P (mg/L)	22	31
K (mg/L)	201	235
Ca (mg/L)	70	200
S (mg/L)	26	64
Mg (mg/L)	20	48

7.3.3 Response of hydroponic lettuce plants grown in FDFO nutrient solutions

The response of hydroponic plants grown using different nutrient solutions obtained from FDFO has been assessed in terms of different growth parameters including fresh biomass production (aerial parts and roots) and dried biomass (oven dried at 60 °C for 72 h). Growth performance results are gathered in **Fig. 59, which** shows similar growth patterns between the selected treatments indicating that the FDFO nutrient solution could be applicable to any hydroponic applications using different plant species. The fresh and dry weights of aerial parts and roots were also comparable to other reports (Sikawa and Yakupitiyage, 2010, Smoleń et al., 2014). Plants grown in T2 (i.e. Optimum Grow - same hydroponic nutrient solution used as DS in FO experiments) revealed the highest biomass production followed by plants grown in T1 (i.e. FDFO nutrient solution) and then T3 (i.e. Half-strength Hoagland's solution). Fresh and dry biomass data displayed in **Fig. 59** show that the fresh weight of aerial parts was 158.53 g (± 14.9 g), 160.32 g (± 20.45 g), and 105.33 g (± 14.42 g) for T1, T2 and T3, respectively. The difference in yield between

T1/T2 and T3 could be due to more cool and warm air movement around the first two treatments which created more plant transpiration, then higher photosynthesis and consequently biomass. Lettuce plants fed with FDFO nutrient solution showed no signs of toxicity or any mortality indicating the suitability of growing lettuce in NFT system with the prescribed conditions.

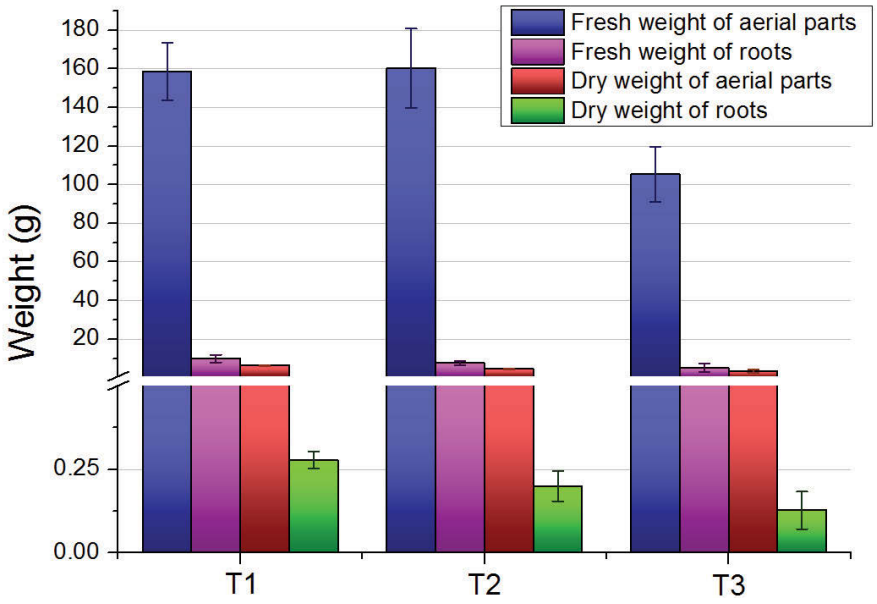

Figure 59. Fresh and dry biomass of hydroponic lettuce grown in three different treatments: T1 feeds with FDFO nutrient solution, T2 feeds with commercial fertilizer diluted with distilled water and T3 feeds with half-strength Hoagland's solution.

7.4 Conclusions

This study investigated the potential of FDFO to produce nutrient solutions for hydroponics through the osmotic dilution of a commercial hydroponic fertilizer solution using wastewater as a sustainable alternative water source. Preliminary bench-scale experiments demonstrated the good performance of the commercial liquid fertilizer in terms of water flux and RSF. The main advantage of using a commercial fertilizer as DS,

in comparison to inorganic salts, relies in its well-balanced macro- and micronutrients composition. The presence of organic nitrogen such as urea can, however, be detrimental to FDFO in terms of nutrient loss by reverse diffusion towards the feed water. Physical cleaning was observed adequate to recover the initial water flux by up to 75% while osmotic backwashing was able to recover flux by 95%, highlighting the low-fouling potential of FDFO. Pilot-scale experiments were carried out in different stages incorporating PAO mode of operations in order to achieve the required dilution for hydroponics. The hybrid FDFO-PAO system was able to produce a suitable hydroponic solution in terms of nutrient concentration and pH and conductivity. Future works are still required to further improve this hybrid system in order to find the optimum trade-off between process footprint (FO) and energy costs (PAO). Finally, the diluted nutrient solution produced by the pilot FDFO process was tested to grow hydroponic lettuce plants and growth pattern were compared with plants grown using standard hydroponic formulations. Growth performance results indicates that the lettuce growth pattern with FDFO diluted fertilizer solution showed similar trends with the standard hydroponic treatments and their biomass were comparable to previous reports. These results are very promising for the future of FDFO for hydroponic applications to grow any types of crops.

8. Conclusions and recommendations

8.1 Conclusions

This thesis aimed to develop the novel FDFO-AnMBR hybrid system and investigated its feasibility for sustainable hydroponics and wastewater reuse. This was achieved by evaluating FDFO for concentrating municipal wastewater, selecting the optimum DS for AnFDFOMBR to understand the developed novel hybrid system, operating AnFDFOMBR for treating concentrated municipal wastewater and applying FDFO produced water for the hydroponic application. For AnFDFOMBR, two hybrid systems (i.e., the combined AnMBR system with FDFO and FDFO as post-treatment of AnMBR) were considered.

8.1.1. FDFO evaluation for concentrating municipal wastewater and sustainable agricultural application

In this study, the FDFO-AnMBR hybrid system was proposed for sustainable wastewater reuse and hydroponic application. This system consisted of 1st staged FDFO for concentrating municipal wastewater and 2nd staged AnFDFOMBR for treating concentrated municipal wastewater and producing bio-methane. Thus, Chapter 3 investigated the potential of FDFO to achieve simultaneous water reuse from wastewater and sustainable agriculture application. Results showed that 95% was the optimum water recovery to achieve in FDFO for further AnMBR treatment. The performance of different fertilizers (i.e. single and blended) as DS was assessed in terms of water flux, RSF, water recovery and final nutrient concentration. While KCl and NH_4Cl showed the highest water flux and water recovery, MAP, MKP and SOA demonstrated the lowest RSF and thus loss of nutrient through back diffusion. The use of wastewater effluent instead of

brackish or seawater as FS in FDFO proved to be beneficial in terms of reducing the final nutrient concentration. In fact, the water fluxes obtained with wastewater as FS was substantially higher than those obtained with high salinity FS (i.e. up to 80% higher). Increasing the DS concentration or blending fertilizers at equal ratio (i.e. 1 M: 1 M) did not provide significant improvement in terms of water flux and final NPK concentration. Finally, although high recovery rate can be achieved during long-term operations (i.e. up to 76.2% for SOA after 4-day operation), the final diluted DS still required substantial dilution (i.e. up to 100 times depending on the targeted crop) before meeting the nutrient standard requirements for hydroponics.

8.1.2. Optimization of AnFDFOMBR via a study to select the suitable fertilizer DS

Prior to investigating 2nd staged AnFDFOMBR, it is required to understand the impact of fertilizer DS on AnFDFOMBR fundamentally since anaerobic microbes as well as FO performance may be very sensitive to fertilizer DS. Therefore, in Chapter 4, a selection procedure of fertilizers as DS for novel AnFDFOMBR was firstly investigated. From preliminary screening and FO experiments, six fertilizers (i.e., MAP, SOA, MKP, KCl, NH_4NO_3, and NH_4Cl) were selected. MAP exhibited the highest biogas production since other fertilizers exhibited the inhibition effect on the anaerobic activity under determined concentrations. Simulation results showed that SOA and MAP were appropriate to OMBR integrated with FDFO since they had less salt accumulation and relatively higher water flux. For these reasons, MAP can be the most suitable DS for AnFDFOMBR. Based on results obtained from this study, two types of the AnMBR-FDFO hybrid systems were operated and further evaluated.

8.1.3. Evaluation of the AnMBR-FDFO hybrid system for the sustainable wastewater reuse and agricultural application

In this study, two types of the AnMBR-FDFO hybrid systems were investigated. At the first, FDFO can be combined as post-treatment with AnMBR to further remove contaminants such as PPCPs which can be toxic to soil environment or plants. Thus, it needs to evaluate FDFO for AnMBR effluent treatment in terms of membrane fouling and OMPs rejection properties since AnMBR effluent contains high contents of organics and inorganics as well as contaminants. In Chapter 5, fouling behaviour in FDFO was systematically investigated using three different fertilizer DS and included OMPs transport behaviour during AnMBR effluent treatment. Under the AL-FS mode of membrane orientation, water flux with FDFO did not decline significantly due to the hydrophilicity of the scaling layer, even though severe scaling occurred when DAP fertilizer was used as DS. Under the AL-DS mode, DAP fertilizer DS showed the highest flux decline followed by KCl and MAP, where scaling was observed within the support layer pores when DAP fertilizer was used as DS. Physical/hydraulic cleaning successfully recovered water flux for the FO membranes operated under the AL-FS mode of membrane orientation. However, for the membranes operated under AL-DS mode, the flux was not fully recovered as the fouling and scaling occurred inside the support layer. Osmotic backwashing significantly enhanced the cleaning efficiency and flux recovery for FO membranes operated under the AL-DS mode. During the AnMBR effluent treatment by FDFO, DAP fertilizer DS exhibited the lowest OMPs forward flux (or the highest OMPs removal of up to 99%) compared to MAP and KCl fertilizers as DS. The higher OMPs flux resulted in higher water flux that enhanced concentrative ECP on the membrane active surface and no significant influence of RSF was observed on the OMPs

flux. These results can be utilized for optimizing FDFO in terms of AnMBR effluent treatment and OMPs rejection.

FDDO can be directly combined with AnMBR internally or externally. Unlike FDFO post-treatment, this hybrid system can be critically influenced by fertilizer DS since fertilizer DS can be directly mixed with anaerobic sludge via RSF. In Chapter 6, it was found out that flux decline was very severe regardless of fertilizer DS due to the absence of aeration and the sticky sludge, while flux recoveries were different amongst the tested fertilizer DS since their effect on biofouling was different. Nutrient accumulation in the bioreactor was influenced by fertilizer properties and exhibited a significant impact on anaerobic activity as well as the sludge. Bacterial community structure was affected by nutrient accumulation while archaeal community structure remained fairly stable, implying that anaerobic activity was mainly depending on variations in bacterial community structure. These results indicate that nutrient accumulation should be well-controlled for the efficient operation of AnFDFOMBR.

8.1.4. Application of FDFO produced water for sustainable hydroponics

After investigating the FDFO-AnMBR hybrid system, the potential of FDFO was lastly assessed in Chapter 7 to produce nutrient solutions for hydroponics through the osmotic dilution of a commercial hydroponic fertilizer solution using wastewater as a sustainable alternative water source. Preliminary bench-scale experiments demonstrated the good performance of the commercial liquid fertilizer in terms of water flux and RSF. The main advantage of using a commercial fertilizer as DS, in comparison to inorganic salts, relies on its well-balanced macro- and micronutrients composition. The presence of organic nitrogen such as urea can, however, be detrimental to FDFO in terms of nutrient loss by reverse diffusion towards the feed water. Physical cleaning was observed adequate to

recover the initial water flux by up to 75% while osmotic backwashing was able to recover flux by 95%, highlighting the low-fouling potential of FDFO. Pilot-scale experiments were carried out in different stages incorporating PAO mode of operations in order to achieve the required dilution for hydroponics. The hybrid FDFO-PAO system could produce a suitable hydroponic solution in terms of nutrient concentration and pH and conductivity. Future works are still required to further improve this hybrid system in order to find the optimum trade-off between process footprint (FO) and energy costs (PAO). Finally, the diluted nutrient solution produced by the pilot FDFO process was tested to grow hydroponic lettuce plants and growth pattern were compared with plants grown using standard hydroponic formulations. Growth performance results indicates that the lettuce growth pattern with FDFO diluted fertilizer solution showed similar trends with the standard hydroponic treatments and their biomass were comparable to previous reports. These results are very promising for the future of FDFO for hydroponic applications to grow any types of crops.

8.2 Recommendations

In this study, the AnMBR-FDFO hybrid process is proposed for sustainable wastewater reuse and agricultural application. The concept of the proposed hybrid process was successfully demonstrated by i) evaluating FDFO with fertilizers as DS to produce diluted fertilizer solutions for hydroponics, ii) evaluating the AnMBR-FDFO hybrid system for municipal wastewater treatment and biogas production as the supply of water and energy for operating the hybrid system, and iii) evaluating the performance of FDFO process as a pre-treatment and post-treatment for AnMBR influent and effluent, respectively. Nevertheless, there are still some challenges to commercialize this novel hybrid process and therefore the following recommendations are suggested:

1. Since the final diluted fertilizer concentration is determined according to osmotic equilibrium, municipal wastewater can be one of the suitable FS due to its low osmotic pressure. However, this study indicates that additional dilution is required to meet the standard of nutrient concentration for plants. Therefore, there is a crucial need to develop an economical model to achieve suitable concentration of the final produced water.
2. FDFO can negatively influence the performance of AnMBR. This is because reverse diffusion of fertilizer draw solute affects anaerobic microbes and thus reduces biogas production in the anaerobic bioreactor. Besides, due to salt accumulation by RSF in the bioreactor, the final product water concentration can be also significantly reduced. To solve these problems, it is required to develop a method to reduce RSF with no impact on the performance of the anaerobic bioreactor as well as FDFO. Either low RSF membrane or large molecular weight DS can be developed to improve the feasibility of FDFO.
3. Hydroponics was tested as a target application of the FDFO-AnMBR hybrid system. However, since hydroponics is one of the agricultural techniques to grow plants, it needs to expand the application of our novel hybrid system from hydroponics to the others (e.g., simple irrigation). It would be recommendable that massive greenhouse or large farming area can be located in a wastewater treatment plant where FDFO can produce safe and reliable diluted fertilizer solution.

References

2004. Environmental Guidelines: Use of Effluent by Irrigation. Sydney: Department of Environment and Conservation (NSW).

2014. *Water Scarcity* [Online]. UNDESA. Available: http://www.un.org/waterforlifedecade/scarcity.shtml [Accessed].

ACHILLI, A., CATH, T. Y. & CHILDRESS, A. E. 2010. Selection of inorganic-based draw solutions for forward osmosis applications. *Journal of Membrane Science,* 364**,** 233-241.

ACHILLI, A., CATH, T. Y., MARCHAND, E. A. & CHILDRESS, A. E. 2009. The forward osmosis membrane bioreactor: A low fouling alternative to MBR processes. *Desalination,* 239**,** 10-21.

AHLUWALIA, S. S. & GOYAL, D. 2007. Microbial and plant derived biomass for removal of heavy metals from wastewater. *Bioresource Technology,* 98**,** 2243-2257.

AL-AGHA, M. R. & MORTAJA, R. S. 2005. Desalination in the gaza strip: drinking water supply and environmental impact. *Desalination,* 173**,** 157-171.

ALBERTSEN, M., KARST, S. M., ZIEGLER, A. S., KIRKEGAARD, R. H. & NIELSEN, P. H. 2015. Back to Basics – The Influence of DNA Extraction and Primer Choice on Phylogenetic Analysis of Activated Sludge Communities. *PLoS ONE,* 10**,** e0132783.

ALBURQUERQUE, J. A., DE LA FUENTE, C. & BERNAL, M. P. 2012. Chemical properties of anaerobic digestates affecting C and N dynamics in amended soils. *Agriculture, Ecosystems & Environment,* 160**,** 15-22.

ALDERSON, M. P., DOS SANTOS, A. B. & MOTA FILHO, C. R. 2015. Reliability analysis of low-cost, full-scale domestic wastewater treatment plants for reuse in aquaculture and agriculture. *Ecological Engineering,* 82**,** 6-14.

ALIDINA, M., HOPPE-JONES, C., YOON, M., HAMADEH, A. F., LI, D. & DREWES, J. E. 2014. The occurrence of emerging trace organic chemicals in wastewater effluents in Saudi Arabia. *Science of The Total Environment,* 478**,** 152-162.

ALMULLA, A., EID, M., C T , P. & COBURN, J. 2003. Developments in high recovery brackish water desalination plants as part of the solution to water quantity problems. *Desalination,* 153**,** 237-243.

ALTAEE, A., MILLAR, G. J., SHARIF, A. O. & ZARAGOZA, G. 2016. Forward osmosis process for supply of fertilizer solutions from seawater using a mixture of draw solutions. *Desalination and Water Treatment,* 57**,** 28025-28041.

ALTURKI, A., MCDONALD, J., KHAN, S. J., HAI, F. I., PRICE, W. E. & NGHIEM, L. D. 2012. Performance of a novel osmotic membrane bioreactor (OMBR) system: Flux stability and removal of trace organics. *Bioresource Technology,* 113**,** 201-206.

ALTURKI, A. A., MCDONALD, J. A., KHAN, S. J., PRICE, W. E., NGHIEM, L. D. & ELIMELECH, M. 2013. Removal of trace organic contaminants by the forward osmosis process. *Separation and Purification Technology,* 103**,** 258-266.

AMBLER, J. R. & LOGAN, B. E. 2011. Evaluation of stainless steel cathodes and a bicarbonate buffer for hydrogen production in microbial electrolysis cells using a new method for measuring gas production. *International Journal of Hydrogen Energy,* 36**,** 160-166.

AMBUCHI, J. J., ZHANG, Z. & FENG, Y. 2016. Biogas Enhancement Using Iron Oxide Nanoparticles and Multi-Wall Carbon Nanotubes. *International Journal of Chemical, Molecular, Nuclear, Materials and Metallurgical Engineering,* 10**,** 1239-1246.

AMERICAN PUBLIC HEALTH, A., EATON, A. D., AMERICAN WATER WORKS, A. & WATER ENVIRONMENT, F. 2005. *Standard methods for the examination of water and wastewater,* Washington, D.C., APHA-AWWA-WEF.

ANDRADE, L. H. D., MENDES, F. D. D. S., ESPINDOLA, J. C. & AMARAL, M. C. S. 2014. Internal versus external submerged membrane bioreactor configurations for dairy wastewater treatment. *Desalination and Water Treatment,* 52**,** 2920-2932.

ANG, W. S., LEE, S. & ELIMELECH, M. 2006. Chemical and physical aspects of cleaning of organic-fouled reverse osmosis membranes. *Journal of Membrane Science,* 272**,** 198-210.

ANGELAKIS, A., DO MONTE, M. M., BONTOUX, L. & ASANO, T. 1999a. The status of wastewater reuse practice in the Mediterranean basin: need for guidelines. *Water Research,* 33**,** 2201-2217.

ANGELAKIS, A. N., MARECOS DO MONTE, M. H. F., BONTOUX, L. & ASANO, T. 1999b. The status of wastewater reuse practice in the Mediterranean basin: need for guidelines. *Water Research,* 33**,** 2201-2217.

ANGELIDAKI, I., ELLEGAARD, L. & AHRING, B. K. 1993. A mathematical model for dynamic simulation of anaerobic digestion of complex substrates: focusing on ammonia inhibition. *Biotechnol Bioeng,* 42**,** 159-66.

ANSARI, A. J., HAI, F. I., GUO, W., NGO, H. H., PRICE, W. E. & NGHIEM, L. D. 2015. Selection of forward osmosis draw solutes for subsequent integration with anaerobic treatment to facilitate resource recovery from wastewater. *Bioresource Technology,* 191**,** 30-36.

AR VALO, J., GARRAL N, G., PLAZA, F., MORENO, B., P REZ, J. & G MEZ, M. Á. 2009. Wastewater reuse after treatment by tertiary ultrafiltration and a membrane bioreactor (MBR): a comparative study. *Desalination,* 243**,** 32-41.

ARIYANTO, E., SEN, T. K. & ANG, H. M. 2014. The influence of various physico-chemical process parameters on kinetics and growth mechanism of struvite crystallisation. *Advanced Powder Technology,* 25**,** 682-694.

ARKHANGELSKY, E., WICAKSANA, F., CHOU, S., AL-RABIAH, A. A., AL-ZAHRANI, S. M. & WANG, R. 2012. Effects of scaling and cleaning on the performance of forward osmosis hollow fiber membranes. *Journal of Membrane Science,* 415**,** 101-108.

ASLAN, M., SAAT I, Y., HANAY, Ö. & HASAR, H. 2014. Membrane fouling control in anaerobic submerged membrane bioreactor. *Desalination and Water Treatment,* 52**,** 7520-7530.

ASSESSMENT, M. E. 2005. *Ecosystems and human well-being,* Washington, DC, Island Press

BABICH, H. & STOTZKY, G. 1983. Toxicity of nickel to microbes: environmental aspects. *Adv Appl Microbiol,* 29**,** 195-265.

BAE, H.-S., MOE, W. M., YAN, J., TIAGO, I., DA COSTA, M. S. & RAINEY, F. A. 2006. Brooklawnia cerclae gen. nov., sp. nov., a propionate-forming bacterium isolated from chlorosolvent-contaminated groundwater. *International Journal of Systematic and Evolutionary Microbiology,* 56**,** 1977-1983.

BAEK, S. H., PAGILLA, K. R. & KIM, H.-J. 2010. Lab-scale study of an anaerobic membrane bioreactor (AnMBR) for dilute municipal wastewater treatment. *Biotechnology and Bioprocess Engineering,* 15**,** 704-708.

BAHRI, A. 2009. Managing the Other Side of the Water Cycle: Making Wastewater an Asset. Mölnlycke.

BELAY, N. & DANIELS, L. 1987. Production of Ethane, Ethylene, and Acetylene from Halogenated Hydrocarbons by Methanogenic Bacteria. *Applied and Environmental Microbiology,* 53**,** 1604-1610.

BENJAMIN, M. M., WOODS, S. L. & FERGUSON, J. F. 1984. Anaerobic toxicity and biodegradability of pulp mill waste constituents. *Water Research,* 18**,** 601-607.

BLANDIN, G., VERLIEFDE, A. R., TANG, C. Y. & LE-CLECH, P. 2015. Opportunities to reach economic sustainability in forward osmosis–reverse osmosis hybrids for seawater desalination. *Desalination,* 363**,** 26-36.

BLANDIN, G., VERLIEFDE, A. R. D., TANG, C. Y., CHILDRESS, A. E. & LE-CLECH, P. 2013. Validation of assisted forward osmosis (AFO) process: Impact of hydraulic pressure. *Journal of Membrane Science,* 447**,** 1-11.

BLUM, D. J. W. & SPEECE, R. E. 1991. A Database of Chemical Toxicity to Environmental Bacteria and Its Use in Interspecies Comparisons and Correlations. *Research Journal of the Water Pollution Control Federation,* 63**,** 198-207.

BOO, C., ELIMELECH, M. & HONG, S. 2013. Fouling control in a forward osmosis process integrating seawater desalination and wastewater reclamation. *Journal of Membrane Science,* 444**,** 148-156.

BORJA, R., S NCHEZ, E. & DUR N, M. M. 1996a. Effect of the clay mineral zeolite on ammonia inhibition of anaerobic thermophilic reactors treating cattle manure. *Journal of Environmental Science and Health . Part A: Environmental Science and Engineering and Toxicology,* 31**,** 479-500.

BORJA, R., SANCHEZ, E. & WEILAND, P. 1996b. Influence of Ammonia Concentration on Thermophilic Anaerobic-Digestion of Cattle Manure in Upflow Anaerobic Sludge Blanket (Uasb) Reactors. *Process Biochemistry,* 31**,** 477-483.

BORNARE, J., RAMAN, V., SAPKAL, V., SAPKAL, R., MINDE, G. & SAPKAL, P. 2014. An overview of membrane bioreactors for anaerobic treatment of wastewaters. *Int. J. In. Res. Ad. Eng,* 1**,** 91-97.

BOWDEN, K. S., ACHILLI, A. & CHILDRESS, A. E. 2012. Organic ionic salt draw solutions for osmotic membrane bioreactors. *Bioresource Technology,* 122**,** 207-216.

BRECHNER, M., BOTH, A. & STAFF, C. Hydroponic Lettuce Handbook. *Cornell Controlled Environment Agriculture*.

BURN, S., MUSTER, T., KAKSONEN, A. & TJANDRAATMADJA, G. 2014. Resource Recovery from Wastewater: A Research Agenda. *Water Intelligence Online,* 13.

CABIROL, N., BARRAGAN, E. J., DURAN, A. & NOYOLA, A. 2003. Effect of aluminium and sulphate on anaerobic digestion of sludge from wastewater enhanced primary treatment. *Water Sci Technol,* 48**,** 235-40.

CAI, X. & ROSEGRANT, M. W. 2003. 10 World Water Productivity: Current Situation and Future Options. *Water productivity in agriculture: limits and opportunities for improvement,* 1**,** 163.

CAPORASO, J. G., KUCZYNSKI, J., STOMBAUGH, J., BITTINGER, K., BUSHMAN, F. D., COSTELLO, E. K., FIERER, N., PE A, A. G., GOODRICH, J. K., GORDON, J. I., HUTTLEY, G. A., KELLEY, S. T., KNIGHTS, D., KOENIG, J. E., LEY, R. E., LOZUPONE, C. A., MCDONALD, D., MUEGGE, B. D., PIRRUNG, M., REEDER, J., SEVINSKY, J. R., TURNBAUGH, P. J., WALTERS, W. A., WIDMANN, J., YATSUNENKO, T., ZANEVELD, J. & KNIGHT, R. 2010. QIIME allows analysis of high-throughput community sequencing data. *Nature methods,* 7**,** 335-336.

CAPORASO, J. G., LAUBER, C. L., WALTERS, W. A., BERG-LYONS, D., HUNTLEY, J., FIERER, N., OWENS, S. M., BETLEY, J., FRASER, L., BAUER, M., GORMLEY, N., GILBERT, J. A., SMITH, G. & KNIGHT, R. 2012. Ultra-high-throughput microbial community analysis on the Illumina HiSeq and MiSeq platforms. *The ISME Journal,* 6**,** 1621-1624.

CATH, T. Y., CHILDRESS, A. E. & ELIMELECH, M. 2006. Forward osmosis: Principles, applications, and recent developments. *Journal of Membrane Science,* 281**,** 70-87.

CATH, T. Y., ELIMELECH, M., MCCUTCHEON, J. R., MCGINNIS, R. L., ACHILLI, A., ANASTASIO, D., BRADY, A. R., CHILDRESS, A. E., FARR, I. V. & HANCOCK, N. T. 2013. Standard methodology for evaluating membrane performance in osmotically driven membrane processes. *Desalination,* 312**,** 31-38.

CHEKLI, L., KIM, Y., PHUNTSHO, S., LI, S., GHAFFOUR, N., LEIKNES, T. & SHON, H. K. 2017. Evaluation of fertilizer-drawn forward osmosis for sustainable agriculture and water reuse in arid regions. *Journal of Environmental Management,* 187**,** 137-145.

CHEKLI, L., PHUNTSHO, S., KIM, J. E., KIM, J., CHOI, J. Y., CHOI, J.-S., KIM, S., KIM, J. H., HONG, S., SOHN, J. & SHON, H. K. 2016. A comprehensive review of hybrid forward osmosis systems: Performance, applications and future prospects. *Journal of Membrane Science,* 497**,** 430-449.

CHEKLI, L., PHUNTSHO, S., SHON, H. K., VIGNESWARAN, S., KANDASAMY, J. & CHANAN, A. 2012. A review of draw solutes in forward osmosis process and their use in modern applications. *Desalination and Water Treatment,* 43**,** 167-184.

CHEN, H., CHANG, S., GUO, Q., HONG, Y. & WU, P. 2016. Brewery wastewater treatment using an anaerobic membrane bioreactor. *Biochemical Engineering Journal,* 105, Part B**,** 321-331.

CHEN, J. L., ORTIZ, R., STEELE, T. W. J. & STUCKEY, D. C. 2014a. Toxicants inhibiting anaerobic digestion: A review. *Biotechnology Advances,* 32**,** 1523-1534.

CHEN, L., GU, Y., CAO, C., ZHANG, J., NG, J.-W. & TANG, C. 2014b. Performance of a submerged anaerobic membrane bioreactor with forward osmosis membrane for low-strength wastewater treatment. *Water Research,* 50**,** 114-123.

CHEN, Y., CHENG, J. J. & CREAMER, K. S. 2008. Inhibition of anaerobic digestion process: A review. *Bioresource Technology,* 99**,** 4044-4064.

CHIU, S.-F., CHIU, J.-Y. & KUO, W.-C. 2013. Biological stoichiometric analysis of nutrition and ammonia toxicity in thermophilic anaerobic co-digestion of organic substrates under different organic loading rates. *Renewable Energy,* 57**,** 323-329.

CHOI, Y.-J., CHOI, J.-S., OH, H.-J., LEE, S., YANG, D. R. & KIM, J. H. 2009. Toward a combined system of forward osmosis and reverse osmosis for seawater desalination. *Desalination,* 247**,** 239-246.

CLAY, J. 2004. *World Agriculture and the Environment: A Commodity-by-Commodity Guide to Impacts and Practices*, Island Press.

CLAY, J. 2013. *World agriculture and the environment: a commodity-by-commodity guide to impacts and practices,* Washington, DC, Island Press.

CODAY, B. D., YAFFE, B. G., XU, P. & CATH, T. Y. 2014. Rejection of trace organic compounds by forward osmosis membranes: a literature review. *Environmental Science & Technology,* 48**,** 3612-3624.

COLLERAN, E., PENDER, S., PHILPOTT, U., O'FLAHERTY, V. & LEAHY, B. 1998. Full-scale and laboratory-scale anaerobic treatment of citric acid production wastewater. *Biodegradation,* 9**,** 233-245.

CORBAT N-B GUENA, M.-J., ÁLVAREZ-BLANCO, S. & VINCENT-VELA, M.-C. 2014. Salt cleaning of ultrafiltration membranes fouled by whey model solutions. *Separation and Purification Technology,* 132**,** 226-233.

CORNELISSEN, E. R., HARMSEN, D., DE KORTE, K. F., RUIKEN, C. J., QIN, J.-J., OO, H. & WESSELS, L. P. 2008. Membrane fouling and process performance of forward osmosis membranes on activated sludge. *Journal of Membrane Science,* 319**,** 158-168.

CUETOS, M. J., G MEZ, X., OTERO, M. & MOR N, A. 2010. Anaerobic digestion and co-digestion of slaughterhouse waste (SHW): Influence of heat and pressure pre-treatment in biogas yield. *Waste Management,* 30**,** 1780-1789.

D'HAESE, A., LE-CLECH, P., VAN NEVEL, S., VERBEKEN, K., CORNELISSEN, E. R., KHAN, S. J. & VERLIEFDE, A. R. D. 2013. Trace organic solutes in closed-loop forward osmosis applications: Influence of membrane fouling and modeling of solute build-up. *Water Research,* 47**,** 5232-5244.

DE BAERE, L. A., DEVOCHT, M., VAN ASSCHE, P. & VERSTRAETE, W. 1984. Influence of high NaCl and NH4Cl salt levels on methanogenic associations. *Water Research,* 18**,** 543-548.

DOMINGUES, D. S., TAKAHASHI, H. W., CAMARA, C. A. & NIXDORF, S. L. 2012. Automated system developed to control pH and concentration of nutrient solution evaluated in hydroponic lettuce production. *Computers and electronics in agriculture,* 84**,** 53-61.

DUAN, J., LITWILLER, E., CHOI, S.-H. & PINNAU, I. 2014. Evaluation of sodium lignin sulfonate as draw solute in forward osmosis for desert restoration. *Journal of Membrane Science,* 453**,** 463-470.

DVOŘ K, L., G MEZ, M., DOLINA, J. & ČERN N, A. 2016. Anaerobic membrane bioreactors—a mini review with emphasis on industrial wastewater treatment: applications, limitations and perspectives. *Desalination and Water Treatment,* 57**,** 19062-19076.

DVOŘ K, L., G MEZ, M., DVOŘ KOV , M., RŮŽIČKOV , I. & WANNER, J. 2011. The impact of different operating conditions on membrane fouling and EPS production. *Bioresource Technology,* 102**,** 6870-6875.

EL-MASHAD, H. M., ZEEMAN, G., VAN LOON, W. K. P., BOT, G. P. A. & LETTINGA, G. 2004. Effect of temperature and temperature fluctuation on thermophilic anaerobic digestion of cattle manure. *Bioresource Technology,* 95**,** 191-201.

EPA, U. S. 2012. Guidelines for water reuse. *Environmental Protection Agency, Municipal Support Division Office of Wastewater Management Office of Water Washington, DC. Agency for International Development Washington DC, EPA/625/R-04/108, Cincinnati, OH US EPA/625/R-04/108*.

ERSU, C. B., ONG, S. K., ARSLANKAYA, E. & LEE, Y.-W. 2010. Impact of solids residence time on biological nutrient removal performance of membrane bioreactor. *Water Research,* 44**,** 3192-3202.

FAM, W., PHUNTSHO, S., LEE, J. H. & SHON, H. K. 2013. Performance comparison of thin-film composite forward osmosis membranes. *Desalination and Water Treatment,* 51**,** 6274-6280.

FANG, H. H. P., CHEN, T. & CHAN, O. C. 1995. Toxic effects of phenolic pollutants on anaerobic benzoate-degrading granules. *Biotechnology Letters,* 17**,** 117-120.

FEDERATION, W. E. & ASSOCIATION, A. P. H. 2005. Standard methods for the examination of water and wastewater. *American Public Health Association (APHA): Washington, DC, USA*.

FERN NDEZ, J., P REZ, M. & ROMERO, L. I. 2008. Effect of substrate concentration on dry mesophilic anaerobic digestion of organic fraction of municipal solid waste (OFMSW). *Bioresource Technology,* 99**,** 6075-6080.

FERRO, G., FIORENTINO, A., ALFEREZ, M. C., POLO-L PEZ, M. I., RIZZO, L. & FERN NDEZ-IB EZ, P. 2015. Urban wastewater disinfection for agricultural reuse: effect of solar driven AOPs in the inactivation of a multidrug resistant E. coli strain. *Applied Catalysis B: Environmental,* 178**,** 65-73.

GALLERT, C., BAUER, S. & WINTER, J. 1998. Effect of ammonia on the anaerobic degradation of protein by a mesophilic and thermophilic biowaste population. *Appl Microbiol Biotechnol,* 50**,** 495-501.

GAO, W. J. J., LIN, H. J., LEUNG, K. T. & LIAO, B. Q. 2010. Influence of elevated pH shocks on the performance of a submerged anaerobic membrane bioreactor. *Process Biochemistry,* 45**,** 1279-1287.

GARCIA-CASTELLO, E. M., MCCUTCHEON, J. R. & ELIMELECH, M. 2009. Performance evaluation of sucrose concentration using forward osmosis. *Journal of Membrane Science,* 338**,** 61-66.

GE, Q., SU, J., AMY, G. L. & CHUNG, T.-S. 2012. Exploration of polyelectrolytes as draw solutes in forward osmosis processes. *Water Research,* 46**,** 1318-1326.

GRABOWSKI, A., TINDALL, B. J., BARDIN, V., BLANCHET, D. & JEANTHON, C. 2005. Petrimonas sulfuriphila gen. nov., sp. nov., a mesophilic fermentative bacterium isolated from a biodegraded oil reservoir. *International Journal of Systematic and Evolutionary Microbiology,* 55**,** 1113-1121.

GRAY, G. T., MCCUTCHEON, J. R. & ELIMELECH, M. 2006. Internal concentration polarization in forward osmosis: role of membrane orientation. *Desalination,* 197**,** 1-8.

GREENBERG, G., HASSON, D. & SEMIAT, R. 2005. Limits of RO recovery imposed by calcium phosphate precipitation. *Desalination,* 183**,** 273-288.

GREENLEE, L. F., LAWLER, D. F., FREEMAN, B. D., MARROT, B. & MOULIN, P. 2009. Reverse osmosis desalination: Water sources, technology, and today's challenges. *Water Research,* 43**,** 2317-2348.

GROBICKI, A. & STUCKEY, D. 1989. The role of formate in the anaerobic baffled reactor. *Water Research,* 23**,** 1599-1602.

GU, Y., CHEN, L., NG, J.-W., LEE, C., CHANG, V. W. C. & TANG, C. Y. 2015. Development of anaerobic osmotic membrane bioreactor for low-strength wastewater treatment at mesophilic condition. *Journal of Membrane Science,* 490**,** 197-208.

GUMAELIUS, L., MAGNUSSON, G., PETTERSSON, B. & DALHAMMAR, G. 2001. Comamonas denitrificans sp. nov., an efficient denitrifying bacterium isolated from activated sludge. *International Journal of Systematic and Evolutionary Microbiology,* 51**,** 999-1006.

GUO, C. X., ZHAO, D., ZHAO, Q., WANG, P. & LU, X. 2014. Na+-functionalized carbon quantum dots: a new draw solute in forward osmosis for seawater desalination. *Chemical Communications,* 50**,** 7318-7321.

GWAK, G., JUNG, B., HAN, S. & HONG, S. 2015. Evaluation of poly (aspartic acid sodium salt) as a draw solute for forward osmosis. *Water Research,* 80**,** 294-305.

H LSEN, T., BARRY, E. M., LU, Y., PUYOL, D., KELLER, J. & BATSTONE, D. J. 2016. Domestic wastewater treatment with purple phototrophic bacteria using a

novel continuous photo anaerobic membrane bioreactor. *Water Research,* 100**,** 486-495.

HANCOCK, N. T. & CATH, T. Y. 2009. Solute coupled diffusion in osmotically driven membrane processes. *Environmental Science & Technology,* 43**,** 6769-6775.

HANCOCK, N. T., XU, P., HEIL, D. M., BELLONA, C. & CATH, T. Y. 2011. Comprehensive Bench- and Pilot-Scale Investigation of Trace Organic Compounds Rejection by Forward Osmosis. *Environmental Science & Technology,* 45**,** 8483-8490.

HANCOCK, N. T., XU, P., ROBY, M. J., GOMEZ, J. D. & CATH, T. Y. 2013. Towards direct potable reuse with forward osmosis: Technical assessment of long-term process performance at the pilot scale. *Journal of Membrane Science,* 445**,** 34-46.

HARADA, H., UEMURA, S. & MOMONOI, K. 1994. Interaction between sulfate-reducing bacteria and methane-producing bacteria in UASB reactors fed with low strength wastes containing different levels of sulfate. *Water Research,* 28**,** 355-367.

HARTMANN, H. & AHRING, B. K. 2006. Strategies for the anaerobic digestion of the organic fraction of municipal solid waste: an overview. *Water Science and Technology,* 53**,** 7-22.

HEIPIEPER, H. J., WEBER, F. J., SIKKEMA, J., KEWELOH, H. & DE BONT, J. A. M. 1994. Mechanisms of resistance of whole cells to toxic organic solvents. *Trends in Biotechnology,* 12**,** 409-415.

HENDRIKSEN, H. V. & AHRING, B. K. 1991. Effects of ammonia on growth and morphology of thermophilic hydrogen-oxidizing methanogenic bacteria. *FEMS Microbiology Letters,* 85**,** 241-246.

HERRERA-ROBLEDO, M., MORGAN-SAGASTUME, J. M. & NOYOLA, A. 2010. Biofouling and pollutant removal during long-term operation of an anaerobic membrane bioreactor treating municipal wastewater. *Biofouling,* 26**,** 23-30.

HERZBERG, M., KANG, S. & ELIMELECH, M. 2009. Role of Extracellular Polymeric Substances (EPS) in Biofouling of Reverse Osmosis Membranes. *Environmental Science & Technology,* 43**,** 4393-4398.

HOAGLAND, D. R. & ARNON, D. I. 1950. The water-culture method for growing plants without soil. *Circular. California Agricultural Experiment Station,* 347.

HOCHMUTH, G. J. & HOCHMUTH, R. C. 2001. Nutrient solution formulation for hydroponic (perlite, rockwool, NFT) tomatoes in Florida. University of Florida, IFAS Extension.

HOEK, E. M. V. & ELIMELECH, M. 2003. Cake-Enhanced Concentration Polarization: A New Fouling Mechanism for Salt-Rejecting Membranes. *Environmental Science & Technology,* 37**,** 5581-5588.

HOLLOWAY, R. W., ACHILLI, A. & CATH, T. Y. 2015. The osmotic membrane bioreactor: a critical review. *Environmental Science: Water Research & Technology,* 1**,** 581-605.

HONG, S. & ELIMELECH, M. 1997. Chemical and physical aspects of natural organic matter (NOM) fouling of nanofiltration membranes. *Journal of Membrane Science,* 132**,** 159-181.

HOSSEINZADEH, M., BIDHENDI, G. N., TORABIAN, A., MEHRDADI, N. & POURABDULLAH, M. 2015. A new flat sheet membrane bioreactor hybrid system for advanced treatment of effluent, reverse osmosis pretreatment and fouling mitigation. *Bioresource Technology,* 192**,** 177-184.

HUANG, J. & PINDER, K. L. 1995. Effects of calcium on development of anaerobic acidogenic biofilms. *Biotechnol Bioeng,* 45**,** 212-8.

HUETT, D. O. 1993. Precise nutrient solution formulation and management for hydroponically grown crops. *Agricultural Science and Technology* [Online]. Available: http://agris.fao.org/agris-search/search.do?recordID=AU19950062922.

ILANGOVAN, K. & NOYOLA, A. 1993. Availability of micronutrients during anaerobic digestion of molasses stellage using an Upflow Anaerobic Sludge Blanket (UASB) reactor. *Environmental Technology,* 14**,** 795-799.

J.W.H, S., ELFERINK, O., VISSER, A., HULSHOFF POL, L. W. & STAMS, A. J. M. 1994. Sulfate reduction in methanogenic bioreactors. *FEMS Microbiology Reviews,* 15**,** 119-136.

JAIN, S., JAIN, S., WOLF, I. T., LEE, J. & TONG, Y. W. 2015. A comprehensive review on operating parameters and different pretreatment methodologies for anaerobic digestion of municipal solid waste. *Renewable and Sustainable Energy Reviews,* 52**,** 142-154.

JAN, A. O. & BARRY, L. H. 1988. Sulfide-Induced Inhibition of Anaerobic Digestion.

JARRELL, K. F., SAULNIER, M. & LEY, A. 1987. Inhibition of methanogenesis in pure cultures by ammonia, fatty acids, and heavy metals, and protection against heavy metal toxicity by sewage sludge. *Can J Microbiol,* 33**,** 551-4.

JARRELL, K. F., SPROTT, G. D. & MATHESON, A. T. 1984. Intracellular potassium concentration and relative acidity of the ribosomal proteins of methanogenic bacteria. *Canadian Journal of Microbiology,* 30**,** 663-668.

JENSEN, M. H. Hydroponics worldwide. International Symposium on Growing Media and Hydroponics, 1997. 719-730.

JEONG, E., KIM, H.-W., NAM, J.-Y., AHN, Y.-T. & SHIN, H.-S. 2010. Effects of the hydraulic retention time on the fouling characteristics of an anaerobic membrane bioreactor for treating acidifi ed wastewater. *Desalination and Water Treatment,* 18**,** 251-256.

JEONG, H., SEONG, C., JANG, T. & PARK, S. 2016. Classification of Wastewater Reuse for Agriculture: A Case Study in South Korea. *Irrigation and Drainage,* 65**,** 76-85.

JIM NEZ CISNEROS, B. E. & ASANO, T. 2008. *Water reuse : an international survey of current practice, issues and needs,* London, IWA Pub.

JIN, P., BHATTACHARYA, S. K., WILLIAMS, C. J. & ZHANG, H. 1998. EFFECTS OF SULFIDE ADDITION ON COPPER INHIBITION IN METHANOGENIC SYSTEMS. *Water Research,* 32**,** 977-988.

JOHIR, M. A. H., VIGNESWARAN, S., KANDASAMY, J., BENAIM, R. & GRASMICK, A. 2013. Effect of salt concentration on membrane bioreactor (MBR) performances: Detailed organic characterization. *Desalination,* 322**,** 13-20.

JONES JR, J. B. 2016. *Hydroponics: a practical guide for the soilless grower*, CRC press.

JUMPSTART CONSORTIUM HUMAN MICROBIOME PROJECT DATA GENERATION WORKING, G. 2012. Evaluation of 16S rDNA-Based Community Profiling for Human Microbiome Research. *PLoS ONE,* 7**,** e39315.

KABARA, J. J. & VRABLE, R. 1977. Antimicrobial lipids: natural and synthetic fatty acids and monoglycerides. *Lipids,* 12**,** 753-9.

KAUR, S., RANA, D., MATSUURA, T., SUNDARRAJAN, S. & RAMAKRISHNA, S. 2012. Preparation and characterization of surface modified electrospun membranes for higher filtration flux. *Journal of Membrane Science,* 390–391**,** 235-242.

KIM, B., LEE, S. & HONG, S. 2014a. A novel analysis of reverse draw and feed solute fluxes in forward osmosis membrane process. *Desalination,* 352**,** 128-135.

KIM, C., LEE, S., SHON, H. K., ELIMELECH, M. & HONG, S. 2012. Boron transport in forward osmosis: Measurements, mechanisms, and comparison with reverse osmosis. *Journal of Membrane Science,* 419–420**,** 42-48.

KIM, D. I., KIM, J., SHON, H. K. & HONG, S. 2015a. Pressure retarded osmosis (PRO) for integrating seawater desalination and wastewater reclamation: Energy consumption and fouling. *Journal of Membrane Science,* 483**,** 34-41.

KIM, J., SHIN, J., KIM, H., LEE, J.-Y., YOON, M.-H., WON, S., LEE, B.-C. & SONG, K. G. 2014b. Membrane fouling control using a rotary disk in a submerged anaerobic membrane sponge bioreactor. *Bioresource Technology,* 172**,** 321-327.

KIM, J. E., PHUNTSHO, S., LOTFI, F. & SHON, H. K. 2015b. Investigation of pilot-scale 8040 FO membrane module under different operating conditions for brackish water desalination. *Desalination and Water Treatment,* 53**,** 2782-2791.

KIM, J. E., PHUNTSHO, S. & SHON, H. K. 2013. Pilot-scale nanofiltration system as post-treatment for fertilizer-drawn forward osmosis desalination for direct fertigation. *Desalination and Water Treatment,* 51**,** 6265-6273.

KIM, M., AHN, Y.-H. & SPEECE, R. E. 2002. Comparative process stability and efficiency of anaerobic digestion; mesophilic vs. thermophilic. *Water Research,* 36**,** 4369-4385.

KIM, M. S., LEE, D. Y. & KIM, D. H. 2011. Continuous hydrogen production from tofu processing waste using anaerobic mixed microflora under thermophilic conditions. *International Journal of Hydrogen Energy,* 36**,** 8712-8718.

KIM, S., LEE, S., LEE, E., SARPER, S., KIM, C.-H. & CHO, J. 2009. Enhanced or reduced concentration polarization by membrane fouling in seawater reverse osmosis (SWRO) processes. *Desalination,* 247**,** 162-168.

KIM, Y., CHEKLI, L., SHIM, W.-G., PHUNTSHO, S., LI, S., GHAFFOUR, N., LEIKNES, T. & SHON, H. K. 2016. Selection of suitable fertilizer draw solute for a novel fertilizer-drawn forward osmosis–anaerobic membrane bioreactor hybrid system. *Bioresource Technology,* 210**,** 26-34.

KIM, Y., ELIMELECH, M., SHON, H. K. & HONG, S. 2014c. Combined organic and colloidal fouling in forward osmosis: Fouling reversibility and the role of applied pressure. *Journal of Membrane Science,* 460**,** 206-212.

KIM, Y., LEE, S., SHON, H. K. & HONG, S. 2015c. Organic fouling mechanisms in forward osmosis membrane process under elevated feed and draw solution temperatures. *Desalination,* 355**,** 169-177.

KIMURA, K., TOSHIMA, S., AMY, G. & WATANABE, Y. 2004. Rejection of neutral endocrine disrupting compounds (EDCs) and pharmaceutical active compounds (PhACs) by RO membranes. *Journal of Membrane Science,* 245**,** 71-78.

KISO, Y., SUGIURA, Y., KITAO, T. & NISHIMURA, K. 2001. Effects of hydrophobicity and molecular size on rejection of aromatic pesticides with nanofiltration membranes. *Journal of Membrane Science,* 192**,** 1-10.

KJERSTADIUS, H., DE VRIEZE, J., LA COUR JANSEN, J. & DAVIDSSON, Å. 2016. Detection of acidification limit in anaerobic membrane bioreactors at ambient temperature. *Water Research,* 106**,** 429-438.

KOSTER, I. W. & LETTINGA, G. 1988. Anaerobic digestion at extreme ammonia concentrations. *Biological Wastes,* 25**,** 51-59.

KWIETNIEWSKA, E. & TYS, J. 2014. Process characteristics, inhibition factors and methane yields of anaerobic digestion process, with particular focus on microalgal biomass fermentation. *Renewable and Sustainable Energy Reviews,* 34**,** 491-500.

LAY, W. C. L., ZHANG, Q. Y., ZHANG, J. S., MCDOUGALD, D., TANG, C. Y., WANG, R., LIU, Y. & FANE, A. G. 2011. Study of integration of forward osmosis and biological process: Membrane performance under elevated salt environment. *Desalination,* 283**,** 123-130.

LEE, J.-W., KWON, T.-O. & MOON, I.-S. 2006. Performance of polyamide reverse osmosis membranes for steel wastewater reuse. *Desalination,* 189**,** 309-322.

LEE, S., BOO, C., ELIMELECH, M. & HONG, S. 2010. Comparison of fouling behavior in forward osmosis (FO) and reverse osmosis (RO). *Journal of Membrane Science,* 365**,** 34-39.

LEE, S. & ELIMELECH, M. 2007. Salt cleaning of organic-fouled reverse osmosis membranes. *Water Research,* 41**,** 1134-1142.

LEE, S., KIM, Y., KIM, A. S. & HONG, S. 2015. Evaluation of membrane-based desalting processes for RO brine treatment. *Desalination and Water Treatment***,** 1-8.

LEE, S. & KIM, Y. C. 2017. Calcium carbonate scaling by reverse draw solute diffusion in a forward osmosis membrane for shale gas wastewater treatment. *Journal of Membrane Science,* 522**,** 257-266.

LEW, C., HU, J., SONG, L., LEE, L., ONG, S., NG, W. & SEAH, H. 2005. Development of an integrated membrane process for water reclamation. *Water Science and Technology,* 51**,** 455-463.

LI, X.-M., ZHAO, B., WANG, Z., XIE, M., SONG, J., NGHIEM, L. D., HE, T., YANG, C., LI, C. & CHEN, G. 2014. Water reclamation from shale gas drilling flow-back fluid using a novel forward osmosis–vacuum membrane distillation hybrid system. *Water Science and Technology,* 69**,** 1036-1044.

LIAO, B.-Q., KRAEMER, J. T. & BAGLEY, D. M. 2006. Anaerobic Membrane Bioreactors: Applications and Research Directions. *Critical Reviews in Environmental Science and Technology,* 36**,** 489-530.

LIN, H., CHEN, J., WANG, F., DING, L. & HONG, H. 2011. Feasibility evaluation of submerged anaerobic membrane bioreactor for municipal secondary wastewater treatment. *Desalination,* 280**,** 120-126.

LIN, H., PENG, W., ZHANG, M., CHEN, J., HONG, H. & ZHANG, Y. 2013. A review on anaerobic membrane bioreactors: Applications, membrane fouling and future perspectives. *Desalination,* 314**,** 169-188.

LIN, H. J., XIE, K., MAHENDRAN, B., BAGLEY, D. M., LEUNG, K. T., LISS, S. N. & LIAO, B. Q. 2009. Sludge properties and their effects on membrane fouling in submerged anaerobic membrane bioreactors (SAnMBRs). *Water Research,* 43**,** 3827-3837.

LINARES, R. V., YANGALI-QUINTANILLA, V., LI, Z. & AMY, G. 2011. Rejection of micropollutants by clean and fouled forward osmosis membrane. *Water Research,* 45**,** 6737-6744.

LIU, T. & SUNG, S. 2002. Ammonia inhibition on thermophilic aceticlastic methanogens. *Water Science and Technology,* 45**,** 113-120.

LIU, Y. & BOONE, D. R. 1991. Effects of salinity on methanogenic decomposition. *Bioresource Technology,* 35**,** 271-273.

LU, S.-G., IMAI, T., UKITA, M. & SEKINE, M. 2007. Start-up performances of dry anaerobic mesophilic and thermophilic digestions of organic solid wastes. *Journal of Environmental Sciences,* 19**,** 416-420.

LU, Y. & HE, Z. 2015. Mitigation of Salinity Buildup and Recovery of Wasted Salts in a Hybrid Osmotic Membrane Bioreactor–Electrodialysis System. *Environmental Science & Technology,* 49**,** 10529-10535.

LUO, W., HAI, F. I., PRICE, W. E., GUO, W., NGO, H. H., YAMAMOTO, K. & NGHIEM, L. D. 2016. Phosphorus and water recovery by a novel osmotic membrane bioreactor–reverse osmosis system. *Bioresource Technology,* 200**,** 297-304.

LUSTE, S. & LUOSTARINEN, S. 2010. Anaerobic co-digestion of meat-processing by-products and sewage sludge – Effect of hygienization and organic loading rate. *Bioresource Technology,* 101**,** 2657-2664.

MCCUE, T., HOXWORTH, S. & RANDALL, A. A. 2003. Degradation of halogenated aliphatic compounds utilizing sequential anaerobic/aerobic treatments. *Water Sci Technol,* 47**,** 79-84.

MCCUTCHEON, J. R. & ELIMELECH, M. 2006. Influence of concentrative and dilutive internal concentration polarization on flux behavior in forward osmosis. *Journal of Membrane Science,* 284**,** 237-247.

MCCUTCHEON, J. R. & ELIMELECH, M. 2007. Modeling water flux in forward osmosis: implications for improved membrane design. *AIChE journal,* 53**,** 1736-1744.

MCCUTCHEON, J. R. & ELIMELECH, M. 2008. Influence of membrane support layer hydrophobicity on water flux in osmotically driven membrane processes. *Journal of Membrane Science,* 318**,** 458-466.

MCCUTCHEON, J. R., MCGINNIS, R. L. & ELIMELECH, M. 2005. A novel ammonia—carbon dioxide forward (direct) osmosis desalination process. *Desalination,* 174**,** 1-11.

MCCUTCHEON, J. R., MCGINNIS, R. L. & ELIMELECH, M. 2006. Desalination by ammonia–carbon dioxide forward osmosis: Influence of draw and feed solution concentrations on process performance. *Journal of Membrane Science,* 278**,** 114-123.

MCGINNIS, R. L. & ELIMELECH, M. 2007. Energy requirements of ammonia–carbon dioxide forward osmosis desalination. *Desalination,* 207**,** 370-382.

MCILROY, S. J., SAUNDERS, A. M., ALBERTSEN, M., NIERYCHLO, M., MCILROY, B., HANSEN, A. A., KARST, S. M., NIELSEN, J. L. & NIELSEN, P. H. 2015. MiDAS: the field guide to the microbes of activated sludge. *Database: The Journal of Biological Databases and Curation,* 2015**,** bav062.

MENDEZ, R., LEMA, J. M. & SOTO, M. 1995. Treatment of Seafood-Processing Wastewaters in Mesophilic and Thermophilic Anaerobic Filters. *Water Environment Research,* 67**,** 33-45.

MI, B. & ELIMELECH, M. 2008. Chemical and physical aspects of organic fouling of forward osmosis membranes. *Journal of Membrane Science,* 320**,** 292-302.

MI, B. & ELIMELECH, M. 2010. Organic fouling of forward osmosis membranes: Fouling reversibility and cleaning without chemical reagents. *Journal of Membrane Science,* 348**,** 337-345.

MOLDEN, D. 2007. *Water for life: A Comprehensive Assessment of Water Management in Agriculture*, Earthscan Ltd.

MONSALVO, V. M., MCDONALD, J. A., KHAN, S. J. & LE-CLECH, P. 2014. Removal of trace organics by anaerobic membrane bioreactors. *Water Research,* 49**,** 103-112.

MOODY, C. D. 1977. Forward osmosis extractors : theory, feasibility and design optimization. The University of Arizona.

NATIONS, F. A. A. O. O. T. U. 2016. *Direct use of municipal wastewater for irrigation* [Online]. Rome: Food and Agriculture Organization of the United Nations. Available: http://www.fao.org/nr/water/aquastat/wastewater/index.stm [Accessed].

NAWAZ, M. S., GADELHA, G., KHAN, S. J. & HANKINS, N. 2013. Microbial toxicity effects of reverse transported draw solute in the forward osmosis membrane bioreactor (FO-MBR). *Journal of Membrane Science,* 429**,** 323-329.

NG, K. K., SHI, X. & NG, H. Y. 2015. Evaluation of system performance and microbial communities of a bioaugmented anaerobic membrane bioreactor treating pharmaceutical wastewater. *Water Research,* 81**,** 311-324.

NGHIEM, L. D., NGUYEN, T. T., MANASSA, P., FITZGERALD, S. K., DAWSON, M. & VIERBOOM, S. 2014. Co-digestion of sewage sludge and crude glycerol for on-demand biogas production. *International Biodeterioration and Biodegradation,* 95**,** 160-166.

NGUYEN, H. T., CHEN, S.-S., NGUYEN, N. C., NGO, H. H., GUO, W. & LI, C.-W. 2015. Exploring an innovative surfactant and phosphate-based draw solution for forward osmosis desalination. *Journal of Membrane Science,* 489**,** 212-219.

NGUYEN, N. C., CHEN, S.-S., YANG, H.-Y. & HAU, N. T. 2013. Application of forward osmosis on dewatering of high nutrient sludge. *Bioresource Technology,* 132**,** 224-229.

O'FLAHERTY, V. & COLLERAN, E. 1999. Effect of sulphate addition on volatile fatty acid and ethanol degradation in an anaerobic hybrid reactor. I: process disturbance and remediation. *Bioresource Technology,* 68**,** 101-107.

OLESZKIEWICZ, J. A. & SHARMA, V. K. 1990. Stimulation and inhibition of anaerobic processes by heavy metals—A review. *Biological Wastes,* 31**,** 45-67.

OREMLAND, R. S. & TAYLOR, B. F. 1978. Sulfate reduction and methanogenesis in marine sediments. *Geochimica et Cosmochimica Acta,* 42**,** 209-214.

OTTOSON, J., HANSEN, A., BJ RLENIUS, B., NORDER, H. & STENSTR M, T. A. 2006. Removal of viruses, parasitic protozoa and microbial indicators in conventional and membrane processes in a wastewater pilot plant. *Water Research,* 40**,** 1449-1457.

PARK, J., YOON, J.-H., DEPUYDT, S., OH, J.-W., JO, Y.-M., KIM, K., BROWN, M. T. & HAN, T. 2016. The sensitivity of an hydroponic lettuce root elongation bioassay to metals, phenol and wastewaters. *Ecotoxicology and Environmental Safety,* 126**,** 147-153.

PARK, M. J., PHUNTSHO, S., HE, T., NISOLA, G. M., TIJING, L. D., LI, X.-M., CHEN, G., CHUNG, W.-J. & SHON, H. K. 2015. Graphene oxide incorporated polysulfone substrate for the fabrication of flat-sheet thin-film composite forward osmosis membranes. *Journal of Membrane Science,* 493**,** 496-507.

PARKS, S. 2011. *Nutrient management of Asian vegetables*, Horticulture Australia.

PENDERGAST, M. M., GHOSH, A. K. & HOEK, E. M. V. 2013. Separation performance and interfacial properties of nanocomposite reverse osmosis membranes. *Desalination,* 308**,** 180-185.

PEREIRA, M. A., CAVALEIRO, A. J., MOTA, M. & ALVES, M. M. 2003. Accumulation of long chain fatty acids onto anaerobic sludge under steady state and shock loading conditions: Effect on acetogenic and methanogenic activity. *Water Science and Technology.*

PETROTOS, K. B., QUANTICK, P. & PETROPAKIS, H. 1998. A study of the direct osmotic concentration of tomato juice in tubular membrane – module configuration. I. The effect of certain basic process parameters on the process performance. *Journal of Membrane Science,* 150**,** 99-110.

PHILLIP, W. A., YONG, J. S. & ELIMELECH, M. 2010. Reverse draw solute permeation in forward osmosis: modeling and experiments. *Environmental Science & Technology,* 44**,** 5170-5176.

PHUNTSHO, S., HONG, S., ELIMELECH, M. & SHON, H. K. 2013a. Forward osmosis desalination of brackish groundwater: Meeting water quality requirements for fertigation by integrating nanofiltration. *Journal of Membrane Science,* 436**,** 1-15.

PHUNTSHO, S., KIM, J. E., JOHIR, M. A. H., HONG, S., LI, Z., GHAFFOUR, N., LEIKNES, T. & SHON, H. K. 2016. Fertiliser drawn forward osmosis process: Pilot-scale desalination of mine impaired water for fertigation. *Journal of Membrane Science,* 508**,** 22-31.

PHUNTSHO, S., LOTFI, F., HONG, S., SHAFFER, D. L., ELIMELECH, M. & SHON, H. K. 2014. Membrane scaling and flux decline during fertiliser-drawn forward osmosis desalination of brackish groundwater. *Water Research,* 57**,** 172-182.

PHUNTSHO, S., SAHEBI, S., MAJEED, T., LOTFI, F., KIM, J. E. & SHON, H. K. 2013b. Assessing the major factors affecting the performances of forward osmosis and its implications on the desalination process. *Chemical Engineering Journal,* 231**,** 484-496.

PHUNTSHO, S., SHON, H., HONG, S., LEE, S., VIGNESWARAN, S. & KANDASAMY, J. 2012a. Fertiliser drawn forward osmosis desalination: the concept, performance and limitations for fertigation. *Reviews in Environmental Science and Bio/Technology,* 11**,** 147-168.

PHUNTSHO, S., SHON, H. K., HONG, S., LEE, S. & VIGNESWARAN, S. 2011. A novel low energy fertilizer driven forward osmosis desalination for direct fertigation: Evaluating the performance of fertilizer draw solutions. *Journal of Membrane Science,* 375**,** 172-181.

PHUNTSHO, S., SHON, H. K., MAJEED, T., EL SALIBY, I., VIGNESWARAN, S., KANDASAMY, J., HONG, S. & LEE, S. 2012b. Blended Fertilizers as Draw

Solutions for Fertilizer-Drawn Forward Osmosis Desalination. *Environmental Science & Technology,* 46**,** 4567-4575.

PINTO, A. J. & RASKIN, L. 2012. PCR Biases Distort Bacterial and Archaeal Community Structure in Pyrosequencing Datasets. *PLOS ONE,* 7**,** e43093.

PLUGGE, C. M., BALK, M., ZOETENDAL, E. G. & STAMS, A. J. M. 2002. Gelria glutamica gen. nov., sp. nov., a thermophilic, obligately syntrophic, glutamate-degrading anaerobe. *International Journal of Systematic and Evolutionary Microbiology,* 52**,** 401-407.

POLYAKOV, Y. S. & ZYDNEY, A. L. 2013. Ultrafiltration membrane performance: Effects of pore blockage/constriction. *Journal of Membrane Science,* 434**,** 106-120.

QIU, G., LAW, Y.-M., DAS, S. & TING, Y.-P. 2015. Direct and Complete Phosphorus Recovery from Municipal Wastewater Using a Hybrid Microfiltration-Forward Osmosis Membrane Bioreactor Process with Seawater Brine as Draw Solution. *Environmental Science & Technology,* 49**,** 6156-6163.

QIU, G. & TING, Y.-P. 2014. Direct phosphorus recovery from municipal wastewater via osmotic membrane bioreactor (OMBR) for wastewater treatment. *Bioresource Technology,* 170**,** 221-229.

RAVAL, H. D. & KORADIYA, P. 2016. Direct fertigation with brackish water by a forward osmosis system converting domestic reverse osmosis module into forward osmosis membrane element. *Desalination and Water Treatment,* 57**,** 15740-15747.

RENARD, P., BOUILLON, C., NAVEAU, H. & NYNS, E.-J. 1993. Toxicity of a mixture of polychlorinated organic compounds towards an unacclimated methanogenic consortium. *Biotechnology Letters,* 15**,** 195-200.

RESH, H. M. 2012. *Hydroponic food production: a definitive guidebook for the advanced home gardener and the commercial hydroponic grower,* Boca Raton, FL, CRC Press.

RIJSBERMAN, F. R. 2006. Water scarcity: Fact or fiction? *Agricultural Water Management,* 80**,** 5-22.

RIVIERE, D., DESVIGNES, V., PELLETIER, E., CHAUSSONNERIE, S., GUERMAZI, S., WEISSENBACH, J., LI, T., CAMACHO, P. & SGHIR, A. 2009. Towards the definition of a core of microorganisms involved in anaerobic digestion of sludge. *ISME J,* 3**,** 700-714.

ROMANO, R. T. & ZHANG, R. 2008. Co-digestion of onion juice and wastewater sludge using an anaerobic mixed biofilm reactor. *Bioresource Technology,* 99**,** 631-637.

SAHEBI, S., PHUNTSHO, S., EUN KIM, J., HONG, S. & KYONG SHON, H. 2015. Pressure assisted fertiliser drawn osmosis process to enhance final dilution of the fertiliser draw solution beyond osmotic equilibrium. *Journal of Membrane Science,* 481**,** 63-72.

SCHMIDT, J. E. & AHRING, B. K. 1993. Effects of magnesium on thermophilic acetate-degrading granules in upflow anaerobic sludge blanket (UASB) reactors. *Enzyme and Microbial Technology,* 15**,** 304-310.

SEMIAT, R. 2008. Energy Issues in Desalination Processes. *Environmental Science & Technology,* 42**,** 8193-8201.

SEPP L , A. & LAMPINEN, M. J. 2004. On the non-linearity of osmotic flow. *Experimental Thermal and Fluid Science,* 28**,** 283-296.

SHAFFER, D. L., YIP, N. Y., GILRON, J. & ELIMELECH, M. 2012. Seawater desalination for agriculture by integrated forward and reverse osmosis: Improved product water quality for potentially less energy. *Journal of Membrane Science,* 415–416**,** 1-8.

SHANNON, M. A., BOHN, P. W., ELIMELECH, M., GEORGIADIS, J. G., MARINAS, B. J. & MAYES, A. M. 2008. Science and technology for water purification in the coming decades. *Nature,* 452**,** 301-310.

SHE, Q., JIN, X., LI, Q. & TANG, C. Y. 2012. Relating reverse and forward solute diffusion to membrane fouling in osmotically driven membrane processes. *Water Research,* 46**,** 2478-2486.

SHE, Q., WANG, R., FANE, A. G. & TANG, C. Y. 2016. Membrane fouling in osmotically driven membrane processes: A review. *Journal of Membrane Science,* 499**,** 201-233.

SIKAWA, D. C. & YAKUPITIYAGE, A. 2010. The hydroponic production of lettuce (Lactuca sativa L) by using hybrid catfish (Clarias macrocephalus× C. gariepinus) pond water: Potentials and constraints. *Agricultural water management,* 97**,** 1317-1325.

SIKKEMA, J., DE BONT, J. A. & POOLMAN, B. 1995. Mechanisms of membrane toxicity of hydrocarbons. *Microbiological Reviews,* 59**,** 201-222.

SMOLEŃ, S., KOWALSKA, I. & SADY, W. 2014. Assessment of biofortification with iodine and selenium of lettuce cultivated in the NFT hydroponic system. *Scientia Horticulturae,* 166**,** 9-16.

SNYDER, S. A., WESTERHOFF, P., YOON, Y. & SEDLAK, D. L. 2003. Pharmaceuticals, Personal Care Products, and Endocrine Disruptors in Water: Implications for the Water Industry. *Environmental Engineering Science,* 20**,** 449-469.

SONG, X., MCDONALD, J., PRICE, W. E., KHAN, S. J., HAI, F. I., NGO, H. H., GUO, W. & NGHIEM, L. D. 2016. Effects of salinity build-up on the performance of an anaerobic membrane bioreactor regarding basic water quality parameters and removal of trace organic contaminants. *Bioresource Technology,* 216**,** 399-405.

SONG, Z., WILLIAMS, C. J. & EDYVEAN, R. G. J. 2001. Coagulation and Anaerobic Digestion of Tannery Wastewater. *Process Safety and Environmental Protection,* 79**,** 23-28.

SOTO, M., M NDEZ, R. & LEMA, J. M. 1993a. Methanogenic and non-methanogenic activity tests. Theoretical basis and experimental set up. *Water Research,* 27**,** 1361-1376.

SOTO, M., M NDEZ, R. & LEMA, J. M. 1993b. Sodium inhibition and sulphate reduction in the anaerobic treatment of mussel processing wastewaters. *Journal of Chemical Technology & Biotechnology,* 58**,** 1-7.

SPAGNI, A., CASU, S., CRISPINO, N. A., FARINA, R. & MATTIOLI, D. 2010. Filterability in a submerged anaerobic membrane bioreactor. *Desalination,* 250**,** 787-792.

SRINIVASAN, S. & CHI, T. 1973. Effect of imperfect salt rejection on concentration polarization in reverse osmosis systems. *Desalination,* 13**,** 287-301.

STERRITT, R. M. & LESTER, J. N. 1980. Interactions of heavy metals with bacteria. *Sci Total Environ,* 14**,** 5-17.

STUCKEY, D. C. 2012. Recent developments in anaerobic membrane reactors. *Bioresource Technology,* 122**,** 137-148.

SUTARYO, S., WARD, A. J. & M LLER, H. B. 2012. Thermophilic anaerobic co-digestion of separated solids from acidified dairy cow manure. *Bioresource Technology,* 114**,** 195-200.

TAN, C. H. & NG, H. Y. 2008. Modified models to predict flux behavior in forward osmosis in consideration of external and internal concentration polarizations. *Journal of Membrane Science,* 324**,** 209-219.

TAN, C. H. & NG, H. Y. 2010. A novel hybrid forward osmosis - nanofiltration (FO-NF) process for seawater desalination: Draw solution selection and system configuration. *Desalination and Water Treatment,* 13**,** 356-361.

TANG, C. Y., SHE, Q., LAY, W. C. L., WANG, R. & FANE, A. G. 2010. Coupled effects of internal concentration polarization and fouling on flux behavior of forward osmosis membranes during humic acid filtration. *Journal of Membrane Science,* 354**,** 123-133.

TCHOBANOGLOUS, G., THEISEN, H. & VIGIL, S. A. 1993. *Integrated solid waste management : engineering principles and management issues,* New York, McGraw-Hill.

TEAM, R. C. 2015. R: A language and environment for statistical computing [Internet]. Vienna, Austria: R Foundation for Statistical Computing; 2013. *Document freely available on the internet at:* http://www. *r-project. org*.

TIRAFERRI, A., YIP, N. Y., STRAUB, A. P., ROMERO-VARGAS CASTRILLON, S. & ELIMELECH, M. 2013. A method for the simultaneous determination of transport and structural parameters of forward osmosis membranes. *Journal of Membrane Science,* 444**,** 523-538.

TORRES, A., HEMMELMANN, A., VERGARA, C. & JEISON, D. 2011. Application of two-phase slug-flow regime to control flux reduction on anaerobic membrane bioreactors treating wastewaters with high suspended solids concentration. *Separation and Purification Technology,* 79**,** 20-25.

VALLADARES LINARES, R., LI, Z., YANGALI-QUINTANILLA, V., LI, Q. & AMY, G. 2013. Cleaning protocol for a FO membrane fouled in wastewater reuse. *Desalination and Water Treatment,* 51**,** 4821-4824.

VALLADARES LINARES, R., YANGALI-QUINTANILLA, V., LI, Z. & AMY, G. 2011. Rejection of micropollutants by clean and fouled forward osmosis membrane. *Water Research,* 45**,** 6737-6744.

VALLEE, B. L. & ULMER, D. D. 1972. Biochemical effects of mercury, cadmium, and lead. *Annu Rev Biochem,* 41**,** 91-128.

VAN BEELEN, P. & VAN VLAARDINGEN, P. 1994. Toxic effects of pollutants on the mineralization of 4-chlorophenol and benzoate in methanogenic river sediment. *Environmental Toxicology and Chemistry,* 13**,** 1051-1060.

VAN DER WIELEN, P. W. J. J., ROVERS, G. M. L. L., SCHEEPENS, J. M. A. & BIESTERVELD, S. 2002. Clostridium lactatifermen tans sp. nov., a lactate-fermenting anaerobe isolated from the caeca of a chicken. *International Journal of Systematic and Evolutionary Microbiology,* 52**,** 921-925.

VAN LANGERAK, E. P. A., GONZALEZ-GIL, G., VAN AELST, A., VAN LIER, J. B., HAMELERS, H. V. M. & LETTINGA, G. 1998. Effects of high calcium concentrations on the development of methanogenic sludge in upflow anaerobic sludge bed (UASB) reactors. *Water Research,* 32**,** 1255-1263.

VERSTRAETE, W. & VLAEMINCK, S. E. 2011. ZeroWasteWater: short-cycling of wastewater resources for sustainable cities of the future. *International Journal of Sustainable Development and World Ecology,* 18**,** 253-264.

VOURCH, M., BALANNEC, B., CHAUFER, B. & DORANGE, G. 2008. Treatment of dairy industry wastewater by reverse osmosis for water reuse. *Desalination,* 219**,** 190-202.

WANG, L., WIJEKOON, K. C., NGHIEM, L. D. & KHAN, S. J. 2014a. Removal of polycyclic musks by anaerobic membrane bioreactor: Biodegradation, biosorption, and enantioselectivity. *Chemosphere,* 117**,** 722-729.

WANG, Q., GARRITY, G. M., TIEDJE, J. M. & COLE, J. R. 2007. Naïve Bayesian Classifier for Rapid Assignment of rRNA Sequences into the New Bacterial Taxonomy. *Applied and Environmental Microbiology,* 73**,** 5261-5267.

WANG, X., CHANG, V. W. & TANG, C. Y. 2016. Osmotic membrane bioreactor (OMBR) technology for wastewater treatment and reclamation: Advances, challenges, and prospects for the future. *Journal of Membrane Science,* 504**,** 113-132.

WANG, X., YANG, G., FENG, Y., REN, G. & HAN, X. 2012. Optimizing feeding composition and carbon–nitrogen ratios for improved methane yield during anaerobic co-digestion of dairy, chicken manure and wheat straw. *Bioresource Technology,* 120**,** 78-83.

WANG, X., YUAN, B., CHEN, Y., LI, X. & REN, Y. 2014b. Integration of micro-filtration into osmotic membrane bioreactors to prevent salinity build-up. *Bioresource Technology,* 167**,** 116-123.

WEI, C.-H., HARB, M., AMY, G., HONG, P.-Y. & LEIKNES, T. 2014. Sustainable organic loading rate and energy recovery potential of mesophilic anaerobic membrane bioreactor for municipal wastewater treatment. *Bioresource Technology,* 166**,** 326-334.

WEI, C.-H., HOPPE-JONES, C., AMY, G. & LEIKNES, T. 2015. Organic micro-pollutants' removal via anaerobic membrane bioreactor with ultrafiltration and nanofiltration. *Journal of Water Reuse and Desalination*.

WIJEKOON, K. C., MCDONALD, J. A., KHAN, S. J., HAI, F. I., PRICE, W. E. & NGHIEM, L. D. 2015. Development of a predictive framework to assess the removal of trace organic chemicals by anaerobic membrane bioreactor. *Bioresource Technology,* 189**,** 391-398.

WIJEKOON, K. C., VISVANATHAN, C. & ABEYNAYAKA, A. 2011. Effect of organic loading rate on VFA production, organic matter removal and microbial activity of a two-stage thermophilic anaerobic membrane bioreactor. *Bioresource Technology,* 102**,** 5353-5360.

WISHAW, B. & STOKES, R. 1954. The diffusion coefficients and conductances of some concentrated electrolyte solutions at 25. *Journal of the American Chemical Society,* 76**,** 2065-2071.

WOO, Y. C., KIM, Y., SHIM, W.-G., TIJING, L. D., YAO, M., NGHIEM, L. D., CHOI, J.-S., KIM, S.-H. & SHON, H. K. 2016. Graphene/PVDF flat-sheet membrane for the treatment of RO brine from coal seam gas produced water by air gap membrane distillation. *Journal of Membrane Science,* 513**,** 74-84.

WOO, Y. C., LEE, J. J., TIJING, L. D., SHON, H. K., YAO, M. & KIM, H.-S. 2015. Characteristics of membrane fouling by consecutive chemical cleaning in pressurized ultrafiltration as pre-treatment of seawater desalination. *Desalination,* 369**,** 51-61.

WOO, Y. C., TIJING, L. D., PARK, M. J., YAO, M., CHOI, J.-S., LEE, S., KIM, S.-H., AN, K.-J. & SHON, H. K. Electrospun dual-layer nonwoven membrane for desalination by air gap membrane distillation. *Desalination*.

WOOD, E. J. 1977. Outlines of biochemistry, 4th edition: E. E. Conn and P. K. Stumpf. Pp. 630. John Wiley and Sons, Inc. London and New York. 1976. Hardback, £10.95, softcover, £5.85. *Biochemical Education,* 5**,** 20-20.

WWAP 2012. The United Nations World Water Development Report 4: Managing Water under Uncertainty and Risk. Paris.

XIANG, X., ZOU, S. & HE, Z. 2017. Energy consumption of water recovery from wastewater in a submerged forward osmosis system using commercial liquid fertilizer as a draw solute. *Separation and Purification Technology,* 174**,** 432-438.

XIAO, D., TANG, C. Y., ZHANG, J., LAY, W. C. L., WANG, R. & FANE, A. G. 2011. Modeling salt accumulation in osmotic membrane bioreactors: Implications for FO membrane selection and system operation. *Journal of Membrane Science,* 366**,** 314-324.

XIAO, P., NGHIEM, L. D., YIN, Y., LI, X.-M., ZHANG, M., CHEN, G., SONG, J. & HE, T. 2015. A sacrificial-layer approach to fabricate polysulfone support for forward osmosis thin-film composite membranes with reduced internal concentration polarisation. *Journal of Membrane Science,* 481**,** 106-114.

XIE, M., BAR-ZEEV, E., HASHMI, S. M., NGHIEM, L. D. & ELIMELECH, M. 2015a. Role of Reverse Divalent Cation Diffusion in Forward Osmosis Biofouling. *Environmental Science & Technology,* 49**,** 13222-13229.

XIE, M., NGHIEM, L. D., PRICE, W. E. & ELIMELECH, M. 2012a. Comparison of the removal of hydrophobic trace organic contaminants by forward osmosis and reverse osmosis. *Water Research,* 46**,** 2683-2692.

XIE, M., NGHIEM, L. D., PRICE, W. E. & ELIMELECH, M. 2013a. A Forward Osmosis–Membrane Distillation Hybrid Process for Direct Sewer Mining: System Performance and Limitations. *Environmental Science & Technology,* 47**,** 13486-13493.

XIE, M., NGHIEM, L. D., PRICE, W. E. & ELIMELECH, M. 2013b. Impact of humic acid fouling on membrane performance and transport of pharmaceutically active compounds in forward osmosis. *Water Research,* 47**,** 4567-4575.

XIE, M., NGHIEM, L. D., PRICE, W. E. & ELIMELECH, M. 2014. Relating rejection of trace organic contaminants to membrane properties in forward osmosis: Measurements, modelling and implications. *Water Research,* 49**,** 265-274.

XIE, M., PRICE, W. E. & NGHIEM, L. D. 2012b. Rejection of pharmaceutically active compounds by forward osmosis: Role of solution pH and membrane orientation. *Separation and Purification Technology,* 93**,** 107-114.

XIE, M., ZHENG, M., COOPER, P., PRICE, W. E., NGHIEM, L. D. & ELIMELECH, M. 2015b. Osmotic dilution for sustainable greenwall irrigation by liquid fertilizer: Performance and implications. *Journal of Membrane Science,* 494**,** 32-38.

XU, M., WEN, X., HUANG, X. & LI, Y. 2010a. Membrane Fouling Control in an Anaerobic Membrane Bioreactor Coupled with Online Ultrasound Equipment for Digestion of Waste Activated Sludge. *Separation Science and Technology,* 45**,** 941-947.

XU, Y., PENG, X., TANG, C. Y., FU, Q. S. & NIE, S. 2010b. Effect of draw solution concentration and operating conditions on forward osmosis and pressure retarded osmosis performance in a spiral wound module. *Journal of Membrane Science,* 348**,** 298-309.

YAELI, J. 1992. Method and apparatus for processing liquid solutions of suspensions particularly useful in the desalination of saline water. Google Patents.

YAN, X., BILAD, M. R., GERARDS, R., VRIENS, L., PIASECKA, A. & VANKELECOM, I. F. J. 2012. Comparison of MBR performance and membrane cleaning in a single-stage activated sludge system and a two-stage anaerobic/aerobic (A/A) system for treating synthetic molasses wastewater. *Journal of Membrane Science,* 394–395**,** 49-56.

YASUKAWA, M., MISHIMA, S., SHIBUYA, M., SAEKI, D., TAKAHASHI, T., MIYOSHI, T. & MATSUYAMA, H. 2015. Preparation of a forward osmosis membrane using a highly porous polyketone microfiltration membrane as a novel support. *Journal of Membrane Science,* 487**,** 51-59.

YE, L., PENG, C.-Y., TANG, B., WANG, S.-Y., ZHAO, K.-F. & PENG, Y.-Z. 2009. Determination effect of influent salinity and inhibition time on partial nitrification in a sequencing batch reactor treating saline sewage. *Desalination,* 246**,** 556-566.

YEN, H.-W. & BRUNE, D. E. 2007. Anaerobic co-digestion of algal sludge and waste paper to produce methane. *Bioresource Technology,* 98**,** 130-134.

YEN, S. K., MEHNAS HAJA N, F., SU, M., WANG, K. Y. & CHUNG, T.-S. 2010. Study of draw solutes using 2-methylimidazole-based compounds in forward osmosis. *Journal of Membrane Science,* 364**,** 242-252.

YERKES, D. W., BOONYAKITSOMBUT, S. & SPEECE, R. E. 1997. Antagonism of sodium toxicity by the compatible solute betaine in anaerobic methanogenic systems. *Water Science and Technology,* 36**,** 15-24.

YIP, N. Y. & ELIMELECH, M. 2013. Influence of Natural Organic Matter Fouling and Osmotic Backwash on Pressure Retarded Osmosis Energy Production from Natural Salinity Gradients. *Environmental Science & Technology,* 47**,** 12607-12616.

YIP, N. Y., TIRAFERRI, A., PHILLIP, W. A., SCHIFFMAN, J. D. & ELIMELECH, M. 2010. High Performance Thin-Film Composite Forward Osmosis Membrane. *Environmental Science & Technology,* 44**,** 3812-3818.

YU, H. Q., TAY, J. H. & FANG, H. H. P. 2001. The roles of calcium in sludge granulation during uasb reactor start-up. *Water Research,* 35**,** 1052-1060.

YUN, T., KIM, Y.-J., LEE, S., HONG, S. & KIM, G. I. 2014. Flux behavior and membrane fouling in pressure-assisted forward osmosis. *Desalination and Water Treatment,* 52**,** 564-569.

YURTSEVER, A., CALIMLIOGLU, B., G R R, M., ÇıNAR, Ö. & SAHINKAYA, E. 2016. Effect of NaCl concentration on the performance of sequential anaerobic and aerobic membrane bioreactors treating textile wastewater. *Chemical Engineering Journal,* 287**,** 456-465.

ZAYED, G. & WINTER, J. 2000. Inhibition of methane production from whey by heavy metals--protective effect of sulfide. *Appl Microbiol Biotechnol,* 53**,** 726-31.

ZHANG, J., LOONG, W. L. C., CHOU, S., TANG, C., WANG, R. & FANE, A. G. 2012. Membrane biofouling and scaling in forward osmosis membrane bioreactor. *Journal of Membrane Science,* 403–404**,** 8-14.

ZHANG, M., SHE, Q., YAN, X. & TANG, C. Y. 2017. Effect of reverse solute diffusion on scaling in forward osmosis: A new control strategy by tailoring draw solution chemistry. *Desalination,* 401**,** 230-237.

ZHANG, S., WANG, P., FU, X. & CHUNG, T.-S. 2014. Sustainable water recovery from oily wastewater via forward osmosis-membrane distillation (FO-MD). *Water Research,* 52**,** 112-121.

ZHANG, X., YUE, X., LIU, Z., LI, Q. & HUA, X. 2015. Impacts of sludge retention time on sludge characteristics and membrane fouling in a submerged anaerobic-oxic membrane bioreactor. *Appl Microbiol Biotechnol,* 99**,** 4893-903.

ZHAO, S., ZOU, L. & MULCAHY, D. 2012. Brackish water desalination by a hybrid forward osmosis–nanofiltration system using divalent draw solute. *Desalination,* 284**,** 175-181.

ZONTA, Ž., ALVES, M. M., FLOTATS, X. & PALATSI, J. 2013. Modelling inhibitory effects of long chain fatty acids in the anaerobic digestion process. *Water Research,* 47**,** 1369-1380.

ZOU, S., GU, Y., XIAO, D. & TANG, C. Y. 2011. The role of physical and chemical parameters on forward osmosis membrane fouling during algae separation. *Journal of Membrane Science,* 366**,** 356-362.

ZOU, S. & HE, Z. 2016. Enhancing wastewater reuse by forward osmosis with self-diluted commercial fertilizers as draw solutes. *Water Research,* 99**,** 235-243.